*Ph.D. Thesis*

# STUDIES ON THE DEVELOPMENT OF ZIRCONIA BASED ADSORBENTS/CATALYSTS FOR LIQUID FUEL DESULFURIZATION


***By***

***Sachin Kumar***

**COLLEGE OF ENGINEERING STUDIES**


***Submitted in partial fulfillment of the requirement of the degree of***

***Doctor of Philosophy (Engineering)***

*to*



**UNIVERSITY OF PETROLEUM & ENERGY STUDIES**
**DEHRADUN -248007, INDIA**


**OCTOBER, 2011**

# CANDIDATE'S DECLARATION

I hereby declare that the work, which is being presented in the dissertation entitled ***"Synthesis and characterization of zirconia based adsorbents/catalysts for liquid fuels desulfurization"*** for the partial fulfillment of the requirements of the award of the degree of doctorate of philosophy in engineering submitted in Department of Chemical Engineering, University of Petroleum & Energy Studies (UPES), Dehradun and Department of Chemical Engineering, Indian Institute of Technology (IIT), Roorkee, is an authentic record of my own work carried out during the period from Jan 2007 to July 2011 under supervision of Dr RP Badoni, UPES, Dehradun and Dr VC Srivastava, IIT, Roorkee.

The matter, embodied in this dissertation has not been submitted by me for the award of any other degree/diploma/certificate.

Date:

**Place: Dehradun** **(SACHIN KUMAR)**

# CERTIFICATE 1

# (By Dr.R.P Badoni)

# CERTIFICATE 2

# (By Dr.V.C Srivastava)

# ACKNOWLEDGEMENT

I express my deep sense of gratitude to my guide **Dr R P Badoni**, Distinguished Professor, Department of Chemical Engineering, University of Petroleum & Energy Studies (UPES), Dehradun for his keen interest, constant guidance and encouragement throughout the course of this work, his experience, assiduity and deep insight of the subject held this work always on a smooth and steady course. Useful criticism and constant help extended in the hours of need had been immensely useful.

It is a great pleasure for me in expressing my profound sense of gratitude, indebtness and heartful thanks to my guide **Dr V C Srivastava**, Assistant Professor, Department of Chemical Engineering, Indian Institute of Technology (IIT) Roorkee, who showed admirable forbearance and provide me valuable guidance in carrying out this work. Their everlasting encouragement and valuable suggestions at each and every step and his analytical skills made it feasible to carry out the work to conclusion.

Thanks are due to **Dr S J Chopra,** Honorable Chancellor, UPES, Dehradun and **Dr Parag Dewan**, Honorable Vice Chancellor, UPES, Dehradun, for providing various facilities during this dissertation at research & development laboratories, UPES, Dehradun.

I would also like to thank **Dr I D Mall**, Prof. and Head, Department of Chemical Engineering, IIT, Roorkee, and **Dr I M Mishra**, Prof., Department of Chemical Engineering, IIT, Roorkee and Dean (Saharanpur Campus) IIT, Roorkee for his useful guidance and encouragement provided to me during this dissertation.

I also extend my thanks to **Mr R S Kaushik,** Research Resource Officer, R&D laboratories, UPES for their wholehearted co-operation, encouragement and their valuable advice at each and every step of my work.

I am thankful to Mr R Bhatnagar (Senior Technical Assistant), Industrial Pollution Abatement Lab., Department of Chemical Engineering, IIT, Roorkee for the continuous help provided during the experimental work.

I am greatly indebted to my friends namely Dr Suresh Sundarmurty, Assistant Professor, Department of Chemical Engineering, National Institute of Technology (NIT) Bhopal (M.P), Dr Hitendra Singh, Assistant Professor, Department of Chemistry, Gov. Degree College, Tehri-Garwal (U.k), Dr Vibha Kr. Singh, Assistant Professor, Department of Chemistry, Gov. Degree College, Tehri-Garwal (U.k), Dr Nidhi Taygi, Mr Upendre Satti, Safety Officer, Sivani Gas, Mr Devendra Rawat, R&D Laboratories, UPES, Mr Charu Pant, R&D Laboratories, UPES whom enthusiastic support, encouragement and help, made me come up with this report. It is very hard to express my feeling in proper words for my parents who apart from providing me the best available education have encouraged me in all my endeavours. I owe much of my academic success to them. Though it is not possible to mention everyone, none can be forgotten for their direct/ indirect help.

Finally, I am thankful to my parents, who introduced me to the Life, Nature, The Lord and Science and Technology.

**SACHIN KUMAR**

# EXECUTIVE SUMMARY

Removing sulfur (S) from the petroleum products has been a challenging task for petroleum refiners for last many decades. Research work is still going on to develop suitable processes and catalysts to bring down the S level to parts per billion (ppb) levels, especially in gasoline and diesel streams. Presently hydrodesulfurization (HDS) is the major process in the refineries for S removal. It is a catalytic process conducted under high temprature, pressure and Hydrogen ($H_2$) gas. However, even with the novel catalysts materials which are presently be used in the process still the level of sulfur cannot be brought down to the desired level. Various novel desulfurization techniques such as oxidative desulfurization (ODS) and adsorptive desulfurization (ADS) are also emerging as a potential technique apart from the catalytic HDS. In light of the above, the present study focused on the development of the materials having twin functions of behaving like adsorbent as well as catalyst. With this objective zirconia based materials were synthesized, characterize and evaluated for their use as adsorbents/catalysts in ADS/ODS. Large number of such materials were synthesised using various preparation techniques such as precipitation, co-precipitation, sol-gel etc. The prominent of them identified in terms of some basic properties are: zirconia dried at 393 K (ZD393), zirconia calcined at 893 K (ZC893), sulfated zirconia calcined at 893 K (SZC893) and chromium promoted sulfated zirconia calcined at 893 K (CSZC893).

The advanced state-of-art tools such as scanning electron microscopic (SEM) for morphology, energy-dispersive atomic X-ray analysis (EDAX) for elemental distribution, fourier transform infra red spectral analysis (FTIR) to identify characterstics functional groups, Brunauer–Emmett–Teller surface area analysis (BET) to evaluate pore surface area, transmission electron microscopic analysis (TEM) to understand the sample pattern, thermo gravimetric/derivative thermo gravimetric analysis (TG/DTG) to understand thermal profile, electron probe microscopic analysis (EPMA) to map the elemental distribution, electron spin resonance spectroscopic analysis (EPMA) to confirm the presence of metal species, neutron activation analysis (NNA) to detect the exact metal concentration, has been used for the physico-chemical

characterization of developed materials. Bulk density of developed materials was found to be 0.89-0.99 g/cm$^3$. The developed material showed highest surface area before calcination. After calcination at 893 K, sample ZC893 showed some crystalline peaks. Majority of these peaks were monoclinic in nature. In addition, a small portion of tetragonal phase of zirconia was also observed in ZC893. XRD pattern of CSZC893 indicated that the introduction of chromium further stabilized the metastable tetragonal zirconia phase and crystallinity was further increased with chromium loading. SEM analysis showed that CSZC893 is more crystalline in nature as compared to ZC893 and SZC893. EDAX analysis showed presence of 0.98 wt% Cr in addition to Zr, O and S in CSZC893 which was reconfirmed by NAA. ZD383 was found to be fully stable upto 1273 K with a minute 2% wt loss from ambient to 1273 K. SZC393 was found to be stable upto 773 K only. Various types of functional groups were found on the surface of sample.

ADS of DBT present in model hydrocarbon (DBT in iso octane) at different concentration level were studied using three adsorbents namely ZD393, ZC893 and SZC893. The effect of adsorbent dosage (*m*) on the uptake of DBT by the adsorbent was studied. Optimum dosage for various adsorbent was found to be 10 g/l. The study of the effect of contact time on then removal of DBT showed that the equilibrium adsorption time was found to be 22 h. The rate of DBT removal was found to be very rapid during the initial 30 min, and thereafter the rate of removal decreases. During the initial stage of adsorption a large number of vacant surface sites are available for adsorption. After a lapse of sometime the DBT molecules found it difficult to attach onto the remaining vacant surface sites. Besides, the DBT adsorbed into the macro- and meso-pores that get almost saturated with DBT during the initial stage of adsorption. Thereafter, the DBT molecules have to traverse farther and deeper into the micro-pores encountering much larger resistance. This results in the slowing down of the adsorption during the later period of adsorption. Various kinetic models, viz. pseudo-first-order and pseudo-second-order and intra-particle diffusion models have been tested to investigate the adsorption of DBT onto adsorbents. The pseudo-second-order kinetics represented the adsorption data well. An increase in temperature induced a negative effect on the adsorption process. Equilibrium adsorption data were analyzed by applying different isotherm models using non-linear regression technique. DBT

adsorption onto adsorbents has been tested using the two-parameter Freundlich and Langmuir isotherm equations and the three parameter Redlich-Peterson (R-P) equation and BET isotherm equations. Brunauer, Emmett and Teller (BET) isotherm generally well represented the equilibrium adsorption of DBT onto various zirconia based adsorbents. The adsorption process was well described by multistage diffusion model. The adsorption of DBT onto developed materials was found to be exothermic in nature. ADS of DBT from model hydrocarbon by various adsorbents were found to follow the following trend: ZD393 < ZC893 < SZC893.

ODS of DBT present in model hydrocarbon at different concentration level was studied using four catalysts namely ZD393, ZC893, SZC893 and CSZC893. Optimum catalyst dose for all catalyst were found to be 5 g/l. Optimum reaction time was found to be 6 h for maximum DBT conversion. Reaction kinetics was found to follow pseudo first order kinetics. Effect of temprature on ODS was studied in the range of 303-353 K. An increase in temprature induced a positive effect on the ODS upto 333 K. ODS of DBT from model hydrocarbon by various catalysts was found to follow the following trend: ZD393 < ZC893 < SZC893 < CSZC893. XRD patterns of CSZC893 before ODS indicated that the doping of chromium can stabilize the metastable tetragonal zirconia phase, XRD patterns of CSZC893 after ODS shows that the peaks get shifted also the intensity and tetragonal nature of the peak gets reduced after ODS.The signifies the fact that the tetragonal phase is responsible for catalytic activity of CSZC893. The EPMA studies shows the chromium species were well dispersed on the surface of CSZ before ODS reaction however, its distribution gets marginally disturbed after ODS reaction. TGA thermogram of CSZ shows 2.2% wt loss due to dehydration of CSZ before ODS and 7.5% wt loss due to vaporization of DBT-sulfones after ODS. Optimum oxidative-desulfurization of sulfur from model hydrocarbon was achieved at 333 K with CSZ dose was found to be 5 g/l with optimum reaction time of 6 h.

The present study show that ODS can remove same amount of DBT in lesser time with lesser amount of zirconia material than ADS. However, ODS requires higher temperature than ADS along with some minor amount additional chemicals like oxidants and acids.

# CONTENTS

# LIST OF FIGURES

# LIST OF TABLES

# GREEK LETTERS

| | |
|---|---|
| $\beta$ | Exponent ($0<\beta<1$) (in Redlich-Peterson isotherm) |
| $\Delta S$ | Change in the entropy for active complex formation, k J/mol |
| $\Delta H$ | Enthalpy for active complex formation, kJ/mol |
| $\Delta G$ | Gibbs free energy for active complex formation, kJ/mol |
| $\Delta S^o$ | Change in the entropy for adsorption, kJ/mol |
| $\Delta H^o$ | Enthalpy of adsorption, kJ/mol |
| $\Delta G^o$ | Gibbs free energy of adsorption, kJ/mol |
| $\rho$ | Density, $kg/m^3$ |
| $\varepsilon_r$ | Residual error |
| $\alpha_T$ | Degree of transformation, fractional pyrolysis of the adsorbent |
| $\beta_o$ | Intercept parameter |
| $\beta_i$ | Slope or linear effect of the input factor $x_i$ |
| $\beta_{ii}$ | Quadratic parameters of input factor $x_i$ |
| $\beta_{ij}$ | Interaction parameters between the input factor $x_i$ and $x_j$ |
| $\sigma^2$ | Error variance |
| $\chi$ | Transmission coefficient |
| $2\theta$ | Scattering angle |
| $\gamma$ | Distribution coefficient |
| $\omega$ | Probability |
| $\mu$ | Chemical potential |
| $\eta$ | Fraction of the solute sorption |
| $\in$ | Energy of the system |
| $g_y, g_x, g_z$ | Lande g-factor |
| $g \perp$ | Lande g-factor at $90^o$ |
| g// | Lande g-factor |

# NOMENCLATURE

| | |
|---|---|
| $C_o$ | Initial concentration of model hydrocarbon |
| $C_i$ | Concentration of adsorbate solution at equilibrium (mg/l) |
| $K$ | Adsorption rate constant (1/min) |
| $K_a$ | Rate constant, liquid/mg of adsorbate, (l/mg) |
| $K_L$ | Langmuir isotherm constant, (l/mg) |
| $K_T$ | Tempkin isotherm constant, (l/mg) |
| $K_R$ | Redlich Peterson isotherm constant, (l/mg |
| $K_F$ | Freundlich isotherm constant $[1/(mg/l)^{1/n}]$ |
| $K_o$ | Apperent Rate Constant in ODS,(1/min) |
| $k_f$ | First order rate constant,$(min^{-1})$ |
| $k_s$ | Second order rate constant,(g/mg.min) |
| n | Freundlich isotherm constant |
| $Q_t$ | Amount of adsorbate adsorbed per unit amount of adsorbent at time t, (mg/g) |
| $Q_e$ | Amount of adsorbate adsorbed per unit amount of adsorbent at equilibrium, (mg/g) |
| $Q_m$ | Limiting adsorbing capacity, (mg/g) |
| $R_L$ | Separation Factor |

Chapter – I

# INTRODUCTION

## 1.1 GENERAL

A modern refinery is a highly integrated industrial plant employing different physical and chemical processes such as distillation, extraction, reforming, hydrogenation, cracking, blending, etc to convert crude oil to higher value products [Babich and Moulijn, 2003]. The main products obtained from crude oil are liquid motor gasoline, aviation gasoline, liquid petroleum gas and diesel fuels, wax, lubricants, bitumen and petrochemicals.

Crude oil is the largest and most widely used source of energy in the world and its are limited and non-renewable and the amount left is also not accurately known. Figure 1.1 shows the use of fossil-fuel resources as source of liquid fuels.

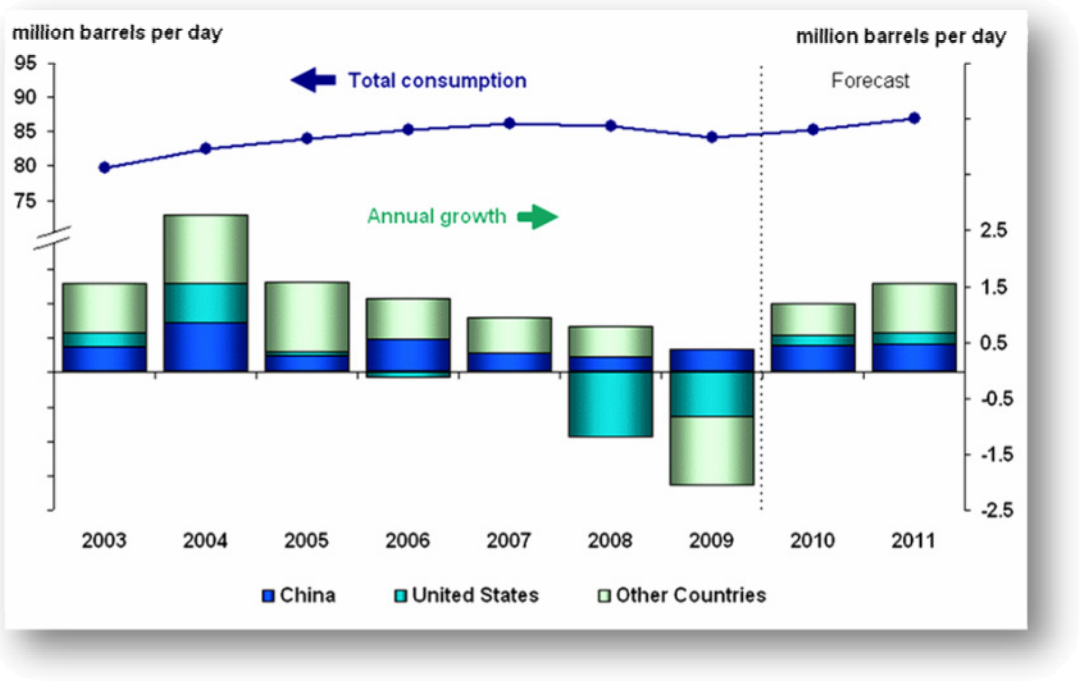


**Figure 1.1 World's liquid Fuel Consumption [US Energy Information Administration, Short-Term Energy Outlook, Feb. 2010].**

According to United States Energy Information Administration (EIA) global liquid fuels consumption to grow by 1.2 million bbl/day in 2010 and 1.6 million bbl/d

in 2011 after showing annual declines in 2008 and 2009. Non- Organization for Economic Co-operation and Development (OECD) countries are expected to account for the majority of this growth in both 2010 and 2011 [US Energy Information Admistration, Short term Energy Outlook, Feb 10, 2010].

Sulfur is one of the major impurities present in the crude oil. After carbon and hydrogen, sulfur is considered as the most abundant element in petroleum [Soleimani et al., 2007]. Crude oils with higher density contain more sulfur compounds. Distillation fractions with higher boiling point contain higher concentrations of sulfur compounds [Kropp and Fedorak, 1998; Schulz et al., 1999]. The average amount of total sulfur in crude oil may vary from 0.03 wt% to 7.89 wt%.

Organic sulfur compounds in crude oil are generally aromatic or saturated forms of thiols, sulfides and heterocyclic. Tables 1.1 and 1.2 show the presence of sulfur compounds and/or their derivatives in different refinery fuel streams [Song, 2003a]. Among these, aromatic compounds such as dibenzothiophene (DBT) or its derivatives are of significant importance because they have higher boiling points (more than 473 K) and it is difficult to remove them from atmospheric tower outlet streams (e.g middle distillates) [Kawatra et al., 2001,Shennan, 1996].

$SO_2$ is one of five major air pollutants worldwide. Mexico City experiences some of the most severe air pollution in the world [Komarnisky et al., 2003]. The deleterious effects of heteroatoms (S, O, and N) in corrosion of engine parts, $NO_x$ and $SO_x$ emissions, as well as the deactivation of refinement catalysts, emissions of $SO_2$ and $NO_x$ are the primary sources of acidic deposition. Acidic deposition has contributed to the degradation of forest ecosystems, especially the high elevation forests and the acidification of surface waters [Gbondo-Tugbawa and Driscoll, 2002]. Acidic deposition has direct and indirect effects on trees. Indirect effects occur through changes in soil chemistry including: decreases in pH, increases in chemical weathering, increases in solubility of toxic metals, alteration in mycorrhizal development, impaired root function [Haines and Carlson, 1989], and enhanced nutrient loss from soil, all these causes have made the removal of these species an issue of importance.

The removal of sulfur compounds is technologically and economically a matter of concern to the refiner over the years [Ho et al., 1999; Kocal, 2001]. The technology

options vary depending upon the product streams and the type of sulfur compounds. However, the major problem has been in particular for the removal of thiophene (TH), benzothiophene (BT) and substituted BT. Various desulfurization processes have been developed over the years to bring down the sulfur level in various fuel streams to ppm level. To meet the emerging fuel norms more stringent requirements are being enforced, especially for gasoline and diesel fuels. Motivated by forthcoming shortage in crude oil and other environmental concerns, other carbon sources are considered as feed stock material for the production of fuels, which include heavy crudes and residues, coal and biomass resources.

Several research groups world over are working on different methods such as adsorptive desulfurization (ADS), biodesulfurization (BDS), hydrodesulfurization (HDS), oxidative desulfurization (ODS), etc for the removal of sulfur from various fuel streams.

In general, diesel and gasoline contain 20–30% aromatics but less than 1% sulfur compounds, hence, removing the sulfur compounds without removing the aromatics is difficult, particularly in HDS process which also potentially hydrogenates (saturates) aromatics. It is preferable, however, to include certain aromatic compounds such as toluene and naphthalene in the fuel as they contribute significantly to fuel quality [Wang et al., 2001; Grossman et al., 2001] and maintaining other fuel requirements such as oxygen content, vapor pressure, benzene content, overall aromatics content, boiling range and olefin content for gasoline, and cetane number, density, polynuclear aromatics content, and distillation 95% point for diesel fuel [ EPA, 1999; Venner, 2000; Hattiangadi. et al., 2000; Miller et al., 2001].

In order to meet future fuel specifications efforts are being made for developing techniques that can reduce or remove such refractory compounds by ADS, ODS and BDS [Liotta and Han, 2003; Farcasiu et al., 1979; Wang et al., 2001; Kocal et al., 2002; Grossman et al., 2001; Yen et al., 2002; Gore, 2000].

However, the present need is to explore a suitable adsorbent/catalyst which could be effective in removal of sulfur from compound such as DBT. Present work is an attempt to develop a suitable zirconia based adsorbent/catalyst for the effective removal of these difficult compounds

**Table 1.1 Typical Sulfur Compounds and Corresponding Refinery Streams for Fuels [Song, 2003a].**

| Sulfur compounds | Refinery streams | Fuel Type |
|---|---|---|
| Mercaptanes; sulfides; disulfides; thiophene and its alkylated derivatives, benzothiophene | SR-naphtha; FCC naphtha; coker naphtha | Gasoline (298-498 K) |
| Mercaptanes; benzothiophene, alkylated benzothiophenes | Kerosene; heavy naphtha; middle distillate | Jet fuel (403–573 K) |
| Alkylated benzothiophenes; dibenzothiophene; alkylated dibenzothiophenes | Middle distillate; FCC LCO; coker gas oil | Diesel fuel (433–653 K) |
| Greater than or equal to three-ring polycyclic sulfur compounds, including dibenzothiophene, benzonaphtho-thiophene, phenanthro [4, 5-b, c, d] thiophene and their alkylated derivatives and naphthothiophenes | Heavy gas oils; vacuum gas oil; distillation resides | Fuel oils (non-road fuel and heavy oils) |

**Table 1.2 Typical Sulfur Compounds and Their Boiling Range [Song, 2003a].**

| Sulfur Species | Boiling Range (K) |
|---|---|
| Gasoline Range Sulfur | < 491.5 |
| Benzothiophene | 493.744 |
| $C_1$- Benzothiophenes | 494.3 - 533.22 |
| $C_2$- Benzothiophenes | 533.22 – 552.68 |
| $C_3$- Benzothiophenes | 552.68 - 579.92 |
| $C_{4+}$ - Benzothiophenes | 579.924 - 605.5 |
| Dibenzothiophene | 607.168 |
| $C_1$- Dibenzothiophene | 636.08 - 655.54 |
| $C_2$- Dibenzothiophene | 636.08 - 655.54 |
| 4, 6 – Dimethyldibenzothiophenes | 639.416 |
| $C_{3+}$ - Dibenzothiophene | 655.54 |

## 1.2 EMISSION NORMS IN INDIA [SIMA, 2009]

According to the Euro V norms, the fuel sulfur content have to be reduced to as low as 10 ppm. Figure 1.2 shows the journey of emission standards in India. It was only in 1991 that the first stage emission norms came into force for petrol vehicles and in 1992 for diesel vehicles. From April 1995, mandatory fitment of catalytic converters in new petrol passenger cars sold in the four metros of Delhi, Calcutta, Mumbai and Chennai along with supply of unleaded petrol (ULP) was affected. Availability of ULP was further extended to 42 major cities and now it is available throughout the country. Since India embarked on a formal emission control regime only in 1991, there is a gap in comparison with technologies available in the USA or Europe. Currently, India is behind Euro norms by few years, however, emission norms are being aligned with Euro standards and vehicular technology is being accordingly upgraded. Vehicle manufactures are also working towards bridging the gap between Euro standards and Indian emission norms. There is a need for a holistic approach so that up gradation in engine technology can be optimized for maximum environmental benefits.

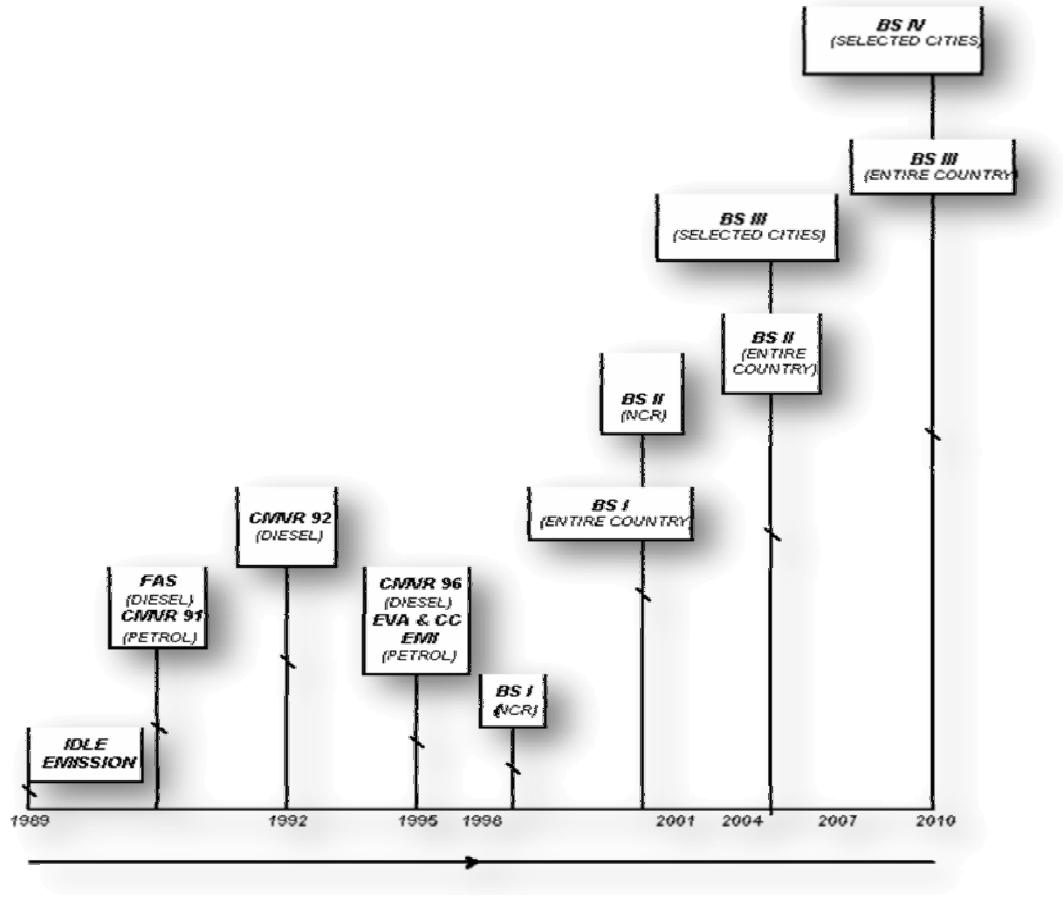


**Figure 1.2 The Journey of Emission Standards in India.**

Table 1.3 shows the fuel specifications (gasoline and diesel fuels) as per various Bharat-Stage norms in India. The latest regulations in India have reduce the gasoline sulfur content from current maximum of 150 ppm to 50 ppm and to cut the diesel sulfur content from current 350 ppm to 50 ppm. Refineries are facing major challenges to meet the fuel sulfur specification along with the required reduction of aromatics contents [**Auto Fuel Policy, 2003**].

**Table 1.3 Fuel Quality Specifications for Gasoline and Diesel in India.**

| Standard | Gasoline | | Diesel | | | |
|---|---|---|---|---|---|---|
| | Lead (ppm) | Benzene (%) | Sulfur (ppm) | Sulfur (ppm) | Cetane Number | Density ($kg/m^3$) |
| **India 2000** | 130 | 3 (Metros) 5 (Rest of India) | 1000 | 2500 | 48 | 820-860 |
| **Bharat Stage II** | 130 | 1 (Metros) 3 (Rest of India) | 500 | 500 | 48 | 820-860 |
| **Bharat Stage III** | 50 | 1 | 150 | 350 | 51 | 820-845 |
| **Bharat Stage IV** | 50 | 1 | 50 | 50 | 51 | 820-845 |

## 1.3 VARIOUS DESULFURIZATION PROCESSES

Desulfurization processes can be classified on the basis the fate of the organosulfur compounds during desulfurization, the role of $H_2$, or the nature of the physio-chemical process used [Babich and Moulijn, 2003]. Classification of desulfurization on the basis of key physico-chemical processes is shown in figure 1.3.

The organosulfur compounds can get decomposed, or separated from refinery stream without decomposition, or both separated and then decomposed are transformed during the desulfurization process. In the first type of process, when organosulfur compounds get decomposed, gaseous or solid sulfur products are formed and the $H_2$ part can be recovered and remains in the refinery streams. Conventional HDS is the

most typical example of this type of process. In second type of process, the organosulfur compounds are simply separated from the refinery streams either as such without any change or by first transforming the organosulfur compounds into other compounds then separating it from the refinery streams. When streams are desulfurized by separation, not only some desired products also get lost but also disposal of the retained organosulfur molecules also creates a future problem. In other processes, organosulfur compounds are separated from the streams and simultaneously decomposed in a single reactor unit rather than in a series of reaction and separation vessels. Catalytic distillation is the one such example [Babich and Moulijn, 2003].

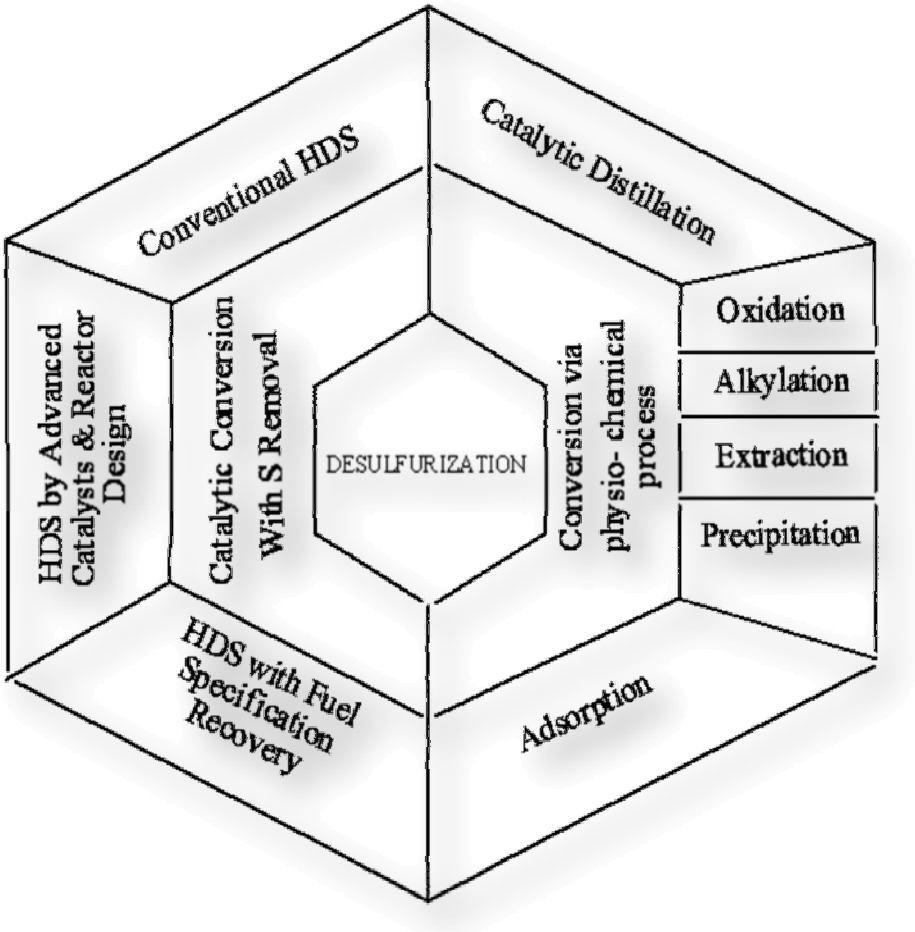


**Figure 1.3 Desulfurization Processes Classification on the basis of key physico-chemical processes.**

Desulfurization processes can be also classified in two groups, 'HDS based' and 'non-HDS based', depending on the role of $H_2$ in removing sulfur. In HDS based processes, $H_2$ is used to decompose organosulfur compounds and eliminate sulfur from fuel streams while non-HDS based processes do not require $H_2$. Catalytic HDS of crude oil and refinery streams carried out at elevated temperature and $H_2$ partial pressure converts organosulfur compounds to hydrogen sulfide ($H_2S$) and hydrocarbons [Topsøe et al., 1996; Furimsky and Massoth, 1999]. The conventional HDS process is usually conducted over sulfided $CoMo/Al_2O_3$ and $NiMo/Al_2O_3$ catalysts [Topsøe et al., 1996].

Non-HDS based desulfurization technologies include catalytic decomposition of organosulfur compounds without using $H_2$ and attaining high levels of sulfur removal by shifting the boiling point of sulfur containing compounds, separating by extraction or adsorption, and decomposition via selective oxidation.

Extractive desulfurization is based on the fact that organosulfur compounds are more soluble than hydrocarbons in an appropriate solvent. The general process flow is transferred from the fuel oil into the solvent due to their higher solubility in the solvent. Subsequently, the solvent fuel mixture is fed into a separator in which hydrocarbons are separated from the solvent. The desulfurized hydrocarbon stream is used either as a component to be blended into the final product or as a feed for further transformations. The organosulfur compounds are separated by distillation and the solvent is recycled.

Desulfurization by extractive photochemical oxidation combines photochemical reactions with extraction of the organosulfur compounds into an aqueous-soluble solvent [Shiraishi et al., 1998, 1999a, b, 2001]. The sulfur containing hydrocarbons are suspended in an aqueous-soluble solvent and irradiated by UV or visible light in a specially designed photoreactor. This results in the oxidation of the sulfur compounds. The polar compounds formed are rejected by the non-polar hydrocarbon phase and are concentrated in the solvent.

Many commercial technologies have been developed for desulfurization of liquid fuels combining various techniques. Some of the well-known licensed desulfurization processes are given in table 1.4.

**Table 1.4 Well Known Licensed Industrial Process Applied for Desulfurization.**

| Industrial processes | Adsorbent/ Catalyst | Temp(K) | Pressure Range ($kg/cm^2$) | Reactor Type | Licensed/ Patented by |
|---|---|---|---|---|---|
| Sulfur adsorption and S-Zorb process | Phillips adsorbent | 650- 775 | 7 – 21 | Fluidized bed | Phillips Petroleum |
| The IRVAD process | Activated Alumina | 513 | Low Pressure | Continuous cross-flow reactivator | Black & Veatch Irritchard Inc. and Alcoa Industrial Chemicals |
| TReND process | - | - | - | - | Research Triangle Institute |
| The SynSat process | Metal sulfide as catalyst | 588 - 673 | 31 - 63 | Fluidized bed | Criterioummus [Maxwell, 1997; Suchanek, 1996; ABB Lummus, 1998]. |
| Prime D Process | Ni-Mo catalyst | - | - | - | IFP's [EPA420-R-00-026, 2000] |
| Prime $G^+$ Process | | - | Low Pressure | - | Axens-IFP |
| Haldor–Topsoe process | Base-metal catalyst (TK-573) | - | - | - | Haldor–Topsoe [Cooper et al., 1994] |

Contd…

**Table 1.4. (Contd……..)**

| Industrial processes | Adsorbent/ Catalyst | Temp(K) | Pressure Range (kg/cm$^2$) | Reactor Type | Licensed/ Patented by |
|---|---|---|---|---|---|
| ASAT Technology | ASAT catalyst (platinum and palladium) | - | - | - | United Catalysts and Sud-Chemie AG [EPA420-R-00-026, 2000] |
| SARS (selective adsorption: SARS-I & -II processes) | - | - | - | - | Pennsylvania State University [Song, 2002; Ma et al., 2002] |
| Oct-Gain processes | - | - | - | Fixed bed | ExxonMobil |
| ISAL processes | CoMo–P/$Al_2O_3$ associated to a Ga-Cr/ HZSM-5 zeolite | - | - | Fixed bed | UOP-INTEVEP |
| Exomer Process | Caustic extraction | - | - | - | Merichem, ExxonMobil |

## 1.4 ADSORPTION AS A DESULFURIZATION TECHNIQUE

Desulfurization by adsorption is an alternative method to remove sulfur compounds with modified metal oxides, molecular sieves and activated carbon as adsorbents under ambient conditions. The sulfur compounds can be removed from commercial fuels either via reactive adsorption by chemisorption [Hernandez-Maldonado and Yang, 2004a], π-complexation [Song and Ma, 2003b; Takahashi et al., 2002; Hernandez-Maldonado and Yang, 2003a; Hernandez-Maldonado and Yang 2003b], or van der Waals and electrostatic interactions [Mikhail et al., 2002].

Various investigators have utilized this technique for the removal of sulfur from various types of fuels and model hydrocarbons by various types of adsorbents [Weitkamp et al., 1991; Ma et al., 2002; Hernandez and Yang, 2004a; McKinley 2003; Sano et al., 2005]. Desulfurization by adsorption faces the challenge of developing easily remunerable adsorbent with a high adsorption capacity. Adsorbents developed must have high selectivity for the adsorption of refractory aromatic sulfur compounds that do not get removed during the HDS process and that these adsorbents should be able to remove sulfur compounds present in minute quantity [Srivastav and Srivastava, 2009].

## 1.5 OXIDATION AS A DESULFURIZATION TECHNIQUE

The ODS process consists generally of two stages: the first stage is oxidation of organic sulfur-containing compounds in fuels, and the following step is removal of oxidized sulfur-containing compounds by extraction. In the oxidation process, the sulfur containing compounds is oxidized to sulfone by chemical reaction using an oxidant viz. $H_2O_2$, $H_2SO_4$, etc [Ali et al., 2006; Lu et al., 2006; Mei, 2003; Yang et al., 2002]. The sulfone compound can then be easily extracted from the fuel due to its higher polarity. The extraction of oxidized sulfur-containing compounds is considered to be a useful method for removal of sulfur compounds [Shiraishi et al., 1999b; Otsuki et al., 2000; Shiraishi et al., 2002; Shiraishi et al., 2004]. Otsuki et a1.[2000] reported that the thiophene and thiophene derivatives with lower electron densities on the sulfur atoms could not be oxidized in the $H_2O_2$/formic acid system at 323 K while dibenzothiophenes with higher electron densities were oxidized. Kong et a1.[2004] reported that the thiophene could be oxidized over TS-1 catalyst slowly by $H_2O_2$ in water or t-butanol, but it could not be oxidized in methanol or acetonitrile solvent.

## 1.6 RESEARCH OBJECTIVES

Only scarce work has been found in the open literature for use of zirconia based materials for ADS/ODS of liquid materials. Moreover no study is reported for synthesis and characterization of chromium doped sulfated zirconia and application in ODS. In view of the literature survey and the necessity of developing a treatment process for desulfurization, the following aims and objectives have been set for the present work.

1. To develop zirconia based materials and characterize these materials for their physico-chemical. These characteristics include scanning electron microscopic (SEM) and energy-dispersive atomic X-ray analysis (EDAX), fourier transform infra red spectral (FTIR) analysis, Brunauer–Emmett–Teller (BET) surface area, transmission electron microscopic (TEM) analysis, thermo gravimetric (TG) and derivative thermo gravimetric(DTG) analysis, etc.
2. To utilize uncalcined, calcined and calcined-sulfated zirconia as adsorbents for the removal of DBT present in model hydrocarbon (DBT dissolved in iso-octane).
    a) To study the effect of various parameters like adsorbent dose ($m$), contact time ($t$), initial concentration ($C_o$) and temperature (T) on the removal of DBT from the model hydrocarbon in batch study.
    b) To carry out kinetic and equilibrium studies for the adsorption of DBT onto developed materials and to analyze the experimental data using various kinetic and isotherm models.
    c) To understand the thermodynamics of adsorption and to estimate the heat of adsorption for DBT from the model hydrocarbon using developed materials as adsorbents.
3. To utilize developed materials as catalysts for the ODS of DBT present in model hydrocarbon (DBT dissolved in iso-octane).
    a) To study the effect of various parameters like catalyst dose ($w$), contact time ($t$), initial concentration ($C_o$) and temperature (T) on the ODS of DBT from the model hydrocarbon in batch ODS study.
    b) To carry out kinetic studies for the ODS of DBT using various kinetic model.

## Chapter – II

# LITRATURE REVIEW

### 2.1 GENERAL

This chapter has been divided into three parts: the first part deals with review of various studies on the adsorptive (ADS) and oxidative desulfurization (ODS) of model oil. In the second part, a comprehensive review of literature on the catalytic activity of various types of modified and promoted zirconia, its application, operational parameters, etc. has been reported. The third part gives theory related to adsorption as reported in the literature.

### 2.2 DESULFURIZATION

The current industrial method for removal of sulfur from fuels is hydrodesulfurization (HDS), which is a high temperature, high pressure catalytic process. This makes HDS a very costly option for deep desulfurization. Moreover, HDS is not effective for removing heterocyclic sulfur compounds such as dibenzothiophene (DBT) and its derivatives, especially 4, 6-dimethyldibenzothiophene (4, 6-DMDBT). Deep desulfurization of gasoline (from 500 to <15 ppm sulfur) is restricted largely by DBT and its derivatives. Different types of alternative technologies have been developed to meet the urgent needs of clean fuels in recent years [Wardencki and Straszewski, 1974; Koranyi et al., 1995; Collins et al., 1997; Takahashi and Yang, 2001; Mikhail et al., 2002; Ma et al., 2002; Jiang et al., 2003; Aladin et al., 2004; Shan et al., 2004;; King et al., 2000; Richardeau et al., 2004; Chica et al., 2005; Ma et al., 2005; Velu et al., 2005; Lanju et al., 2007; Dehkordi et al., 2009; Kumar et al., 2012]. Adsorptive desulfurization (ADS), Catalytic oxidative desulfurization (ODS), oxidation-extraction desulfurization (OEDS) and bio-desulfurization (BDS) are the other desulfurization techniques that have the potential to produce ultra clean fuels. BDS has drawn wide attention recently because of its green processing of fossil fuel. However, the slowness of the removal process is a major hindrance in the use of BDS process.

The main classes of sulfur compounds usually removed using these technologies are thiols, dialkyl and cycloalkyl sulfides, alkyl aryl sulfides, as well as heteroaromatic compounds such as benzothiophene (BT), dibenzothiophene (DBT), 4-methyl dibenzothiophene (4-MDBT), and 4,6-dimethyldibenzothiophene (4,6-DMDBT).Many investigators use DBT, 4-MDBT, 4,6-DMDBT as model compounds for desulfurization studies.

### 2.2.1 Adsorptive Desulfurization Fundamentals

ADS is based on the ability of a solid adsorbent to selectively adsorb organosulfur compounds from fuel streams [Babich and Moulijn, 2003; Muzica et al., 2010].Adsorption occurs when the sulfur molecules attach to the adsorbent and remain there separate from the fuel. On the basis of interaction of the sulfur compounds with the adsorbent, ADS can be divided into two groups: 'adsorptive desulfurization' and 'reactive adsorption desulfurization'. Regeneration of the adsorbent is usually done by flushing the spent adsorbent with a desorbent, resulting in a high organosulfur compound concentration flow. Reactive adsorption desulfurization employs chemical interaction of the organosulfur compounds and the adsorbent. Efficiency of the desulfurization is mainly determined by the adsorbent properties: its adsorption capacity, selectivity for the organosulfur compounds, durability and regenerability.

Many porous materials have been investigated as adsorbents for removing organic sulfur compounds from model solutions or actual fuels; mesoporous SBA-15 [McKinley and Angelici, 2003], activated carbon [Salem, 1994; Jiang et al., 2003], silica gel [Ma et al., 2002], magnetic alumina [Shan et al., 2004], microporous zeolites [Salem, 1994; Velu et al., 2003; Hernandez-Maldonado and Yang, 2003a, b; Hernandez-Maldonado et al., 2005; Xue et al., 2005], and other materials [Mikhail et al., 2002]. Other then these types of porous materials, zirconia has also been found to be one of the effective adsorbents for sulfur removal [Baeza et al., 2008]. The key challenge of this approach is the development of adsorbents with high adsorption capacities and selectivities for sulfur compounds over other aromatic and olefinic compounds.

Table 2.1 compares the various types of studies as reported in literature for ADS. Salem and Hamid [1994, 1997] studied ADS for removing sulfur from naphtha with a 550 ppm initial sulfur level in a batch reactor using activated carbon (AC),

zeolite 5A, and zeolite 13X as solid adsorbents. AC showed the highest capacity, but a low level of sulfur removal. Zeolite 13X was superior for sulfur removal from low sulfur streams at room temperature. AC, zeolites, CoMo catalysts, and silica–alumina adsorbents were tested for adsorptive desulfurization of a mid-distillate stream with 1200 ppm sulfur in a fixed bed reactor [Savage et al., US Patent 5, 454, 933]. The process was specially aimed at the elimination of refractory 4- and 4, 6-substituted dibenzothiophenes which are pre-dominantly present in the feed after hydro treatment. AC was claimed to possess good desulfurization performance at 373 K for 75 min. Regeneration of the adsorbent is usually done by flushing the spent adsorbent with a desorbent, resulting in a high organosulfur compound concentration flow. Reactive ADS employs chemical interaction of the organosulfur compounds and the adsorbent. Sulfur got fixed in the adsorbent, usually as sulfide, and the sulfur free hydrocarbon got released into the purified fuel stream. Regeneration of the spent adsorbent resulted in sulfur elimination as $H_2S$, S, or $SO_x$, depending on the process applied.

An adsorption-based desulfurization technology called IRVAD (combination of the inventor name 'IRVine' and 'ADsorption') was developed by Black and Veatch Pritchard engineering company and claimed to be a low-cost process for making low-sulfur gasoline [Irvine, 1998; Irvine et al., 1999]. The process uses an alumina-based adsorbent to counter-currently contact liquid hydrocarbon in a multistage absorber. The adsorbent is regenerated in a continuous cross-flow reactivator using heated reactivation gas. The process operates at lower pressure, does not consume $H_2$ or saturate olefins [Babich and Moulijn, 2003]. However, since it is based on polarity, it is not expected to be very selective towards sulfur compounds in liquid fuels such as gasoline, diesel fuels and jet fuels. Work on the IRVAD process is currently discontinued [Babich and Moulijn, 2003].

In the ADS, organosulfur compounds are only concentrated. Additional downstream treatment, preferably high-pressure hydrotreating, is required to eliminate sulfur. Efficiency of the process can be increased by optimizing the adsorbent properties in order to improve hydrocarbon recovery during the reactivation treatment. Some of the operating parameters, such as adsorbent particle size, number of adsorption–reactivation steps, weight ratio of the hydrocarbon feed to the adsorbent, appropriate adsorption, and reactivation temperature, must also be optimized before commercial application is possible.

**Table 2.1 Comparative studies of various adsorbents applied for different desulfurization process.**

| Adsorbent | Adsorbate | Applications | References |
|---|---|---|---|
| Mesoporous carbon | Petroleum fuels | ▪ Mesoporous carbon, CMK-3, was prepared using hexagonal Al-SBA-15 mesoporous silica, instead of SBA-15, as a template.<br>▪ The performance of this adsorbent was compared with SBA-15 and Al-SBA-15, through which CMK-3 showed higher sulfur adsorption capabilities due to a larger mesopore volume and a higher specific surface area.<br>▪ The uptake capacity for DBT followed the order CMK-3 > Al-SBA-15 > SBA-15.<br>▪ Langmuir and Freundlich isotherm models were used to fit equilibrium data for CMK-3. The equilibrium data were best represented by the Langmuir isotherm. Kinetic studies were carried out and showed the sorption kinetics of dibenzothiophene was best described by a pseudo-second-order kinetic model. | [Anbia and Parvin, 2011] |
| Activated carbons | real and model diesels | ▪ Adsorptive affinity of PASHs and PAHs on activated carbons and the effect of PAHs on the adsorption performance of PASHs were studied.<br>▪ The adsorption results showed that adsorptive affinities of molecules with polycyclic aromatic skeleton structure are primarily governed by the π- π dispersive interaction between the aromatic rings and the grapheme layers of activated carbons.<br>▪ The adsorption capacity of PASHs decreases significantly in the presence of PAHs as result of the adsorption competition due to similar structure, molecular diameter and adsorption mechanisms. | [Bu et al., 2011] |

| Adsorbent | Adsorbate | Applications | References |
|---|---|---|---|
| Ag/Titania sorbent | n-octane | ▪ Adsorption, desorption and structure of the surface chemical compounds formed upon interaction of DBT in solution of n-octane with the sulfur-selective Ag/Titania sorbent for the ultradeep desulfurization of liquid fuels was characterized by the temperature-programmed XPS and ESR.<br>▪ Adsorption of DBT proceeds via chemisorption via the oxygen-containing surface groups. Desorption of DBT and thermal regeneration of the "spent" Ag/Titania were studied by the complementary temperature-programmed XPS and ESR from 25 to 525$^{o}$C, in the high vacuum vs. air. The XPS spectrum of the pure DBT is reported for the first time. | [Samokhvalova et al., 2011] |
| Activated carbon fiber and a granular coconut-shell activated carbon | mixture of ndecane and toluene | ▪ The adsorption behavior of DBT on an ACF)and a GCSAC in the solvents n-hexane, n-decane, toluene, and mixture of n-decane and toluene was investigated.<br>▪ At low equilibrium concentrations of < 2 mass ppm-S, GCSAC displayed greater capacity for DBT adsorption than did ACF in all the tested solvents.<br>▪ The adsorption kinetics of ACF and GCSAC in all the tested solvents were governed by a pseudo-second-order model. | [Kumagai et al., 2010] |
| Ni-loaded mesoporous molecular sieve | Ultra low sulfur diesel | ▪ High-performance nickel-based sorbent was developed by loading nickel on a mesoporous molecular sieve, MCM-48, for ADS of commercial ULSD for fuel cell applications.<br>▪ Effects of the ultrasonic aid in incipient wetness impregnation (IWI), nickel loading amount and support materials on the sorbent performance were examined.<br>▪ Using MCM-48 as a support with 20 wt% nickel loading (Ni20/MCM-48) can lead to an excellent nickel-based sorbent with a breakthrough capacity of 2.1mg-S/g-sorb for ADS of the ULSD at a breakthrough sulfur level of 1ppmw. | [Sentorun-Shalaby et al., 2010] |

| Adsorbent | Adsorbate | Applications | References |
|---|---|---|---|
| Activated carbon | Straight run gas Oil ; DBT in n-octane | ▪ The highest total capacity for adsorption of sulfur and nitrogen species as 0.098 g sulfur and 0.039 g nitrogen per 1 g of the activated carbon, respectively, among the carbon materials examined.<br>▪ Removal of both nitrogen and sulfur species was found very effective to achieve UD-HDS under conventional HDS conditions.<br>▪ SRGO treated over activated carbon contained only 11 ppm of sulfur, while non-treated SRGO contained still 193 ppm of sulfur in its HDS product. | [Sano et al., 2004; Zhou et al., 2009] |
| Polymer-derived carbons | Simulated diesel | ▪ The surface features of the carbons were evaluated using adsorption of nitrogen, potentiometric titration, Boehm titration, thermal analysis and FTIR.<br>▪ The results suggest that the amount adsorbed is mainly governed by the volume of micropores, where dispersive interactions are predominant.<br>▪ Acidic groups located in larger pores are also important to attract additional molecules DBT and 4, 6-DMDBT via specific interactions with the progress of adsorption. | [Seredych et al., 2009] |
| Activated C and Ni Supported System | Gas Oil | ▪ The modified activated carbon samples showed better adsorption capacity when compared with that of activated carbon samples and metal supported systems. | [Selvavathi et al., 2009] |
| Activated carbon produced from dates' stones and activated by $ZnCl_2$ | DBT in n-decane | ▪ Textural characteristics of GAC were determined by nitrogen adsorption at 77 K along with application of BET equation for determination of surface area.<br>▪ Pore size distribution and pore volumes were computed from $N_2$ adsorption data by applying the nonlinear density function theory (NLDFT).<br>▪ More than 86% of DBT is adsorbed in the first 3 h which gradually increases to 92.6% in 48 h and no more sulfur is removed thereafter. | [Yahia et al., 2009] |

| Adsorbent | Adsorbate | Applications | References |
|---|---|---|---|
| | | ▪ The efficiency of sulfur removal by GAC is reduced when applied to commercial diesel fuel.<br>▪ Linear regression of experimental data was able to predict the critical pore diameter for DBT adsorption (0.8 nm) and validating the reported impact of average pore diameter of activated carbon on the adsorption capacity. | |
| Rice husk activated carbon. | Kerosene | ▪ Rice husk activated at 1123 K for 1 h showed an acceptable adsorption capacity for DBTs, despite a much lower specific surface area (473 $m^2/g$) and total pore volume (0.267 $cm^3/g$), when compared to micro-porous activated carbon fiber with a large specific surface area (2336 $m^2/g$) and total pore volume (1.052 $cm^3/g$).<br>▪ The volumes of ultra micropores acting as DBTs adsorption sites and of mesopores leading DBTs into the ultra micropores were closely related to the DBTs adsorption capacity of the RHACs. | [Kumagai et al., 2009] |
| Thermally oxidized activated carbon | Model diesel fuel | ▪ The effect of thermal oxidation of activated carbon (AC) on adsorption capacity of dibenzothiophene (DBT) was investigated.<br>▪ Thermal oxidation was done at different temperature 473, 573 and 673K.<br>▪ The oxygen functional groups on the surfaces were determined separately by DRFTIR spectroscopy and Boehm titration.<br>▪ Thermal oxidation reduced its total basicity, while total acidity was increased. | [Yu et al., 2009] |
| 13X Type Zeolite | Commercial diesel | ▪ Kinetic characterization of the adsorption process was performed applying Lagergren's pseudo-first order, pseudo-second order and intra-particle diffusion models.<br>▪ Statistical analysis involved the calculation of effects of individual parameters and their interactions on sulfur adsorption and the development of statistical models of the process. | [Muzic et al., 2009] |

| Adsorbent | Adsorbate | Applications | References |
|---|---|---|---|
| Ag-MAS, Ag-MCM-41, Ag-Y | DBT and Naphthalene in i-octane | ▪ The adsorption was operated at 303 K with equilibrium method. The ratio of oil to adsorbent was chosen as 100 ml/g.<br>▪ Adsorption properties of Ag-MAS, Ag-MCM-41, and Ag-Y were tested with hydrotreated diesel at 303 K, Ratio of adsorbents to oil is 20 ml/g; Surface area measured by BET Method and was found as 940, 906, 647 for MCM 41,MAS and NaY,respectively | [Wang et al., 2009] |
| Activated alumina | DBT in n-hexane | ▪ Sulfur species were adsorptively removed.<br>▪ The BET surface area of alumina was found to decrease from 143.6 to 66.4$m^2$/g after the loading of DBT at optimum conditions.<br>▪ The carbon-oxygen functional groups present on the surface of alumina were found to be effective in the adsorption of DBT onto alumina. Optimum adsorbent dose was found to be 20 g/l.<br>▪ Langmuir isotherm best represented the equilibrium adsorption data. The heat of adsorption and change in entropy for DBT adsorption onto alumina was found to be 19.5 kJ/mol and 139.2 kJ/mol K, respectively. | [Srivastav & Srivastava, 2009] |
| Ni loading on silica–alumina and Activated carbon | Model diesel oil | ▪ The sorbents carrying 45% and 30% of Ni on Si-Al showed a breakthrough uptake capacity of nearly, respectively, 2 and 2.6 times higher than SudChemie sorbent as a consequence of their higher Ni dispersion and surface area; Activated carbons and the sample with 28%Ni on AC showed even higher breakthrough uptake capacities. | [Hernandez et al., 2009] |
| Molecular sieve | Kerosene | ▪ Sulfur species were adsorptively removed; The proposed method, combines selective photooxidation of highly reactive S compounds and adsorptive desulfurization of reactive and non-reactive sulfur compounds in kerosene; Non-reactive sulfur compounds DBTs were removed by adsorbents such as MS and GAC. | [Tao et al., 2009] |
| Ni loading supported on silica–alumina and activated carbon | A model diesel oil | ▪ Sulfur species were adsorptively removed.<br>▪ The influence on adsorbents uptake capacity of the presence of aromatics in amounts representative of real diesel oils was studied. | [Hernandez et al., 2009] |

| Adsorbent | Adsorbate | Applications | References |
|---|---|---|---|
| | | The sorbents carrying 45% and 30% of Ni on Si Al showed a breakthrough uptake capacity of nearly, respectively, 2 and 2.6 times higher than SudChemie sorbent as a consequence of their higher Ni dispersion and surface area. The activated carbons and the sample with 28%Ni on AC showed an even higher breakthrough uptake capacity.<br>▪ In particular, the deposition of nickel on activated carbon is an innovative approach which takes advantage of the selectivity of Ni towards S-species and the high adsorptive capacity of AC support. | |
| Polystyrene-based activated carbon spheres | DBT in n-heptane | ▪ Sulfur species were adsorptively removed.<br>The textural structure was characterized by SEM, $N_2$ adsorption, TG and aqueous adsorption.<br>▪ Results show that the adsorbent with BET surface areas up to 979-1672 $m^2/g$ were obtained. The maximum adsorption capacity of PACS to DBT was 109.36 mg/g and the adsorption capacity was related to the volume of narrow micropores, independent of surface area/total pore volume. Irreversible adsorption existed between DBT and adsorbent.. | [Qin et al., 2009] |
| Na-Y and AgNa-Y zeolites | Tetrahydrothiophene | ▪ Chemical composition of the prepared samples was analyzed by an ICP-AES and the results were used to calculate the level of $Ag^+$-exchange with $Na^+$.<br>▪ Experiment was performed at atmospheric pressure using vertically placed tubular fixed bed glass reactors (i.d. = 9 mm).<br>▪ All the adsorption experiments were conducted in the absence of water vapor.<br>▪ The flow rate of the feeds was fixed at 55 $cm^3$/ min (NTP). | [Lee et al., 2008] |
| Zinc titanate | $H_2S$ from fuel gas | ▪ Sulfur species were adsorptively removed.<br>▪ The effect of the reactant gas composition and concentration and reaction temperature on the sulfidation and regeneration behavior of the $Zn_2TiO_4$ sorbent was investigated with a fixed bed reactor and a TG analyzer. | [Huang et al., 2008b] |

| Adsorbent | Adsorbate | Applications | References |
|---|---|---|---|
| | | The unreacted shrinking core model can be used to correlate with the experimental data.<br>▪ The regeneration is controlled by the chemical reaction in the early stage of reaction and by the diffusion through the product layer at the latter stage | |
| Cu supported on zirconia | Thiophene in n-octane | ▪ Sulfur species were adsorptively removed.<br>▪ The capacity of Cu on zirconia to adsorb thiophene increases as the copper content increases, reaching a maximum at a concentration of 3% of copper.<br>▪ The adsorption capacity also depends on the treatment used, and the higher capacities are observed in adsorbents treated with a flow of $N_2O$ at 363 K. | [Baeza et al., 2008] |
| Metallic Ni nanoparticles supported on mesoporous silica (SBA-15 and KIT-6 by impregnation) | Commercial diesel | ▪ Sulfur species were adsorptively removed; The best adsorption capacity observed was 1.7 mg/g at 10mg/l S breakthrough level with a high sulfur diesel (240 ppmw) on 30 wt% Ni/SBA-15; for a low sulfur diesel (11.7 mg/l), the corresponding result was 0.47 mg/g for the same adsorbent at 0.1 mg/l S breakthrough level, which is suitable for fuel cell applications. | [Park et al., 2008] |
| CuCl/MCM-41, $PdCl_2$/MCM-41, CuCl/SBA-15 and $PdCl_2$/SBA-15 | JP-5 light fraction as fuel. | ▪ Desulfurization was achieved by π-complexation adsorption with $CuCl_2$ and $PdCl_2$ supported on the MCM-41 and SBA-15 mesoporous materials at room temprature.<br>▪ The spent $PdCl_2$/SBA-15 was regenerated by purge with benzene at 343 K, and the regenerated $PdCl_2$/SBA-15 was tested again for the desulfurization. | [Wang et al., 2008] |
| Zeolites | Thiophene and BT in n-hexane solution | ▪ Adsorption capacity of our developed zeolites was compared to those of commercial zeolites, i.e. NaY, HUSY, beta, and ZSM-5 obtained via the conventional synthesis methods.<br>▪ The results suggested a potential of zeolites derived from Mae Moh coal fly ash for removal of refractory sulfur compounds, such as benzothiophene | [Ngamcharussrivichai et al., 2008] |

| Adsorbent | Adsorbate | Applications | References |
|---|---|---|---|
| Cu(I)Y Zeolite | Gasoline and diesel fuel | ▪ The adsorption mechanisms in deep denitrogenation of gasoline and diesel fuels and the effect of nitrogen compounds on desulfurization by the density functional theory (DFT) method.<br>▪ The $\eta^2$ adsorption mode has been found to be energetically preferred for neutral $N_2$ compounds, i.e. indole and carbazole; while for basic ones, quinoline/acridine, the $\eta^1$-N adsorption mode is the most preferential one, implying that in the competitive adsorption aromatics show a strong preference over neutral nitrogen compounds than over basic ones.<br>▪ Deep denitrogenation and desulfurization could be carried out simultaneously over Cu(I)Y zeolite under ambient temperature, while for Cu(I)Y zeolite the adsorption of nitrogen compounds is preferable to that of sulfur compounds, and good selectivity will be shown for the basic nitrogen compounds during denitrogenation | [Liu et al., 2008] |
| Modified C derived from the recycled PET | DBT in n-hexane | ▪ Sulfur species were adsorptively removed.<br>▪ The adsorption of DBT is governed by two types of contributions: physisorption on the microporous network of the carbons and chemisorption; Introduction of surface acidic groups enhanced the performance of the carbons as a result of their specific interactions with DBT; The nature of the acidic groups is a decisive factor in the selectivity of the reactive adsorption process. | [Ania et al., 2007] |
| PDMS–AgY Zeolite Mixed Membrane | Thiophene & 2-methylthiophene mixture of n-octane | ▪ Attributed to the Knudsen diffusion of the feed species in the macro-and meso-pores existing in AgY zeolite.<br>▪ The difference between enrichment factors of non-filled and filled membranes become unapparent when the temperature increases, implying that a kinetic barrier in the sorption and desorption process on the surface or within the pores of AgY zeolites might exist. | [Qi et al., 2007] |

| Adsorbent | Adsorbate | Applications | References |
|---|---|---|---|
| | | ▪ Experimental points of AgY-filled PDMS membranes locate above the upper bound curve of pure PDMS membranes for separation of *n*-octane/thiophenes, indicating that higher permeability was gained with little expense of selectivity using PDMS–AgY zeolite mixed matrix membranes. | |
| NaX Zeolite | n-heptane, 1-octene and xylenes and their mixtures | ▪ Competitive adsorption from xylenes reduced adsorption capacity for thiophene from mixtures containing large concentration of xylenes.<br>▪ Langmuir model is applied to describe observed competitive adsorption.<br>▪ Selective adsorption of organic sulfur compound could be used as a polishing step in a purification scheme which allows sulfur removal from hydrocarbons at low temperature and without the use of expensive hydrogen. | [Reut and Prakash, 2006] |
| La(III)-exchanged NaY Zeolite | | ▪ IR spectra of thiophene adsorption indicate that thiophene is adsorbed onto La(III) via direct S–La(III) interaction and Na(I) ions via $\pi$-electronic interaction for La(III) exchanged zeolite NaY, but only via $\pi$-electronic interaction with Na+ ions for NaY.<br>▪ The amount of adsorbed thiophene on La(III) exchanged zeolite Y was slightly decreased by co-adsorption of benzene, but greatly reduced on NaY. The adsorption of thiophene via interaction with La(III) on La(III)-exchanged zeolite Y is hardly replaced by benzene co-adsorption. | [Tian et al., 2006] |
| Cu(I) Y Zeolite | Thiophene in 80% n-octane + 20% benzene | ▪ Oxygenates (i.e. ethanol and MTBE as required additives in gasoline) and moisture were found to have strong inhibiting effects on desulfurization by adsorption with zeolite.<br>▪ Ab initio molecular orbital calculations showed that the adsorption bond energies with Cu(I)Y were: 21.4 kcal/mol for thiophene; 31.0 kcal/mol for MTBE and 41.6 kcal/mol for ethanol. | [Li et al., 2006] |

| Adsorbent | Adsorbate | Applications | References |
|---|---|---|---|
| | | ▪ In addition, the desulfurization capacity was strongly dependent on the liquid hourly space velocity because of the diffusion limitation of thiophene in the zeolite crystals. | |
| Activated carbon, Activated alumina and Ni based adsorbent | Model diesel | ▪ Adsorptive desulfurization and denitrogenation were studied.<br>▪ A fixed-bed adsorption system was used.<br>▪ The adsorptive capacity and selectivity for the various compounds were examined and compared on the basis of the breakthrough curves.<br>▪ The electronic properties of the adsorbates were calculated by a semi-empirical quantum chemical method and compared with their adsorption selectivity.<br>▪ For Ni-based adsorbent direct interaction between the heteroatom in the adsorbate and the surface nickel played an important role.<br>▪ The adsorption selectivity on the activated alumina depends dominantly on the molecular electrostatic potential and the acidic–basic interaction.<br>▪ The activated carbon shows higher adsorptive capacity and selectivity for both sulfur and nitrogen compounds, especially for the sulfur compounds with methyl substituents, such as 4,6-MDBT. | [Kim et al., 2006] |
| MnO blended with activated bentonite, in addition to Ni-W/kaolinite | DMDS in cyclohexane solution. | ▪ The morphological and structural changes of the different materials were investigated via surface area, XRD, and SEM.<br>▪ The results indicated that the sorbent containing zinc–chromium iron oxides was the most active one towards desulfurization, where DMDS removal reached ~58% compared with the other prepared sorbents.<br>▪ This activity was related to the ferromagnetic properties of both chromium and iron oxides. | [Zaki et al., 2005] |

| Adsorbent | Adsorbate | Applications | References |
|---|---|---|---|
| Faujasite type zeolites with Cu(I), Ni(II), Zn(II) cations | Diesel, gasoline, and jet fuels | ▪ The sorbents were obtained by ion exchanging using different techniques, including liquid phase ion exchange (LPIE).<br>▪ Hydrolysis of the cations in aqueous solutions should be avoided in order to increase the ion exchange level when aqueous solutions are used.<br>▪ The deep-desulfurization (sulfur levels of <1 ppmw) tests were performed using fixed-bed adsorption techniques.<br>▪ Molecular orbital calculations indicate the sorbents performance decreases as follows: Cu(I) > Ni(II) > Zn(II).<br>▪ The best sorbent, Cu(I)-Y(VPIE), has breakthrough adsorption capacities of 0.395 and 0.278 mmol S/g of sorbent for commercial jet fuel (364.1 ppmw S) and diesel (297.2 ppmw S), respectively. | [Hernandez-Maldonado et al., 2005] |
| Acid-activated kaolinite, acid-activated bentonite, charcoal, petroleum coke and cement kiln dust. | DMDS in cyclohexane | ▪ An economically attractive alternative method for desulfurization of petroleum fraction.<br>▪ The acid-activated bentonite was found to be the most suitable adsorbent studied, at the lowest reaction temperature 303 K.<br>▪ The higher efficiency of the activated-clay towards sulfur adsorption may be attributed to that, the silicate–silicate bentonite structure possesses Brönsted acid sites, which resulted from the dissociation of the water molecule in between silicate sheets.<br>▪ In addition, the clay surface, after acid treatment would possess positive hydrogen sites. Therefore, the increase in acid sites, disturbs the charge equilibrium in the bentonite-clay lattice, creates strain that arises new active sites for adsorption, which would interact more favorably with the basic sulfur compounds. | [Mikhail et al., 2002] |

### 2.2.2 Oxidative Desulfurization Fundamentals

New processes capable of a higher desulfurization efficiency to produce low sulfur fuels are being developed. In particular, the oxidative desulfurization (ODS) appears very promising and is currently receiving growing attention.

In ODS, the sulfur containing compounds is oxidized to sulfone by chemical reaction using an oxidant viz. organic peroxides, $H_2O_2$, $H_2SO_4$, etc. The utilization of $H_2O_2$ as an oxidizing agent during oxidative desulfurization received significant attention [Strukul, 2003; Kaczorowska et al., 2005; Jones et al., 1999], owing to its high effective-oxygen content, cleanliness (it produces only water as by-product; when water accumulation is not desired it can be removed by extraction or other process [Ramırez-Verduzco et al., 2004]), and acceptable safety in storage and operation. Homogeneous [Strukul, 2003] and heterogeneous catalysis [Ratnasamy et al., 2004; Ziolek , 2004; Roger et al., 1994; Sheldon et al., 1998] application can be regarded for $H_2O_2$ due to its inherent property as a soft oxidizing agent.

In catalytic ODS, the divalent sulfur of DBT can be oxidized first to DBTO (mono-sulfoxide) and finally to $DBTO_2$ (di-sulfoxide) by the electrophilic addition reaction of oxygen atoms to the hexavalent sulfur of sulfones [Di-shun et al., 2009].

These sulfones are highly polarized compounds having significantly different chemical and physical properties from those of hydrocarbon in fuel oil, such that they can easily removed by subsequent solvent extraction using water-soluble polar solvents, such as NMP, DMF, DMSO and MeOH, etc. [Rappas, US Patents US 6, 402, 940; US 6, 406, 616, Wachs WO 03/051798], distillation, adsorption and decomposition. By combination of the processes, the sulfur content of the diesel can be reduced to $\leq 50$ ppm [Sampanthar et al., Patent Application PCT/SG2004/00016016].

The ODS process is usually carried out under mild conditions which present competitiveness over the conventional HDS process [Rappas, US Patents US 6, 402, 940; US 6, 406, 616, Wachs WO 03/051798]. One of the main advantages of the ODS is that the most refractory sulfur compounds (e.g. alkylated dibenzothiophenes) show a higher reactivity than that of HDS in which expensive hydrogen is used. The reactivities of the compounds seem to correlate well with their electronic density except with the 4, 6-dimetyl dibenzothiophene [Li et al., 2003].

Various studies on the ODS process have reported the use of differing oxidizing agents and catalysts, such as $H_2O_2$/acetic acid [Fairbridge et al., 2001] and $H_2O_2$/formic acid [Tam et al., 1990], $H_2O_2$/heteropolyacids [Collins et al., 1997; Yazu et al., 2001], $H_2O_2$/inorganic solid acids [Ramirez-Verduzco et al., 2004], $NO_2$/heterogeneous catalysts [US Patent 4, 493, 765], ozone/heterogeneous catalysts [Nonaka et al., 1999], tert-butylperoxides/heterogeneous catalysts [Sughrue et al., US Patent Application 20, 040, 007, 50] and $O_2$/aldehyde/cobalt catalysts [Murata et al., 2004].

Wang et al. [2003] studied the oxidation of sulfur compounds in kerosene with *tert*-butyl hydroperoxide (*t*-BuOOH) in the presence of various catalysts. The oxidation activities of DBT in kerosene for a series of Mo catalysts supported on $Al_2O_3$ with various Mo contents were estimated. The results show that the oxidation activity of DBT increased with increasing Mo content up to about 16 w% and decreased when Mo content was beyond this value. The oxidation of BT, DBT, 4-MDBT and 4, 6-DMDBT dissolved in decaline was also carried out on 16 w% Mo/$Al_2O_3$ catalyst with *t*-BuOOH to investigate the oxidation reactivities of these sulfur compounds. The results indicated that the oxidation reactivities of these sulfur compounds decreased in the order of DBT > 4-MDBT > 4,6-DMDBT > BT. Analyses of the oxidative reactions of the sulfur compounds suggested that the oxidative reaction of each sulfur compound can be treated as a first-order reaction.

The oxidation of sulfur-containing compounds in diesel was conducted by Lu et al. [2006], in emulsion oxidative system composed of diesel, 30 wt% $H_2O_2$, and an amphiphilic catalyst $[C_{18}H_{37}N(CH_3)_3]_4$-$[H_2NaPW_{10}O_{36}]$ under mild conditions. The amphiphilic catalyst exhibits very high catalytic activity such that all sulfur-containing compounds in either model or actual diesel can be selectively oxidized into their corresponding sulfones using $H_2O_2$ as an oxidant. The catalytic oxidation reactivity of sulfur-containing compounds was found to be in the following order: BT < 5-MBT < DBT < 4, 6-DMDBT.

Table 2.2 shows the comparison of various types of studies as reported in literature for catalysts based desulfurization processes.

**Table 2.2 Various types of catalysts based desulfurization processes.**

| Catalyst | Process | Target | Application | References |
|---|---|---|---|---|
| polyoxotungstate emulsion catalysts | Oxidative desulfurization | S compound in decalin | ▪ The Dawson-type polyoxotungstate emulsion catalysts Q18P2W18, Q18P2W17, and Q18P2W12 were successfully synthesized and characterized by IR and 31P MAS NMR.<br>▪ used for the oxidation of sulfur-containing compounds such as 4,6-DMDBT, DBT, BT, and 2,5-DMT with $H_2O_2$ as an oxidant under mild conditions. | [Yongna et al., 2011] |
| Hexagonal mesoporous silicate | Oxidative desulfurization | model oil | ▪ Well-ordered HMS materials with various contents of HPW were synthesized via an original direct synthesis method.<br>▪ Compared with the conventional wet impregnation method, the samples obtained by the original direct synthesis method have better HPW dispersion and larger specific surface area.<br>▪ | [Li et al., 2011] |
| Granular activated carbon | Oxidative desulfurization | commercial Malaysian diesel | ▪ The development of granular functionalized-activated carbon as catalysts in the catalytic oxidative desulfurization (Cat-ODS) of commercial Malaysian diesel using hydrogen peroxide as oxidant.<br>▪ Granular functionalized-activated carbon was prepared from oil palm shell using phosphoric acid activation method and carbonized at 500°C and 700°C for 1 h.<br>▪ The rates of the catalytic oxidative desulfurization reaction were found to increase with the temperature, and $H_2O_2$/S molar ratio. | [Haw et al., 2010] |

| Catalyst | Process | Target | Application | References |
|---|---|---|---|---|
| Pt-zeolite | Hydrodesulphurization and benzene hydrogenation | DLCO | ▪ The catalysts contained finely dispersed Pt nanoparticles (2–5nm) located on montmorillonite and zeolite surfaces as: $Pt^{o}$ ($\nu_{CO}$ = 2070–2095 $cm^{-1}$), $Pt^{\delta+}$ ($\nu_{CO}$ = 2128 $cm^{-1}$) and $Pt^{2+}$ ($\nu_{CO}$ = 2149–2155 $cm^{-1}$).<br>▪ The catalytic activity in the HDS reaction was evaluated as the rate (WHDS, mol $C_4H_4S$/mol Pt*h) of the pseudo-first-order thiophene HDS reaction.<br>▪ The benzene hydrogenation reaction was studied at 573 K, pressure 20 atm, feed ($C_6H_6 + H_2$) flow rate 10 $cm^3/s$.<br>▪ A U23 pilot plant was used. This plant contains an isothermal fixed bed reactor operating in the up flow mode.<br>▪ The reactor with the catalyst volume of 40ml has an interior diameter of 19 mm and is equipped with an interior thermometric probe. | [Ismagilov et al., 2009] |
| Decatungstates | Oxidative desulfurization | DBT in n-octane | • n(DBT):n(catalyst):n($H_2O_2$) = 1:0.01:3, 333 K for 0.5 h, under which the DBT conversion can reached 99.6% with the catalyst.<br>• The sulfone can be separated from the oil using N, N-dimethylformamide (DMF) as an extractant, and the sulfur content can be lowered from 1000 to 4 ppm.<br>• For real diesel, the sulfur removal can reach 93.5% after five times extraction. | [Jiang et al., 2009] |

| Catalyst | Process | Target | Application | References |
|---|---|---|---|---|
| Sulfuric acid | Oxidative desulfurization | hydro treated diesel oil | ▪ The results showed that the sulfone content in the oxidation product increased rapidly with an increase in acetic acid and sulfuric acid ratios from 1:0 to 2:1 mole ratios.<br>▪ The maximum DBT conversion (w%) was at 2:1 mole ratio of acetic acid/sulfuric acid.<br>▪ Sulfur species in typically hydro treated diesel and ring number distribution in 527–658 K cut are also reported. | [Ali et al., 2009] |
| $VO_x/Al_2O_3$ | Oxidative desulfurization | DBT in acetonitrile | ▪ Reaction was carried out in a batch reactor at 33K.<br>▪ Reaction products analyzed by PONA capillary column. | [Gomez-Bernal et al., 2009] |
| Pt-Zeolite catalysts | Hydrodesulfurization | Thiophene in model fuel | ▪ Data obtained by HRTEM, XPS, EXAFS and FTIR Spectroscopy.<br>▪ The catalysts contained finely dispersed Pt nanoparticles (2–5 nm) located on montmorillonite and zeolite surfaces. It was shown that the state of Pt depended on the Si/Al zeolite ratio, montmorillonite presence and Pt precursor. | [Zinfer et al., 2009] |
| ZSM-5 zeolite dispersed in a silica matrix | Catalytic oxidation | Thiophene in n-octane mixtures | ▪ Catalytic experiments are carried out in the CREC riser simulator under mild conditions.<br>▪ The experimental results obtained shows that thiophene conversion proceeds via ring opening and alkylation yielding $H_2S$, alkyl-thiophenes, benzothiophene, and coke, with no measurable thiophene saturation or dimerization reactions observed. The experimental results are also supported with an extensive thermodynamic. | [Jaimes et al., 2009] |

| Catalyst | Process | Target | Application | References |
|---|---|---|---|---|
| Mo and/or V oxides supported on alumina pellets | Oxidative desulfurization | Commercial diesel fuel | • Oxidative desulfurization using tert-butyl hydroperoxide (TBHP)/ $H_2O_2$ as oxidant.<br>• The performance of the catalysts was discussed in terms of reduced species of vanadium oxide, prevailing on the catalysts, which increase the sulfone yield of refractory Hydrodesulfurization compounds (DBT, 4-MDBT and 4,6-DMDBT). | [Gonza lez-Garcıa et al., 2009] |
| Molecular sieve | Catalytic desulfurization | | • A new reaction pathway was discovered and investigated using C-13 NMR, GC, GC-MS, HPLC, ion chromatography, and XANES.<br>• The thiophene oxidized to thiophene-sesquioxide [3a,4,7,7a-tetrahydro-4,7-epithiobenzo[b]-thiophene 1,1.8-trioxide] and the sesquioxide oxidized mostly to sulfate. 2-Methyl-thiophene and 2, 5 dimethylthiophene also oxidized to sulfate and sulfone products. | [Nemeth et al., 2008] |
| Ni compounds: $[Ni(dippe)H]_2$, $[Ni(dcype)H]_2$, $[Ni(dtbpe)H]_2$, $NiCl_2{\cdot}6H_2O$, $[Ni(dippe)(Me)_2]$ | Deoxy-desulfurization | Model Fuel Oil | • Catalysts reacted with MeMgBr to yield the straightforward deoxydesulfurization of sulfones of dibenzothiophene (DBTO2), 4-methyl-dibenzothiophene (MeDBTO2) and 4,6-dimethyldibenzothiophene (Me2DBTO2), thereof producing the corresponding sulfur-free biphenyls (85–100% yield) when using a solvent mixture of toluene–THF, 10:2 v/v. | [Oviedo et al., 2008] |
| silica-supported 12-phosphotungstic (HPW) and 12-silicotungstic (HSiW) acids | Hydrodesulfurization | FCC Feed | • Stirred slurry tank reactor was used.<br>• Deactivation was measured in a continuous trickle bed reactor (micro-pilot), using the same feed composition at a spatial velocity of 74 $h^{-1}$, 358 K under 0,01 MPa. | [Arias et al., 2008] |

| Catalyst | Process | Target | Application | References |
|---|---|---|---|---|
| $Fe^{2+}/H_2O_2$/Acid System. | Oxidative desulfurization + Fenton's reagent system both without/with ultrasound | Hydrotreated Middle East diesel fuel as a feedstock | • The mixture system (Feed + reagents is irradiated by ultrasound under different powers at 300 K or 313 K.<br>• An ultrasound apparatus with ultrasonic frequency 28 kHz is home made; its ultrasonic powers can be changed between 50 W to 200 W.<br>• reaction mechanics fitted apparent first-order kinetics.<br>• best operating condition for Oxidative desulfurization : temperature 313 K, ultrasonic power 200 W, ultrasonic frequency 28 kHz, $Fe^{2+}/H_2O_2$ 0.05 mol/mol, pH 2.10 in aqueous phase and reaction time 15min, the sulfur content in the diesel. fuels was decreased from 568.75 μg/g to 9.50 μg/g. | [Daia et al., 2008] |
| Ti-Beta Catalysts | Catalytic oxidation | Oxidation of 1-hexene | • Synthesized by different procedures and characterized by XRD, SEM, DRS in the UV-Vis region, and XPS.<br>• The Ti and Al content and the distribution of both elements along the crystallites of Ti-Beta was seen to affect the intrinsic activity of the Ti.<br>• The simultaneous presence of Al and Ti in the same crystal region reduces the intrinsic activity of titanium for the oxidation reaction.<br>• It was found that the intrinsic activity of the Ti atom in Ti-Beta is lower than in TS-1. | [Camblor et al., 2008] |

| Catalyst | Process | Target | Application | References |
|---|---|---|---|---|
| $Mo/\gamma\text{-}Al_2O_3$ | Oxidative desulfurization | Commercial Mexican diesel fuel | • The results showed that the activity for sulfur elimination depends mainly on the presence of hepta-and octamolybdates species on the catalyst support and the use of a polar aprotic solvent; The $H_2O_2$/sulfur molar ratio was about 11; on the basis of the results obtained a mechanistic proposal for this reaction is described, as an oxidation mechanism by nucleophilic attack of the sulfur atom on peroxo species of hepta-and octamolybdates, but a mechanism involving the singlet oxygen presence can be discarded. | [Garcıa-Gutierrez et al., 2008] |
| $TiO_2$-Phosphotungstic acid. | Oxidative desulfurization | DBT in n-octane | • The calcined mesoporous $TiO_2$ materials by STAB were characterized by XRF, XRD, FTIR TEM and $N_2$ adsorption/desorption measurements; The $N_2$ adsorption/desorption isotherms exhibit the characteristics of mesoporous structure; TEM results indicate that the disordered wormhole-like mesostructure without discernible long-range order is formed by the agglomerization of $TiO_2$ nanoparticles.<br>• The $TiO_2$ materials exhibit good performance in DBT oxidation. | [Huang et al., 2008] |
| HPWA-SBA-15 | Oxidation followed by adsorption for desulfurization | DBT in i-octane | • Catalyst characterized by XRD, FTIR, TEM, $^{31}P$-NMR.<br>• Results concluded that HPWA-SBA-15 has both catalytic oxidation ability and adsorption ability.<br>• The non-polar DBT can be converted into polar DBT sulfone that is easily absorbed on HPWA-SBA-15. | [Yang et al., 2007] |

| Catalyst | Process | Target | Application | References |
|---|---|---|---|---|
| | | | • FTIR characterization indicates the existence of intermediate of [O–O] structure in the desulfurization.<br>• Both the $^{31}P$ NMR spectra of HPWA-SBA-15 before and after regeneration and the desulfurization results of these two samples indicated that HPWA-SBA-15 has good regenerating ability. | |
| Sulfided Mo-$\gamma$ -$Al_2O_3$, Ni-Mo-$\gamma$ -$Al_2O_3$ | HDS | | • The rate constants of all steps in the kinetic network of the HDS of DMDBT could be measured over Mo/$\gamma$ -Al2O3, and those of some steps could be measured over NiMo/$\gamma$ -$Al_2O_3$.<br>• Before the reaction, the catalysts were activated by in situ sulfidation with a mixture of 10% $H_2S$ in $H_2$ (50 ml/min) at 673 K and 1 MPa for 4 h.<br>• Opening of the sulfur-containing ring in DMDBT and its hydrogenated intermediates occurs by C–S hydrogenolysis rather than by elimination. | [Li et al., 2007] |
| Activated carbon modified with Ag(I), Cu(II), Ni(II), Zn(II), Fe(III) ions | Temperature programmed studies | - | • Temperature programmed desorption experiments were conducted to measure the TPD curves of DBT on these modified activated carbons, and the desorption activation energy, *E*d, of DBT on the activated carbon surfaces were estimated.<br>• The TPD experiments were conducted respectively at different heating rates from 5 to 10 K/min. | [Yu et al., 2007] |

| Catalyst | Process | Target | Application | References |
|---|---|---|---|---|
| $Co–Mo/Al_2O_3$ | Hydrodesulfurization | Gas oil feed (straight-run gas oil-SRGO and coker gas oil-CGO) | • Higher degree of desulfurization was achieved with reduction of T95 from N 633 K to B 613 K.<br>• The effect of lowering the T95 on deep desulfurization of two gas oil feeds was studied.<br>• A high pressure fixed bed micro-reactor unit by Vinci Technologies, France, was used.<br>• Surface area, 240 $m^2/g$ and pore volume,0.74 ml/g was observed by BET Method. | [Al-Barood et al., 2007] |
| Activated carbon-supported lead dioxide ($\beta$-$PbO_2/C$) was anode and copper pillar was cathode, with electrolyte was aqueous NaOH solution. | Electrochemically catalytic oxidation and extraction | | • An electrochemical fluidized-bed reactor was used for the study.<br>• Results indicated that the optimal desulfurization conditions were as follows: the cell voltage, the pH value of the electrolyte, feed volume flow rate and the $\beta$-$PbO_2$ percentage by weight were 3.2 V, pH value 13.1, 300 ml/min and 5.0 wt.%, respectively; Concentration of sulfur in gasoline was reduced from 310 to 40 μg/g. | [Wang et al., 2007a] |
| Activated carbon-supported ($CeO_2/C$) was anode and copper pillar was cathode, with electrolyte was aqueous cerium nitrate solution solution. | Electrochemically catalytic oxidation and extraction | | • An electrochemical fluidized-bed reactor was used for the study; The $CeO_2/C$ particle group anode could remarkably accelerate the electrochemical reaction rate and promote the electrochemical catalysis performance for the electrochemical desulfurization reaction.<br>• The experimental results indicated that the optimal desulfurization conditions were as follows: the cell voltage, concentration of the Ce(III) ions, feed volume flow rate and the $CeO_2$ percentage by weight were 3.2 V, 0.08 mol/l, 300 ml/min and 5.0wt%, respectively. | [Wang et al., 2007b] |

| Catalyst | Process | Target | Application | References |
|---|---|---|---|---|
| | | | • Concentration of sulfur in gasoline was reduced from 300 to 50 μg/g. | |
| CoMo supported on a Ti-loaded hexagonal mesoporous SBA-15 | Hydrodesulfurization | DBT in decaline | • Experiment carried out in a batch reactor at 623 K and with a total hydrogen pressure of 3.1 MPa.<br>• Under steady-state conditions, the CoMoS-$TiO_2$ catalyst with a Si/Ti ratio of 20 was the most active among the catalysts studied.<br>• The Ti-SBA-15 supports and the CoMo/Ti-SBA-15 catalysts were studied by $N_2$ adsorption–desorption isotherms, XRD, TEM, FTIR of adsorbed pyridine and NO, UV–Vis DRS, TPR, micro-Raman and XPS spectroscopy. | [Nava et al., 2007] |
| $Na_2WO_4$ | Oxidative desulfurization | Diesel | • GC coupled with FID was used to identify the various sulfur compounds and their concentrations in the model solutions.<br>• The $Na_2WO_4$ formed a homogeneous biphasic catalytic system. The role of the acetic acid in this reaction is to increase the dispersion of the catalyst and to promote and stabilize the activation of $H_2O_2$. | [Al-Shahrani et al., 2007] |
| Ti-HMS/TS-1 | Oxidative desulfurization | DBT, BT and Thiophene in n-octane | • The catalytic performances of the composite materials were investigated by means of sulfur compounds oxidation.<br>• UV–visible analysis indicated the existence of framework tetra coordination titanium species Ti(IV).<br>• Composite Ti-HMS/TS-1 exhibits excellent activities in the oxidation of both small and bulky molecular sulfur compounds, which is superior to the pure materials of TS-1 and Ti-HMS. | [Jin et al., 2007] |

| Catalyst | Process | Target | Application | References |
|---|---|---|---|---|
| $[C_{18}H_{37}N(CH_3)_3]_4.$ $[H_2NaPW_{10}O_{36}]$ | Oxidative desulfurization | Commercial Diesel | • Amphiphilic catalyst in the W/O emulsion system exhibits very high catalytic activity. | [Lu et al., 2006] |
| Mn and Co oxide supported on g-$Al_2O_3$ | Oxidative desulfurization | DBT, 4-MDBT, 4, 6-DMDBT, 4, 6-DEDBT in n-tetradecane. | • The sulfones were removed by extraction with polar solvent to reduce the sulfur level in diesel to 40–60 mg/l; The reactions were carried out at a temperature range of 263-453 K, during which air was introduced via a gas disperser at a constant flow rate of 100 ml/min while the reaction mixture was stirred throughout the experiment. | [Jeyagowry et al., 2006] |
| Ti-MCM-41 | Diesel Fuel | T, 2-MT, BT, 2-MBT, DBT, 4-MDBT, 4,6-DMDBT | • A continuous fixed-bed reactor was used.<br>• $MoO_x/Al_2O_3$ catalysts were active, but rapid deactivation occurs due to metal leaching and sulfone adsorption.<br>• Calcined Ti-MCM-41 was more active, did not leach Ti, and deactivated more slowly than $MoO_x/Al_2O_3$ | [Chica et al., 2006] |
| Formic acid and acetic acid | Oxidative desulfurization | DBT in toluene and hexane | • Three experiments using HCl, formic acid and acetic acid were conducted at 323 K.<br>• GC–MS technique was used to identify the sulphones during the oxidation of thiophenes. | [Ali et al., 2006] |
| Sulfided CoMo/ γ-$Al_2O_3$ | Catalytic desulfurization through partial oxidation in SCW. | Model sulfur-containing compound BT | • Investigated in a bomb reactor at 623–723K and 30–40MPa over; VR was used to confirm the desulfurization rate and efficiency, and the desulfurization mechanism of VR determined by the pyrolysis temperature.<br>• The thermodynamic equilibrium of in situ $H_2$ generation was a controlling factor of the desulfurization pathway. | [Yuan et al., 2005] |

| Catalyst | Process | Target | Application | References |
|---|---|---|---|---|
| Activated carbon | Oxidative desulfurization /Adsorptive desulfurization | Commercial diesel fuel | • The effect of carbon surface chemistry on DBT adsorption and catalytic activity was also investigated; Adsorption of DBT shows a strong dependence on carboxylic group content.<br>• The oxidative removal of DBT increases as the surface carbonyl group content increases.<br>• Reaction studied in a batch reactor. | [Yu et al., 2005] |
| $TiO_2$ anatase supported $V_2O_5$ | Oxidative desulfurization | 2-MT, 2,5-DMT, BT, DBT, 4-MDBT, 4,6-DMDBT in hexadecane | • The oxidation was performed through a vanadium based catalyst in the presence of hydrogen peroxide under mild reaction conditions, atmospheric;<br>• Pressure and temperature range of 303–343 K in a batch reactor.<br>• The rate constant at 343 K for DBT oxidation was 0.41 $min^{-1}$ and 0.14 $min^{-1}$ for 4,6-DMDBT. The apparent activation energies of all compounds were obtained from the slopes of the Arrhenius plots, and were 35.3 – 48.4 kJ/mol. | [Caero et al., 2005] |
| $WO_x/ZrO_2$ | Oxidative desulfurization followed by extraction. | SRGO | • Experiments were carried out in a glass batch reactor under stirring at 1000 rpm at atmospheric pressure; EDXFS was used to determine the total sulfur in samples. | [Ramırez-Verduzco et al., 2004] |
| Titanium silicalite | Oxidative desulfurization | TH in n-octane | • FT-IR and UV–Vis characterization shown the presence of framework titanium in all TS-1 samples.<br>• Resulting mixture was stirred for 6h at 333 K and analyzed periodically. Catalysts were centrifuged off and the organic phases were subjected to gas chromatographic analysis with FID detector on a capillary column SE-54. | [Kong et al., 2004] |

## 2.3 ZIRCONIA MATERIALS

Zirconia ($ZrO_2$) is a widely researched material because of its thermal stability, mechanical properties, and its basic, acidic, reducing and oxidizing surface properties [Nakano et al., 1979]. Zirconia may exist in two crystal phases after calcination at low (less than approximately 1073 K) temperatures: a metastable tetragonal phase and the thermodynamically favored monoclinic phase [Heuer and Ruihle, 1984; Rijnten, 1970]. The tetragonal phase becomes the stable phase above about 1373 K; however, the transition to the monoclinic phase is so rapid that the tetragonal phase is not obtained even upon rapidly cooling from a high temperature. The tetragonal phase may be stabilized by the addition of a second metal, and Y and Ca are frequently used for this purpose. Sulfate also stabilizes the tetragonal phase so that at temperatures to about 973 K, the second metal is not needed to retain the tetragonal phase [Srinivasan et al., 1991]. Nevertheless, the tetragonal phase can be generated at much lower temperatures then those mentioned above [Veiga Blancoet al., 1980].

### 2.3.1 Importance of Solid Acid and Base Catalysts

Almost all the acid-base catalyzed reactions are traditionally carried out using liquid acids and bases. But, the enforcement of stringent environmental regulations have demanded the replacement of these environmentally hazardous materials, which left with the use of solid acid and base catalysts as the only possible options.

More than three hundred solid acids and bases have been developed in the last four decades [Tanabe and Holderich, 1999]. The surface properties and the structures have been clarified by the newly developed sophisticated analytical techniques. The characterized solid acids and bases have been applied as catalysts to various reactions and the role of acid-base properties has been studied extensively. Now, the solid acid-base catalysis is one of the most economically and ecologically important fields in catalysis. The need for materials in agreement with environmental concerns and regulations has led to the preparation of solid super acid catalysts than in liquid superacids with particular capacities, including (i) high conversion and selectivity toward reaction, (ii) stability under reaction, (iii) low sensitivity to poisoning, and (iii) easy regeneration.

### 2.3.2 Importance of sulfated zirconia (SZ) as solid acid material

SZ is one of the benign alternatives for the substitution of liquid acids answering the demand for clean technologies [Ahmad et al., 2003]. Much work has been devoted to SZ, which is compiled in several reviews [Arata, 1990; Corma, 1995; Song and Sayari, 1996]. SZ has reached a lot of interest due to its high activity for the isomerization of light alkanes at low temperatures [Song and Sayari, 1996]. The industrial use of SZ is currently restricted to the isomerization of $C_5$–$C_6$ paraffinic cuts for enhancing the octane number of gasoline. Anything having acid strength more than that of 100% sulfuric acid is called a super acid. For this, SZ was termed as solid super acid.

After the pioneering work of Hino et al. [1980], a great deal of research has been carried out across the globe to utilize SZ for several acid catalyzed reactions, but the matter of its super acidic nature has been a controversy since its discovery [Song and Sayari, 1996]. Some recent researchers have reported that it is not a super acid, but a strong solid acid having strength equivalent to that of 100% sulfuric acid.

Table 2.3 shows the application of sulfated zirconia ion various conversion processes. Yadav and Nair [1999] have published a review on the utilization of SZ for different acid catalyzed reactions such as isomerization, alkylation, esterification, cracking, etc. The excellent catalytic activity of SZ to isomerize alkane at room temperature made it so interesting for the catalyst chemists to work with [Song and Sayari, 1996].

Like zirconia , other metal oxides such as $TiO_2$, $SiO_2$, $F_2O_3$ etc., when modified with different anions such as sulfate, phosphate, tungstate, etc. show acidic character [Campelo et al., 1982] and have been studied for several acid catalyzed reactions [Hino and Arata, 1979 a, b, 1980; Scurrel, 1987; Yamaguchi, 1990].

**Table 2.3 Application of zirconia based catalysts in various conversion processes.**

| Catalyst | Target | Application | References |
|---|---|---|---|
| SZ | TH in n-heptane | ▪ Catalysts characterized by XPS, FT-IR, XRD, and SEM; The products were detected by gas chromatography–mass spectrometry (GC–MS).<br>▪ The slurry reactor was used for experimentation; Total efficiency of desulfurization from thiophene with ozone near to 100% has been obtained with the SZ catalytic oxidation reaction. | [Wang et al., 2009] |
| Zirconia | BT in n-heptane | ▪ Incorporation of $N_2$ into the bulk material is the key step in the preparation of N-doped transition metal oxides.<br>▪ In the surface process, molecular and dissociative adsorption of nitrogen ($N_2$) and ammonia ($NH_3$) at the perfect and oxygen-deficient (111) surface of cubic zirconia has been studied theoretically at hybrid density functional level.<br>▪ In agreement with experimental observation $N_2$ does not interact with the non-defective surface. Anionic adsorbed species, mainly $N_2$-are observed in the presence of oxygen vacancies in the top most layer independent of coverage. $NH_3$ adsorbs molecularly also on the defect-free surface whereas at the defective surface both molecular and dissociative adsorption is found. | [Reimann and Bredow, 2009] |
| Cu supported on Zirconia | Thiophene in n-octane | ▪ Sulfur species were adsorptively removed.<br>▪ The capacity of Cu on zirconia to adsorb thiophene increases as the copper content increases, reaching a maximum at a concentration of 3% of copper.<br>▪ The adsorption capacity also depends on the treatment used, and the higher capacities are observed in adsorbents treated with a flow of $N_2O$ at 363 K. | [Baeza et al., 2008] |
| SZ | Mixture of ketene silyl acetal and aldimine | ▪ Catalyzed Mannich-type reactions of ketene silyl acetals and aldimines proceeded smoothly at room temperature to afford b-amino esters in good to high yields.<br>▪ In addition, the heterogeneous it was easily recovered from the reaction mixture and then reused without significant loss of effectiveness | [Wang et al., 2007] |

| Catalyst | Target | Application | References |
|---|---|---|---|
| SZ | Light Naphtha Isomerization | ▪ Studied on the function of the metal in the sulfated zirconia catalyst for the isomerization reaction of light paraffins. | [Watanabe et al., 2005] |
| SZ | n-butane, iso-butane and 1-butene. | ▪ The interaction of $C_4$-hydrocarbons with SZ has been investigated for isomerization of $C_4$ hydrocarbons by using the temporal analysis of products (TAP) reactor.<br>▪ Heats of adsorption from van't Hoff plots were modelled for *n*-butane and isobutane and are comparable to calorimetry data for this system thus giving the opportunity to model the first step in a microkinetic model appropriately | [Breitkopf et al., 2005] |
| Pt/Mo-SZ | Organic synthesis and transformations | ▪ Imprignation technique was applied for promotion of zirconia.<br>▪ Addition of promoters enhanced the tetragonal zirconia phase and the surface acidity.<br>▪ All catalysts exhibit good catalytic activity for synthesis of diphenylureas, coumarines and 1,5-benzodiazepines, acylation of alcohols,phenols and amines, and protection of carbonyl compounds. | [Reddy et al., 2005] |
| SZ | Isomerization of n-butane and Isobutane | ▪ The skeletal isomerization of butane has been shown to be initiated by oxidative dehydrogenation of the alkane.<br>▪ This is followed by the formation of alkoxy groups/carbenium ions at the surface, induced by strong Brønsted acid sites.<br>▪ With increasing conversion, the selectivity decreased linearly, leading to propane and pentanes up to 40% of conversion.<br>▪ Transient experiments show conclusively that the isomerization of the carbenium ion and not the hydride transfer from the alkane to the carbenium ion is the rate-determining step. | [Li et al., 2005] |
| Platinum-iron-promoted tungstated zircon | Isomerization of n-butane | ▪ Doubly promoted P/F1.2WZ catalys showed much higher than the sum of the singly promoted P/WZ and F1.2WZ catalysts.<br>▪ The exceptionally high activity of P/F1.2WZ catalyst in n-butane isomerization reaction is explained by a cooperative effect. | [Wang et al., 2005] |

| Catalyst | Target | Application | References |
|---|---|---|---|
| | | ▪ The diffusion of activated n-butane species stabilized by iron promoter to the Brønsted acid sites created by platinum promoter will be improved as both promoters are in close proximity to each other. The interaction between iron promoter and n butane or its activated species is shown by the influence of iron on the propane selectivity of the reaction; In addition, the close proximity of platinum and iron promoters in P/F1.2WZ catalyst is shown by TPR; Results revealed that the iron promoter is located on the surface of F1.2WZ catalyst. XANES, EXAFS, and EPR studies suggest that the iron promoter exists as highly dispersed Fe(III) species either bound to $WO_x$ surface or located at the surface vacant sites of zirconia.<br>▪ In addition, EPR study indicated the presence of fine a-$Fe_2O_3$ clusters on the surface of catalyst.<br>▪ The TPR peak at 694 K was probably due to Fe–O–Fe of this species. | |
| $WO_x/ZrO_2$ | Oxidative desulfurization followed by extraction of SRGO. | ▪ Experiments were carried out in a glass batch reactor under stirring at 1000 rpm at atmospheric pressure; EDXFS was used to determine the total sulfur in samples; The oxidation reaction was carried out with hydrogen peroxide at 30 wt.%, in a heterogeneous system with a $WO_x/ZrO_2$ catalyst at 15wt.% of W. | [Ramırez-Verduzco et al., 2004] |
| SZ | Interaction of hydrogen and n-pentane | ▪ Interaction of $H_2$ with the sample evacuated at 673 K leads to the formation of new hydroxyl groups; It was shown that hydrides and protonated cyclopentadienes form at low temperatures. At higher temperatures, aromatic compounds are formed mainly. | [Paukshtis et al., 2000] |
| Pt-promoted M and T-SZ | Hydroconversion of n-hexadecane | ▪ The catalysts contained 27–86% of the monoclinic phase.<br>▪ The catalysts were activated just prior to activity studies with *n*-hexadecane; This synthesis route and pretreatment produced mixed-phase catalysts which yielded comparable conversion and selectivity data to that of a purely tetragonal catalyst using optimum conditions.<br>▪ The data show that an active catalyst can be obtained with the monoclinic phase present and that addition of sulfate after development of the crystalline phases can yield an active catalyst. | [Robert et al., 1999] |

#### 2.3.2.1 Zirconia ($ZrO_2$)

Zirconia (Zirconium dioxide) is an important transition metal oxide which finds use as a catalyst or as a carrier or support material for a catalyst [Tanabe, 1985] and as a good adsorbent [Baeza et al., 2008]. The surface of zirconium oxide is known to possess all these catalytic activities. Also it is probably the only metal oxide, which is amphoteric in nature and has all four properties, i.e. acid, base, oxidizing and reducing. These properties are influenced by the pretreatment conditions. The catalytic activity and selectivity of zirconia are thus dependent on the preparation methods and activation conditions [Yamaguchi, 1990].

#### 2.3.2.2 Sulfated Zirconia (SZ)

Catalytic properties of SZ were first described by Holm and Bailey [1962]. SZ has been widely used to catalyze reactions such as hydrocarbon isomerization, methanol conversion to hydrocarbons, alkylation, acylation, etherification, condensation, nitration, cyclization [Yadav and Nair, 1999].

Zirconia, when modified with anions, such as sulfate ions known as sulfated zirconia (SZ), forms a highly acidic or super acidic catalyst that exhibits superior catalytic activity to catalyze many reactions. Hino et al. [1979c, 1980] in their work on zirconia, for the first time showed that when sulfate ions were adsorbed on this oxide, the material became highly acidic. Based on the Hammett indicator methods, they measured the acid strength of sulfate adsorbed zirconia to be $10^4$ times more than that of 100% sulfuric acid [Hino et al., 1980]. Arata et al. [1980] also claimed that sulfate anion treated zirconia possesses superacidity with a Hammett acidity function $H_0 \leq 16$. Arata [1996] has identified a range of active sulphated oxides, viz. $SO_4^{2-}$/Zirconia, $SO_4^{2-}/Fe_2O_3$, $SO_4^{2-}/SmO_2$, $SO_4^{2-}/TiO_2$, etc. whose surface properties and mainly surface acidity significantly vary with sulphation and with changes in sulphate concentration. SZ is a non-halide alternative for chlorinated alumina and has attracted considerable attention [Holm and Bailey, 1962; Yamaguchi et al., 1986; Clearfield et al., 1994; Lunsford et al., 1994; Riemer et al., 1994]. SZ is known to possess the highest acidity amongst all known solid super acids, a considerable amount of research is centered on further improvement of catalytic activity and stability towards deactivation.

Numerous investigations on SZ is still focused on basic aspects, e.g., the nature of its active sites [Arata and Hino, 1990; Adeeva et al., 1995; Clearfield et al., 1994;

Song and Kydd, 1998a] and the reaction mechanism [Adeeva et al., 1995; Fogash et al., 1996; Liu et al., 1996a; Matsushita et al., 1999; Suzuku and Okuhara, 2000]. It is well known that heterogeneous catalysis is a surface phenomenon. In general, a catalyst having larger surface area will have higher catalytic activity. On the other hand, to form a catalyst that has shape selectivity for larger molecules, in the same way that zeolites do for smaller molecules, narrow pore size distributions need to be created. To improve its textural properties, various ways have been attempted. For example, SZ was supported on mesoporous silica materials with high surface areas, such as MCM-41 [Chen et al., 2001; Xia et al., 2002;Ghedini et al., 2006], SBA-15 [Hua et al., 2001; Landau et al., 2003] and HMS [Ecormier et al., 2005]. Mesoporous SZ was synthesized by liquid-crystal templating method [Huang et al., 1996; McIntosh and Kydd, 2000; Yang et al., 2002; Sun et al., 2003; Signoretto et al., 2006]. Nanosized [Althues and Kasel, 2002; Mishra et al., 2003; Sun et al., 2002] and macroporous [Al-Daous and Stein, 2003] SZ were also prepared.

Many preparation methods for SZ have been reported in the literature. Most of them concern the classical two-step method [Hino et al., 1979; Hino and Arata, 1980], which consists of the synthesis of an amorphous zirconium hydroxide precursor and its impregnation with sulfuric acid or ammonium sulfate. An alternative is the one-step sol–gel synthesis, to which many of the recent publications are devoted [Morterra et al., 1997; Signoretto et al., 1997; Tichit et al., 1996; Li and Gonzalez, 1996]. The structure of SZ as proposed by Kumbhar et al. [1989] is given in figure 2.1.

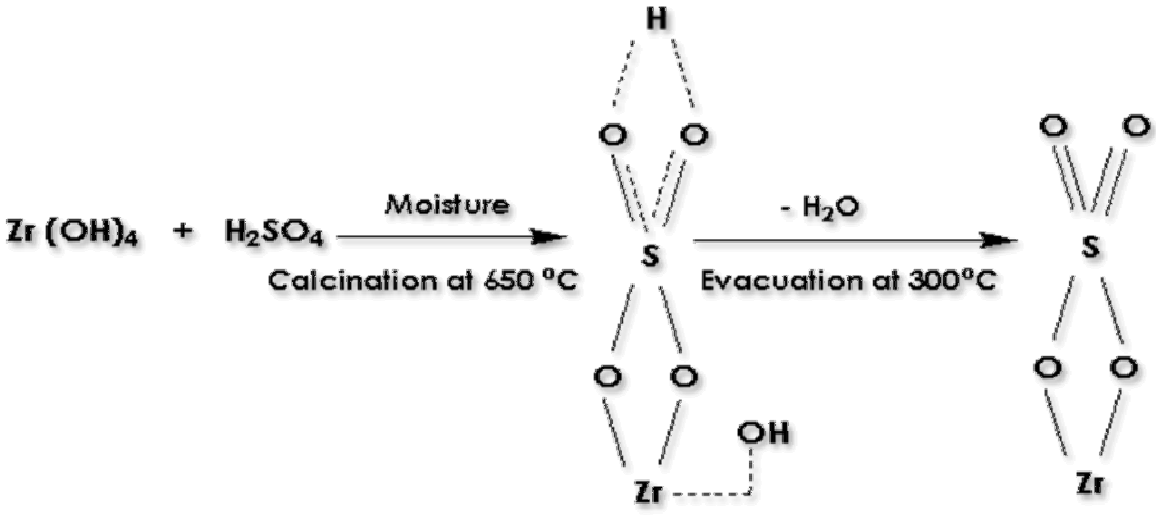


**Figure 2.1 Structure of SZ as proposed by Kumbhar et al. [1989].**

SZ is known to function as both lewis and brønsted acids as shown in figure 2.2 [Corma, 1995]. It has been reported [Jin et al., 1986; Yamaguchi et al., 1986] that the addition of anions such as $SO_4^{2-}$, $PO_4^{3-}$ to modifies the structural and catalytic behaviour. It is also believed that these anions enhance the acidity of zirconia and make it a super acid catalyst [Corma, 1995]. Furthermore the anions disturb the transition of one crystallographic form of zirconia to another. This in turn affects the catalytic properties of zirconia.

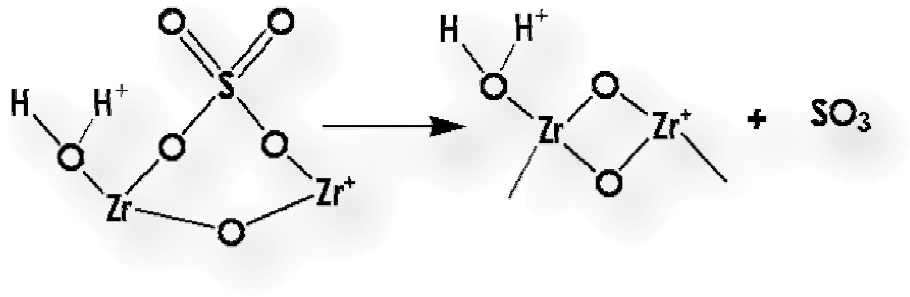


**Figure 2.2 Lewis and bronsted acidity in SZ**

The superacidity of SZ is generated by the interaction between the oxide and $SO_4^{2-}$ ion. The presence of an asymmetric vibrational mode of a S=O is considered to be responsible for the presence of superacidity [Kayo et al., 1983; Tanabe and Takeshita, 1967 ].The lewis acid strength of $Zr^{4+}$ becomes stronger by the inductive effect of S=O in the complex.

Davis et al. [1994] reported that the sulfate ions stabilize the zirconia surface favoring the formation of the tetragonal crystalline phase at calcination temperature above 813 K, and this is responsible for the enhanced activity of SZ. But the fast deactivation of these catalysts prevented its use in commercial processes and the recent research is mainly focused on overcoming this effect. Several suggestions have been made in order to explain the deactivation process, among them:

(1) Formation of hydrocarbon surface deposits (coke**)** [Li et al., 1998; Gonzalez et al., 1998; Vera et al., 1999; Comelli et al., 1995; Chen et al., 1993; Fogash et al., 1998; Kim et al., 2000; Nascimento et al., 1993; Spielbauer et al., 1996].

(2) Surface reduction ($Zr^{4+} \rightarrow Zr^{3+}$) by the reacting hydrocarbon [Vera et al., 1999],

(3) Reduction of the oxidation state of sulfur in the surface sulfate from $S^{6+}$ to lower oxidation states resulting in a decrease in acid strength [Sohn and Kim, 1989; Yori. et al., 1989; Li and Gondez, 1997].

(4). The transformation of the catalytically active surface tetragonal phase into the inactive monoclinic phase [Li and Stair, 1996; Li et al., 1996].

(5) Surface poisoning by water **[**Comelli et al., 1995].

(6). Possible removal of sulfur as $H_2S$ [Flora and Horvat, 1995].

(7). Changes in the surface acidity [Ward and Ko, 1994; Gonzalez et al., 1997].

**2.3.2.3 Metal Promoted Sulfated Zirconia (MSZ)**

Holm and Bailey [1962] were the first to disclose in the early $60^s$, that Pt containing sulfate-modified zirconia was an acid catalyst suitable for alkylation of hydrocarbons. However, SZ as such suffers fast deactivation when in contact with hydrocarbons due to several factors such as carbon formation [Keogh et al., 1994], loss of acidity [Li and Gonzalez, 1996], removal of sulfur entities [Li and Gonzalez, 1997] or a combination of these, restricting its industrial usage. A number of transition metals (either as ions or oxides) (e.g. Ti, V, Cr, Mn, Fe, Co, Ni, Cu, Zn, Pd, Ir, Pt etc.) have been added to SZ resulting in catalysts with higher activity than unmodified SZ, amongst these modifying agents Mn, Fe and Pt tend to exhibit better activity till now. Addition of promoters, such as Fe and Mn, enhances the activity at low temperatures, whereas addition of modifiers, such as Pt and Cu, decreases the rate of deactivation. The role of promoters or modifiers is not very well understood and differing views exist even for the state of Pt in Pt-modified SZ (Pt/SZ) catalysts [Song and Sayari, 1996].

For SZ catalyst, the catalytic activity is often not strong enough. Miao et al. [1996] have reported that the doping of SZ with various transition metals, such as Cr or V, could enhance its catalytic activity for reactions at low temperature in the absence of hydrogen, which were two to three times more active than sulfated Fe−Mn−Zr, however, the doped catalysts are not stable at high temperature in the presence of hydrogen yet. The role of the promoters in the presence of hydrogen is still an unresolved issue. The differences of catalytic behavior over unprompted and promoted SZ have been discussed in terms of crystalline phase, sulfate content, and acidity [Gao

et al., 1998; Moreno et al., 2001].The enhanced activity of promoted SZ was attributed to iron-oxy species Wan et al. [1996]. Promoters such as Fe or Mn, which enhance the activity by 1–2 orders of magnitude, form a solid solution with tetragonal zirconia, as indicated e.g. by the shrinkage of the unit cell with promoter content.

A number of late transition metals promoters (e.g., Mn and Ni) have also been added to SZ, resulting in catalysts with higher activity than unmodified SZ [Coelho et al., 1995]. Such promotional effects come mostly from synergism between redox and acid sites and from the stabilization of tetragonal phase **[**Jentoft et al., 2004].

Some researchers [Song et al., 1996; Yori et al., 1989; Tabora et al., 1996] also introduced transition metals such as Ni, Pt, Pd, Rh, Ru, Co, W, and Mo in SZ in order to overcome the deactivation problem.

#### 2.3.2.3.1 Aluminum Promoted Sulfated Zirconia (ASZ)

The addition of p-block metal oxide, such as $Al_2O_3$ and $Ga_2O_3$ give an increased steady activity. Gao and co-workers [Miao et al., 1997; Hsu et al., 1992; Coelho et al., 1995; Gao et al., 1998] reported that the addition of small amount of $Al_2O_3$ to the SZ system leads to a catalyst with superior activity than the unpromoted SZ. The promoting and stabilizing effect of Al on SZ (denoted as ASZ; A and SZ standing for alumina and SZ) was subsequently confirmed by other groups [Olindo et al., 2000; Moreno et al., 2001]. The steadiness of activity is important for SZ catalyst to be industrially viable. The effect of alumina on SZ catalyst has been suggested to be due to increased sulfur retention and thus density of acid sites [Moreno et al., 2001]. Later, however, it was reported that the redistribution of acid types is more closely correlated to catalytic activities. The remarkable activity and stability of the Al-promoted catalysts are due to an enhanced amount of the weak Brønsted acid sites [Wang et al., 2005]. Xia et al. [1999] showed that the addition of Al to persulfated zirconia helps to stabilize the surface sulfate complex on the oxide and increase the number of effective acid sites on the catalyst. The remarkable activity and stability of the Al-promoted catalyst under $H_2$ at higher temperatures are caused by an appropriate distribution of acid site strengths and an enhancement in the number of acid sites with intermediate acid strengths. Tabora and Davis [1995], suggested that the promoter does not modify the zirconia phase but may play a separate role in the reaction scheme.

#### 2.3.2.3.2 Iron/Cerium Promoted Sulfated Zirconia (FSZ)

The influence of promoter and sulfate content on the catalyst activity has been addressed in a limited number of studies. A sulfate content of 4.0% was found to be optimal for a catalyst with 1.5% Fe and 0.5% Mn [Lin and Hsu, 1992], whereas at the opposite, no relationship was observed between activity and sulfate content in Fe-promoted sulfated zirconia [Hino and Arata, 1996]. Coelho et al. [1995] investigated a series of FSZ catalysts and observed an optimal Fe content of 0.2% for samples with 8% nominal sulfate content. For similar catalysts, but under different reaction conditions, Song et al. [1998a] reported an optimum activity for 4% Fe without specifically considering the effect of the actual sulfate content of their catalysts.

Wan et al. [1996] provided strong experimental evidence of redox active sites on iron and manganese promoted SZ. Tabora et al. [1995] showed by Fe and Zr K-edge EXAFS that iron is not incorporated isomorphously into the tetragonal zirconium oxide but is located on the surface or at defects.

Sohn et al. [2006] prepared a new solid super acid catalyst, CeSZ simply by doping $ZrO_2$ with Ce and modifying with sulfate simultaneously. The characterization of prepared catalysts was performed using FTIR, XRD and DSC. The surface area of calcined at 923 K was very high (121.2 $m^2/g$) compared to that of SZ (56.0 $m^2/g$). This high surface area of CeSZ was due to the doping effect of Ce, which makes zirconia a stable tetragonal phase as confirmed by XRD. CeSZ exhibited maximum catalytic activities for reactions, 2-propanol dehydration and cumene dealkylation.

#### 2.3.2.3.3 Platinum Promoted Sulfated Zirconia (PSZ)

It has been reported in several papers that the presence of a noble metal (Pt) greatly enhances the catalytic performance of SZ [Hosoi et al., 1988; Ebitani et al., 1989]. Addition of platinum to SZ reduces the rate of deactivation [Iglesia et al., 1993].

The role of added Pt on the reactivity of SZ is even less clear. Platinum promotion of SZ is suggested to occur by increasing the acidity of SZ [Ebitani et al. 1988; Ebitani et al., 1991; Ebitani et al., 1992], increasing hydride transfer to reaction intermediates [Iglesia et al., 1993], or reducing deactivation of the catalyst by preventing coke formation [Garin et al., 1991; Yori et al., 1995]. Pt-promoted SZ has been suggested to play a different role [Comelli, 1996]. Pt is reported to be present on the catalyst surface as metallic Pt, even at calcination temperatures as high as 873 K

and above, and these metallic Pt centers acts as active sites [Sayari and Dicko, 1994]. On the other hand, Ebitani et al. [1992] have explained the role of Pt in enhancing the acidity of Pt/SZ catalysts. They suggested that hydrogen molecule dissociates into hydrogen atoms on Pt sites and then spills over to SZ, where the conversion of an H atom to $H^+$ occurs with the formation of $H^-$ on a lewis acid site. However, Zhang et al. [1994] reported that the presence of Pt did not affect the distribution of acid sites. From XPS studies, Ebitani et al. [1992, 1993] concluded that Pt on SZ exists in the cationic state, possibly as platinum oxide. Sayari et al. [1994] reached a similar conclusion from TPR, XRD, and XPS experiments. Zhao et al. [1994] found from X-ray absorption spectroscopy that platinum supported on SZ is present in a metallic state after calcination in air at 1000 K.

#### 2.3.2.3.4 Tungsten Promoted Sulfated Zirconia (WSZ)

Kuba et al. [2001] proposed a non-catalytic redox process for the activation of n-pentane on WZ. This process involves a homolytic C–H bond cleavage reaction on $WO_x$, followed by one-electron transfer steps that yield surface $W^{5+}$ ions, OH groups, and carbenium ions. Carbenium ion then acts as a chain carrier in the catalytic cycle of isomerization reaction. The carbenium ion could also act as an initiator for C–H bond dissociation. Thus, the redox property of $W^{6+}$ in $WO_x$ is thought to play a crucial role in this initiation process of n-pentane isomerization reaction.

### 2.3.2.4 Doubly Promoted Sulfated Zirconia (DMSZ)

Addition of second promoter such as iron, aluminum or gallium on zirconia increases the performance of this doubly promoted zirconia material which shows further improvement in catalytic activity, stability and selectivity. However, the role of the additional promoter still remains unresolved. Based on the characterization and catalytic results, several propositions have been made on the promotional effect of iron [Lukinskas et al., 2003; Kuba et al., 2003]: (a) ensemble effect, which stabilizes the platinum particles in a highly dispersed state (b) diffusional effect, which facilitates the migration of activated molecules from platinum to the acid sites (c) redox effect which enhances the reducibility of $W^{6+}$ to $W^{5+}$ in WOx. A promoter may promote the reaction through a combination of these effects. The action of gallium promoter may be explained by a redox effect and the aluminum promoter by an acidity effect [Chen et al., 2003, 2004; Wong et al., 2003]. In the study of iron-promoted WZ catalyst, the

nature and location of iron promoter in the catalyst are of great interest. However, relatively few studies on the nature and location of iron promoter on WZ have been reported so far [Lukinskas et al., 2003; Scheithauer et al., 2000]. Nonetheless, there is a diversity of opinions. Tabora and Davis [1995] suggested that iron does not substitute in the tetragonal structure but was present as nanometer-sized oxide clusters or rafts supported on zirconia. On the other hand, Yamamoto et al. [1999] concluded that iron atoms form interstitial-type solid solution in the lattice of zirconia, that is, the atoms are located at the center of distorted oxygen octahedra. Okamoto et al. [2000] reported on a study of metal oxide-support interaction in Iron/zirconia catalysts by Mossbauer spectroscopy. Quite recently, Carrier et al. [2004] characterized the state of iron promoter in tungstated zirconia (WZ) catalysts and suggested that iron occupy substitutional positions in the first surface layer of zirconia with a distorted octahedral coordination for Fe (III). Unfortunately, no catalytic data were provided to correlate the significance of their characterization results.

Iron-promoted tungstated zirconia (FWZ) and platinum–iron-promoted tungstated zirconia (PFWZ) catalysts was studied and correlated to the catalyst characterization results by Wong et al. [2005].

### 2.3.3 Causes and types of Acidity in Sulfated Zirconia

Acidity is the most important function of SZ and it is evidently connected to the presence of $SO_4^{2-}$ groups because zirconium oxide exhibits low acidic properties irrespective of the method used for its synthesis [Tanabe et al., 1989]. Structural characterizations indicate a very inhomogeneous surface: isolated sulfate groups as well as polymeric sulfate species and zirconium oxide are equally accessible. In addition, samples prepared via colloidal sol-gel procedure very probably also contain supported sulfuric acid. Concerning lewis acidity, a good agreement seems to exist. S=O double bonds exhibit an electron inductive effect which increases the electron deficient nature of the zirconium atom attached to the sulfate group, thus strengthening the lewis acid character. This model was first proposed by [Kayo et al., 1983; Jin et al., 1986] and after that confirmed by all other studies [Saur et al., 1986].

Mesoporous materials with large surface areas are beneficial towards spreading a large amount of zirconium sulfate and the subsequent formation of tetragonal SZ which is the catalytic active phase in the isomerization of hydrocarbon. Several

successful attempts in preparing mesoporous SZ have been reported [Huang et al., 1996; Yang et al., 2002]. Recently, Xiao and co-workers prepared mesoporous zirconia oxide, using a triblock copolymer, with alumina promoter and showed that these materials are catalytically active in butane isomerization [Xiao et al., 2004]. However, the acid sites in the catalyst were not identified. Further, to be suitable for use as a catalyst or catalyst carrier in many applications, it is also important that the zirconia product has sufficient strength for the required application. This is particularly the case when the catalyst comprises particles of zirconia which have been shaped, for example by extrusion. Zirconia exists in a number of crystalline forms, dependent upon the prevailing conditions. Thus, zirconia exists under ambient conditions of temperature and pressure as a stable, monoclinic crystalline structure. Under extreme pressures or at higher temperatures, typically of the order of 723–1273 K, zirconia exists as a tetragonal crystalline structure. At even higher temperatures, typically in excess of 1773 K, a cubic crystalline phase forms. Catalytic sites with a dual function i.e., bronsted acidity and function associated with dispersed metal species such as Ga, Zn, Cr, Fe, Co, In and Sn needs to be investigated.

### 2.3.4 Mechanism for Acidity Generation

Chen et al. [1993], proposed a possible mechanism for the generation of the acid sites on the surface of SZ. This mechanism suggests the formation of acid sites to be a two-step chemical reaction between the superficial hydroxyl groups and the sulfate anions being adsorbed. The first chemical reaction occurs during the impregnation with $SO_4^{2-}$ and the subsequent drying:

$$Zr(OH)_{4n} + x\,H_2SO_4 \rightleftharpoons Zr_n(OH)_{4n-2x}(SO_4)_x + 2x\,H_2O$$

$$Zr_n(OH)_{4n-2x}(SO_4)_x \longrightarrow Zr_n(O)_{2n-x}(SO_4)_x + (2n-x)\,H_2O$$

Several observations, such as higher surface area, increased sintering resistance and stability of tetragonal phase and smaller crystallite size as a result of presence of sulfate anions, support this type of mechanism. The incorporation of the sulfate anions on the surface of zirconia has been found to probably increase the number and strength of the lewis acid sites [Yamaguchi, 1990; Parera, 1992; Bensitel et al., 1988; Jin, 1986; Corma, 1994].

Yamaguchi [1990] (figure 2.3) proposed a scheme for the formation of acid sites. According to this hypothesis, irrespective of the starting material used for sulfation are the oxidations during the thermal treatment results in the formation of the structure II. This structure is essential for the catalysis of reactions by such catalysts. It has further been suggested that such a structure may develop at the edge or corner of the metal oxide surfaces. This latter view is supported by the fact that the first doses during a stepwise loading of the acid on microcrystalline zirconia selectively form sulfate groups on crystal defects such as corners and edges [Morterra et al., 1993].

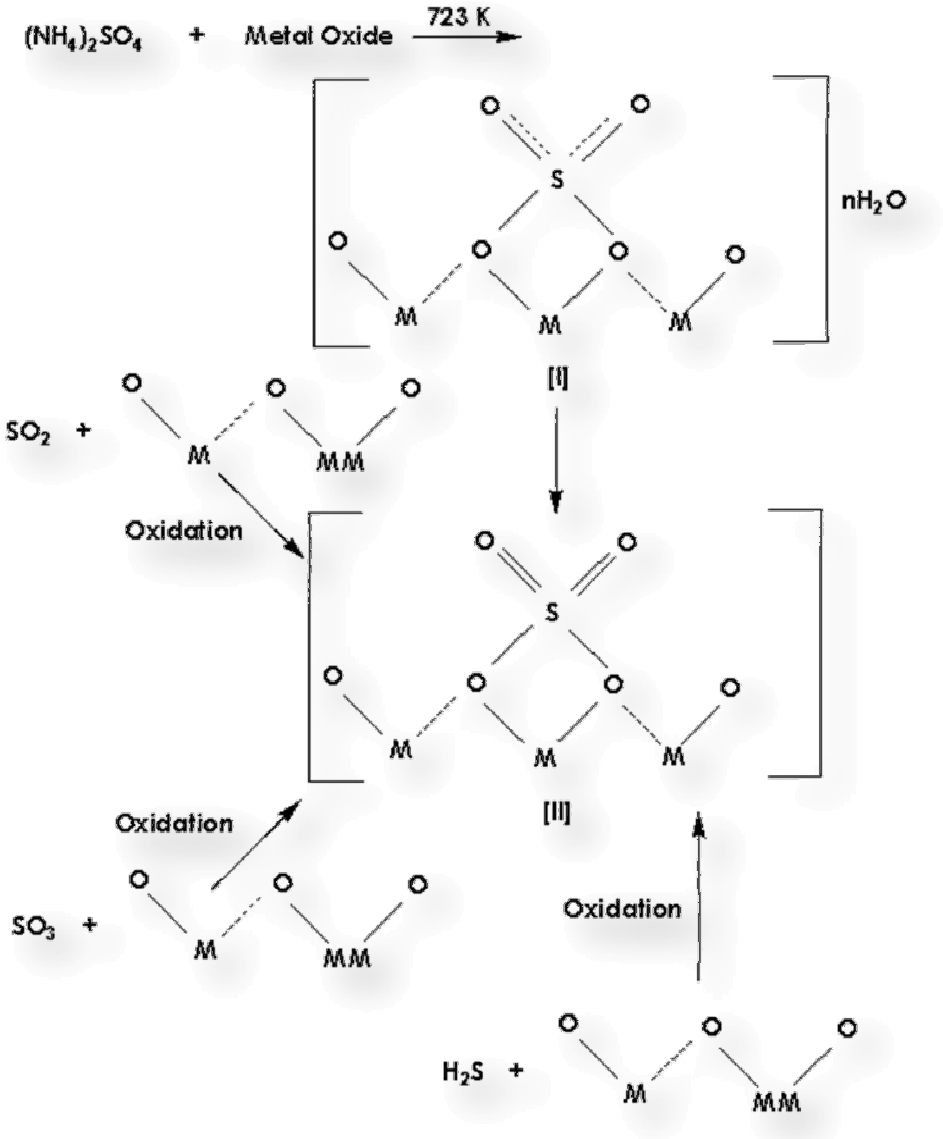


**Figure 2.3 Model for the formation of acid sites on zirconia proposed by Yamaguchi [1990].**

Another model has been proposed by Arata and Hino [1990] **(**figure 2.4) for the structure of the active site, wherein the sulfate bridges across two zirconium atoms. They takes into account the formation of Bronsted sites as a result of the uptake of water molecules as a weak lewis base on the lewis acid site, as has been evidenced\by the IR studies. This model has also been accepted by Davis et al. [1995] (figure 2.5), who suggested that the changes in the structure and valence occurring during the catalyst preparation and thermal activation do not seem to confirm with the chemical bonding. Hence, they have proposed a different scheme that is able to explain the loss of surface $SO_4^{2-}$ as $SO_3$ on heating above 923 K.

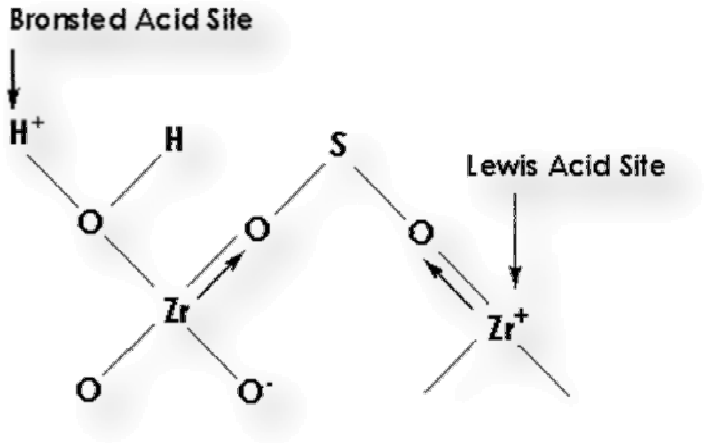


**Figure 2.4 Model for the structure of the active site proposed by Arata and Hino [1990].**

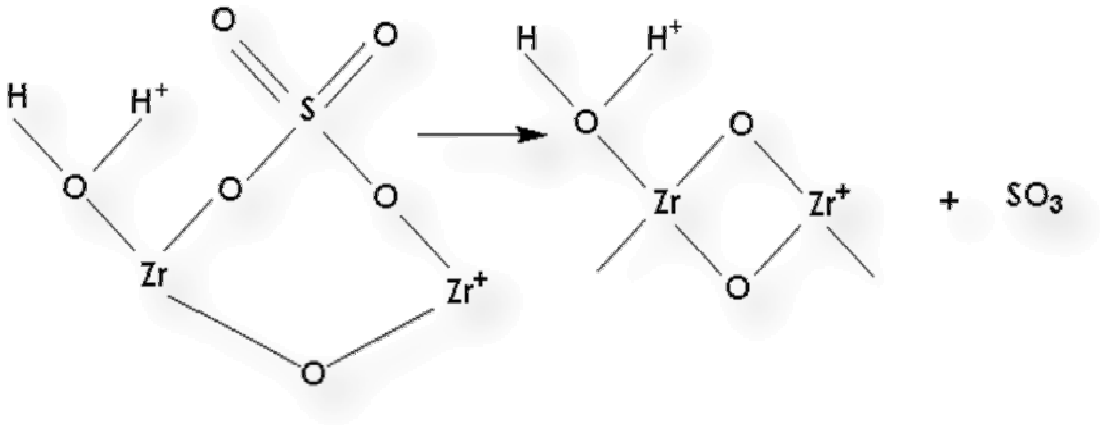


**Figure 2.5 Model explain the loss of surface $SO_4^{2-}$ as $SO_3$ on heating above 923 K proposed by Davis et al. [1994].**

Contrary to the above models, Clearfield et al. [1994] proposed a model that allows for the formation of bronsted sites. This model is based on the assumption that the predominant species in sulfuric acid media is the bisulfate ion, which can displace a Zr-OH-Zr bridge during chemisorption on the surface of hydrated zirconia (I). On heating, either the bisulfate ion can react with an adjacent hydroxyl group or two adjacent hydroxyl groups can react with each other, liberating water and keeping the bisulfate ion intact. The former results in to the generation of lewis-type acidity, whereas the latter leads to the formation of a bronsted-type site. The Clearfield et al. model [1994], in figure 2.6 describes the one step formation of both types of acidic site.

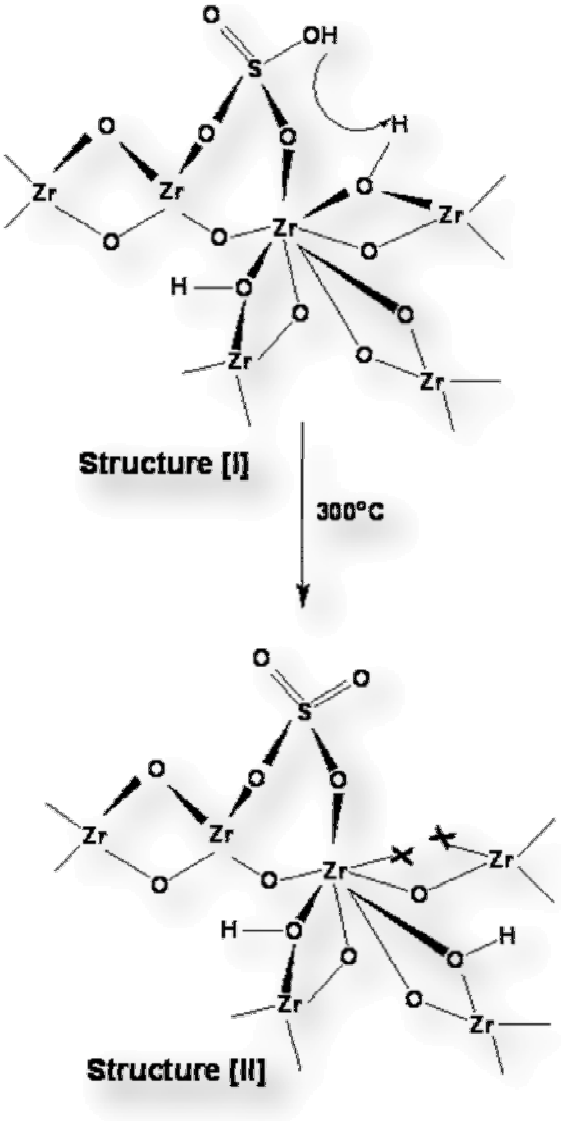


**Figure 2.6 Model describes the one step formation of both types of acidic site on SZ proposed by Clearfield et al. [1994].**

This type of bronsted acidity generation has also been proposed by Kustov et al. [1994], who have postulated that the sulfate treatment of hydrous zirconia results in the elimination of the terminal ZrOH species [Hertl, 1989] due to their substitution by bisulfate anions and enhances the acid strength of the bridging ZrOH groups **.** They have proposed schemes for both an ionic structure with a proton forming a multicenter bond with the $SO_4^{2-}$ anion and a covalent structure with hydrogen-bonded hydroxyl groups.

Hattori [1993] proposed a possible mechanism of protonic acid site generation on Pt-modified SZ in the presence of $H_2$. An IR study of adsorbed pyridine has revealed that protonic acid sites are generated on the catalyst surface in compensation for elimination of lewis acid sites when exposed to $H_2$. He has proposed a dissociative adsorption of $H_2$ on the Pt particles to form H atoms, which subsequently undergo spillover on to the support shown in figure 2.7. The H atom migrates on the surface of SZ to lewis acid sites where it loses an electron to form a proton stabilized on the surface O atoms near the lewis acid site. Similar results have been forwarded by Ebitani and co-workers [Hattori, 1993; Ebitani et al., 1992].

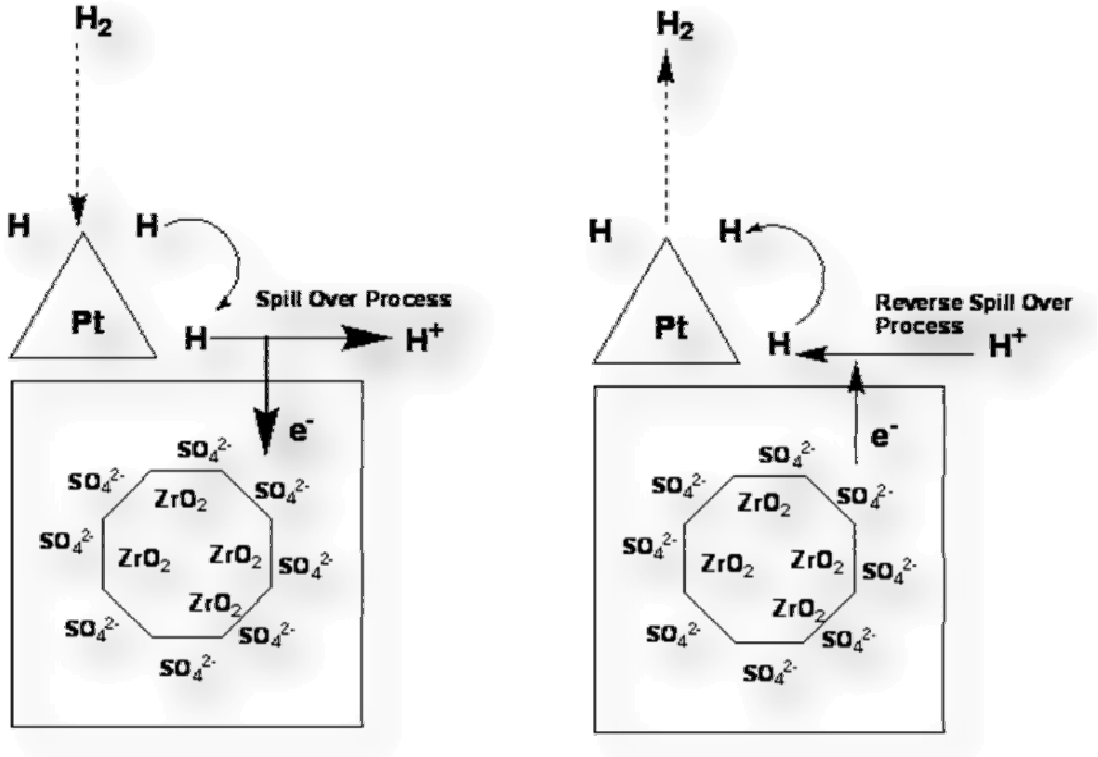


**Figure 2.7 Mechanism of hydrogen spillover on SZ [Hattori, 1993].**

Kustov et al. [1994] have explained the modification of lewis acid sites by $HSO_4^-$ anions (figure 2.8). The lewis acidity enhancement was attributed to the increase of the electron-accepting properties of three-coordinate zirconium cations via the inductive effect of $SO_4^{2-}$ anions, which withdraw electron density from the zirconium cations through the bridging oxygen atom. Furthermore, with the IR study of benzene adsorption, they have reported that the strength of the Bronsted sites of SZ is stronger than the silanol groups of silica gel, but weaker than the bridging OH groups in HX zeolites.

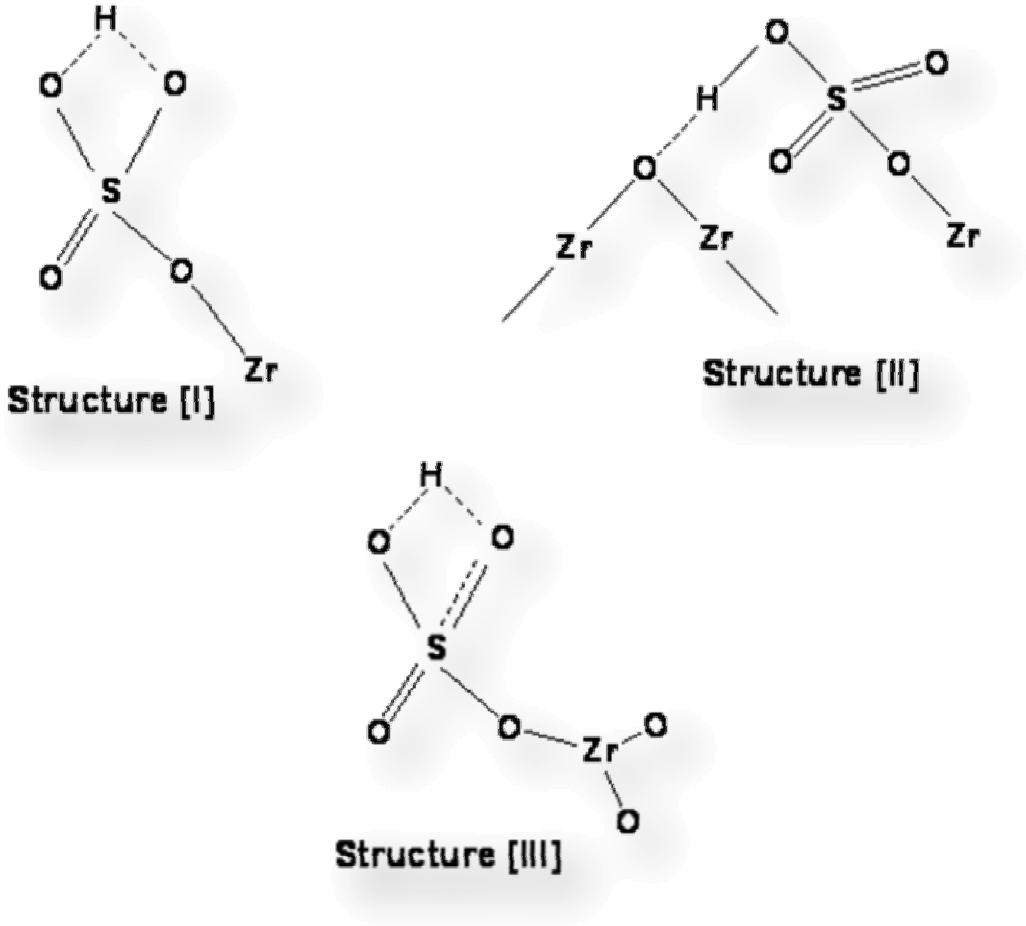


**Figure 2.8 Model explained the modification of lewis acid sites by $HSO_4^-$ anions proposed by Kustov et al. [1994].**

Babou et al. [1995] have postulated a different structure for the active sites at the surface of SZ as shown in figure 2.9. They have proposed that the interaction of the zirconia support with sulfuric acid solution results in the trapping of the protons by the zirconium hydroxide surface. Sulfate ions then get trapped on this ionized surface. Dehydration at temperatures below 473 K results in the loss of a first water molecule, leading to the formation of the structure II. Further dehydration at higher temperatures liberates a second water molecule with the formation of ($SO_3$) ads linked by dative bonds to the support. Such a model is based on quantum chemical calculations and describes the acidity to be near that of sulfuric acid but not to be super acidic.

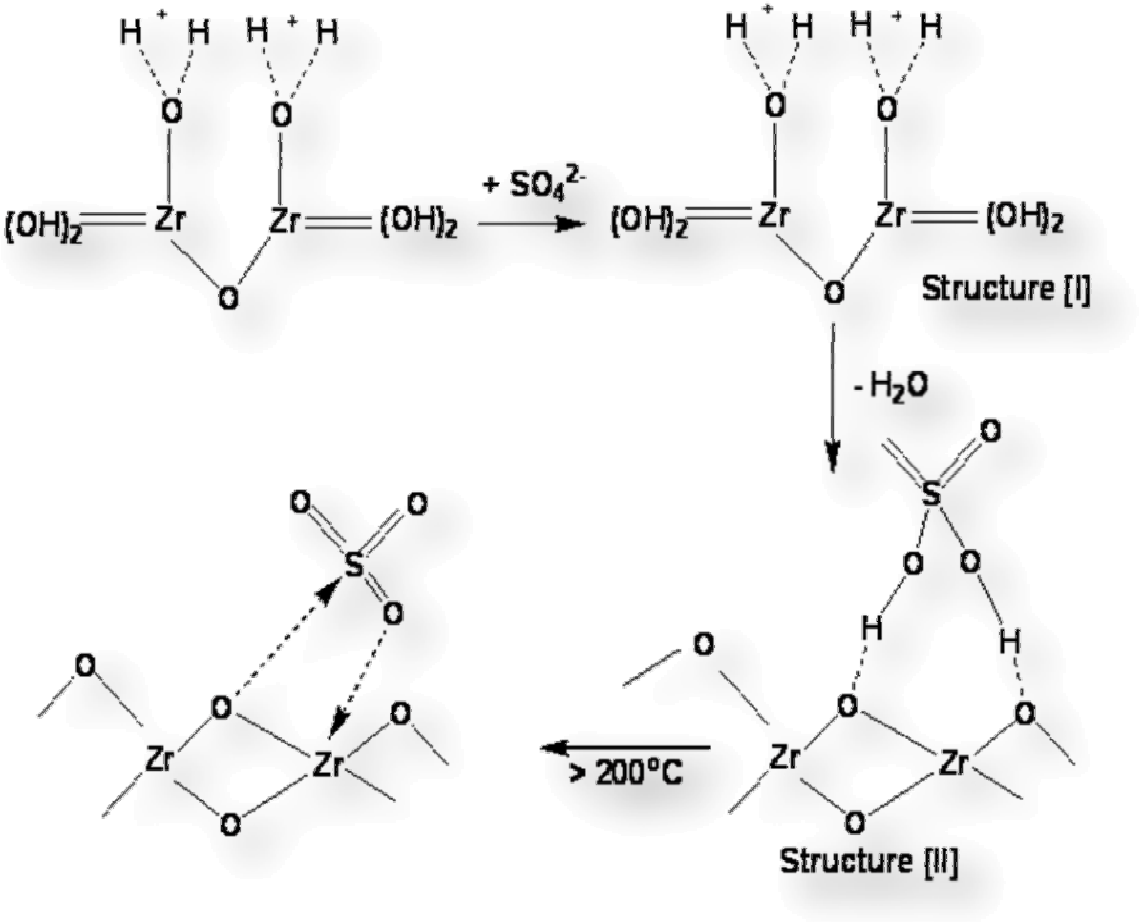


**Figure 2.9 Model postulated a different structure for the active sites at the surface of SZ proposed by Babou et al. [1995].**

Similar arguments based on P-NMR studies have been put forward by Adeeva et al. [1995] in figure 2.10, who has proposed that the acid strength of the Bronsted sites in SZ is similar to that of the lower OH-frequency protons in HY, but is weaker than that of the protons in H ZSM-5. It has also been speculated that the extraordinary activity of these catalysts is not due to its superacidity, but it results from the stabilization of the transition state complex as alkyl $SO_4^{2-}$ or surface alkoxy groups at the catalytic site.

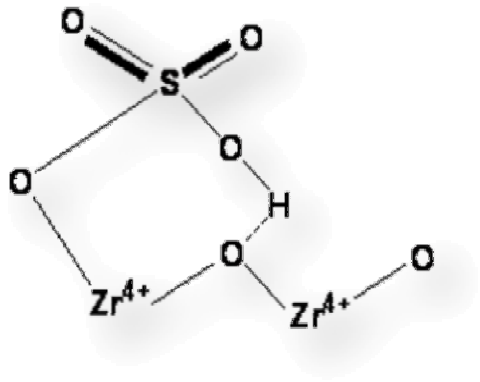


**Figure 2.10 Model proposed that the acid strength of the bronsted sites in SZ proposed by Adeeva et al. [1995].**

Pinna et al. [1994] and Morterra and co-workers [1993, 1993, 1994] have proposed that the $SO_4^{2-}$ responsible for the bronsted acidity of these catalysts represent the most labile fraction of the overall $SO_4^{2-}$ and no bronsted acidity is irreversibly lost $SO_4^{2-}$ and no Bronsted acidity is irreversibly lost for thermal activation temperatures above 923 K. Lewis acidity is shown by the $SO_4^{2-}$ located in the crystallographically defective sites such as edges and corners. Increasing surface sulfation results in the shielding of the surface $Zr^{4+}$ cations located on the low index planes. Most of these $SO_4^{2-}$ - have been proposed to induce Bronsted acidity, this effect being more pronounced if the $SO_4^{2-}$ - are in the form of polynuclear pyro-$SO_4^{2-}$ resulting from high loadings of $SO_4^{2-}$. Yamaguchi and co-workers [1986, 1987] have reported the existence of only the lewis type of acidity on the surface of SZ catalysts. Micro calorimetric studies of ammonia adsorption on the catalyst by Fogash et al. [1995] have revealed the presence of a spectrum of acid sites with different acid strengths. Their study also reveals that the initial doses of ammonia are coordinately bound to the

support. For higher amounts of ammonia dosed, IR spectroscopy shows the presence of $NH_4^+$ions adsorbed on the surface which points to the existence of Bronsted acidity in association with the lewis type acid sites. Lunsford and co-workers [1994] used P-NMR spectroscopy to probe the nature of the sites and have provided the evidence for the existence of both types of acidities. Similarly, Arata and co-workers [1980, 1990], Sohn and Kim [1989], Guo et al. [1994], and Clearfield et al. [1994] have supported the view that both the lewis and bronsted types of acidity are present on the surface of SZ Babou et al. [1995] have found from IR studies of adsorbed bases, such as butane, CO, $H_2O$ and pyridine, that two types of lewis site and one type of Bronsted site exist at the surface of sulfate-modified zirconia. Of these active sites, one lewis type site is associated with the zirconia support and the rest exist due to the presence of surface $SO_4^{2-}$.

### 2.3.5 Effects of Various Parameters on Zirconia Based Materials (Adsorbents/Catalysts) properties

Many parameters have been found to impact the catalytic activity of SZ. Catalyst preparation and pretreatment conditions determine the sulfur content, total surface area, crystallinity of zirconia, and the concentrations of lewis and Bronsted acid sites [Gonzalez et al., 1996; Gonzalez et al., 1997; Ward et al., 1995; Kobe. et al., 1996; Li and Gonzalez 1996; Clearfield et al., 1994; Song and Kydd, 1998a; Corma et al., 1994; Comelli et al., 1995; Shimizu et al., 1998]. Despite extensive research efforts on SZ in the last two decades, our understandings about its preparation, characterization of its active sites and its catalytic mechanism are still incomplete. The acid type is especially controversial. There are claims that the catalytic activity derives from Brønsted acid sites [Niwa et al., 2003]. Other authors are convinced, however, that the active sites are combination of bronsted and lewis types [Hammache et al., 2003].There has been a wide discrepancy in interpretation of the origin of the acidity and the catalytic activity of SZ. Various attempts have been made to elucidate the nature of the active site responsible for its activity. For example, the acidity (site density and strength) of SZ is apparently similar to the acidity of the iron and manganese promoted SZ [Adeeva et al., 1995; Tabora et al., 1995; Wan et al., 1996].

### 2.3.5.1 Effect of the Preparation Procedures

Preparation conditions have significant effects on the amount of sulfation in zirconia. Tichit et al. [1998] stressed the importance of both the pre-hydrolysis steps and the conditions in which gelifcation is carried out in the polymerization sol-gel procedure. Morterra et al. [1997] also prepared sulfate zirconia catalysts using polymerization sol-gel procedure with the gelifcation done overnight. Contrary to the polymerization sol-gel, the colloidal sol-gel procedure is a slow process. Solutions after peptization with $H_2SO_4$ or with a mixture of $CH_3COOH$ and $H_2SO_4$ completely gelifcate only after three weeks. In such conditions, the quantity of retained sulfate is high (over 50 wt%) and greatly exceeds the values reported in the literature for polymerization sol-gel procedure. Moreover the presence of $CH_3COOH$ in solution with $H_2SO_4$ favors higher sulfur content. In all the impregnated samples, the content of sulfur retained on the zirconium oxide is in the range generally reported in the literature. Prolonged heating under reflux of the suspension containing $Zr(OH)_4$ makes this more reactive, the sulfur content in the dried samples being higher than in the case of unheated $Zr(OH)_4$. Also, the prolonged contact of the $Zr(OH)_4$ with $H_2SO_4$ leads to an increase in the sulfur content. In conclusion, the use of the colloidal sol-gel technique in the presence of $H_2SO_4$ as peptizing agent leads to a high $SO_4^{2-}$ adsorbent zirconia. The presence of acetic acid in the peptization solution increased the selectivity of the zirconia gel and the sulfur content in the resulting catalyst is slowly increases comparatively with the samples peptized only with $H_2SO_4$.

### 2.3.5.2 Effect of Precursor and Sulfating Agents

It has been found that the use of ammonia or urea for precipitation of hydrated zirconia significantly affects the surface area of the catalyst [Yamaguchi et al., 1986] Precipitation with $NH_4OH$ yields catalysts with higher surface areas. The specific surface area obtained by sulfating precrystallized zirconia is somewhat lower than that obtained by sulfating amorphous hydrous zirconia [Sarzanini et al., 1995]. Moreover, catalysts obtained by sulfating the amorphous hydrated zirconia possess significantly higher activity than that obtained by sulfating the microcrystalline samples [Guo, 1994]. Sohn and Kim [1989] have studied the effect of using various sulfating agents, such as $H_2SO_4$, $(NH_4)_2SO_4$, $H_2S$, $SO_2$ and $CS_2$. The effects of different sulfating gents, and their post-treatment with oxygen and hydrogen, have been studied for 1-butene

isomerization. It was observed that the superacidity obtained in these catalysts is independent of the sulfur source used for the sulfation of the metal oxide precursor. It has been reported that, for sulfate concentrations above an average half monolayer, sulfation with $H_2SO_4$ leads to contents of sulfate that are appreciably lower than the nominal concentration. On the other hand, sulfation with ammonium sulfate produces high nominal sulfate concentration. Parera [1992] compared the surface sulfate concentration and the surface area of the catalysts when the sulfation is accomplished using sulfuric acid and ammonium sulfate. It is seen that higher sulfate concentrations and surface area are obtained with sulfuric acid than ammonium sulfate. Zeng et al. [1994] have found that higher concentrations of the solutions used for carrying out sulfation result in higher tetragonal content of the catalyst. Higher concentrations also increase the sulfur content the catalyst samples [Chen et al., 1993]. Most of the excess sulfate is, however, lost during the thermal activation of the catalyst. These $SO_4^{2-}$ thus represent most labile forms of the grafted $SO_4^{2-}$ [Sarzanini et al., 1995]. It has been found using HRTEM and XRD techniques that the nature of the surface $SO_4^{2-}$ grafted by any of the techniques on amorphous or precrystallized zirconia is much the same. When monoclinic microcrystalline zirconia is doped with sulfuric acid, the first doses of the acid selectively graft sulfate groups on to the crystal defects Morterra et al [1993]. The latter doses react with the regular crystal faces of the crystallites. It has been found that the relative amounts of the lewis and bronsted sites depend largely on the surface concentration of the $SO_4^{2-}$ and their nature [Morterra et al., 1993; Nascimento et al., 1993]. At low sulfate loadings, when only $SO_4^{2-}$ located in the crystallographically defective sites are present, there is a fair amount of lewis acidity formed, but no Bronsted acidity is formed. Isolated sulfate species observed for higher sulfate loadings and the existence of pyrosulfate on a few low index planes lead to the formation of Bronsted acid sites. Morterra et al. [1991] have studied the effect of sulfate concentration on the Bronsted acidity of the catalyst. Their results suggest increase in Bronsted acidity with an increase in sulfate concentration up to a certain maximum, after which the amount of Bronsted acidity remains constant. This trend has also been reported by Nascimento et al. [1993]. Thus, $SO_4^{2-}$ present above this concentration are lost during the thermal activation and represent the thermally more labile fraction.

### 2.3.5.3 Effect of Activation Temperature

The atmospheres in which the samples are activated are also found to contribute both to the density and to the strength of the acid sites. Thus, activation in air leads to a slow decrease in the sulfur content. This decrease occurs concomitantly with a slow decrease in the surface area and an increase of the acidity strength. Therefore one can suppose that the presence of air catalyzes the nucleation of the superficial sulfate groups.

Thermal treatment of the catalyst under vacuum below 723 K affects only the surface hydration degree, which in turn affects the covalency of the surface sulfates, thus altering the bronsted : lewis (B:L) site ratio [Morterra et al., 1993]. This effect is depicted in table 2.4. Activation temperatures above 723 K under vacuum start affecting the overall surface hydration degree as well as the concentration of the surface sulfates [Bensitel et al., 1988; Morterra et al., 1994]. At higher temperatures, some of the sulfates decompose to form $SO_2$. A possible pathway for this decomposition has been suggested by Chen et al. [1993] as:

$$2Zr^{4+} + SO_4^{2-} \longrightarrow 2Zr^{3+} + SO_2 + O_2$$

Comelli et al. [1995] have found that calcination temperatures above 753 K lead to a reduction in surface area. For instance, calcination at 663 K produces a surface area of 117 $m^2/g$, which decreases to 104 $m^2/g$ at 893 K. Similar results have been reported by Chen et al. [1993].

**Table 2.4 Percentage of acid sites on the SZ that are of the bronsted type[a] [Zhang et al., 1994].**

| Treatment Temperature (K) | | Bronsted sites (% of total ) | | | |
|---|---|---|---|---|---|
| **Pre** | **Post** | **0.0 Wt % $SO_4^{2-}$** | **1.17 Wt % $SO_4^{2-}$** | **9.87 Wt % $SO_4^{2-}$** | **13.6 Wt % $SO_4^{2-}$** |
| 373 | 373 | 0 | 47 | 98 | 98 (97)[C] |
| 373 | 673 | 0 | 49 | 93 | 95 (89)[C] |
| 673 | 273 | 42 | - (45)[b] | 63 | 68 (70)[C] |
| 673 | 673 | 46 | - (42)[b] | 80 | 83 (64)[C] |

[a] All samples were calcined at 898 K, exposed to air prior to the pretreatment in situ at 373 K or 673 K prior to pyridine adsorption; [b] $SO_4^{2-}$ content of the precursor before 923 K calcination; [C] Numbers in parentheses are for Pt-containing material.

### 2.3.5.4 Effect of Calcination Temperature

The catalytic activity of SZ is found to depend on the calcination temperature as well as the pre-calcination temperature of SZ. The super acidic SZ is produced when the pre-calcination temperature is between 373 K and 523 K, and the calcination temperatures upon sulfation are below 753 K .

Precalcination temperatures beyond 753 K, lead to a reduction in super acidity. In fact, the test reaction of isomerization of n-butane to isobutane [Nascimento et al., 1993] has shown that there is a combination of calcination temperature and concentration of sulfuric acid to give a better catalyst; for example, 873 K and 0.3 N $H_2SO_4$ or 923 K and 0.5 N $H_2SO_4$, produce almost identical activities. Table 2.5 shows the effect of calcination temprature on the acidity of SZ.

**Table 2.5 Effect of calcination temperature before and after sulfation on acid strength [Guo et al., 1994]**

| Pre-calcination temp. of zirconia (K) | Calcination temp. of SZ (K) | Acid strength, $H_o$ |
|---|---|---|
| 473 | 923 | $\geq$ - 16.12 |
| 673 | 923 | $\geq$ - 16.12 |
| 773 | 923 | $\geq$ - 13.75 |
| 873 | 923 | $\geq$ - 12.70 |
| 1073 | 923 | > - 12.70 |
| 383 | 473 | > - 12.70 |
| 383 | 673 | $\leq$ - 12.70 |
| 383 | 923 | $\leq$ - 16.12 |
| 383 | 1073 | $\leq$ - 12.70 |

### 2.3.5.5 Effect of Water of Hydration

The effect of water of hydration in acid catalysis has long been known to catalytic scientists. Some authors have reported an enhancement in the activity of these catalysts in the presence of minute amounts of water adsorbed on their surface [Tanabe et al., 1990]. On the other hand, some of the researchers have found water, even at very low concentrations, to be detrimental for the catalytic activity [Keogh et al., 1995; Wen et al., 1990]. There are still other reports that describe no effect of small amounts of water on the catalytic activity [Parera, 1992].

The nature of adsorbed water has been investigated by Keogh et al. [1995] and Morterra et al. [1993]. These authors have employed a combined TGA/DTA/MS technique for the characterization of the catalysts and proposed that water adsorbed on the catalyst converts some of the strong lewis acid sites into bronsted sites. It has further been proposed that these sites formed are not the catalytically active ones. Morterra et al. [1994] have studied the effect of partial rehydration on the catalytic activity of SZ. According to them, the $SO_4^{2-}$ detected on the surface of SZ exhibit a strongly covalent character at medium to high degrees of dehydration. Partial rehydration, however, tends initially to impart a less covalent character to the surface $SO_4^{2-}$ . Higher doses of water convert these $SO_4^{2-}$ to the ionic form. Thus, water dosing results in the transformation of bronsted sites, not catalytically active, at the expense of the strongest lewis centers. Thus, this explains the loss of activity on rehydration of these catalysts. The initial activity can be recovered by repeating the activation step. This reversible transformation of lewis and bronsted sites, on adsorption and desorption of water, has also been reported by Zecchina et al. [1987]. Iglesia et al. [1993] have proposed that the presence of small amounts of water in the hydrocarbon feed can lead to the formation of surface hydroxyl groups with highly polarized O-M-H bonds. These sites can function as the strong Bronsted site for the reaction. With the use of IR spectroscopy, Babou et al. [1995] have pointed out that there is a reversible effect of water on the sulfate species on the surface of SZ. They have detected four $SO_4^{2-}$ species on the surface, which are assumed to be in equilibrium with adsorbed water. The scheme proposed by them is as follow:

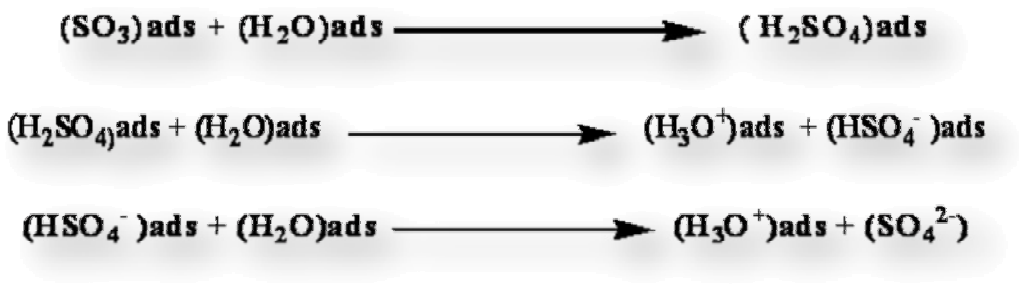


The superacidity generated on the surface of SZ has been a matter of debate. Small amounts of water tend to balance the bronsted and lewis acid sites in specific reactions, leading to much higher activities.

Chapter – III

# PREPARATION OF ADSORBENTS/CATALYSTS

## 3.1 GENERAL

This chapter deals with the method of preparation of adsorbents/catalysts. The physico-chemical properties of adsorbents/catalysts depend upon the preparation conditions and the procedure followed. This work was undertaken to prepare zirconia, their promoted forms to study their physico-chemical properties and adsorptive/catalytic activity towards adsorptive/oxidative desulfurization of model oil. In this context, it is well known that the preparation procedure adopted and the post-synthesis treatment done determines the adsorptive/catalytic activity of the prepared adsorbents/catalysts.

## 3.2 METHOD OF PREPARATION

Zirconia is an interesting material because of its thermal stability, mechanical properties, and its basic, acidic, reducing and oxidizing surface properties [Nakano et al., 1979]. The zirconia precursor is nearly always prepared by precipitation from a zirconium solution by adding a base. With zirconia this is not a simple procedure since the salt utilized to prepare the solution may have a significant impact upon the crystal phase of the zirconia obtained following drying and calcination [Srinivasan et al., 1992]. Starting with anhydrous zirconium tetrachloride, control of the final pH [Davis, 1984] and the rate of addition of the base [Srinivasan et al., 1988] make it possible to prepare a hydrous zirconium oxide that will produce either the tetragonal or monoclinic form as the predominant phase following calcination in the 673-973 K range. However, starting with many of the salts or salt solutions that are commercially available, only the tetragonal phase is obtained following calcination irrespective of the preparation procedure employed.

Zirconia can be prepared by different methods such as: (1) Precipitation and impregnation [Rezaei et al., 2006; Wang et al., 2006], (2) Sol-gel synthesis [Xie, 1999;

Fiona et al., 2004; Akkari et al., 2007], (3) Co-precipitation [Feng-Chau WU, 1989; Mishra et al., 2002] and hydrothermal [Ardizzone et al, 1998; Kaya et al., 2002; Feng et al., 2008] methods. For the preparation of zirconia, the mechanical mixing is generally followed. But, for use as an adsorbent or catalyst support, precipitation and impregnation or either sol-gel method is considered better as these methods help in forming bond between Zr and doped metal at atomic levels (more homogeneous mixture) [Chatry et al., 1994]. Sol-gel route is preferred as it produces materials with better texture such as high surface area, etc. Similarly, precipitation method followed by impregnation method, which produces highly homogeneous mixture, is followed to prepare sulfated zirconia (SZ) and metal promoted SZ.

### 3.2.1 Apparatus, Instruments, Reagents and Accessories required during preparations

Electric muffle furnace, magnetic stirrer, Whatman No. 42, 44, filter paper ash-less, normal filter paper discs, vacuum filtration assembly (1litre), distillation assembly, pH paper, silica crucible, sintered glass crucible, platinum crucible, nickel spatulas', disposable medical hand gloves, heating mantle, etc. were used for the preparation of adsorbents/catalysts.

Beakers (1000 ml, 500 ml, 250 ml, 100 ml), round bottom distillation flask 250 ml, conical flask (250 ml and 500 ml), pipette (25 ml, 50 ml), glass beads 2 mm (Pyrex), funnel (No.20, 40), etc. glasswares were used for the preparation of adsorbents/catalysts.

The following reagents were used to synthesize zirconia /sulfated zirconia (SZ) and Cr-promoted sulfated zirconia (CSZ):

i. Zirconium Oxychoride Octahydrate ($ZrOCl_2.8H_2O$), (96%, GR), (B.No.06066) CDH, New Delhi, India.
ii. Ammonia Solution ($NH_4OH$), (25%, sp.gr. 91, LR), (B.No.HJ7H570864), Merck, Mumbai, India.
iii. Ammonium Carbonate [$(NH_4)_2CO_3$], (96% LR), (B.No.61750105001049), Merck, Mumbai, India

iv. Silver Nitrate ($AgNO_3$), (N/50, LR), (B.No.37303) Qualignes, Mumbai, India.

v. Acetic Acid ($C_2H_4O_2$), (99.98% LR), (B.No.HF9H590386) Merck, Mumbai, India.

vi. Chromium (III) Nitrate [$Cr(NO_3)_3.9H_2O$], (98%, AR), (B.No.01120), CDH, New Delhi, India.

vii. Sulphuric Acid (35 % LR, Sp.Gr.1.84), (B.No.HE6H560392), Merck, Mumbai, India.

viii. Oxalic acid ($C_2H_2O_4.2H_2O$), (99% LR), (B.No.MA8M573425), Merck, Mumbai, India.

ix. Sodium hydroxide (NaOH), (97% GR), (B.No.MF9D590044), Merck, Mumbai, India.

x. Double-distilled water.

### 3.2.2 Preparation and standardization of Zirconium Oxychioride ($ZrOCl_2.8H_2O$) Solution

Pre-determined and pre-weighed amount of $ZrOCl_2.8H_2O$ was dissolved in 500 ml of double distilled water. It was then transferred to a 1 litre volumetric flask and the volume was made up to the mark by double distilled water. The weight of the salt per volume was so chosen so as to keep the strength of the solution approximately 0.10, 0.25, 0.50, 1.00 N. The exact strength of the solution was estimated by using the following standard procedure reported earlier [Vogel, 1966]:

5 ml of the above $ZrOCl_2$ solution was diluted to 250 ml in a volumetric flask. 10 ml of this diluted solution was pipette out into a 500 ml cleaned glass beaker. To this, l00 ml of 10% diammonium hydrogen phosphate (Merck) was added followed by 30 ml of concentrated sulphuric acid (sulphuric acid was added drop wise under constant stirring in order to avoid hazard due to highly exothermic nature of the reaction). The final volume was made to 300 ml with triply distilled water. Two more sets as above were prepared, and all the three were heated in a water bath for l h. These were then cooled to 323 K and the precipitate was filtered through Whatman No. 42 filter paper (ash-less). The residues were washed thoroughly first with double distilled water, and then with 1 M acid solution. Finally, to make the residue sulfate free, they

were washed with 10% aqueous ammonium nitrite solution. The residues along with the filter paper were transferred to platinum crucibles and dried at 100°C for three hours. Finally, they were calcined at 1273 K for 5 h in an electric muffle furnace and weighed as zirconium pyrophosphate ($ZrP_2O_7$). The strength of the original solution was estimated to be 0.235 N.

### 3.2.3 Preparation and Standardization of Sulphuric Acid Solution

190.21 ml of $H_2SO_4$ was dissolved in 500 ml of slightly hot double distilled water (prepared in the laboratory) with constant stirring along the side wall of 1 litre beaker. It was then transferred to a 1 litre volumetric flask and the volume was made up to the mark by double distilled water. The weight of the liquid per volume was so chosen to keep the strength of the solution approximately 7 N. The other acid solutions of different strength were made by diluting 7 N solution using equivalence equation. The exact strength of the solution was estimated by using the following standard procedure [Scott, 1959a]:

Sulphuric acid solution was standardized by back titration method using NaOH solution which was previously standardized by standard method [Lambert and Muir, 1965; Scott, 1959a].

### 3.2.4 Preparation and Standardization of Chromium Nitrate Solution

Pre-determined and pre-weighed amount of $Cr(NO_3)_3.9H_2O$ ($LD_{50}$ = 3250 mg/kg; solubility at 293 K = 81 g/100 ml) was dissolved in 250 ml of double distilled water (prepared in the laboratory). It was then transferred to a 500 ml volumetric flask and the volume was made up to the mark. The weight of the salt per volume was so chosen so as to keep the strength of the solution approximately 0.5, 1.0, 1.5 N. The exact strength of the solution and standardization was estimated by following the standard procedure reported earlier [Scott, 1959b].

### 3.2.5 Spot Test for Cr (III) in Presence of Cr (IV), Co and Ni Salt Interference

A drop of the test solution is mixed with a few cg of the disodium salt of chenta acid and then heated in a boiling water bath for 5 min. A red-violet color indicates the presence of Cr (III) salt provided Cu, Co and Ni salts are absent [Feigl et al., 2003].

### 3.2.6 Liquid Ammonia as a Precipitant in Zirconia Preparation

Liquid ammonia ($NH_3.H_2O$) also known as liquor ammonia ($NH_4OH$), is one of the most extensively studied non-aqueous solvents. It is a protonic solvent and its water like properties have made it a highly useful solvent and a reaction medium for carrying out several types of organic and inorganic reactions. $NH_3$ molecules are, however, less strongly associated through H-bonding in liquid ammonia. Physical properties of $NH_3$ and $H_2O$ are given in table 3.1. Consequently, the freezing and boiling point of liquid ammonia are lower than those of water. Another similarity is its polarity like water because of its pyramidal structure. Auto-ionization of liquid ammonia is somewhat similar to water represented as given below:

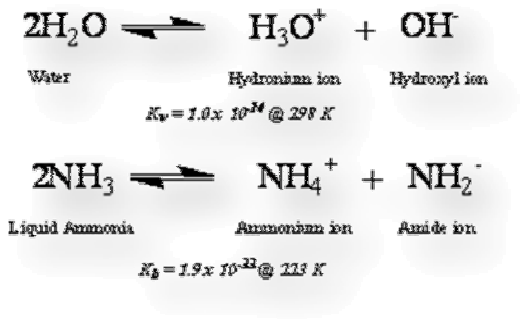


**Table 3.1 Physical properties of ammonia and water [Sharma et al., 2001a].**

| Properties | Water | Liquid Ammonia |
|---|---|---|
| Boiling Point (K) | 373.00 | 239.65 |
| Freezing Point (K) | 273.0 | 195.3 |
| Density (g/ml) | 0.9998 | 0.6874 |
| Dielectric Constant | 78.5 (@298 K ) | 722.0(@203.5 K ) |
| Specific Conductance ($ohm^{-1}cm^{-1}$) | $6.0x10^{-8}$(@298 K ) | $1.3x10^{-11}$(@203.5 K ) |
| Viscosity (cP) | 0.959 (@298 K ) | 0.254 (@203.5 K ) |
| Dipole Moment (D) | 1.850 | 1.470 |
| Trouton Constant (J/K-mol) | 109.0 | 101.2 |

### 3.2.7 Chromium as a Promoter (dopent) of SZ as Catalysts

Chromium (III) salts dissolve in water to give violet solution. The violet color is due to the hydrated Cr(III) ion, $[Cr\ (H_2O)_6]^{3+}$. This is a highly stable ion and can be exposed to air without any oxidation or reduction. It is now well established that six water molecules surrounding the Cr(III) ion are located at the apices of a regular octahedron. The solution of Cr(III) ion is slightly acidic on account of hydrolysis as [Sharma et al., 2001b]

$$[Cr(H_2O)_6]^{3+} \rightleftharpoons [Cr(H_2O)_5OH]^{2+} + H^+$$

Chromium nitrate $[Cr\ (NO_3)_3.9H_2O]$ has taken as a source of Cr(III) dissolved in double distilled water at room temprature with constant stirring. Cr(III) has been doped on SZ by wetness impregnation technique and the % adsorption of Cr(III) on the catalyst was determined by various analytical methods.

## 3.3 SYNTHESIS OF ZIRCONIA ($ZrO_2$), SULFATED ZIRCONIA (SZ) AND Cr-PROMOTED SULFATED ZIRCONIA (CSZ)

The method of preparation of SZ plays a vital role. The surface as well as bulk properties of the various zirconia change significantly with the preparation conditions. Till today, the most frequently used precursor for sulphation is dilute sulphuric acid or ammonium sulphate. One of the earlier reports revealed that sulphation of zirconia with dilute sulphuric acid and ammonium sulphate produced catalysts with both Lewis and Brönsted acidity [Morterra et al., 1997]. However, Kemnitz et al. [1998] reported that treatment of $(NH_4)_2SO_4$ with zirconia gives a catalyst with high Bronsted acidity and low Lewis acidity, whereas sulphuric acid generates sufficient amounts of Lewis as well as Bronsted acid sites. So, use of various precursors alters the Lewis and Bronsted acidity substantially. Summary of effect of preparation techniques, chemical and thermal treatment on activity of adsorbents/catalysts as given in literature is given in table 3.2.

In present study, the precipitation method followed by impregnation method was used to synthesize SZ and activate the synthesized material with thermal treatment and metal doping.

**Table 3.2 Effect of preparation techniques, chemical and thermal treatment on activity of adsorbents/catalysts.**

| Catalysts | Preparation Techniques | Thermal Treatment (K) | | Acidity (L/B) | Surface Area ($m^2/g$) | Remarks | Authors |
|---|---|---|---|---|---|---|---|
| | | Drying | Calcination | | | | |
| SDZ | Co-precipitation; Impregnation | - | - | Both | - | Crystallization & Phase Transformation | [Feng-Chau W.U, 1989] |
| SZ | Precipitation Method | 393@12h | 873@4h | Both | - | - | [Garin et al., 1991] |
| SZ | Precipitation Method | 383@15h | 873@3h | Both | - | - | [Parera.J.M, 1992] |
| SZ(5% S) | Precipitation Method | 197@5h | - | Both | 150 & 290 | Washing with hot distilled water | [Kustov et al., 1994] |
| SZ | Precipitation | 383@12h | 923@3h | Both | 104; 117 | Slight decrease in temperature on increasing calcination temprature | [Comelli et al., 1994] |
| SZ | Precipitation; Impregnation | 393@12h | 823@12h | Both | - | B-sites disappeared above 350 $^oC$; reappear on water adsorption | [Babou et al., 1995] |
| SZ | Precipitation Method | 383@12h | 793@3h | Both | 98 | - | [Kobe et al., 1996] |
| SZ(1.8% S) | Precipitation Method | 393@12h | 848@2h | Both | 98 | - | [Fogash et al.1996] |
| SZ | Precipitation Method | 363@12h | 820@3h | Both | 110 | Study of interaction of water with SZ by NMR Technique | [Semmer et al., 1996] |
| SZ | Hydrothermal/Sol-Gel. | 383@12h | 743@3h | Both | - | - | [Ardizzone et al, 1998] |
| SZ | Sol-Gel technique | 383@18h | 923@3h | Both | $ZS_2$ – 58.2;SZ – 113;ASZ - 99 | - | [Parvulesu et. al, 1999] |

| Catalysts | Preparation Techniques | Thermal Treatment (K) | | Acidity (L/B) | Surface Area ($m^2/g$) | Remarks | Authors |
|---|---|---|---|---|---|---|---|
| | | Drying | Calcination | | | | |
| Zirconia | Precipitation Method | 363@12h | - | Both | 170 - 205 | - | [Ardizzone and Bianchi, 1999] |
| SZ(1.6% S) | Precipitation; Impregnation | 393@24h | 893@4h | Both | 94 | Effect of rxn conditions and catalytic deactivation on the mechanism of n-butane Isomerization. | [kim et al., 2001] |
| SZ | Wetness Impregnation. | 393@18h | 793@2h | Both | 411 | - | [Mishra and Parida , 2001] |
| NSZ (1.45% S) | Precipitation; Impregnation | 383@6h | 873@3h | Both | 162 | - | [Mishra et al., 2001] |
| SZ | Wetness Impregnation. | 393@12h | 793@3h | Both | - | - | [Mishra & Parida, 2002] |
| SZ(1.45% S) | Co-precipitation; Impregnation | 358@18h | 1098@3h | Both | - | Studies on the effect of CO & $CO_2$ on n-butane Isomerization | [Mishra et al., 2002] |
| SZ (9.9% $SO_3$) | Precipitation Method | 383@18h | 873@2h | B-50µmol/g | 60 | - | [Luzgin et al., 2003] |
| SZ | Sol-Gel technique | 353@48h | 923@3h | Both | - | - | [Kuba et. al, 2003] |
| NSZ | Wetness Impregnation. | 383@24h | 873@3h | Both | 162;0.39 $cm^3/g$ | - | [Mishra et. al, 2003] |
| HZ | Homogenous Precipitation | - | - | Both | 148 | - | [da.Silva et al., 2004] |

| Catalysts | Preparation Techniques | Thermal Treatment (K) | | Acidity (L/B) | Surface Area ($m^2/g$) | Remarks | Authors |
|---|---|---|---|---|---|---|---|
| | | Drying | Calcination | | | | |
| SZ | Precipitation Method | 393@4h | 873@2h | Both | SZ WW – 30; SZ - 109 | Water Washed SZ(WW) | [Xuebing Li et al., 2004] |
| SZ | Precipitation Method | 383@2h | 873@3h | Both | - | - | [Xuebing Li et al., 2004] |
| SZ | Precipitation; Impregnation | 393@2h | 873@3h | Both | - | Max. conversion@ 463 K is 22% | [Bogdan et al., 2004] |
| SZ clay | Intercalation | 373@2h | 773@3h | Both | 199 – 275 | Using ethanol sodium dodasyl sulfate(SDS);Crystallite size – 25 nm. | [Bergaoui.L et al., 2004] |
| SZ | Precipitation; Impregnation | 373@12h | 723@3h | Both | - | Supercritical conditions. | [Funamoto.T et al., 2005] |
| SZ | Precipitation Method | | - | Both | - | Sulfation through $SO_3$ induce high activity | [Xuebing Li et al., 2006] |
| SZ | Precipitation; Impregnation | 383@12h | 873@3h | Both | - | the properties of SZ affected by the amount of sulfate ion loading. | [Sugeng et al., 2006] |
| SZ | Precipitation Method | 363@12h | 873@2h | Both | - | - | [Lohitharn et al., 2007] |
| Silica Supported nano crystalline SZ | Sol-Gel technique | - | - | Both | - | Si/Zr ratio is important; on this basis gelation ratio changes. | [Akkari et al., 2007] |

NB: SZ – Sulfated Zirconia; HZ – Hydrous Zirconia; NSZ – Nano Sulfated Zirconia; SDZ- Stabilized doped Zirconia.

### 3.3.1 Preparation of Zirconia

Schematic block diagram of experimental set-up used for the preparation of zirconia is shown in figure 3.1 and the procedure adopted for the preparation of zirconia is given in figure 3.2. Tables 3.3a and 3.3b shows the conditions applied during the preparation of zirconia samples.

Zirconia can be prepared from different precursors such as $ZrOCl_2.8H_2O$ [Arata and Hino, 1988; Sohn and Jang, 1991], ZrO $(NO_3)_2.2H_2O$ [Garvie, 1965; Yamaguchi et al., 1986], Zr isopropoxide [Bensitel et al., 1987; Morterra et al., 1993], and $ZrCl_2$ [Srinivasan et al., 1992; Ardizzone and Bassi, 1990].

High surface area $(ZrO_2)_x(OH)_{2x}$ (332 $m^2/g$) was prepared by precipitation from zirconium oxychloride solutions with liquor ammonia [Comelli et al., 1995] and few drops of ammonium carbonate solution. Figure 3.3 shows the solution after complete precipitation. This precipitate was refluxed for 6 h and aged for 12 h. Water was removed from the top of the aged solution and the slurry obtained after this process is shown in figure 3.4. The slurry was filtrated and washed repeatedly with $NH_4OH$ solution at controlled pH 10 [Davis, 1984] and hot double distilled water until the elimination of $Cl^-$ ions [Comelli et al., 1995] which was checked by standard method [Jolly, 1963].

Chloride free precipitates before and after vacuum filtration is shown in figure 3.5 and figure 3.6, respectively. Chloride free hydrous zirconia after vacuum filtration and crushing is shown in figure 3.7. Crushed chloride free hydrous zirconia after vacuum filtration was subjected to thermal treatment at 383 K for 24 h. Zirconia powder after drying at 393 K and crushing is shown in figure 3.8. Heating hydrous zirconium oxide at a reasonably rapid rate, an exotherm is observed by [Rijmten, 1979; Srinivasan et al., 1993; Torrolvo et al., 1984] at a temperature about 723 K although the exact temperature may vary slightly for different preparations. This event has been attributed to the conversion of an amorphous material to a crystalline phase. The incorporation of sulfate causes a shift of the exotherm position to a higher temperature [Davis et al., 1984; Torrolvo et al., 1984]. After drying at 383 K for 24 h and sieving to 50, 100, 300 micron (Zirconia powder after calcination at 893 K, crushing and sieving to 50 micron is shown in figure 3.9), the samples were treated thermally in flowing dry air for 3 h at 893 K and nitrogen at 473 K for about 24 h and stored in a desiccator for further use [Kumar et al., 2011, 2012].

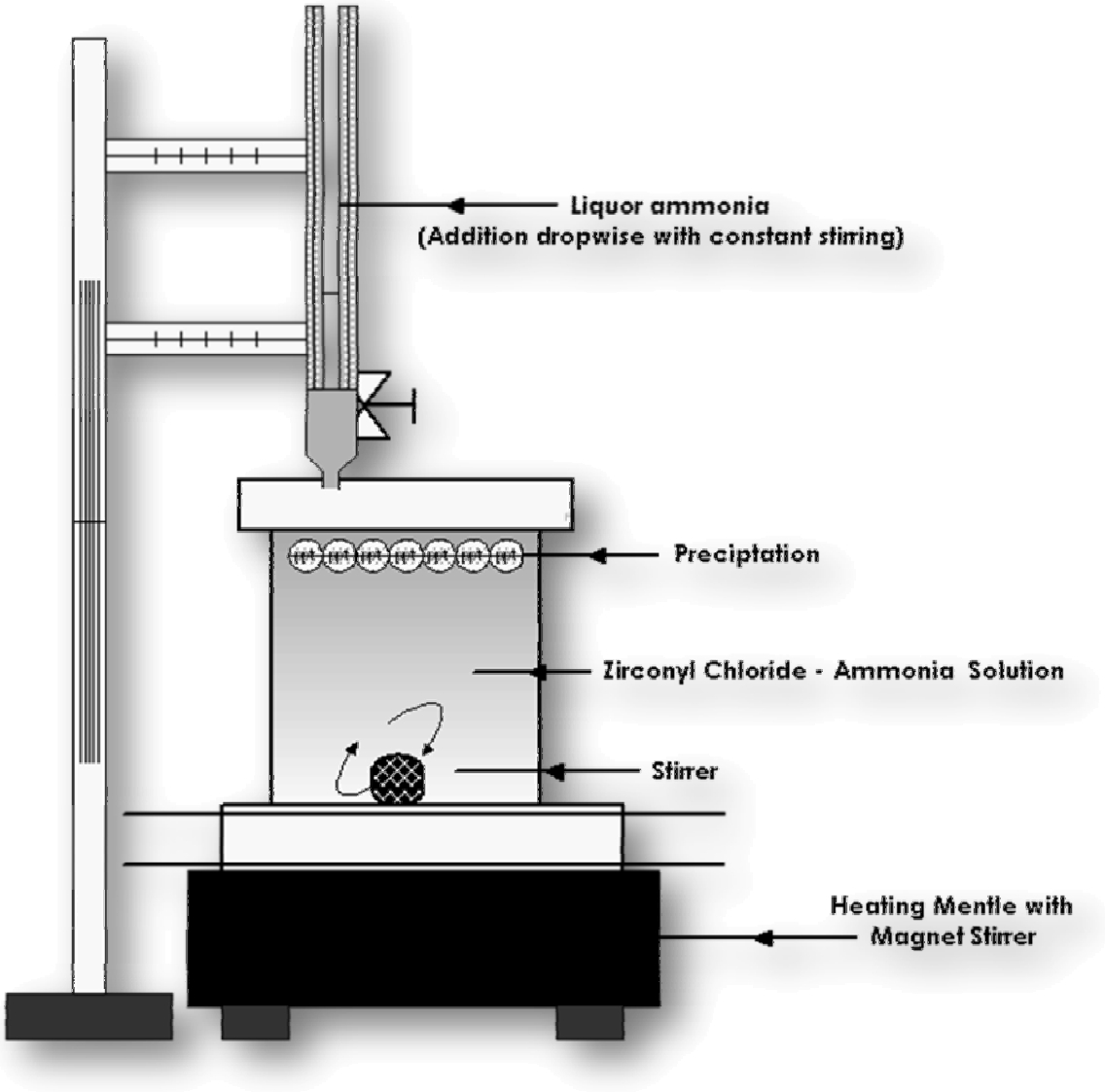


**Figure 3.1 Schematic block diagram of experimental set-up used for the preparation of zirconia.**

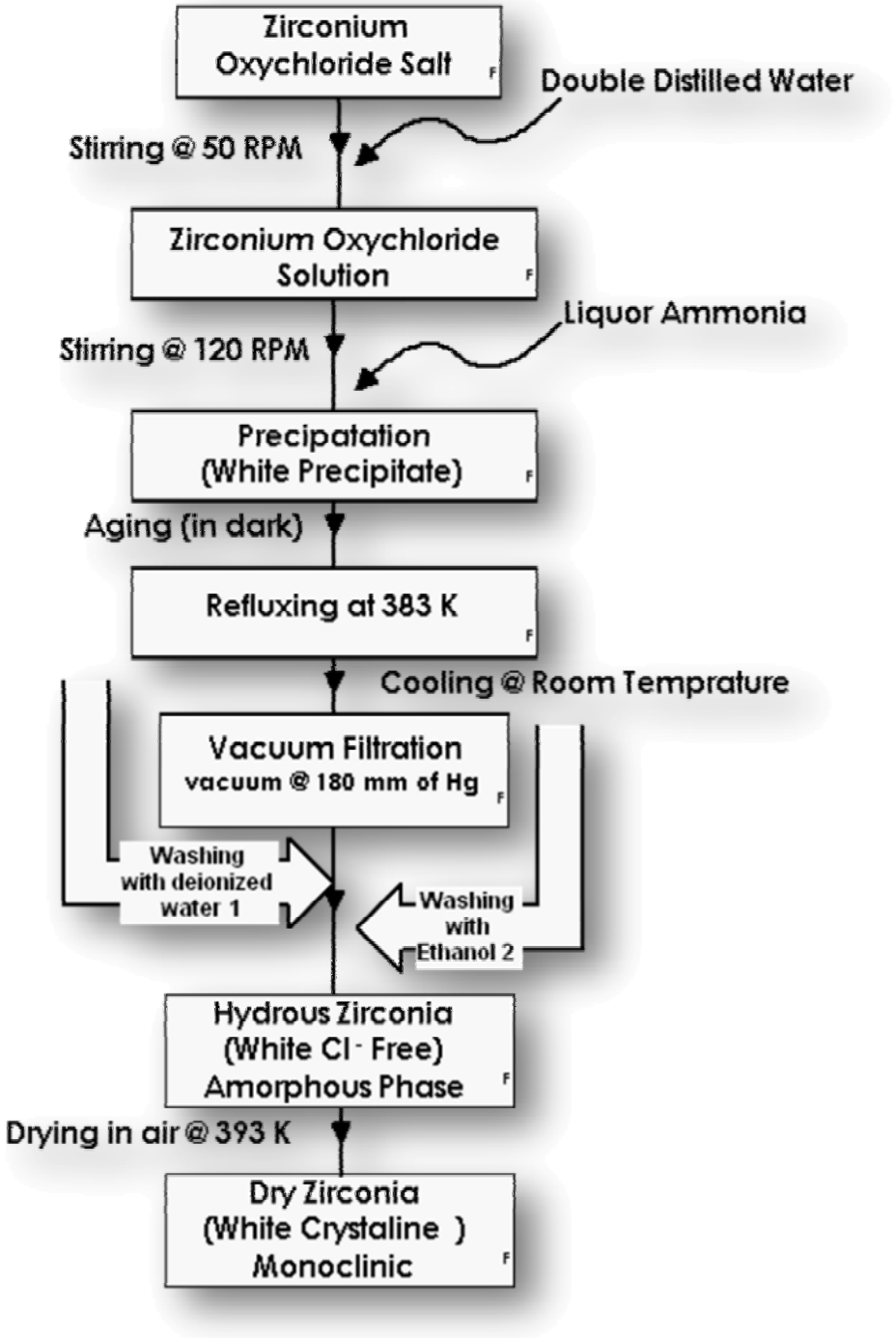


**Figure 3.2 Schematic block diagram of preparation of zirconia based samples**


**Figure 3.3 Hydrous zirconia after precipitation for 4 hour.**

**Figure 3.4 Hydrous zirconia after refluxing-aging at 353 K for 6 h.**

**Figure 3.5 Chloride free hydrous zirconia before vacuum filtration.**

**Figure 3.6 Chloride free hydrous zirconia after vacuum filtration.**

**Figure 3.7 Chloride free hydrous zirconia after vacuum filtration and crushing.**

**Figure 3.8 Zirconia powder after drying at 393 K and crushing.**

**Figure 3.9 Zirconia powder after calcination at 893 K, crushing and sieving to 50 micron.**

**Table 3.3a Preparation conditions for zirconia samples.**

| Precursor sol. (N) | pH change during precipitation | | Stirring Time | | Refluxing Time (h) | Digestion Time (h) | Drying Temp (K) | Calcination Temp (K) |
|---|---|---|---|---|---|---|---|---|
| | Initial | Final | Solution preparation (h) | Precipitation (h) | | | | |
| 0.10 | 0.74 | 11.00 | 0.25 | 3 | 6 | 18 | 393 | 753 & 893 |
| 0.15 | 0.94 | 11.45 | 0.25 | 3 | 6 | 18 | 393 | 753 & 893 |
| 0.20 | 0.95 | 10.24 | 0.50 | 4 | 6 | 18 | 393 | 753 & 893 |
| 0.25 | 1.18 | 10.80 | 0.50 | 4 | 6 | 72 | 393 | 753 & 893 |
| 0.50 | 1.27 | 11.00 | 0.75 | 4 | 8 | 72 | 393 | 753 & 893 |
| 1.00 | 1.45 | 11.80 | 1 | 6 | 8 | 72 | 393 | 753 & 893 |
| 1.50 | 1.48 | 11.07 | 1.5 | 6 | 8 | 96 | 393 | 753 & 893 |
| 2.00 | 1.98 | 12.00 | 2 | 6 | 8 | 96 | 393 | 753 & 893 |

**Table 3.3b Preparation conditions for zirconia samples.**

| Precursor sol. (N) | Wt. of dry zirconia taken (g) | Stirring time for slurry preparation (min) | Refluxing Time (h) | Digestion Time (h) | Drying Temp (K) | Calcination Temp (K) |
|---|---|---|---|---|---|---|
| 0.5 | 40 | 0.50 | 6 | 8 & 12 | 383 | 753 & 893 |
| 1.0 | 40 | 0.75 | 6 | 8 & 12 | 383 | 753 & 893 |
| 2.0 | 40 | 0.75 | 6 | 8 & 12 | 383 | 753 & 893 |
| 3.0 | 40 | 1 | 6 | 8 & 12 | 383 | 753 & 893 |
| 4.0 | 40 | 1 | 8 | 8 & 12 | 383 | 753 & 893 |
| 5.0 | 40 | 1.5 | 8 | 8 & 12 | 383 | 753 & 893 |
| 6.0 | 40 | 1.5 | 8 | 8 & 12 | 383 | 753 & 893 |
| 7.0 | 40 | 1.5 | 8 | 8 & 12 | 383 | 753 & 893 |

### 3.3.2 Sulfation Methods

SZ powders show strong acid features and consequently have recently attracted great interest due to their potential as solid ‘‘super acid’’ catalysts for numerous processes as selective hydrocarbon isomerization, acylation and esterification reactions [Arata, 1996; Arata and Hino, 1990; Yamaguchi, 1990; Chuah et al., 1996; Denkewiez et al., 1990; Clearfield et al., 1994; Yamaguchi, 1986; Srinivasan et al., 1991; Parera, 1992; Srinivasan and Davis, 1992; Waquif et al., 1992; Song and Sayari, 1995; Davis et al., 1994; Chen et al., 1993; Ishida et al., 1988]. Several parameters may affect the features of the powders, primarily the conditions adopted for the oxide preparation, for sulphate addition and the temperature selected for calcination.The addition of the $SO_4^{2-}$ ions to zirconia produces a very strong acid [Yamaguchi et al., 1987; Tanabe, 1984; Waqif et al., 1992].

The route followed to obtain the oxide precursor to be doped with $SO_4^{2-}$ ions plays a major role in imposing the final characteristics of the material [Morterra et al., 1994]. For example, in the case of hydrothermal preparations, even slight variations of the composition of the precipitating mixture (i.e., pH) provoke relevant modifications in the phase composition of $ZrO_2$, these in turn implying differences in specific surface area, degree of hydration and surface electrification [Ardizzone and Bianchi, 1999].

Different procedures for the doping of zirconia with sulphates are reported in the literature (Table 3.4): the more common are impregnation or incipient wetness methods by using either sulphuric acid or $(NH_4)_2SO_4$ solutions [Davis et al, 1994; Wen et al., 1990; Garin et al., 1991; Jatia et al., 1994].

**Table 3.4 Details of SZ preparation methods [Sohn and Kim, 1989].**

| Material | Source of Sulfur | Preparation Method |
|---|---|---|
| $ZrO_2/SO_4^{2-}$ (S) | $H_2SO_4$ | Wet treatment and evacuated at 673 K |
| $ZrO_2/SO_4^{2-}$ (A) | $(NH_4)_2SO_4$ | Impregnation and calcination at 673 K |
| $ZrO_2/SO_4^{2-}$ (S)–$H_2$ | $H_2SO_4$ | $ZrO_2/SO_4^{2-}$ (S) reduced with excess $H_2$ at 773 K |
| $ZrO_2/SO_2$ | $SO_2$ | $ZrO_2$ treated with $SO_2$ at 293 K |
| $ZrO_2/SO_2 – O_2$ | $SO_2$ | $ZrO_2$/ $SO_2$ oxidized with excess $O_2$ at 673 K |
| $ZrO_2/H_2S$ | $H_2S$ | $ZrO_2$ treated with $H_2S$ at 293 K |
| $ZrO_2$/ $H_2S – O_2$ | $H_2S$ | $ZrO_2$/ $H_2S$ oxidized with excess $O_2$ at 673 K |
| $ZrO_2/CS_2$ | $CS_2$ | $ZrO_2$ treated with $CS_2$ at 293 K |
| $ZrO_2/CS_2 – O_2$ | $CS_2$ | $ZrO_2/CS_2$ oxidized with excess $O_2$ at 673 K |

Table 3.5 shows the effect of acid source and weight loaded on the property of SZ. In the case of sol–gel preparations of $ZrO_2$, sulphation may also be produced directly during the oxide preparation by using sulphuric acid as the polycondensation catalyst [Strukul et al., 1996]. In the sulfation by adsorption method, the dried chloride free zirconia slurry is dispersed in different normality (0.5 N to 7.0 N) aqueous sulfuric acid solution [Davis et al., 1994] in the ratio 8 ml of solution per gram of zirconia. The resultant suspension is kept under stirring conditions for l h at room temperature. It is then filtered through a G-4 crucible (not washed) and dried at 393 K for about 24 h and stored in a desiccator for further use **[Parera, 1992].**

**Table 3.5 Properties of SZ obtained with different sulfur compounds in the percolating solution and after heating for 3 h in nitrogen at 893 K [Parera, 1992].**

| S Compounds | S Concentration (Wt %) | Specific Surface Area ($m^2/g$) |
|---|---|---|
| $H_2SO_4$ | 1.48 | 104.1 |
| $(NH_4)_2SO_4$ | 0.81 | 95.3 |
| $(NH_4)_2S_2O_3$ | 0.45 | 45.4 |
| $(NH_4)_2S$ | 0.16 | 45.6 |

Farcasiu et al. [1995, 1997] have proposed a modified impregnation procedure known as sulfation by wetness impregnation method. It is based on the use of a pre-set quantity of sulphuric acid followed by evaporation, to control the final sulphur content of the material more accurately. Also in the case of $SO_4^-$ doping, large differences in the final sulphur content and features of the powders can appear as the consequence of slight variations in the doping procedure.

Sulfation by wetness impregnation method was used in the present study. The schematic block diagram of preparation of sulfated zirconia is given in figure 3.10. In the preparation of SZ method, the nominal sulfate loading on the zirconia surface was varied from 2 to l2 wt%. In a typical experiment, the 393 K dried gel was dispersed in double distilled water and stirred for about 30 min. To this, required amount of different normality (0.5 N to 7.0 N) acid solutions were added by adopting variable acid volume/powder weight ratios i.e., 12, 16, 33, 66, 132 ml/g. It was then evaporated to dryness under stirring conditions by a hot plate cum stirrer (Remi Instruments) maintained at about 383 K. The impregnated samples were firstly dried at 393 K for 24 h and finally in flowing dry air for 3 h at 893 K and nitrogen at 473 K for about 24 h cooled and stored in a desiccator for further use (shown in figure 3.11).

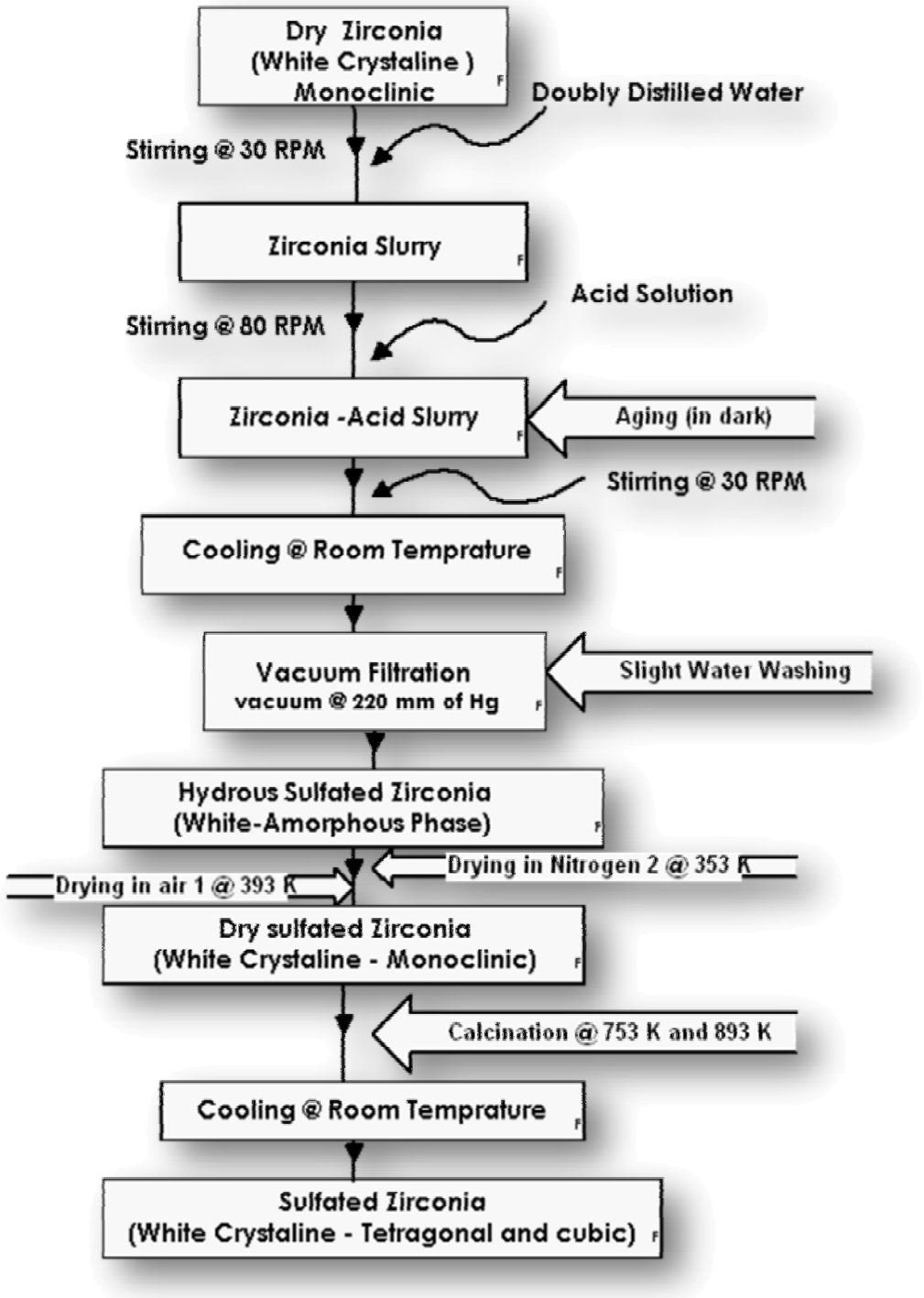


**Figure 3.10 Schematic block diagram of preparation of sulfated zirconia.**

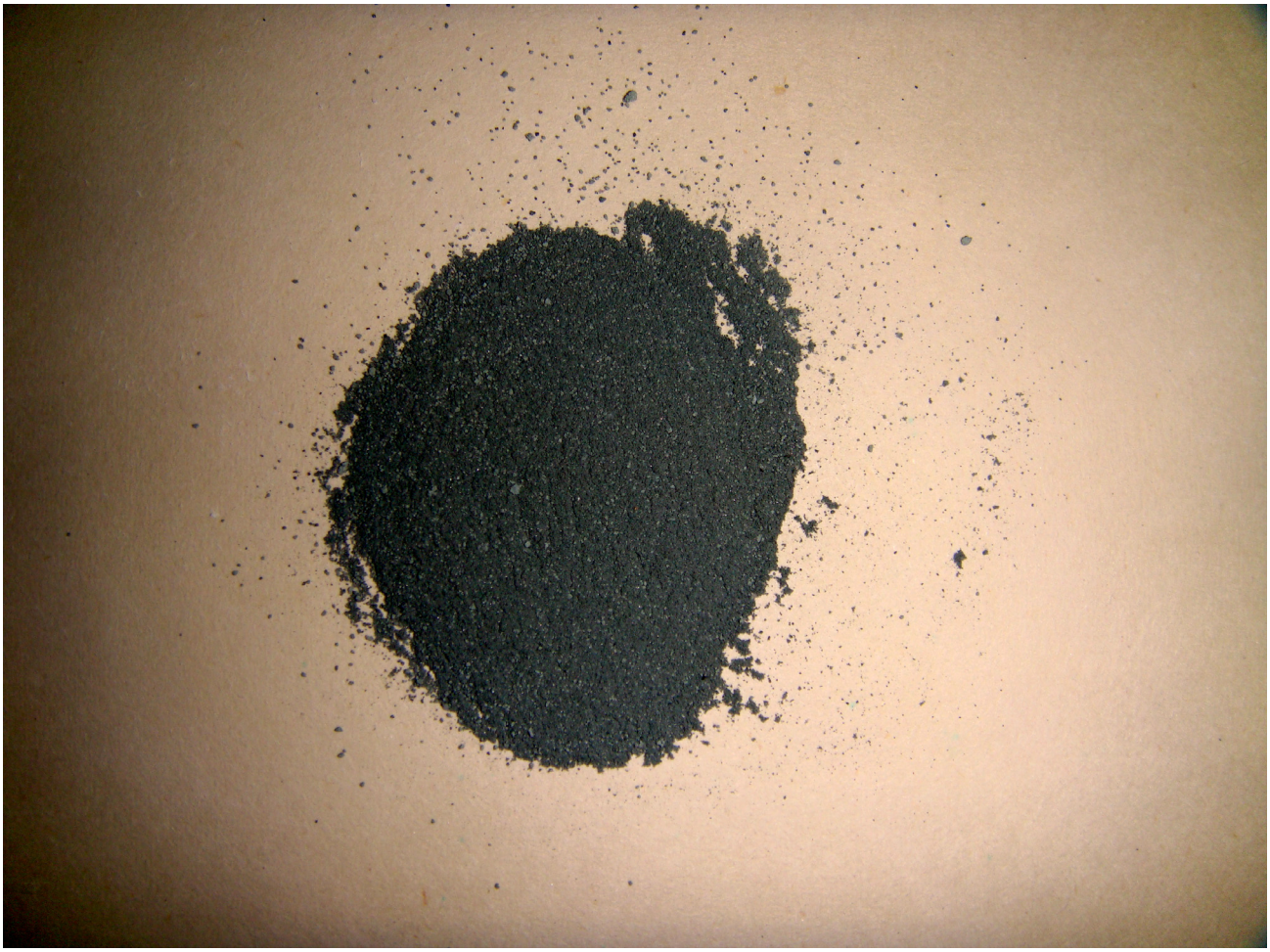

**Figure 3.11 Sulfated zirconia powder after calcination at 893 K, crushing and sieving to 50 micron.**

### 3.3.3 Synthesis of Chromium Promoted Sulfated Zirconia

For the synthesis of chromium promoted sulfated zirconia (CSZ), SZ prepared previously in the laboratory was used as a precursor. The schematic block diagram of preparation of CSZ is given in figure 3.12.

Before impregnation of chromium, the SZ was dried for 24 h at 383 K and cooled to room temperature in a desiccator. Promoters were introduced via the incipient wetness method. Aqueous solution of Cr $(NO_3)_3 \cdot 9H_2O$ was added drop wise with vigorous stirring in a porcelain mortar; 6 ml solution per 12 g powder was always used. The resultant mixture was evaporated to dryness under stirring condition with the help of a hot plate cum stirrer. The wet form of Cr promoted SZ is shown in figure 3.13. The metal promoted samples were dried at 393 K for over-night in flowing dry air in an electric oven, cooled and stored inside a desiccator for further use. Finally, the prepared sample dried in flowing dry air for 3 h at 893 K and nitrogen at 473 K for about 24 h cooled, sieved to 50 micron size (shown in figure 3.14) was stored in a desiccator for further use.

### 3.3.4 Thermal Treatment of Untreated and Treated Zirconia

Calcination was performed in a quartz boat with a volume of 50 ml which was placed in a quartz tube that was purged with 200 ml/min of dry air [Hahn et al., 2001]. The temperatures were selected according to recommendations in the literature; good performance is reported for unprompted SZ after calcination at 823 K [Morterra et al., 1994] and for promoted SZ after calcination at 923 K [Song and Kydd, 1998]. The heating and cooling ramps (as far as possible) were 10 K/min, and the holding time at 753 K or 893 K was 6 h. After cooling, the samples were sieved to 50, 100 and 150 micron and kept in glass sample bottles for further use. Figure 3.15 shows CSZ after calcination at 893 K, crushed and sieved to 50 micron.

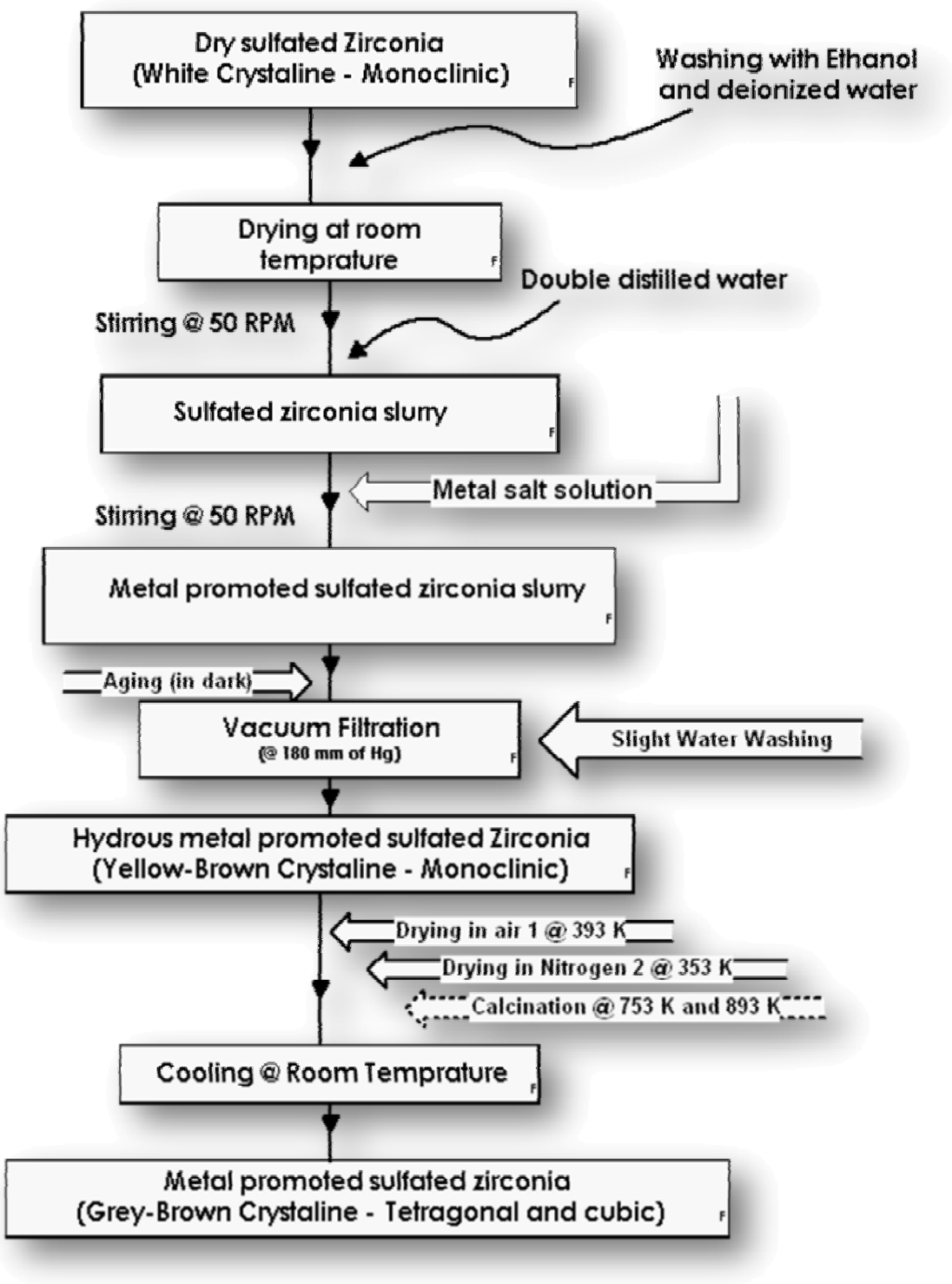


**Figure 3.12 Schematic block diagram of preparation of Cr promoted sulfated zirconia**

**Figure 3.13 Cr promoted, sulfated zirconia slurry before drying.**

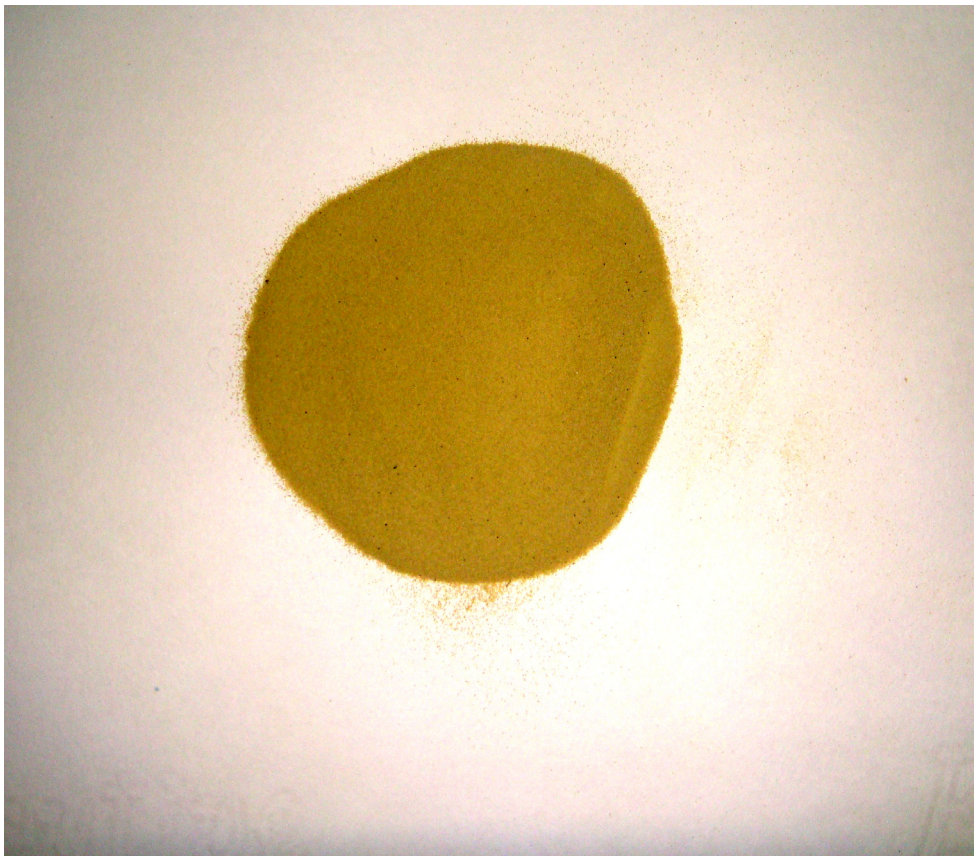

**Figure 3.14 Cr promoted, sulfated zirconia powder after drying at 393 K, crushing and sieving to 50 micron.**

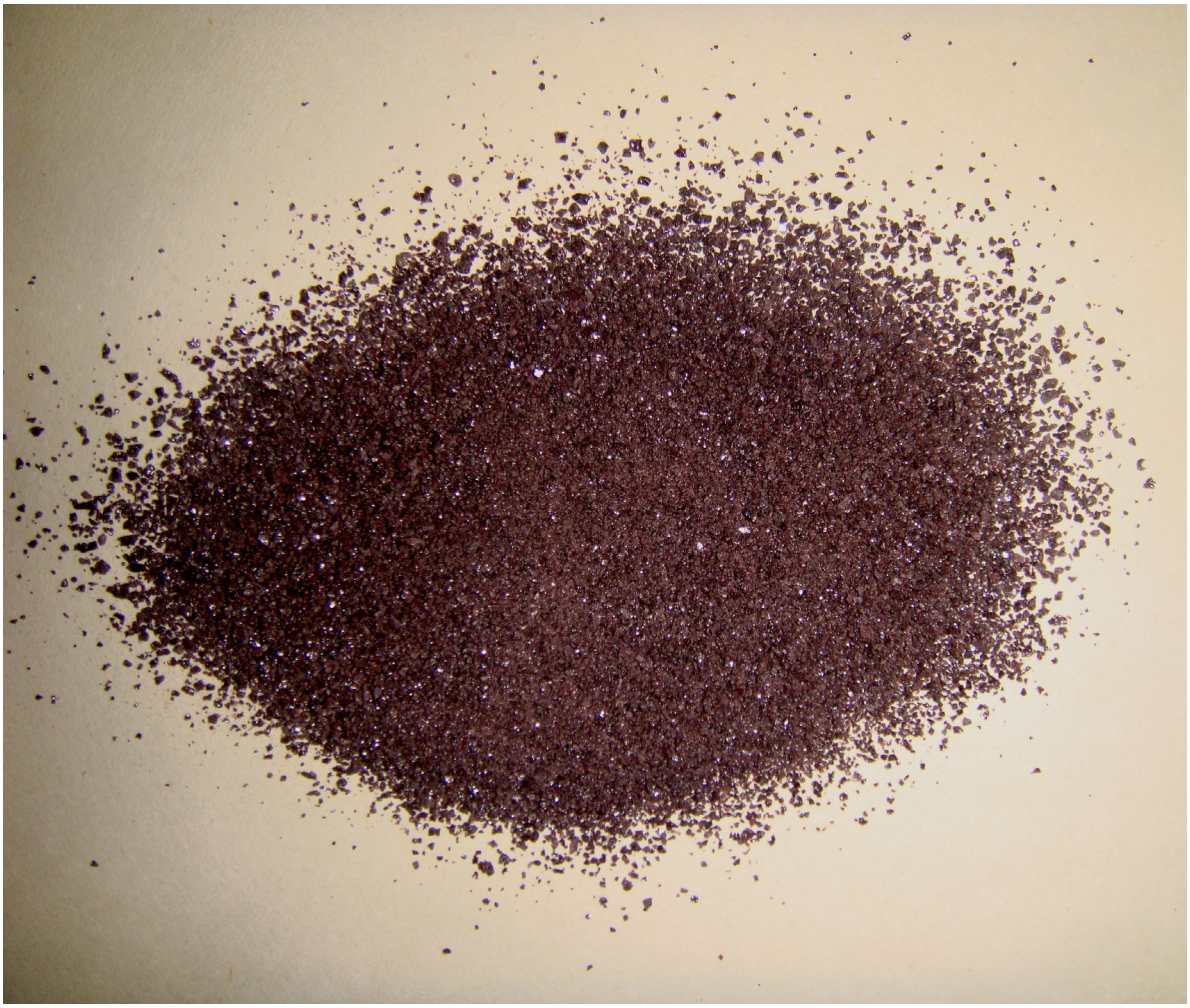

**Figure 3.15 Cr promoted, sulfated zirconia powder after calcination at 893 K, crushing and sieving to 50 micron.**

# Chapter – IV

# EXPERIMENTAL PROGRAMME

This chapter deals with the materials and methods of analysis, and the experimental procedures adopted to collect the experimental data.

## 4.1 MATERIALS

### 4.1.1 Adsorbents/Catalysts

Adsorptive desulfurization (ADS) of dibenzothiophene (DBT) present in model oil (DBT dissolved in iso-octane) at different concentration level was studied using three adsorbents, namely, powdered zirconia dried at 393 K (ZD393), powdered zirconia calcined at 893 K (ZC893), and powdered sulfated zirconia calcined at 893 K (SZC893) which were synthesized in the laboratory as per methods given in previous chapter.

Oxidative desulfurization (ODS) of DBT present in model oil at different concentration level was studied using four catalysts, namely, ZD393, ZC893, SZC893 and powdered chromium-promoted sulfated zirconia calcined (CSZC893).

### 4.1.2 Model hydrocarbon and Other Chemicals

All the chemicals used in the study were of analytical reagent (AR) grade. DBT and iso-octane was procured from Merck, Germany.

DBT was used for the preparation of model oil in iso-octane with initial concentration ($C_o$) varying in the range of 30-1000 mg/l. For this, the required quantity of DBT was accurately weighed and dissolved in a small amount of iso-octane with constant shaking in a 1 litre volumetric flask fixed on a water bath shaker for one hour for complete solubility. The final volume in the volumetric flask was made up to 1 litre by adding iso-octane. Fresh stock solution was prepared as required every day. The $C_o$ was ascertained before the start of each experimental run accordingly. This model oil was used in both ADS and ODS.

AR grade hydrogen-peroxide ($H_2O_2$) (30% by volume) and methanoic acid ($H_2CO_2$) (41% by volume) solutions were procured from Merck, Mumbai, India.

## 4.2 ADSORBENTS/CATALYSTS CHARACTERIZATION

Numerous analytical techniques are used for the characterization of adsorbents/catalysts. Some of these techniques as used by many investigators are listed in table 4.1. The in-house prepared zirconia samples ready to use and reagent for model oil are shown in figure 4.1. In the present study, the physico-chemical characteristics of the adsorbents/catalyst supports were determined by using standard procedure as discussed below:

### 4.2.1 Particle Size

Particle size analysis of the adsorbents was carried out using particle size analyser CIS 100 and LFC101, Ankersmid, Netherland.

### 4.2.2 Density

Bulk densities of the various zirconia based samples (adsorbents/catalyst) were determined by using MAC bulk density meter found to be 0.8990- 0.9993 g/cm$^3$.

### 4.2.3 Acidity

Acidity/Basicity of the prepared solutions was calculated using CyberScan 510 pH meter as per ASTM P228 Method and Radojevic and Baskin [2006].

### 4.2.4 X-Ray Diffraction (XRD) Analysis

The structures of the different adsorbents/catalysts were studied with the help of an X-ray diffractometer (Bruker AXS, Diffractometer D8, Germany) using ASTM D 3960 method, available in the Institute Instrumentation Centre (IIC), IIT, Roorkee, India. The XRD analysis was done using Cu-Kα as a source and Ni as a filter. Goniometer speed was kept at 2º/ min. The range of scanning angle (2θ) was kept at 10-90º. The angular resolution was 0.05$^o$ and 0.01$^o$ for characteristic peaks. The X-ray source was operated at 30 mA and 40 kV. Sample preparation for the X-ray analysis involved gentle grinding of the solid into a fine powder and packing of approximately 0.3–0.5 g of the sample into an aluminium sample holder with light compression to make it flat and tight. The X-ray diffraction patterns of the sample were then recorded and saved in RAW text format for further manipulation. The intensity peaks indicate the values of 2θ, where Bragg's law is applicable. The above diffractometer characteristics made it possible to determine unit cell parameters to an accuracy of 0.02 Å. The identification of compounds was determined by using the ICDD library.

**Table 4.1 Applications of analytical techniques in characterization of different adsorbents/catalysts**

| Analytical techniques | Parameter | Analysis Conditions | References |
|---|---|---|---|
| X-ray Diffraction Analysis (XRD) | Crystallographic phase identifications | The samples were scanned in the range $2\theta = 5 - 80^{\circ}$ at a scanning rate of 2◦/min. | [Mishra et al., 2002; Mishra et al., 2001; Vaudagna et al., 1996; Pichardo et al., 2008; Jentoft et al., 2004; Valigi et al., 2002] |
| X-Ray Absorption Spectra (XRA) | - | The electron storage ring was operated at 8 GeV with a stored current of 75–100 mA. | [Wang et al., 2005; Jentoft et al., 2004] |
| XAS Measurements XANES & EXAFS | To studies on Fe–K-edge and W–LII, III-edge | The electron storage ring was operated at about 1.5 – 8.0 GeV with a ring current of about 75 - 200 mA. | [Valigi et al., 2002; Wong et al., 2005] |
| Extended X-Ray Absorption Fine Structure (EXAFS) | - | - | [Wang et al., 2005] |
| X-Ray Photoelectron Spectroscopy (XPS) | Oxidation state | The spectra were recorded for the 385–420 eV regions to determine the N 1 s present in the sample. | [Wang et al., 2005; Ardizzone et al., 1999; Hino et al., 1980; Garcıa et al., 2001] |
| Thermal Gravimetric Analysis (TGA) / Differential Scanning Colorimetric (DSC) | To determine the thermal properties | Thermal analyses (TG/DSC) were performed on a instrument in flowing air (40 ml/min) with temperature rate set at 10 K/min in the 298–1273 K. temperature range. | [Li et al., 2005; Srinivasan et al., 1994; Akkari et al., 2007; Zane et al., 2006] |

| Analytical techniques | Parameter | Analysis Conditions | References |
|---|---|---|---|
| Temperature-Programmed Oxidation (TPR) | Identify oxidizing species present on the catalyst surface. | The heating rate was 10 K/ min and the flow rate of air was 60 ml/min. | [Wong et al., 2005] |
| Temperature-Programmed Reduction (TPR) | Identify reducing species present on the catalyst surface. | A reducing gas consisting of 2.7 mol% $H_2$ in $N_2$ was passed at the rate of 35 ml/min. The temperature was ramped from room temperature to 1273 K at 10 K/ min. | [Abu et al., 2003; Mishra et al., 2001; Xu et al., 1997; Garcıa et al., 2001] |
| Temperature-Programmed Desorption (TPD) | To determine the distribution of both strong and weak acid sites on the catalyst surface | The TPD experiment was performed using nitrogen as the carrier gas at a heating rate of 10 K/min from 313 to 1073 K.. | [Abu et al. 2003; Mishra et al., 2001; Vaudagna et al., 1997] |
| Brunauer–Emmett–Teller (BET) surface area analyzer | Surface area, Pore Volume | The experiments were performed at liquid nitrogen temperature (77 K). All samples were degassed at 473 K and $10^{-4}$ Torr pressure to remove the physically absorbed moisture from the catalyst surface. | [Abu et al. 2003; Mishra et al., 2002; Mishra et al., 2001; Zane et al., 2006 ] |
| Electron Paramagnetic Resonance (EPR) | To determine the paramagnetic | The samples the EPR tube heated in high vacuum (10−4 hPa) for 1 h at 423 K in the EPR tube and then measured. | [Torralvo et al., 1984; Liu et al., 1995; Che et al., 1983; Morterra et al., 2001; Jentoft et al., 2004] |

| Analytical techniques | Parameter | Analysis Conditions | References |
|---|---|---|---|
| Nuclear Magnetic Resonance (NMR) Spectroscopy | - | The spinning ratewas 10 kHz and the delay between two pulses was varied between 1 and 30 s to ensure that a complete relaxation of the 31P nuclei occurred. The chemical shifts are given relative to external 85% $H_3PO_4$. | [Devassy et al., 2005] |
| Raman Spectroscopy | - | The sample was heated in flowing dry oxygen at 773 K, for 3 h and the spectra were collected at this temp. and after cooling to 298K always in dry oxygen. | [Valigi et al., 2002] |
| Fourier transform infra-red spectroscopy (FTIR) | Surface hydroxyl groups and structure of catalytic species | - | [Mishra et al., 2001; Devassy et al., 2005] |
| Infra Red (IR) Spectroscopy of adsorbed bases | Nature of bonding of different groups | The spectra were scanned in the range 4000–200 $cm^{-1}$ with a resolution of 2 $cm^{-1}$. Prior to the measurements, all samples were dried at 250°C. | [Mishra et al., 2002] |
| Photoacoustic (FTIR-PA) Spectroscopic Studies | To determine the nature of acid sites | Samples pre-treated under nitrogen (35 ml/h) at 150°C for 15 min. with addition of 30ml of pyridine were adsorbed at the same temperature. Each sample flushed with nitrogen for 15 min. | [Mishra et al., 2002; Mishra et al., 2001] |
| Ultraviolet–Visible Diffused Reflectance Studies (DRS) | To determine the nature of surface | The spectra were recorded against boric acid as the reflectance standard; in the range 200–800 nm. | [Mishra et al., 2002] |

| Analytical techniques | Parameter | Analysis Conditions | References |
|---|---|---|---|
| CHNS Analyses | Carbon, Hydrogen, Nitrogen, Sulphur | - | [Mishra et al., 2002] |
| Inductively Coupled Plasma Atomic Emission Spectrometry (ICP-AES) | Elemental Analysis | All the samples were predissolved in $HNO_3/H_2SO_4/HF$ mixed acid and quenched by a large amount of boric acid ($H_3BO_3$). | [Wang et al., 2005; Mishra et al., 2001] |
| High-Resoln. Transmission electron microscopy (HRTEM). | | - | [Wang et al., 2005; Pichardo et al., 2008] |
| Microcalorimetric Studies | To determine the distribution of acid site strengths. | - | [Xia et al., 1999; Fogash et al., 1995] |
| Ion Scattering Spectroscopy | To determine the nature of Surface. | - | [Jentoft et al., 2004] |
| Evolved Gas Analysis (EGA) | To determine the substances released during the TG/DSC thermal Treatment. | A 10 K/min temperature ramp was applied while 40 ml/min of air passed through the sample. | [Zane et al., 2006] |
| Quadrupole Mass Spectroscopy (QMS) | To determine the Molecular Weight | - | [Zane et al., 2006] |
| Ion Chromatographic | To determine the Metal/Non-Metal contents | - | [Sarzanini et al., 1995] |


**Figure 4.1 Prepared samples of zirconia (Normal, Sulfated and Metal promoted) oxidant and acid used in experiments.**

### 4.2.5 Scanning Electron Microscopic (SEM) and Energy-dispersive X-ray analysis (EDAX) Analysis

To understand the morphology of the adsorbents/catalysts before and after ADS/ODS, the SEM micrographs were taken using QUANTA, Model 200 FEG, Neatheland. The particles were first gold coated using Sputter Coater, Edwards S150, to provide conductivity to the samples. The SEM micrographs and simultaneously elemental analysis was done using an EDAX spectrometry.

### 4.2.6 Fourier Transform Infra Red (FTIR) Spectral Analysis

FTIR spectrometer (Thermo Nicolet, NEXUS, USA) was employed to determine the presence of functional groups in the adsorbents/ catalyst before and after the adsorption/oxidation. Pellet (pressed-disk) technique has been used for this purpose. The spectral range was from 4000 to 400 $cm^{-1}$. The study was used to determine the functional groups participating in the adsorption\oxidation process.

### 4.2.7 Brunauer–Emmett–Teller (BET) Surface Area Measurements

Micromeritics flow BET apparatus (Pulse Chemisorb ASAP 2010) which is shown in figure 4.2 was used to measure BET surface areas of adsorbent/ catalysts**.** Prior to any analysis calibration was accomplished by injecting a precise volume of a pure gas or a known composition gas mixture into the instrument through a septum using a syringe and needle. For best results, the ChemiSorb 2720 was made free of air before performing analysis. About 0.5 g of sample was used for the measurement by nitrogen adsorption at 77.15 K. Prior to the single-point $N_2$ adsorption/desorption, the adsorbent was degassed for 30 minutes in an inert gas, He, at 453 K (The upper limit of the heating mantle is about 673 K). Degassing at 473 to 523 K for 15 to 20 min. usually is adequate. Many materials degas well at 393 to 423 K.. The sample was placed in the sample cell and oven-dried under vacuum at 523 K overnight. The sample was then transferred to the BET section for surface area measurement using $N_2$ adsorption/desorption cycle. The specific surface area determined as per Brunauer-Emmett-Teller (BET) method. Nitrogen was used as the cold bath (77.15 K).

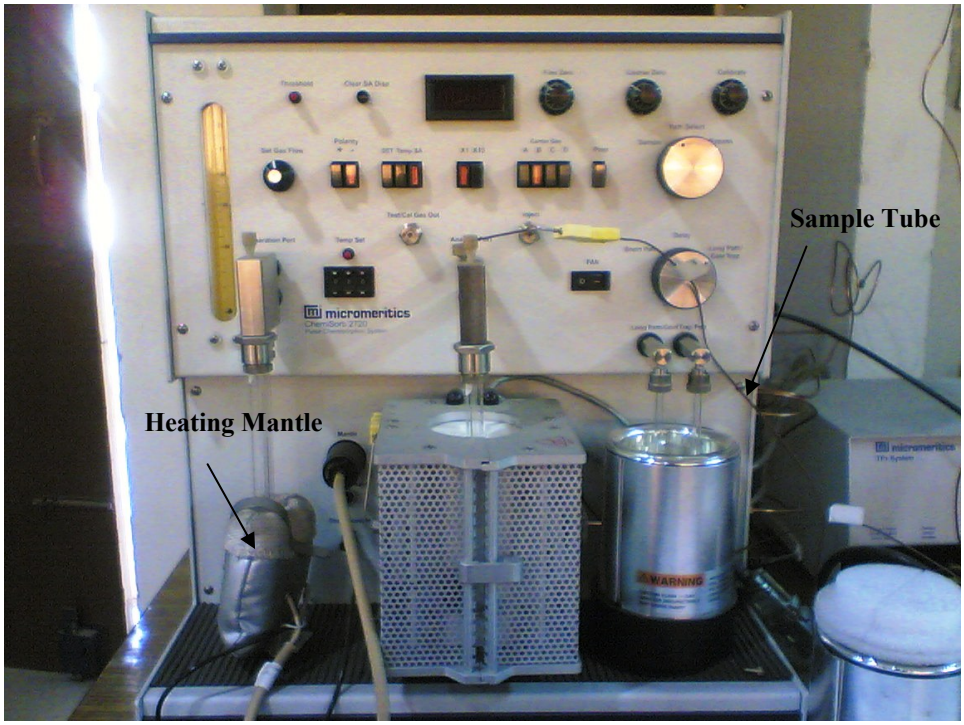


**(a) Surface Area Analyzer**


**(b) Nitrogen adsorption/desorption cell**

**Figure 4.2 Pulse Chemisorb ASAP 2010 Surface Area Analyzer.**

### 4.2.8 Transmission Electron Microscopic (TEM) Analysis

Transmission electron microscopy (TEM) was performed on a Philips CM-30 microscope operating at 200 keV. Specimen preparation consisted of dispersing the material in isopropanol using an ultrasonic bath. A single drop of this dispersion was then deposited on a metallic grid and left to dry.

### 4.2.9 Electron Probe Microscopic (EPM) Analysis

The electron probe microscopic analysis (EPMA) method with high resolution makes it possible to directly map the distribution of any species (chromium in the present study) on the catalyst surface. The EPMA was carried out on a CAMELA SX 100, France system. The vacuum in the EPMA main chamber was typically under $1x10^{-6}$ tor. The EPMA was used with an accelerating voltage of 20kV, a probe current of 0 mA and a probe electron beam diameter of less than 1μm.

### 4.2.10 Electron Paramagnetic Resonance Spectroscopic (EPR) Analysis

The samples were pressed without binder, crushed into 0.10 – 0.20 mm particles and placed in a quartz cell for EPR measurements. EPR spectra have been collected by means of a Bruker model ESP 300 spectrometer using ASTM D 567 method, equipped with either a high temperature cavity ER4111 HT-VT or a low-temperature cavity ST8410.91 and a coaxial quartz gas flow cell, operating at modulation amplitude 2G, modulation frequency 100 KHz, receiver gain $1.6 \times 10^3$. The scanning range is 2000 G, field set 3000G with scanning time 4 minute, Microwave power used 5 mW with microwave frequency 9.1 GHz. Their simulation was done by the SimFonia (Bruker) software. The spectra were recorded at 298 K (RT) and at 70 K (LNT) by means of a special apparatus at IFAM CNR (Pisa). The Bruker ESP300E software and the special Bruker program WIN-EPR (version 901201) were used for data treatment. The Origin 3.5 program for Windows was used for the treatment (baseline correction, double integration, and deconvolution) of the recorded spectra (resolution 4096 points). Resonances for various levels of microwave power were recorded to verify the lack of sample saturation. The gas flow was regulated by four channel readout mass flow controller Model (247C MKS Instruments). This system permitted us to change the composition of the gas mixture and to regulate the flow from 1.5 to 18 $cm^3$/min. Pure helium (99.99%) and the mixtures [10% $O_2$ + He], [0.4% NO + He], [0.2% Propene + He], [5% CO + He], and [5% $H_2$ + He] were used for in situ sample treatment.

### 4.2.11 Neutron Activation Analysis (NAA)

Activation methods are based upon the measurement of radioactivity that has been induced in samples by irradiation with neutrons ($_0n^1$of ~ 0.04 eV) or charged particles such as Hydrogen, Deuterium, or Helium ions [Amiel, 1981]. Bulk chromium concentration determinations were carried out by NAA on CYRUS nuclear reactor. The results obtained are accurate to about 25%.

Approximately 100 mg (accurately weighed) of powdered sample were packed separately in polythene pouches and irradiated for 7 hours of the CIRUS reactor, BARC, Mumbai. For short lived isotopes, accurately weighed powdered samples in the range 20 – 30 mg were irradiated for 1 minute using pneumatic carrier facility (PCF) at the DHRUVA reactor, Mumbai. The neutron flux values in irradiation ~ $10^{13}$ neutrons /cm$^2$ s$^1$ respectively and corresponding % thermal neutron components are 97 and 99. These high neutron densities leads to detection limits that for many elements range from $10^{-3}$ to 10 µg. The gamma activities of the activation products of the samples were assayed after suitable cooling time only for the 7h irradiated samples, using a compton suppressed gamma spectrometer consisting of HPGe detector of 40% relative efficiency coupled to a PC based 8K MCA. The detector resolution was measured to be 2.0 keV at 1332 keV of $^{60}$Co. All spectral data were recorded and analyzed using PHAST software developed in BARC. The peak areas under characteristic gamma rays of various isotopes were used for calculating concentrations of respective elements by the relative method of INAA. Using mass of the element in the standard ($m_{x,std}$) and count rates (counts per second, CPS) of standard ($CPS_{x,std}$) and sample ($CPS_{x,samp}$), mass of the element present in the sample ($m_{x,samp}$) was determined by the following equation:

$$m_{x,samp} = m_{x,std} \times \frac{CPS_{x,samp}}{CPS_{x,std}} \times \frac{D_{std}}{D_{samp}}$$

where, $D$ is the decay factor ($\exp(-\lambda t_d)$) due to cooling, $\lambda$ is the decay constant of the radioisotope and $t_d$ is the cooling time. The $m_{x,samp}$ (mg) was converted to concentration (mg kg$^{-1}$) by normalizing with sample mass (kg).

### 4.2.12 Thermo Gravimetric (TG) and Derivative Thermo Gravimetric (DTG) Analysis

The thermal degradation (gasification) characteristics of the blank and spent adsorbents/catalysts were studied using the thermo-gravimetric and differential analysis techniques. The thermal degradation of the adsorbents was carried out non-isothermally

at the Institute Instrumentation Centre, IIT, Roorkee using the TGA analyzer from Perkin Elmer, Pyris Diamond high-temperature thermal analyzer, Model 9216, at a heating rate of 5 K $min^{-1}$. Calcined alumina was used as reference material. The TGA measures adsorbents/catalysts weight loss caused by the loss of lattice oxygen in a reducing atmosphere. A Cahn 2000 electrobalance, a MicRIcon temperature programmer/controller, a nichrome resistance furnace, and a gas flow system. The system has a temperature range ambient to 1273 K, a maximum capacity of 100 mg, a sensitivity of 0.2 μg and an accuracy of ±0.1 percent. The weight loss, during thermal heating was continuously recorded and downloaded using the software, Muse, Pyris Diamond. The instrument also provided the continuous recording of the DTG and DTA as a function of sample temperature and time. The TG, DTG and DTA curves obtained in each case were analyzed to understand the behavior of thermal degradation.

## 4.3 ANALYTICAL MEASUREMENTS

Analytical methods used in the present study, instruments used for the methods and their operating conditions are summarized in table 4.2.

The concentration of DBT in the sample was determined by using Gas Chromatograph (GC) equipped with flame ionization detector (FID) on a capillary column (L 30 m, I.D. 0.53 mm, Film 0.88 μm). The injector and detector temperatures were set to 553 K and 573 K, respectively. The column temperature started at 373 K for 3 minutes and heated at a rate of 287 K/ min to 553 K, and stayed at 553 K for 30 min. The carrier flow, 15 mL/ min (He). 0.5 μL of the sample volume was injected for each GC-FID run. The sensibility (limit detection) is 2 mg/L. The DBT in model sample were identified and analyzed by the standard samples. The oxidized products, such as dibenzothiophene sulfone (DBTO) and the other major compounds were under same conditions. The percentage removal of DBT and equilibrium adsorption uptake in solid phase, $q_e$ (mg/g), were calculated using the following relationships:

$$\text{Percentage sulfur removal} = 100(C_0 - C_e)/C_0 \quad (1)$$

$$\text{Amount of adsorbed sulfur per g of solid, } q_e = (C_0 - C_e)/m \quad (2)$$

where, $C_o$ is the initial DBT concentration (mg/l), $C_e$ is the equilibrium DBT concentration (mg/l) and $m$ is the adsorbent dose in g per litre of solution. All the experiments were done in triplicate and results were found to show < ±5% deviation from the average value. Reported results are average of these runs.

**Table 4.2 Analytical methods and instruments used in the experiments.**

| Instruments | Objectives | Specifications |
|---|---|---|
| X- Ray Diffractometer | Structures of the different adsorbents/catalysts | **Brucker AXS D8 Advance**<br>Target: Cu, Fe & Mo; Working Voltage:10-100kV; Tube current:4.0 - 80mA<br>Goniometer Scanning range: 0-150$^{o}$; Accessories: High temperature completes analysis software & ICDD library. |
| TGA/DTA Analyser | Thermal degradation characteristics of the materials | **Perkin Elmer Pyris Diamond**<br>Temperature range: Ambient-1773 K; Atmosphere: Air & Nitrogen; Balance type: Horizontal differential type; Thermocopule: Pt-Pt Rh (13%); DTA measuring range: +/- 0.6 μV; DTA measuring range: 0.5 mg/min. - ~ 1 mg/min; Heating rate: 373 K/min; TGA measuring range: 0.2 μg; Sample wt.: 10 – 15 mg (max.100 mg) . |
| Scanning Electron Microscopic Analysis | Surface Analysis | QUANTA, Model 200 FEG, Neatheland with Sputter Coater, Edwards S150, to provide conductivity to the samples. |
| Brunauer–Emmett–Teller surface area analyzer | Surface area of materials analysis | Micromeritics BET apparatus Model Pulse Chemisorb ASAP 2010. |
| Energy-dispersive X-ray analyzer | Elemental analysis | QUANTA, Model 200 FEG, Neatheland . |
| Fourier Transform Infra Red Spectro-photometer | Determination of functional groups in the material before and after the physical/chemical process | Thermo Nicolet, NEXUS, USA; Spectral range 4000 to 400 $cm^{-1}$. |

| Instruments | Objectives | Specifications |
|---|---|---|
| Electron Probe Microscopic analyzer | Mapping the distribution of Metallic species on the material surface. | CAMELA SX 100, France system; Vacuum @ under $1x10^{-6}$ tor; Accelerating voltage of 20kV; P robe current of 0 mA; Probe electron beam diameter of less than 1. |
| Electron paramagnetic resonance spectroscopic analyzer | Electronic structure of metals and surface molecular species. | Bruker model ESP 300<br>Temperature cavity: ER4111 HT-VT (high) - ST8410.91(low); Cell type: coaxial quartz gas flow; Operating modulation amplitude: 2G; Modulation frequency: 100 KHz; Receiver gain:$1.6 \times 10^2 \times 10$; Scanning range: 2000 G - 3000G; Scanning time: 4 min; Microwave power range: 5 mW Microwave frequency range: 9.1 GHz. |
| Nuclear Reactor | Bulk metallic concentration | CIRUS reactor, BARC, Mumbai; neutron flux values in irradiation ~ $10^{13}$ neutrons $/m^2s1$; thermal neutron components are 97 and 99; HPGe detector of 40% relative efficiency coupled to a PC based 8K MCA; Detector resolution 2.0 keV at 1332 keV of $^{60}Co$ with spectral data recording and analysis facility at PHAST software developed in BARC. |
| Densitometer | Bulk Density of adsorbent /catalyst | MAC Bulk Density Appratus; Two 100 ml calibrated Measuring Cylinders; Vibrator. |
| Particle size analyser | Particle size adsorbent/catalyst | Standard sieves and Analyser CIS 100 and LFC101, Ankersmid. |
| UV-Visible Spectrophotometer | Qualitative estimation of organic compounds | UV 1800 Shimadzu Spectrophotometer; Rresolution of 1 nm; Blazed holographic grating with a Czerny-Turner mount result; wavelength range 190 – 1100 nm; accuracy +/- 0.1 nm @ 656.1 nm $D_2$; Baseline stability ≥ 0.0003 Abs/H @ 700 nm with UV probe (standard) Win XP. |

## 4.4 EXPERIMENTAL PROGRAMME

### 4.4.1 Adsorptive Desulfurization Procedure

For each experimental run, 50 ml solution of known concentration of DBT in model oil was taken in 100 ml conical flask containing pre-weighed amount of adsorbents. These flasks were agitated at a constant shaking rate of 120 rpm in a temperature controlled orbital shaker (Remi Instruments, Mumbai) (Figure 4.3) maintained at 298 K to 313 K as the case may be. The flasks were withdrawn at the end of predetermined time ($t$), centrifuged using a research centrifuge (Remi Instruments, Mumbai) at 4000 rpm for 5 min and then the supernatant was analyzed for residual concentration of DBT using gas chromatograph.

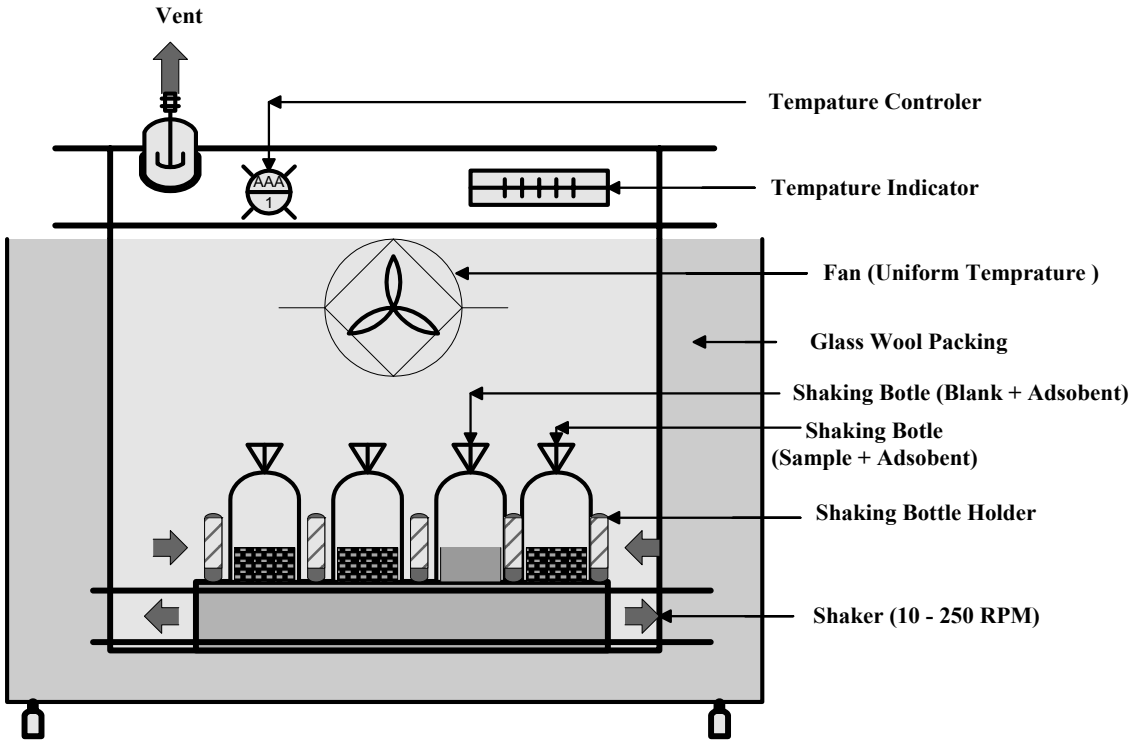


**Figure 4.3 Experimental set-up for adsorptive desulfurization.**

#### 4.4.1.1 Batch Kinetic Study

To determine the time necessary for adsorption, 50 ml of the aqueous solution containing 30-1000 mg/l of the specific DBT was taken in a series of conical flasks. Pre-weighed amounts of the dry and sieved adsorbents were added to different flasks. The flasks were kept in a temperature-controlled shaking water bath and the aqueous

solution-adsorbent mixtures were stirred at constant speed. At the end of the predetermined time, $t$, the flasks were withdrawn, their contents were centrifuged, and the supernatant analyzed for adsorbate concentration. Adsorption kinetics was followed for 24 h and it was observed that after 1 h, there was gradual but very slow removal of the adsorbate from the solution. In order to investigate the kinetics of adsorption of the adsorbate on the adsorbents, various kinetic models, like pseudo-first-order, pseudo-second-order and intra-particle diffusion models have been used.

#### 4.4.1.2 Batch Isotherm Study

For adsorption isotherms, experiments were carried out by contacting a fixed amount of dried and sieved adsorbent with 50 ml of the adsorbate solutions in 250 ml conical flask with glass stopper having $C_o$ in the range of 30-1000 mg/l under static shaking position. After certain contact time (ranges 30–1920 min) the mixture was centrifuged and the adsorbate concentration in the supernatant solution and in the adsorbent was estimated. Three two-parameter models, viz., Langmuir, Freundlich, and Temkin, and one three-parameter model, viz., Redlich-Peterson have been used to correlate the experimental equilibrium adsorption data.

The sum of square of errors (SSE) error function was employed in this study to find out the most suitable kinetic and isotherm models to represent the experimental data respectively.

#### 4.4.1.3 Effect of temperature and estimation of thermodynamic parameters

The effect of temperature on the sorption characteristics was investigated by determining the adsorption isotherms at 298, 303, 308 and 313 K for various adsorbents.

### 4.4.2 Oxidative Desulfurization Procedure

A triple necked glass reactor fitted with a condenser, a magnetic stirrer and a thermocouple, was used to carry out the oxidation reaction. The reactor was immersed in a thermostatically controlled oil bath to carry out the reactions at 303 – 353 K. Actual experimental set-up used in ODS is shown in figure 4.4. Detailed specification of ODS set-up is given in table 4.3.

**Table 4.3 Specification of ODS set-up.**

| Item | Specification |
|---|---|
| Magnetic Stirrer | Remi 5 MLX DX (800 RPM max.) |
| Oil Bath | Asbestos insulated copper bath 500 ml capacity |
| Round Bottom Reactor | Three necked, asbestos insulated 250 ml Borosil Glass Round Bottom Flask |
| Condenser | B20; Horizontal; Water Cooled; Shell-Tube Type |
| Thermocouple | Thermotech TH 102 ((-263 to 573 K) |

In a typical run, the water bath was first heated up and stabilized to the desired reaction temperature called time zero (time t=0 for the reaction was taken when the final temperature was reached). This temperature was maintained constant during one whole experimental run. The reactor was charged with 50 ml model solution and 5 ml methanoic acid solution. When thermal equilibrium was reached, fresh catalyst (5 g/l) was added to the reaction mixture. After $N_2$ introduction in the reactor (0.5 MPa) to remove $CO_2$ from the atmosphere, the mixture was stirred at a rate of 450 rpm and heated up from room temperature to reaction temperature (303-353K) under reflux condition; in the mean time oxidant agent was added dropwise. Reactant and product identifications were achieved by comparing retention times in GC–FID. Hydrogen peroxide (30 w% $H_2O_2$) was used as oxidant. The conversion products dibenzothiophene sulfones in the reaction mixture after the completion of reaction and extraction via methanol shown in figure 4.5 (DBTO2). The degree of advance of the reaction was measured using the conversion of DBT. Part of the $H_2O_2$ reagent was decomposed into oxygen, determined by standard iodometric titration. Table 4.4 shows the operating conditions used in the ODS.

**Table 4.4 Operating conditions used in ODS with various types of catalyst.**

| Parameters | Conditions |
|---|---|
| Model S Compound Solution | DBT in iso-octane |
| Initial DBT concentration | 30-1000 mg/l |
| Hydrogen Peroxide ($H_2O_2$) | 30% (v/v) |
| Methanoic acid ($H_2CO_2$) | 41% (v/v) |
| Working Reactor Volume | 250 ml RBF |
| Working Temperature Range | 303– 353 K |
| Space Time | 6 h |


**Figure 4.4 Experimental set-up for oxidative desulfurization.**

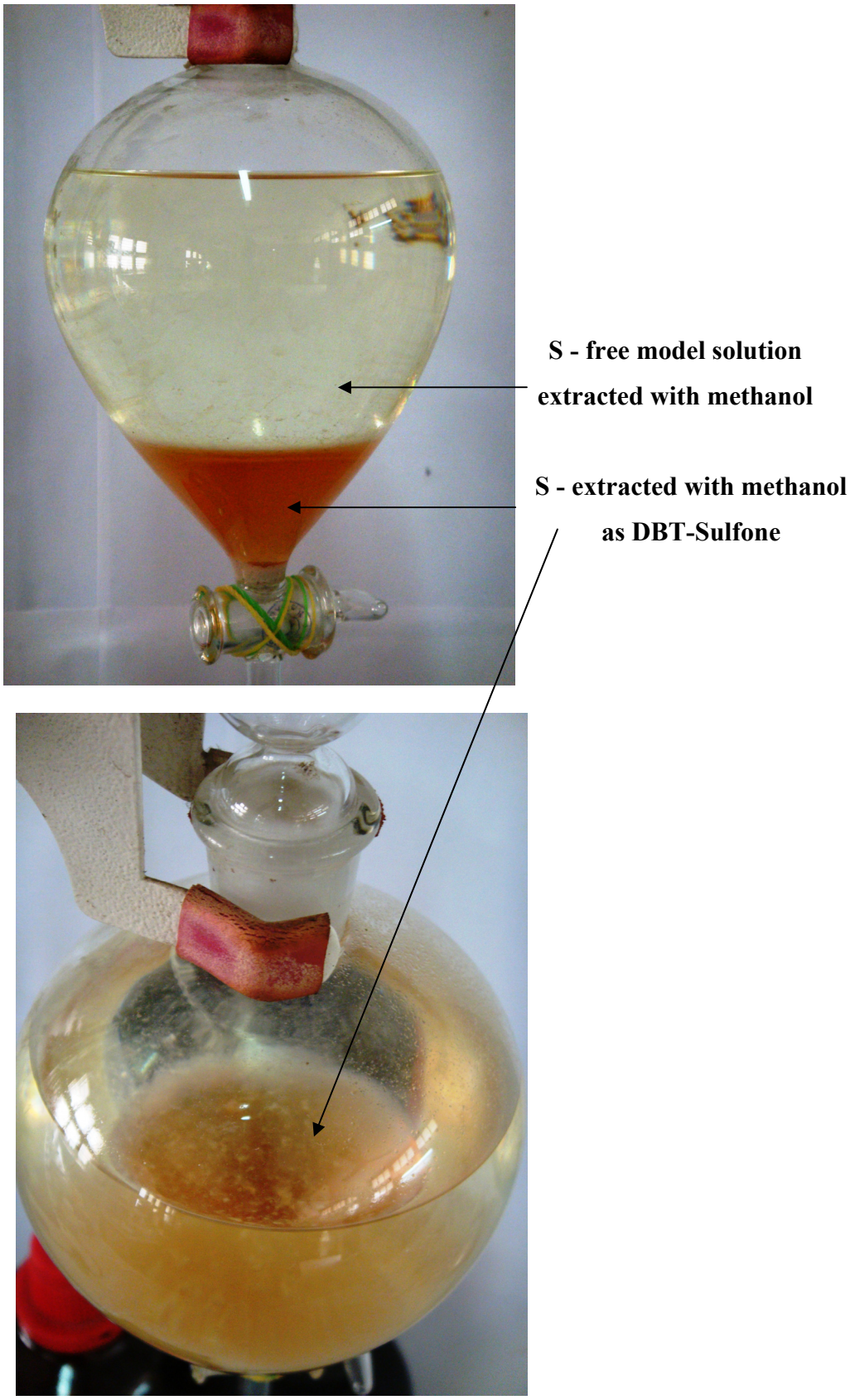


**Figure 4.5 Dibenzothiophene-Sulfone extracted in methanol**

Chapter – V

# RESULT AND DISCUSSION

## 5.1 ADSORBENTS/CATALYSTS CHARACTERIZATION

Adsorptive desulfurization (ADS)/oxidative desulfurization (ODS) of dibenzothiophene (DBT) present in model hydrocarbon (DBT dissolved in iso-octane) at different concentration level was studied using three materials, namely, powdered zirconia dried at 383 K (ZD383), powdered zirconia calcined at 893 K (ZC893), powdered SZ calcined at 893 K (SZC893) and powdered chromium-promoted SZ calcined (CSZC893). The photograph of these materials is given in figure 5.1. These materials were synthesized in the laboratory as per methods given in chapter III. The characterization of ZD383, ZC893, SZC893 and CSZC893 was performed using various physic-chemical and analytical techniques. The instrumental procedures and process parameters followed have already been discussed in chapter IV.

### 5.1.1 Brunauer–Emmett–Teller Surface Area

BET method is probably the most popular method used for the evaluation of the pore surface area. Surface area curve of ZD383 and ZC893 is shown in figure 5.2. Table 5.1 presents the BET surface areas of various samples. It is clear from table that the sample ZD383 (which is Zirconia dried at 383 K before calcination) has highest surface area. The sample ZC893 shows lower surface area then ZD383. This means that the BET surface area of zirconia decreases after calcination.The bulk density of all the zirconia samples were found to be in the range of 0.89 – 0.99 g/l.

**Table 5.1 BET surface area various Zirconia samples.**

| Zirconia samples | BET Surface Area ($m^2/g$) |
|---|---|
| ZD383 | 322.0 |
| ZC893 | 87.43 |
| SZC893 | 87.8 |
| CSZC893 | 90.0 |


**Figure 5.1 Photograph of materials used in desulfurization study.**


**(a) ZD383**

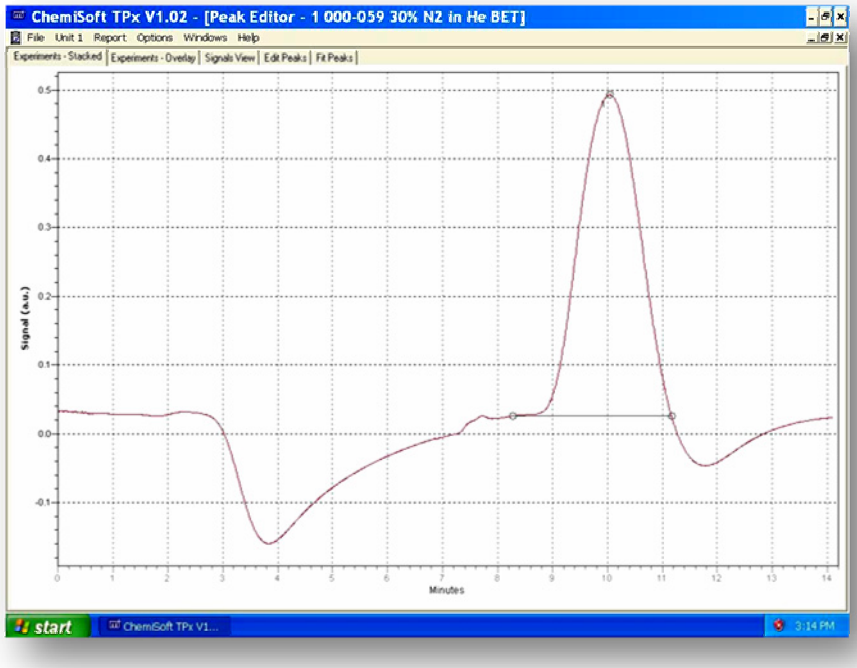


**(b) ZC893**

**Figure 5.2 Surface area curves for zirconia after various thermal treatment.**

In the absence of promoters, calcination of hydrous zirconia normally leads to the formation of thermodynamically more stable monoclinic form with large crystallite sizes [Zalewski et al., 1999] leading to decrease in BET surface area in SC893. SZ before and after chromium loading do not show much change in BET surface area.

Chokkaram et al. [1994] have shown that the surface areas of calcined zirconia don't get much affected by sulfation and promotion by metal loading. The results obtained in the present study show the same results. The values obtained in the present studies are consistent with values reported by Song and Sayari [1996] for unpromoted/unmodified SZ. Incorporated $SO_4^{2-}$ ions in ZC893 retard the formation of larger crystallites of zirconia and stabilize them in the metastable tetragonal phase [Khodakov et al., 1998]. It has been reported that the higher calcination temperature leads to loss of water and loose-bound S species from the surface in the form of $SO_2$ and/or $SO_3$ leading to a decrease in surface area [Srinivasan et al., 1995].

### 5.1.2 X-Ray Diffraction Study

The XRD patterns of the ZD383 and ZC893 are shown in figure 5.3. It may be seen that ZD383 is amorphous in nature with no crystalline peak observed in ZD383. After calcination at 893 K, sample ZC893 shows some crystalline peaks. Majority of these peaks are monoclinic in nature. In addition, small portion of tetragonal phase of zirconia are also observed in ZC893.

XRD patterns of SZC893 and CSZC893 are shown in figure 5.4. XRD pattern of SZC893 indicates that the introduction of $SO_4^{2-}$ anions can stabilize the metastable tetragonal zirconia phase, which is generally believed to be an ideal crystalline phase for the SZ and its analogues [Chen et al., 1993; Yang et al., 2002; Comelli et al., 1995; Miao et al., 1996; Farcasiu et al., 1997].

A strong influence on the phase modification from thermodynamically more stable monoclinic to the metastable tetragonal phase can be observed when various chromium is incorporated into the SZ structure. Generally, the tetragonal phase of zirconia can be stabilized by incorporating the promoters like lanthanum, cerium, and yttrium into the zirconia lattice [Khodakov et al., 1998].

XRD pattern of CSZC893 indicates that the introduction of chromium further stabilizes the metastable tetragonal zirconia phase and crystalinity is further increased with chromium loading. It is well known from the literature that the tetragonal phase of zirconia is more active in catalysis [Yamaguchi, 1994]. Therefore, SZC893 and CSZC893 are expected to show better results.

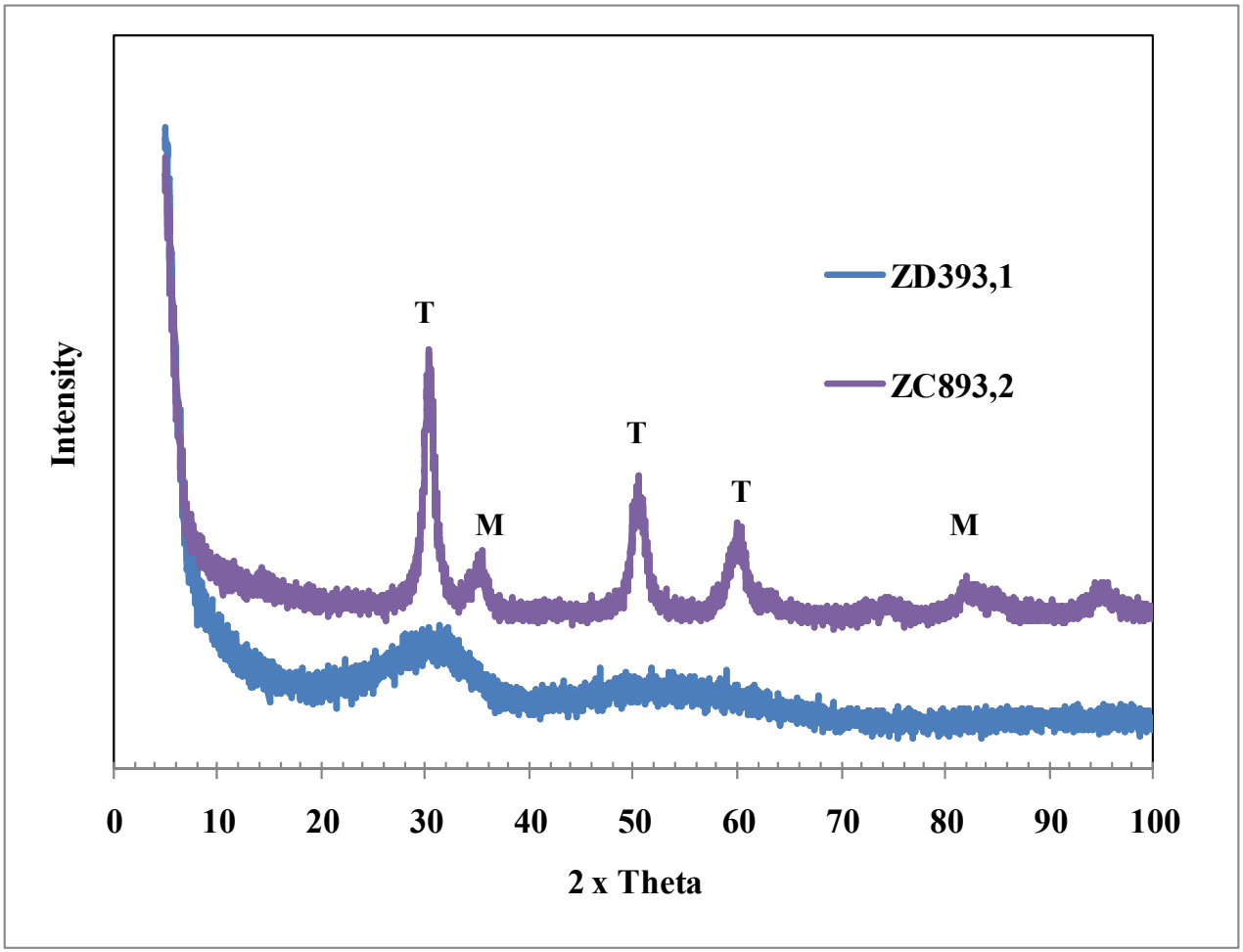


**Figure 5.3 XRD patterns of the ZD383 and ZC893. M: Monoclinic zirconia, T: Tetragonal zirconia.**

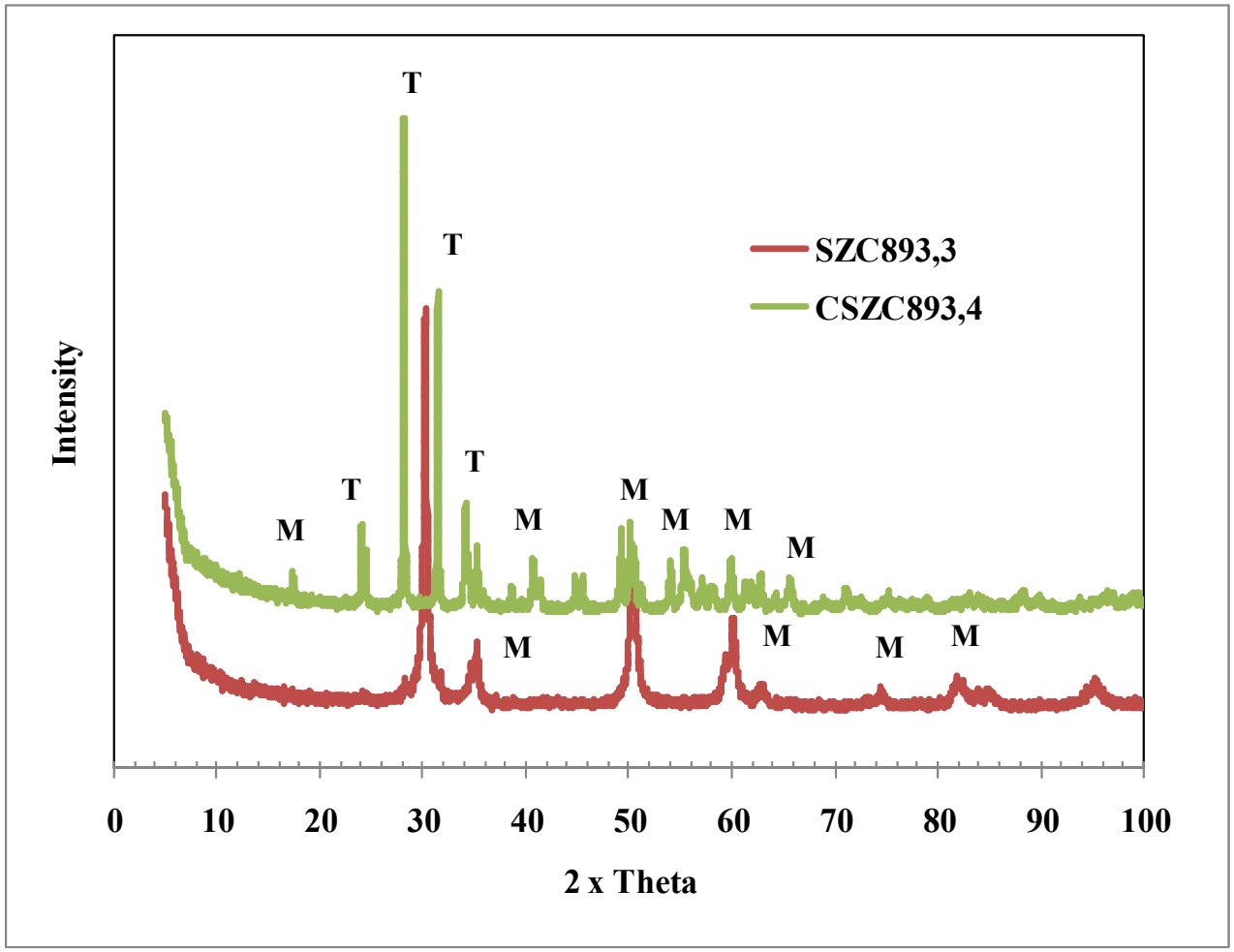


**Figure 5.4 XRD patterns of the SZC893 and CSZC893. M: Monoclinic zirconia, T: Tetragonal zirconia.**

### 5.1.3 Particle Size Analysis

Particle size analysis of ZC893 and SZC893 is given in figure 5.5 and figure 5.6, respectively. Each figure shows number, size, area and volume size distributions separately. A close look into the figures shows that the particle size of SZC893 is much higher than that of increases of ZC893. This shows that the sulfation of increases the particle size. Particle size increases with increase in crystallization [Kuznetsov et al., 2002]. Crystalinity increased from ZC93 to SZC893 as will be shown by XRD patterns in next section. This in turn increased the particle size of SZC893.

### 5.1.4 Transmission Electron Microscopic (TEM) Study

TEM micrographs can be used to understand the pattern of samples of zirconia. TEM of SZC893 is shown in figure 5.7. The TEM images show the presence of polyaggregate particles with a quasi-circular cross section, in which small and disorderly distributed patterns of interferences fringes are observable. This indicates that small domains of regular space crystal planes are in the sample. It is possible that the specimen of SZ893, when observed with the electron microscope, become more crystalline due to the heating effect caused by high-energy electron beam.

### 5.1.5 Scanning Electron Microscopic (SEM) Study

The morphologies of various samples have been examined by SEM analysis. The SEMs of the ZC893, SZC893 and CSZC893 at various magnifications are shown in figure 5.8. These figures reveal surface texture and porosity of the samples. It may be seen in figure at higher magnifications that the CSZC893 is more crystalline in nature as compared to SZC893 and ZC893 in that order.

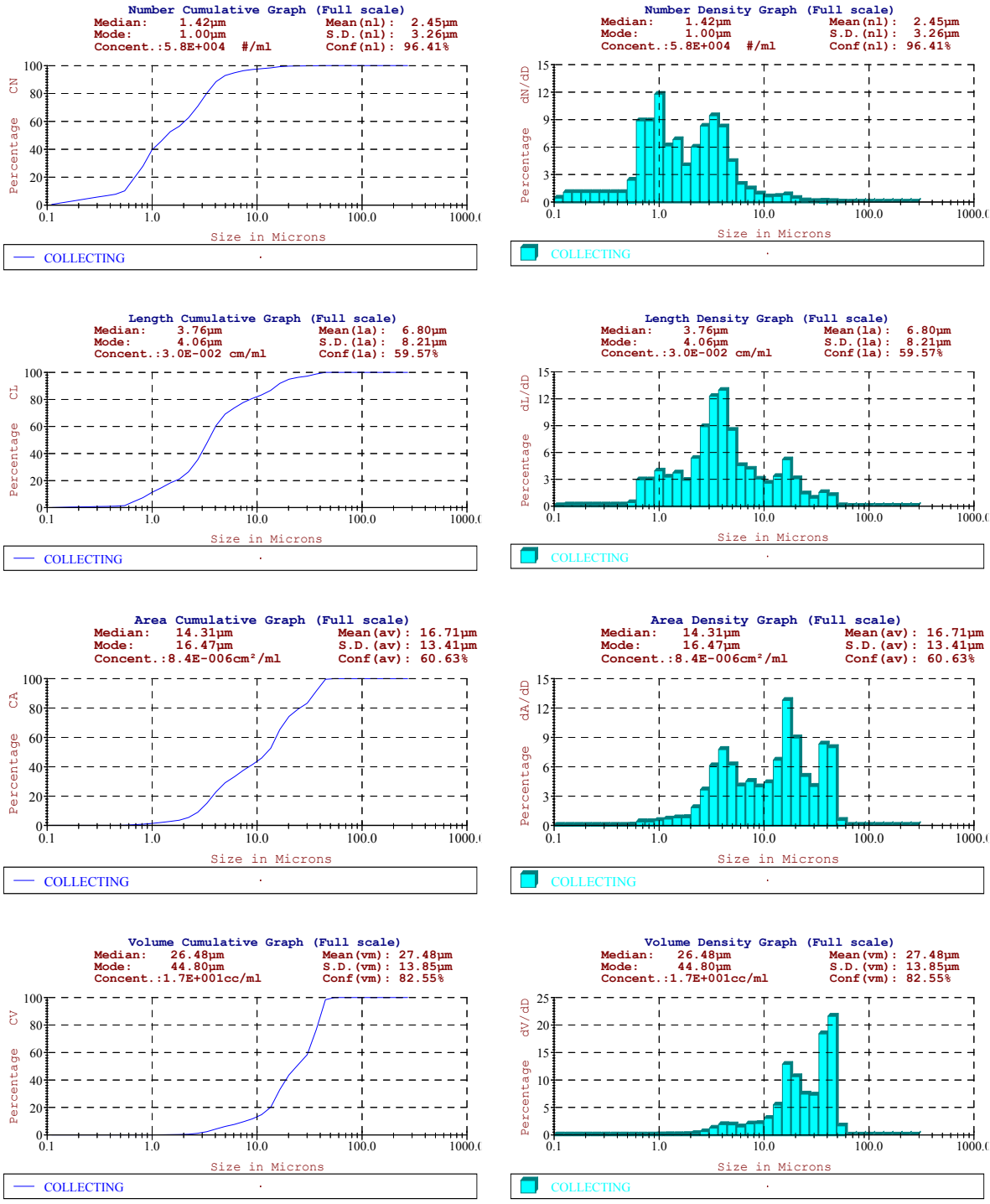


**Figure 5.5 Particle size distribution of ZC893.**

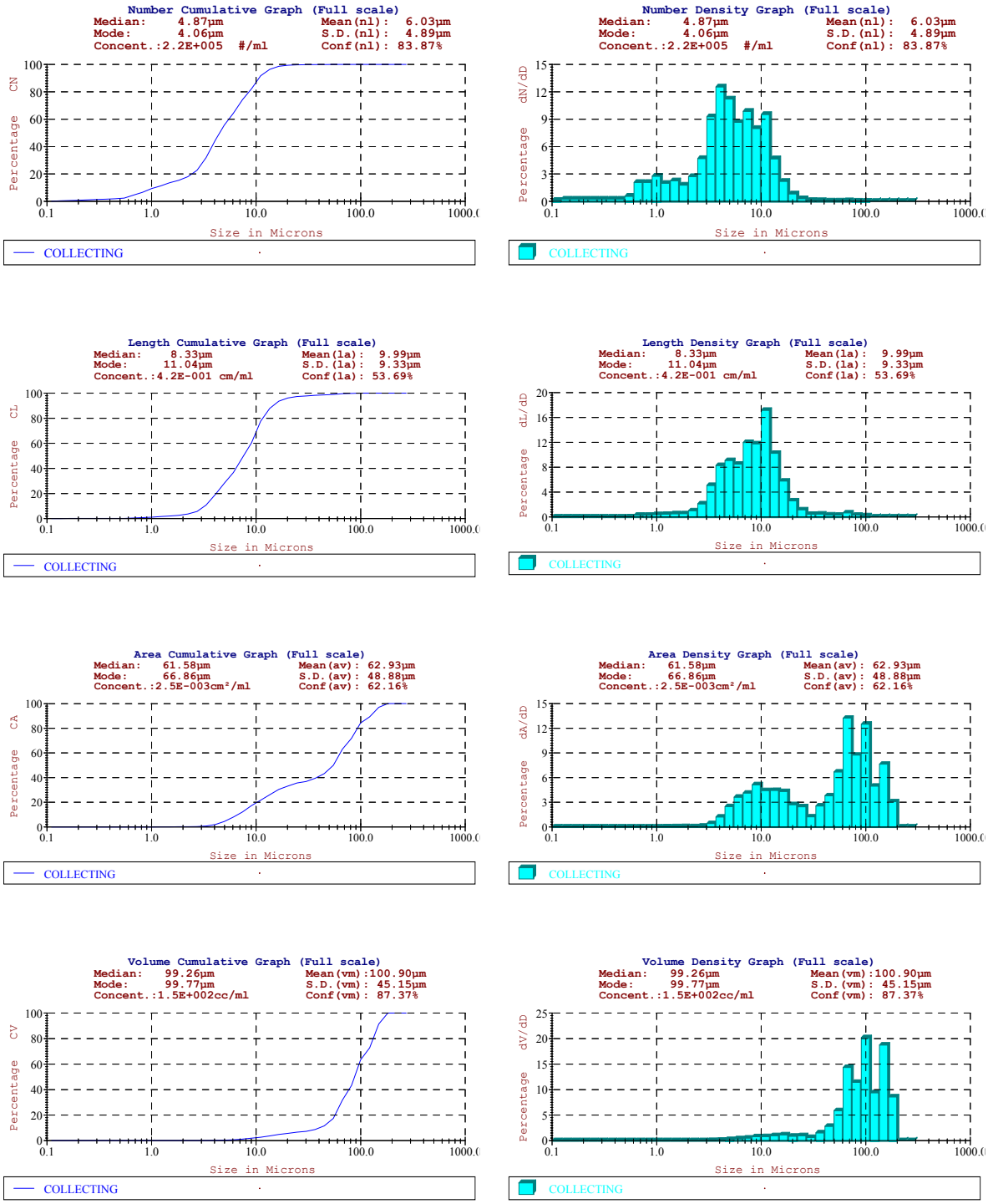


**Figure 5.6 Particle size distribution of SZC893.**

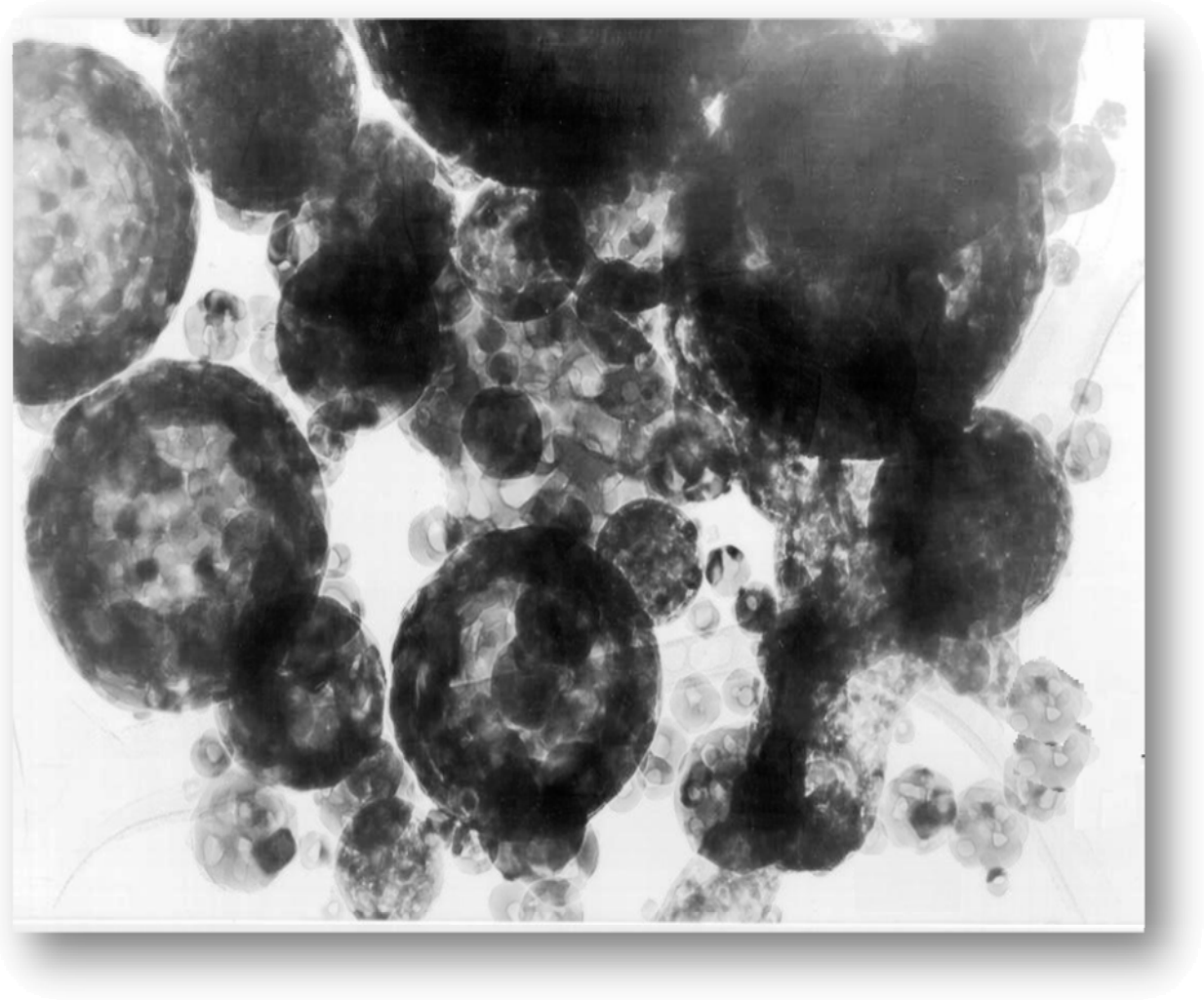

**Figure 5.7 Transmission electron micrographs of SZC893.**

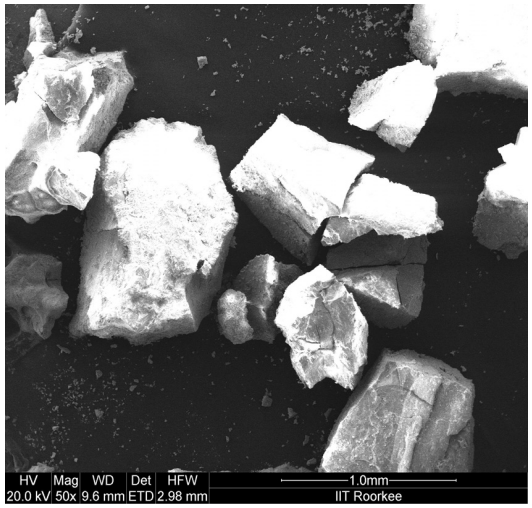


**ZC893-50X**

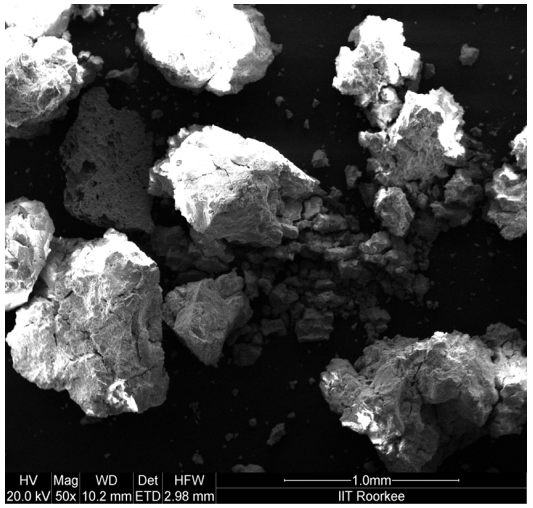


**SZC893-50X**

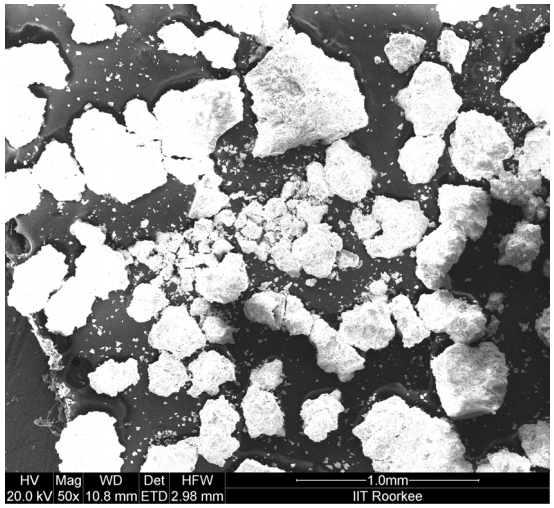


**CSZC893-50X**

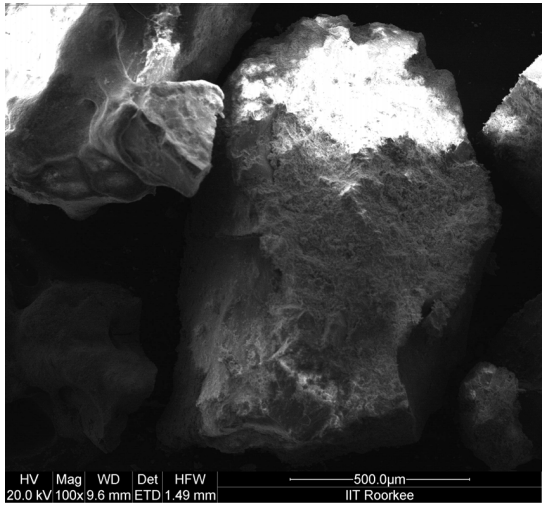


**ZC893-100X**

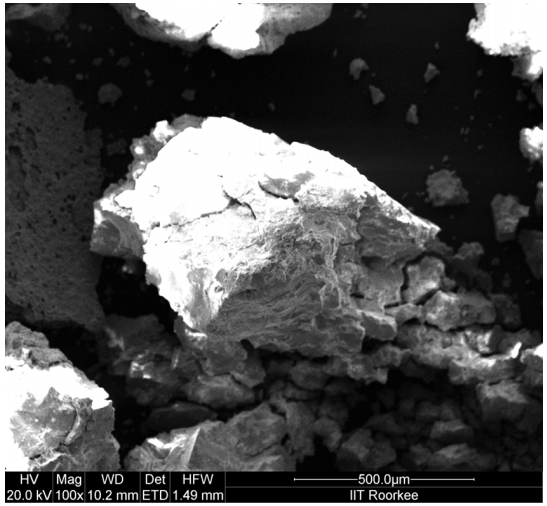


**SZC893-100X**

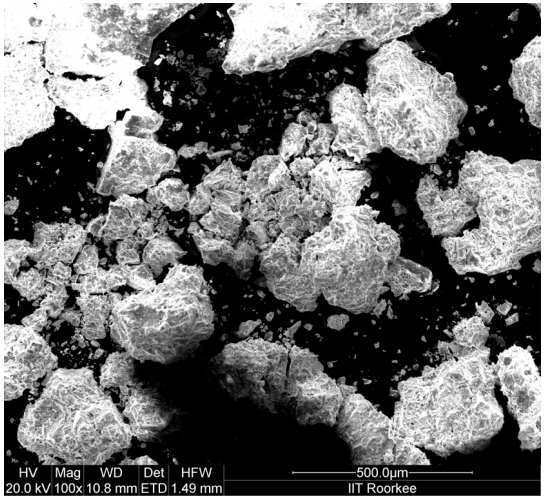


**CSZC893-100X**

**Figure 5.8 SEMs of ZC893, SZC893, and CSZC893 Continued…….**

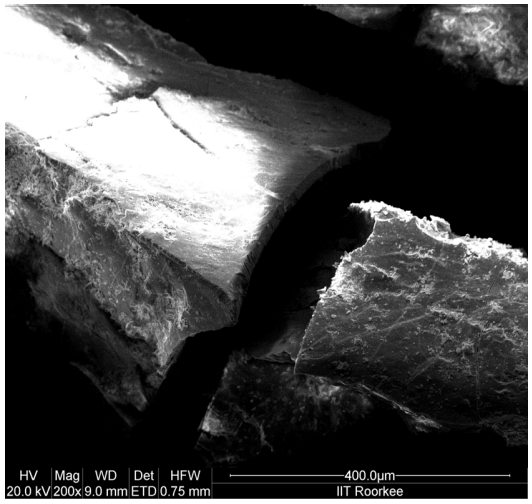


**ZC893-200X**

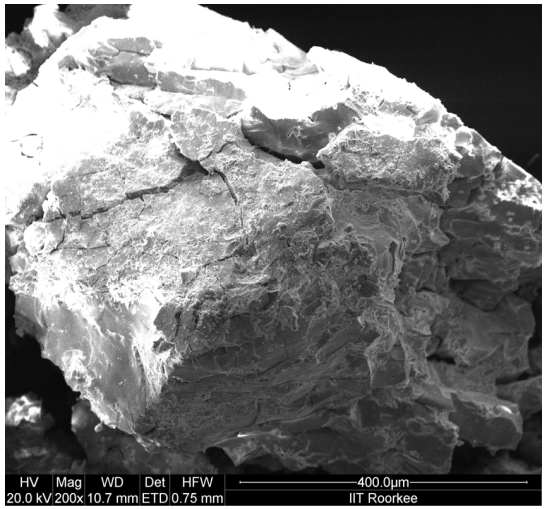


**SZC893-200X**

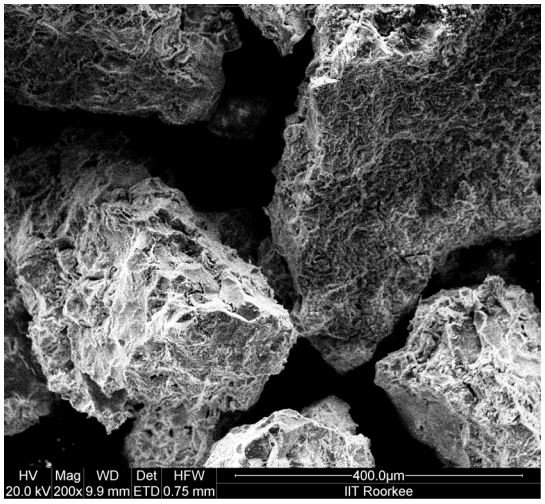


**CSZC893-200X**

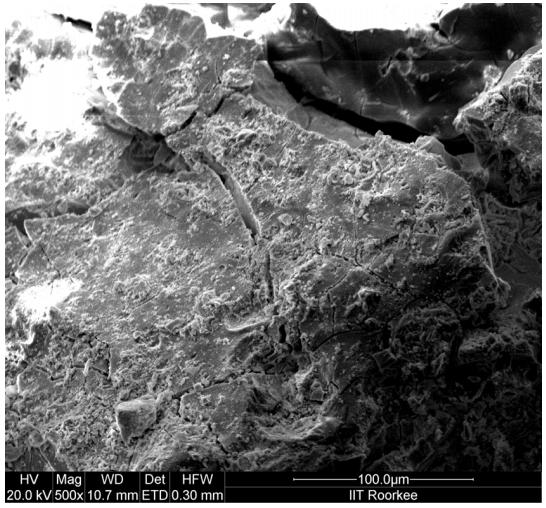


**ZC893-500X**

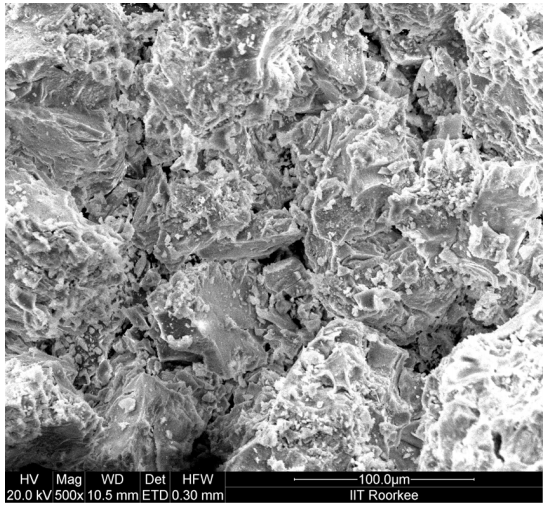


**SZC893-500X**

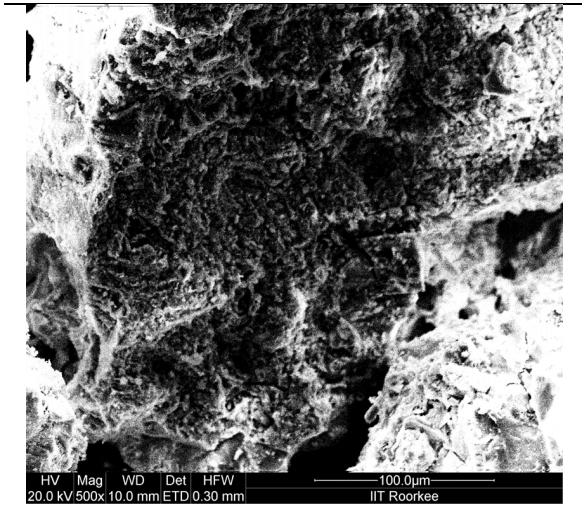


**CSZC893-500X**

**Figure 5.8 SEMs of ZC893, SZC893 and CSZC893 Continued…….**

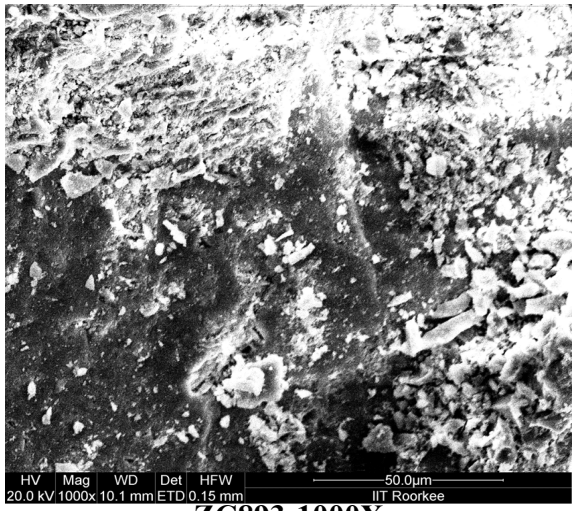


**ZC893-1000X**

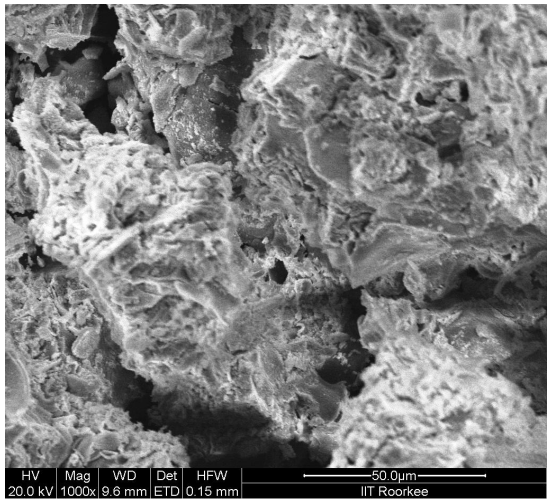


**SZC893-1000X**

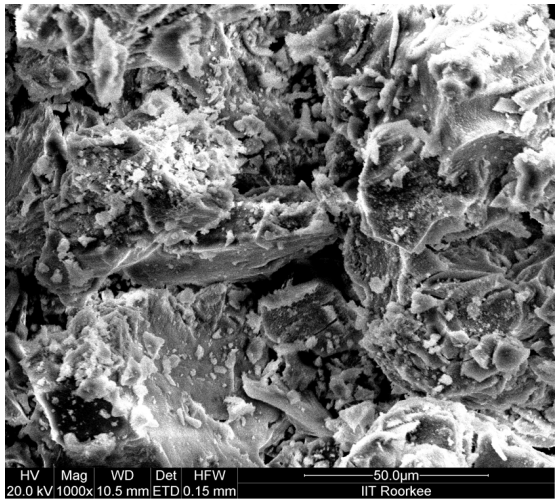


**CSZC893-1000X**

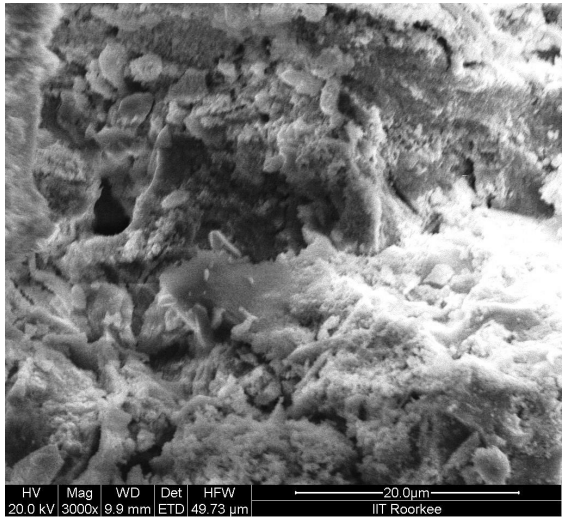


**ZC893-3000X**

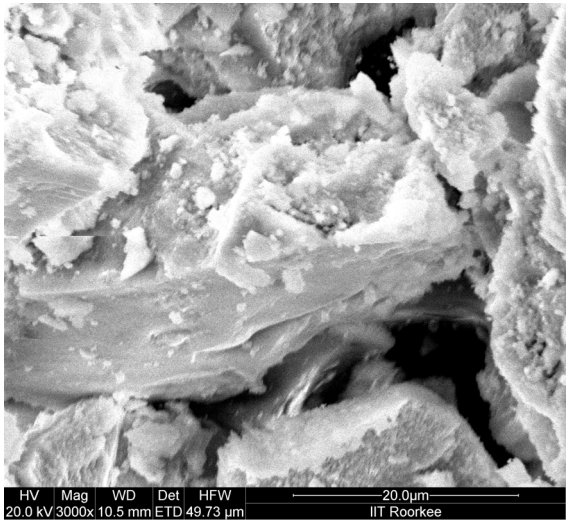


**SZC893-3000X**

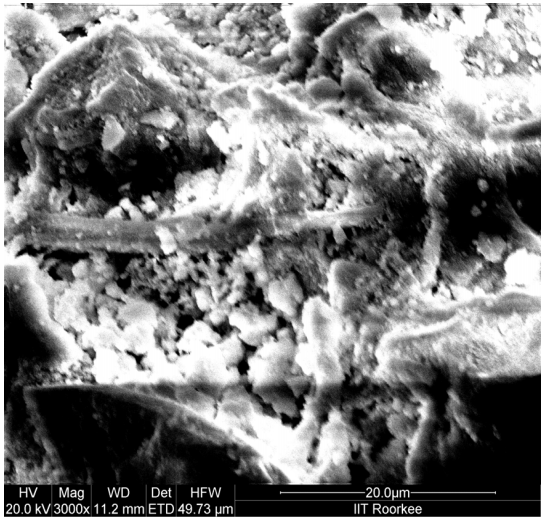


**CSZC893-3000X**

**Figure 5.8 SEMs of ZC893, SZC893 and CSZC893.**

### 5.1.6 Energy Dispersive Atomic X-Ray (EDAX) analysis

EDAX was conducted to study the distribution of the elements in various samples. Figure 5.9 and Figure 5.10 show the EDAX patterns analysis of ZD383, ZC893, SZC893 and CSZC893. Table 5.2 shows the distribution of the elements in these samples. ZD383 and ZC893 were found to contain Zr and O in majority. SZC893 was found to contain 3.55 wt% sulphur, whereas, CSZC893 was found to contain 00.48 wt% sulphur. CSZC893 showed presence of 0.98 wt% Cr in addition to Zr, O and S. NAA also confirms the dispersion of ~900-1000 ppmw chromium on zirconia.

**Table 5.2 Elemental composition of various zirconia's determined by EDAX**

| **Elemental composition of ZD383** | | | **Elemental composition of ZC893** | | |
|---|---|---|---|---|---|
| **Element** | **Wt%** | **At%** | **Element** | **Wt%** | **At%** |
| O K | 10.32 | 39.62 | O K | 15.46 | 50.52 |
| S K | Nil | Nil | S K | 0.96 | 1.56 |
| Cr K | Nil | Nil | Cr K | Nil | Nil |
| Zr K | 89.68 | 60.38 | Zr K | 83.50 | 47.91 |
| **Elemental composition of SZC893** | | | **Elemental composition of CSZC893** | | |
| **Element** | **Wt%** | **At%** | **Element** | **Wt%** | **At%** |
| O K | 18.43 | 54.40 | O K | 8.46 | 34.45 |
| S K | 3.55 | 5.23 | S K | 00.44 | 1.20 |
| Cr K | Nil | Nil | Cr K | 00.98 | 00.86 |
| Zr K | 78.01 | 40.37 | Zr K | 90.12 | 63.48 |

### 5.1.7 Electron Probe Microscopic (EPM) Analysis

The electron probe microscopic analysis (EPMA) was used to map the distribution of chromium species on the adsorbent/catalyst surface. The EPMA method with high resolution makes it possible to directly map the distribution state of the chromium species. EPMA analysis of CSZC893 is shown in figure 5.11. It is clear from figure 5.11 that Cr is loaded in CSZC893 and that it is well dispersed in the whole sample.

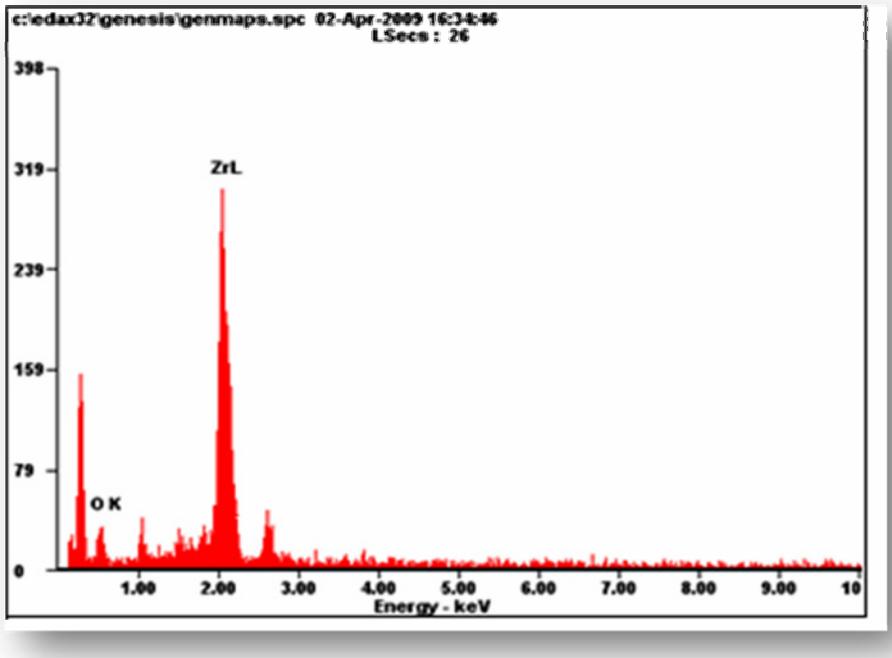


**a. ZD383**

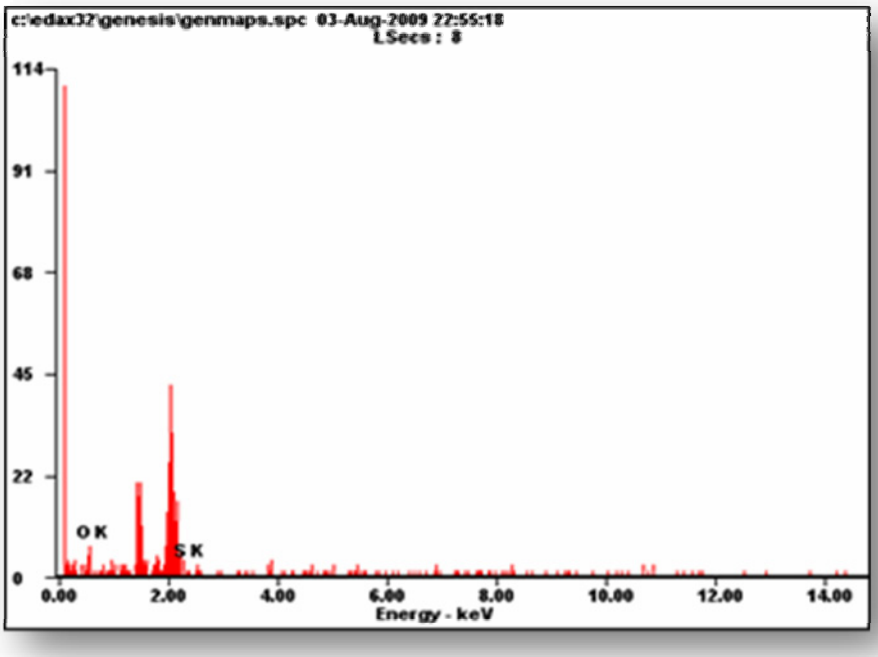


**b. ZC893**

**Figure 5.9 EDAX Spectrum for elemental composition of various samples**

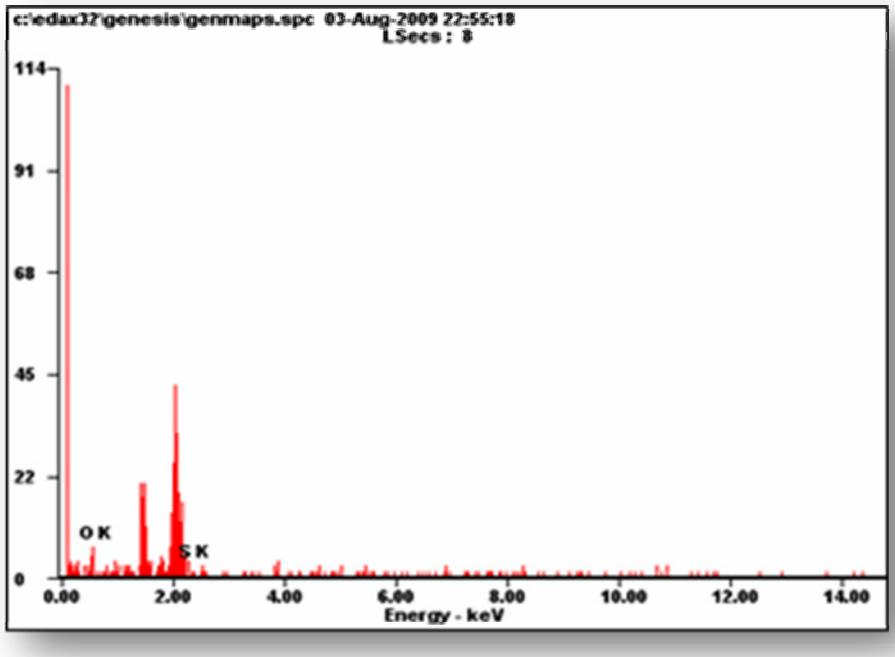


**a. SZC893**

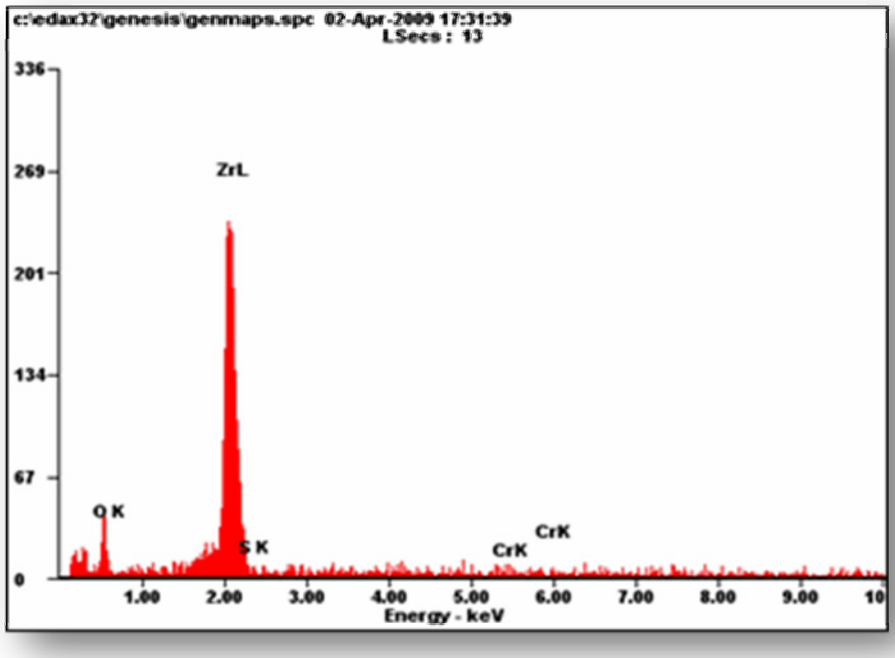


**b. CSZC893**

**Figure 5.10 EDAX Spectrum for elemental composition of various samples**

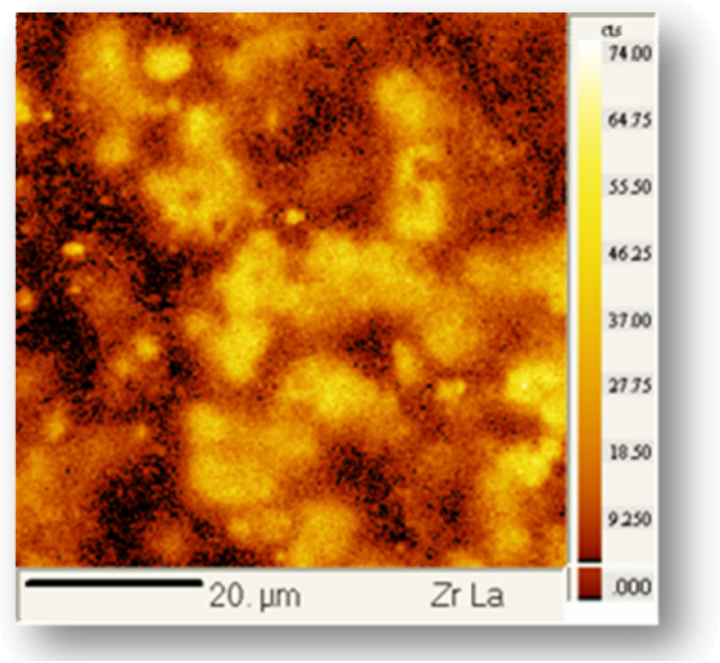


**(a) Zr in CSZC893**

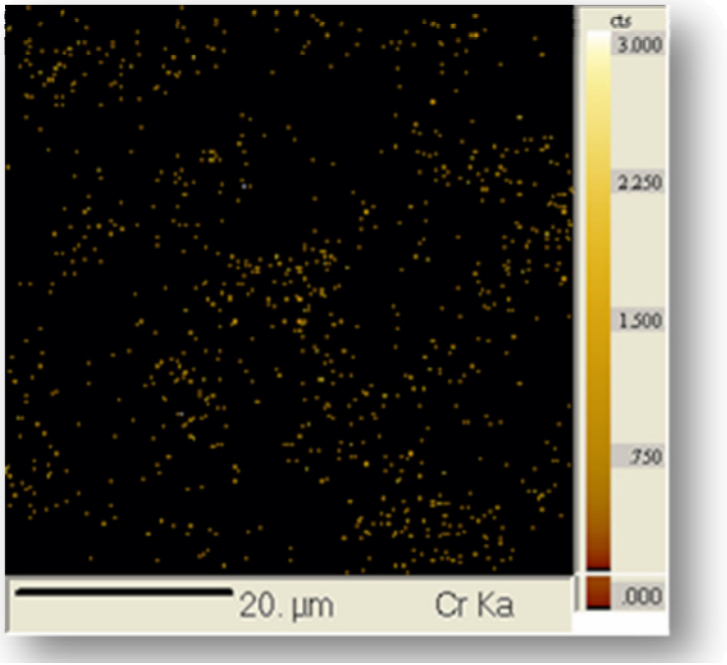


**(b) Cr in CSZC893**

**Figure 5.11 Comparative studies of EPMA images for dispersion of Zr metal and Cr metal on SZC893.**

### 5.1.8 Thermogravimetry (TG) and Differential Thermal (DT) Analysis

The TGA thermogram of DBT is shown in figure 5.12. It shows that DBT is thermally stable upto 423 K. Above 423 K, DBT is thermally unstable and vaporizes completely at 533 K. The TGA thermogram of ZD383 is shown in figure 5.13. It shows that this sample is fully stable upto 1273 K with a minute 2% wt loss from ambient to 1273 K. The TGA thermogram of SZC393 as shown in figure 5.14 shows that the SZC393 is stable upto 773 K. between 773–1043 K, SZC393 shows a wt loss of 38%. This may be due to the decomposition of sulfate species on the surface [Hino et al., 2006].

### 5.1.9 Fourier Transformed Infra-Red (FTIR) Spectroscopy

The FTIR technique is an important tool to identify the characteristic functional groups, which are instrumental in present on the surface of used zirconia samples. The FTIR spectra of the ZD383 and ZC893 are given in figure 5.15. Both ZD383 and ZC893 show transmittance around ~1054 cm-1 region due to the vibration of the CO group in lactones [Davila-Jimenez et al., 2005] and due to -C-OH stretching and –OH deformation. It can be seen that the transmittance is lower for ZC893 as compared to that for ZD383. This means that the zirconia sample after calcination contained higher amount of functional groups corresponding to this wave number as compared to ZD383.

Figure 5.16 shows the FTIR spectra of SZ893 and CSZC893. Broad bands between 3000 and 3700 $cm^{-1}$ in both the samples is indicative of the presence of both free and hydrogen bonded OH groups on the sample surface [Kamath and Proctor, 1998; Larsen et al., 1996]. The peak nearly in the region at 1600 $cm^{-1}$ is assigned to the $\delta_{HOH}$ mode of quasi free $H_3O^+$ species [Morterra et al., 1994].The presence of sharp band at ~1600 $cm^{-1}$ is thought to be the spectral monitor of the residual presence at the surface of hydrated protonic acid centers (hydrated bronsted sites) and is typically SZ [Morterra et al., 1997] water associated with the sulfate [Ward and Ko, 1994] in both of the samples.

An FTIR spectrum of CSZC893 also shows transmittance around ~1110 $cm^{-1}$ region due to the –OH deformation and this peak may also be due to the $SO_2$ symmetric stretching vibrations [Sohn and Kim, 1989]. FTIR spectra of SZC893 show transmittance around ~2340 $cm^{-1}$ region. This stretching may be due to the O-H stretching in sulphinic acid ($-SO_3H$). Although some inference can be drawn about the surface functional groups present on the surface of samples, exact participation of these functional groups in the desulfurization process can only be authenticated after studying the FTIR spectra of samples after the desulfurization process.

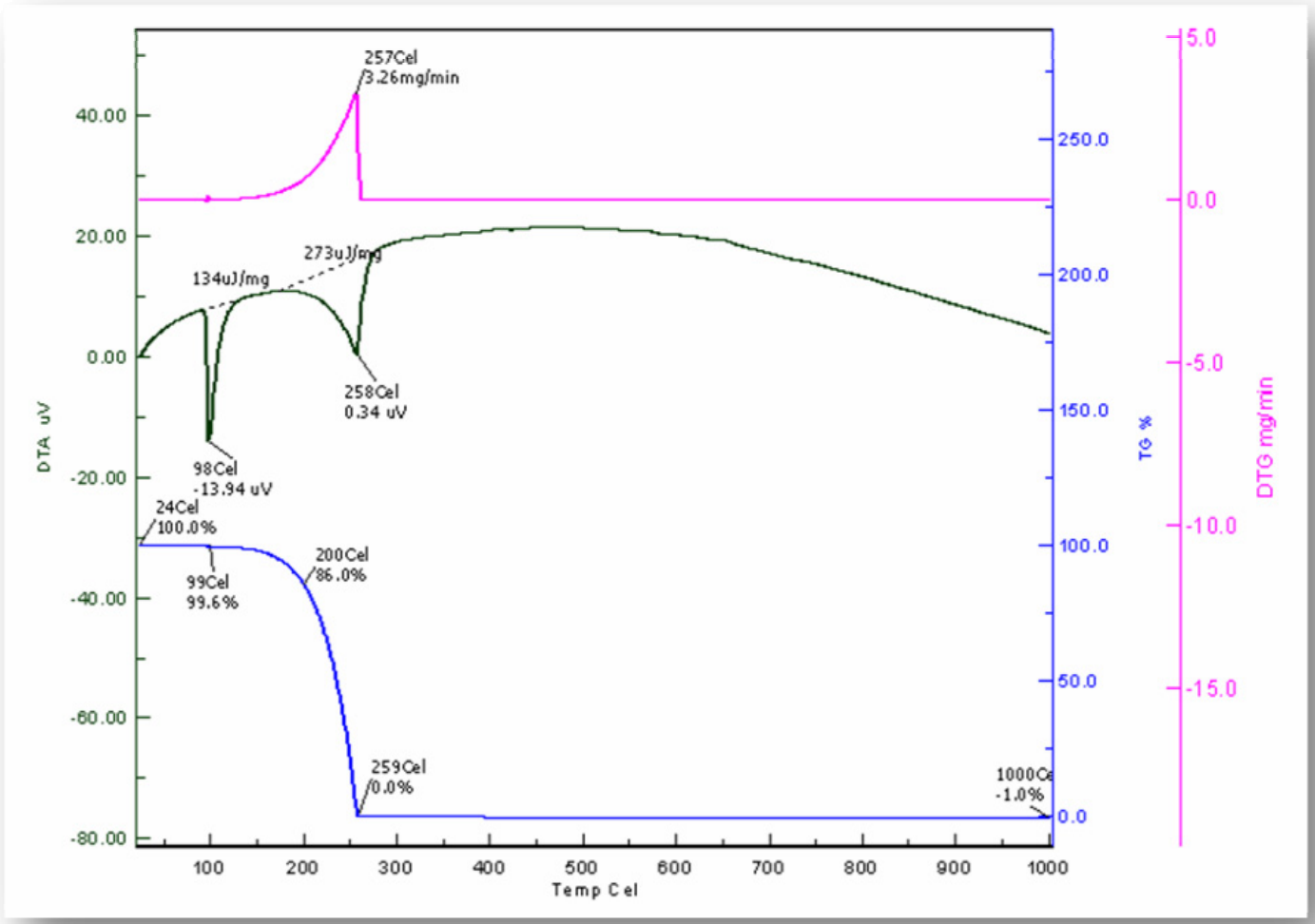


**Figure 5.12 TGD/DTG Thermogram for Pure DBT.**

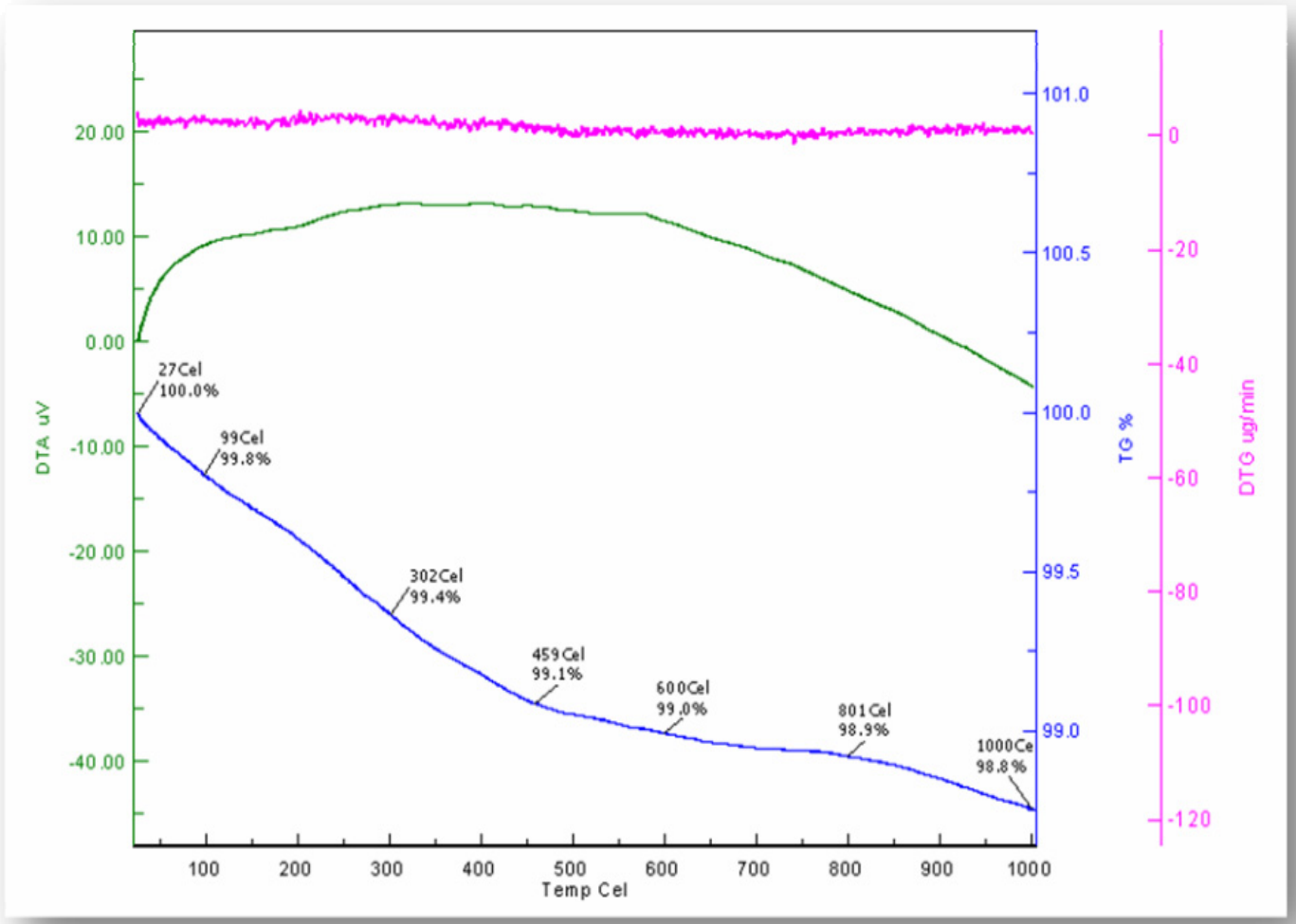


**Figure 5.13 TGD/DTG Thermogram for ZD383.**

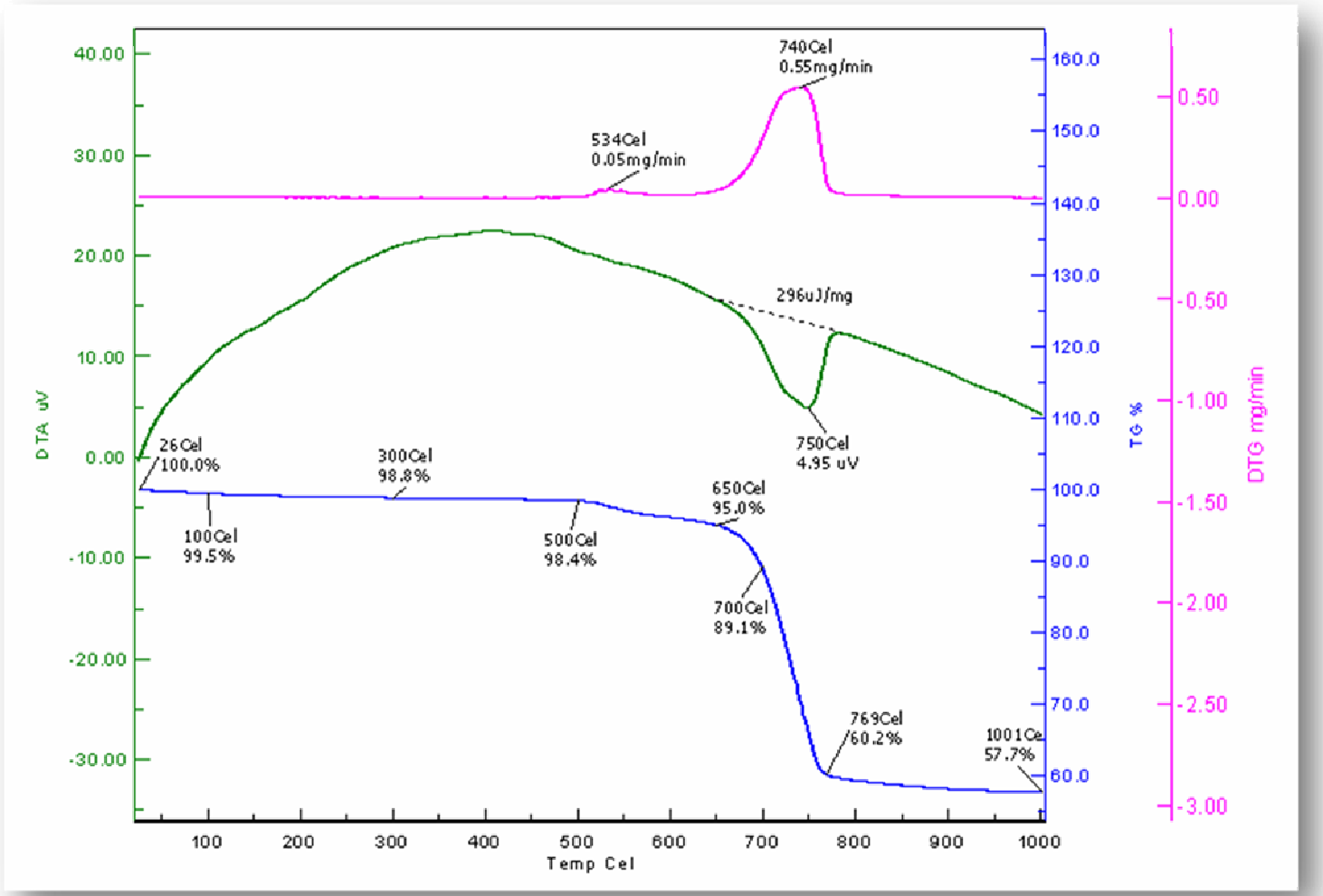


**Figure 5.14 TGD/DTG Thermogram for SZC893.**

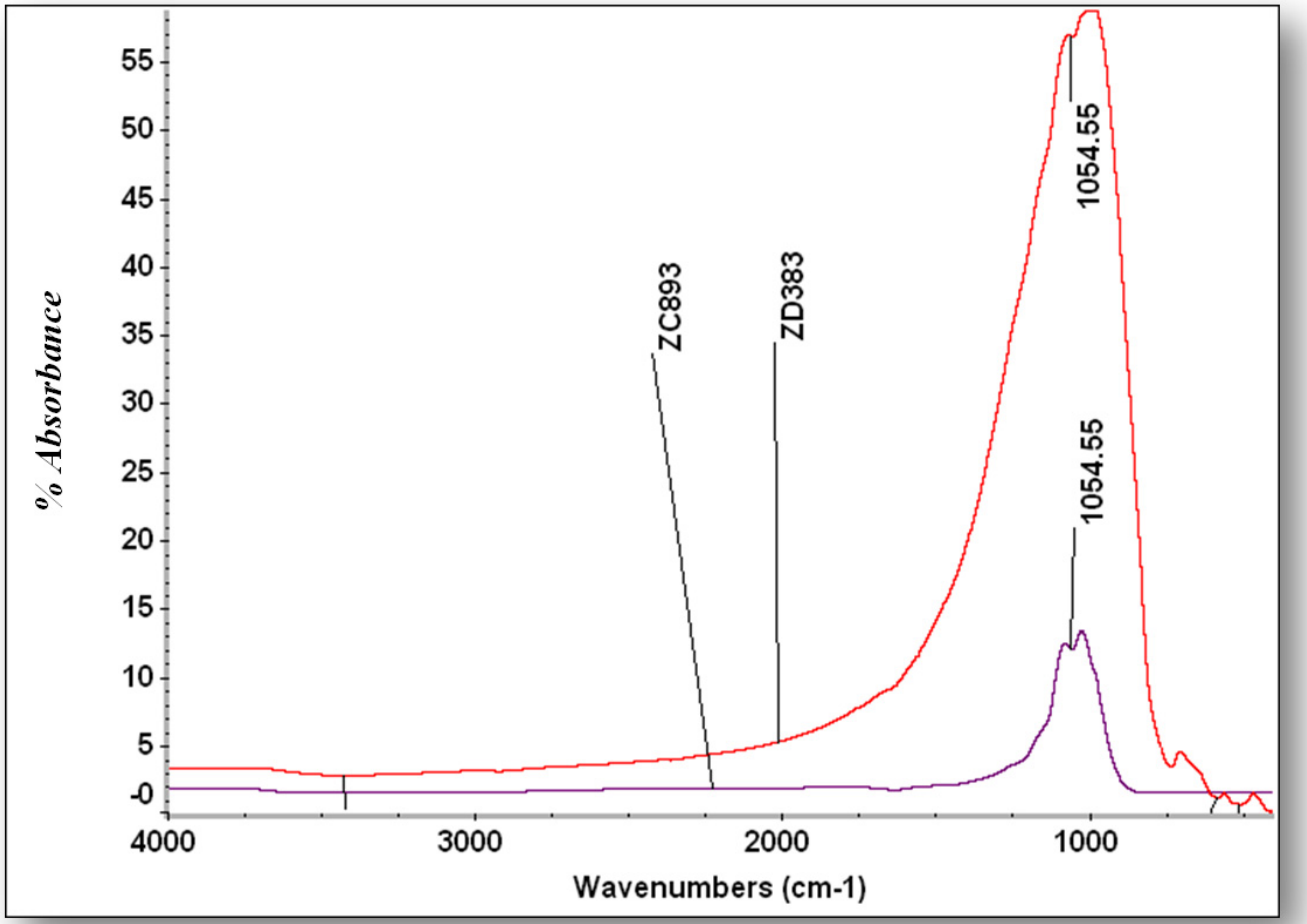


**Figure 5.15 FTIR Spectrum for ZD383 and ZC893.**

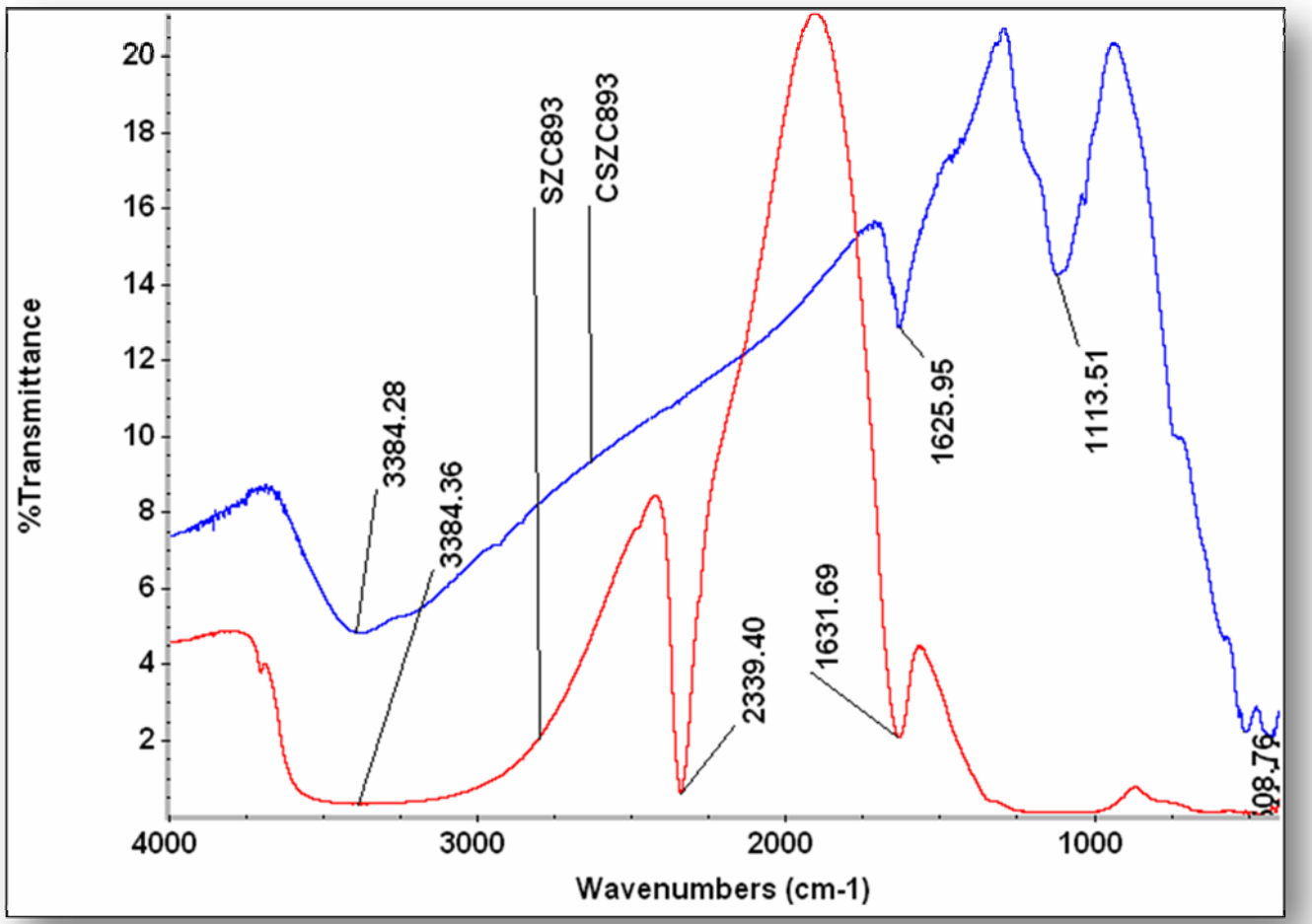


**Figure 5.16 FTIR Spectrum for SZ893 and CSZC893.**

## 5.2 BATCH ADSORPTION DESULFURIZATION STUDIES

Batch adsorption experiments were conducted for adsorptive desulfurization (ADS) of dibenzothiophene (DBT) present in model hydrocarbon (DBT dissolved in iso-octane) at different concentration level was studied using three adsorbents, namely, powdered zirconia dried at 393 K (ZD393), powdered zirconia calcined at 893 K (ZC893), and powdered sulfated zirconia calcined at 893 K (SZC893). Evaluation of various parameters, viz. adsorbent dose ($m$), initial concentration ($C_o$) and contact time ($t$) are of vital importance in the design of any adsorption system for the ADS. The effect of these parameters on the ADS by ZD893, ZC893 and SZC893 is discussed in this section.

### 5.2.1 Effect of Dosage ($m$)

The effect of $m$ on the uptake of DBT onto ZD893, ZC893 and SZC893 was studied at T = 303 K and $C_o$= 30-1000 mg/l and the results are shown in figures 5.17 to 5.19, respectively. The removal of DBT was found to increase with an increase in the $m$ from 1 to 10 g/l. The removal showed marginal change for $m$ > 10 g/l for all the adsorbents. The increase in the adsorption with ZD893, ZC893 and SZC893 dosage can be attributed to the availability of greater surface area and more adsorption sites. At $m$ ≤ 10 g/l, the ZD893, ZC893 and SZC893 surface becomes saturated with DBT and the residual DBT concentration in the solution is large. With an increase in $m$, the DBT removal increases due to increased DBT uptake by the increased amount of ZD893, ZC893 and SZC893. For $m$ > 10 g/l, the incremental DBT removal became low. At about $m$ = 10 g/l, the removal efficiency became almost constant at for DBT removal by ZD893, ZC893 and SZC893. It may be seen in these figures that $m$ =10 g/l seems to be the optimum dosage at all $C_o$.

### 5.2.2 Effect of DBT Concentration ($C_o$)

The effect of $C_o$ on the extent of adsorption of DBT onto ZD383, ZC893 and SZC893 at $m$ = 10 g/l is shown in figure 5.20. It is evident that the DBT removal increases with an increase in $C_o$ due to the decrease in the resistance for the uptake of DBT from the solution.

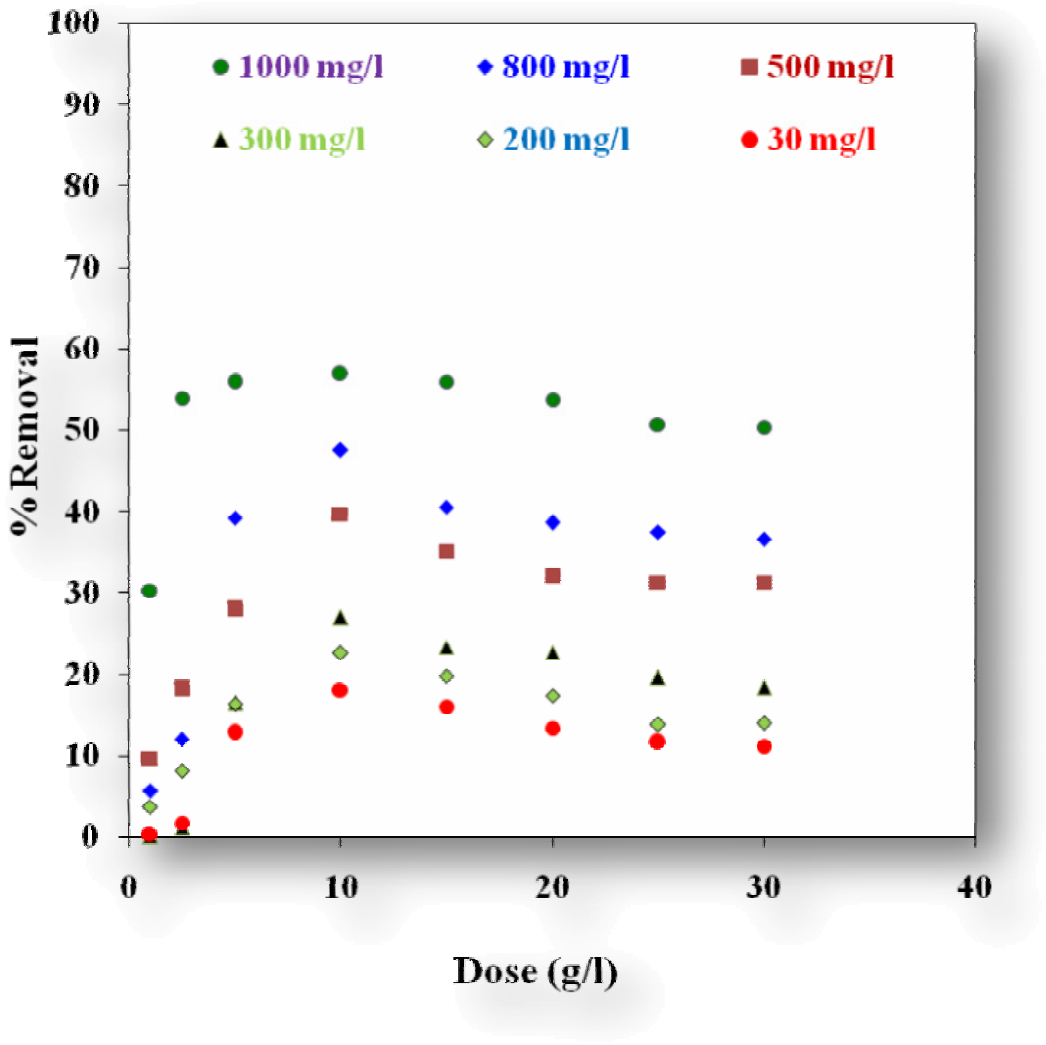


**Figure 5.17 Effect of dosage (*m*) on removal of DBT by ZD383 at various initial concentrations ($C_o$) [$t$ = 22 h; T = 303 K].**

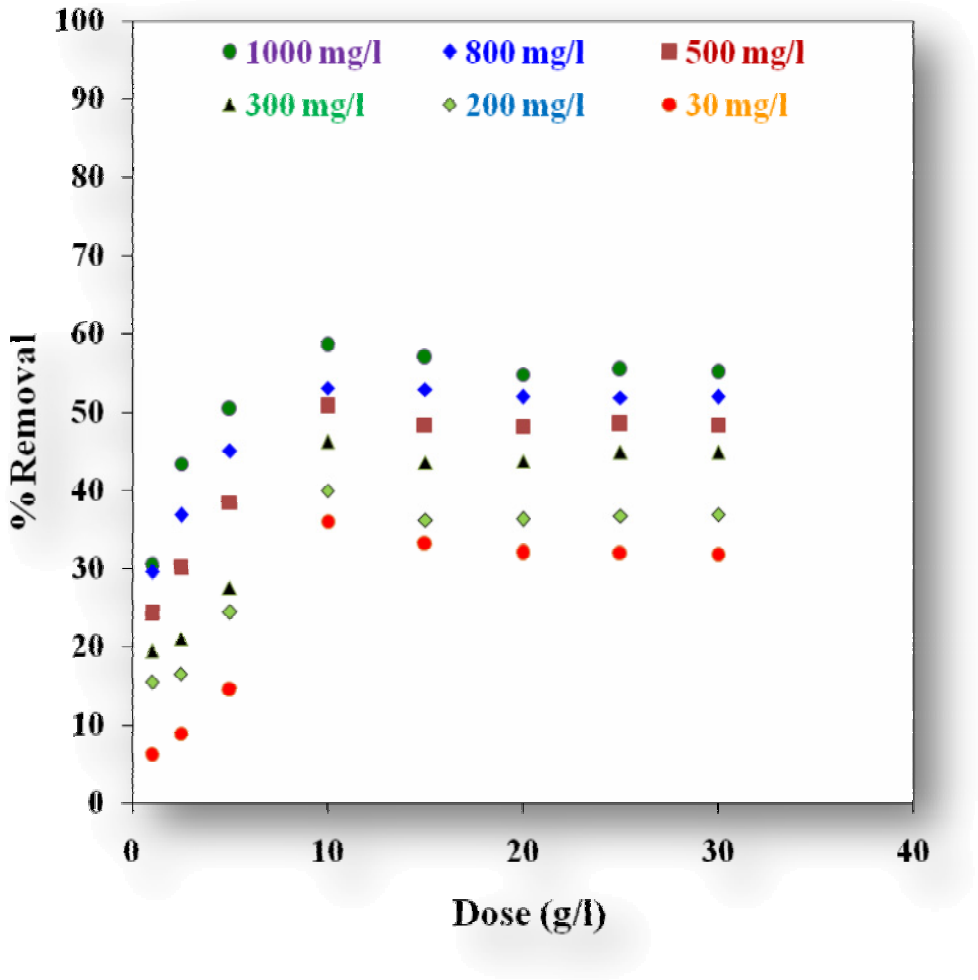


**Figure 5.18 Effect of dosage (*m*) on removal of DBT by ZC893 at various initial concentrations ($C_o$) [$t$ = 22 h; T = 303 K].**

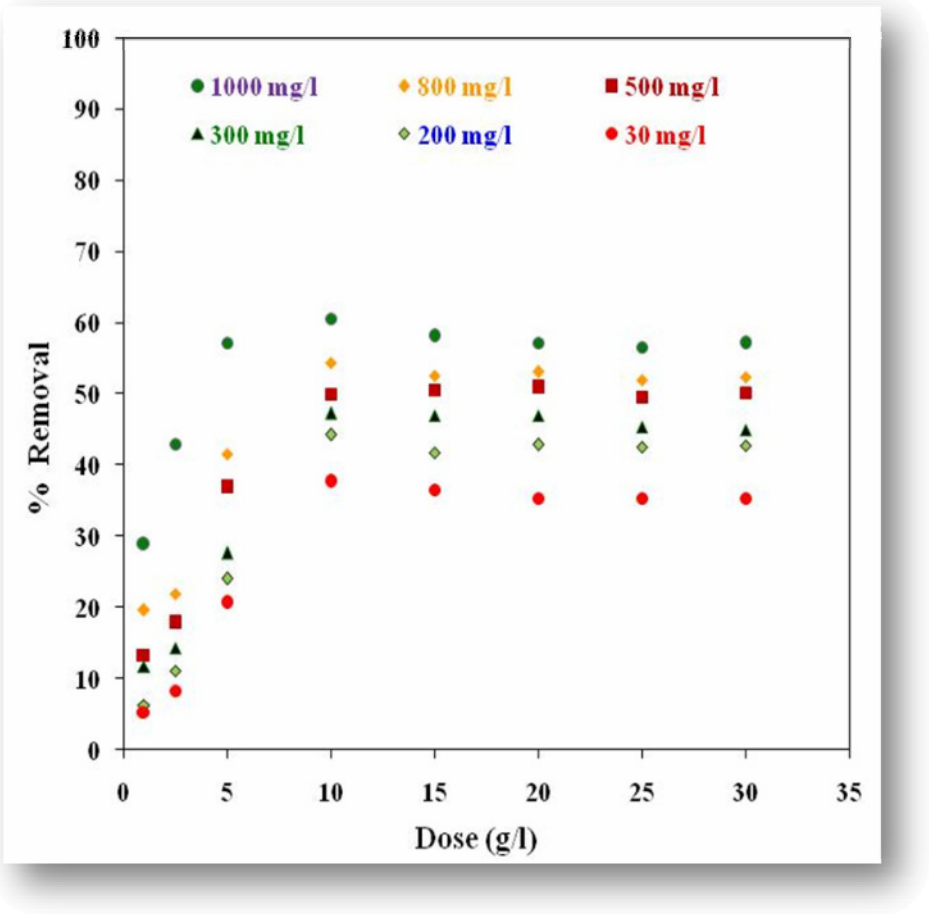


**Figure 5.19 Effect of dosage (*m*) on removal of DBT by SZC893 at various initial concentrations ($C_o$) [$t$ = 22 h; T = 303 K].**

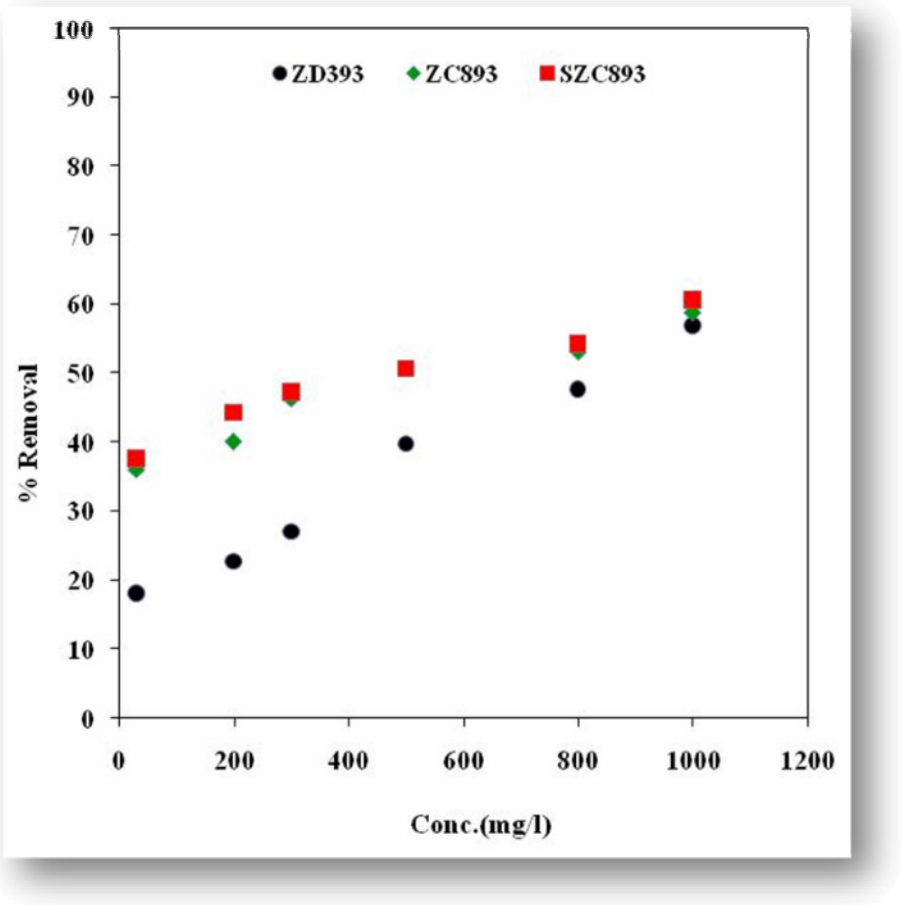


**Figure 5.20 Effect of initial concentration ($C_o$) on removcpal of DBT at T = 303K; $t$ = 22 h by various samples.**

### 5.2.3 Effect of Contact Time (*t*)

The rate and quantity of adsorbate adsorbed by the adsorbent is limited by the size of adsorbate molecules, concentration of adsorbate and its affinity towards the adsorbent, diffusion coefficient of the adsorbate in the bulk and solid phase and the degree of mixing. DBT solutions with different $C_o$ (30, 200, 300, 500, 800 and 1000 mg/l) were kept in contact with ZD383, ZC893 and SZC893 for 32 h.

Figures 5.21 to 5.23 present a plot of the time-course of DBT onto ZD893, ZC893 and SZC893. The residual concentrations at 22 h contact time were found to be varied by a maximum of ~1% than those obtained after 32 h contact time. Therefore, after 22 h contact time, a steady state approximation was assumed and a quasi-equilibrium situation was accepted. Accordingly all the batch experiments were conducted with a contact time of 22 h under vigorous shaking conditions. The rate of DBT removal is found to be very rapid during the initial 30 min, and thereafter, the rate of DBT removal decreases. It is found that the adsorptive removal of the DBT ceases after 22 h of contacting with ZD383, ZC893 and SZC893. A large number of vacant surface sites are available for adsorption during the initial stage, and after a lapse of time, the remaining vacant surface sites are difficult to be occupied due to repulsive forces between the solute molecules on the solid and bulk phases. Besides, the DBT is adsorbed into the macro- and meso-pores that get almost saturated with DBT during the initial stage of adsorption. Thereafter, the DBT molecules have to traverse farther and deeper into the micro-pores encountering much larger resistance. This results in the slowing down of the adsorption during the later period of adsorption.

### 5.2.4 Adsorption Kinetic Modeling (AKM)

The prediction of the batch adsorption kinetics is necessary for the design of industrial adsorption columns. In the present study, the frequently used kinetic models, namely pseudo-first-order and pseudo-second-order models have been tested to investigate the adsorption of DBT onto ZD383, ZC893 and SZC893.

#### 5.2.4.1 Pseudo-First Order and Pseudo-Second Order Model

The adsorption of DBT molecules from oil phase to the solid phase can be considered as a reversible process with equilibrium being established between the solution and the solid phase.

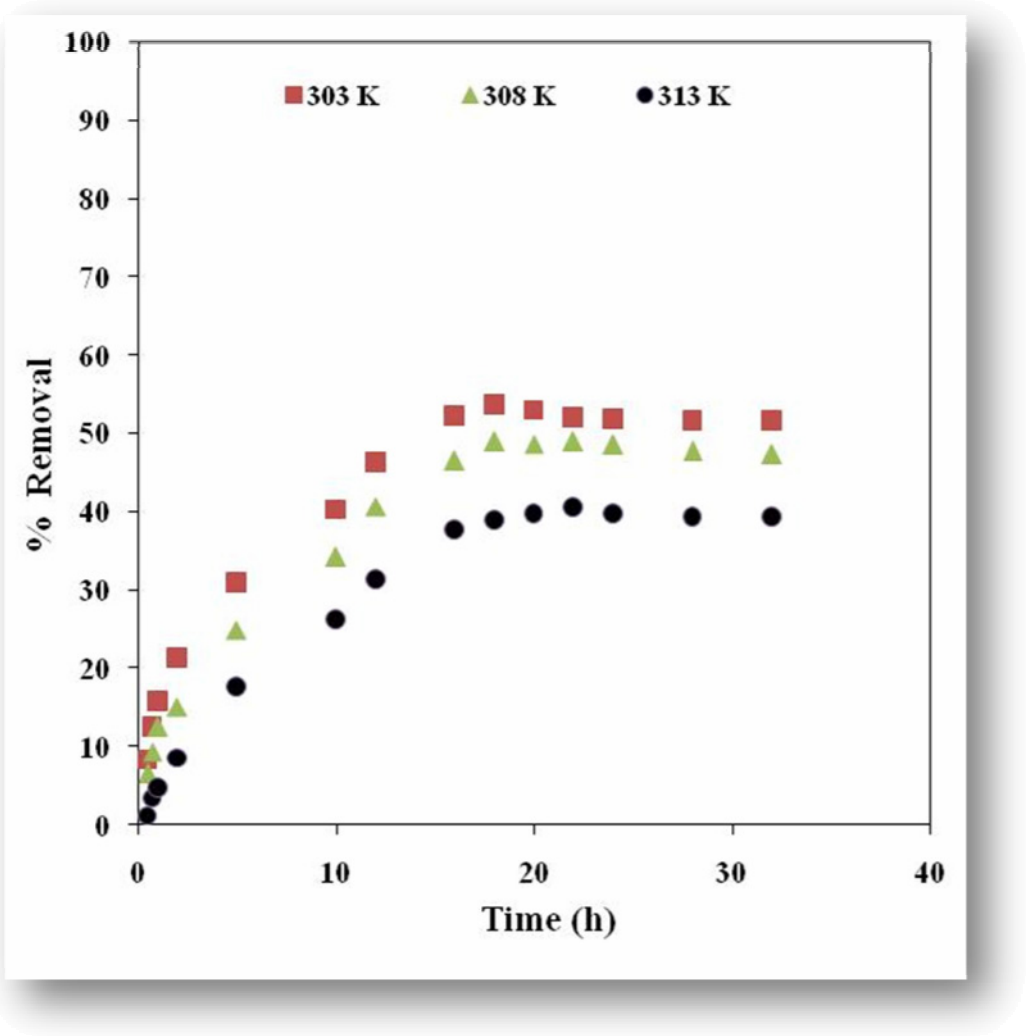


**Figure 5.21 Effect of time on removal of DBT by ZD383 at various temprature (T) [$C_o$=1000 mg/l; $m$ = 10 g/l].**

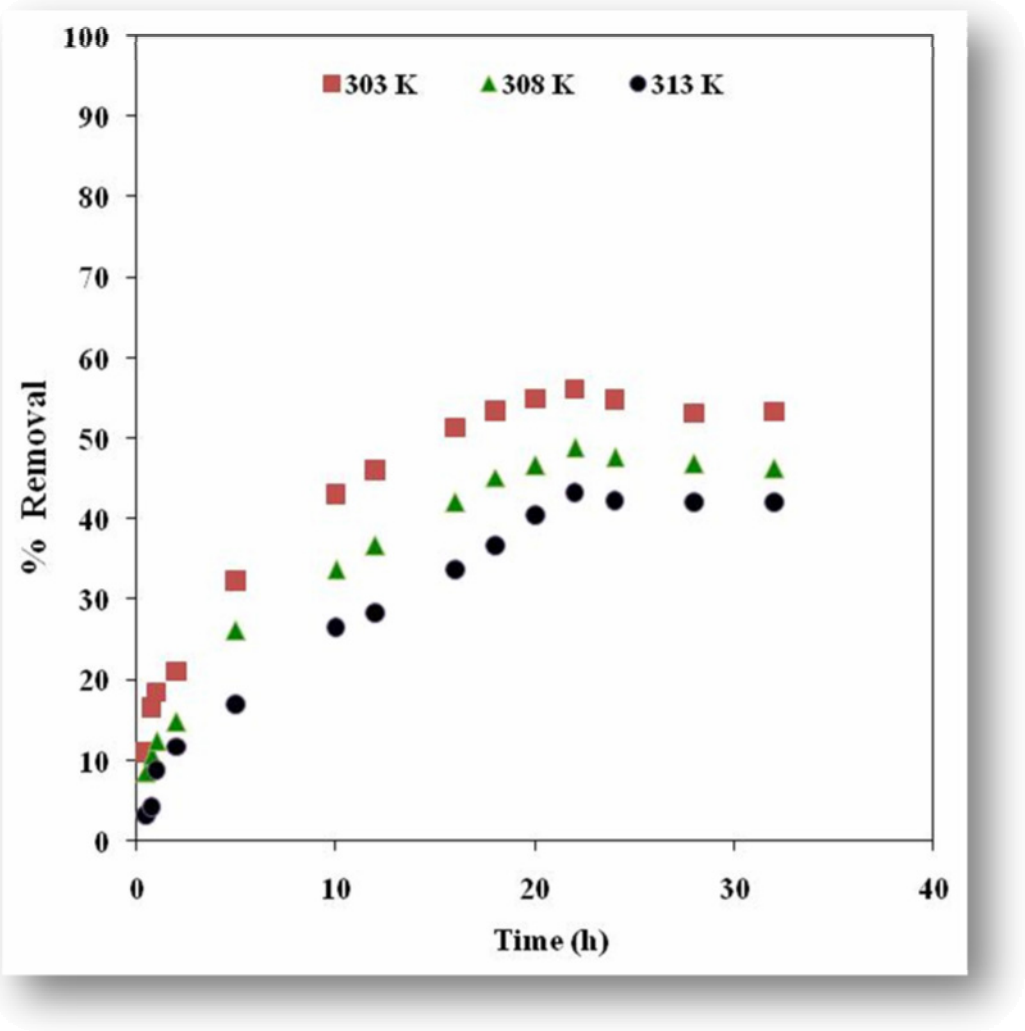


**Figure 5.22 Effect of time on removal of DBT by ZC893 at various temprature (T) [$C_o$=1000 mg/l; $m$ = 10 g/l].**

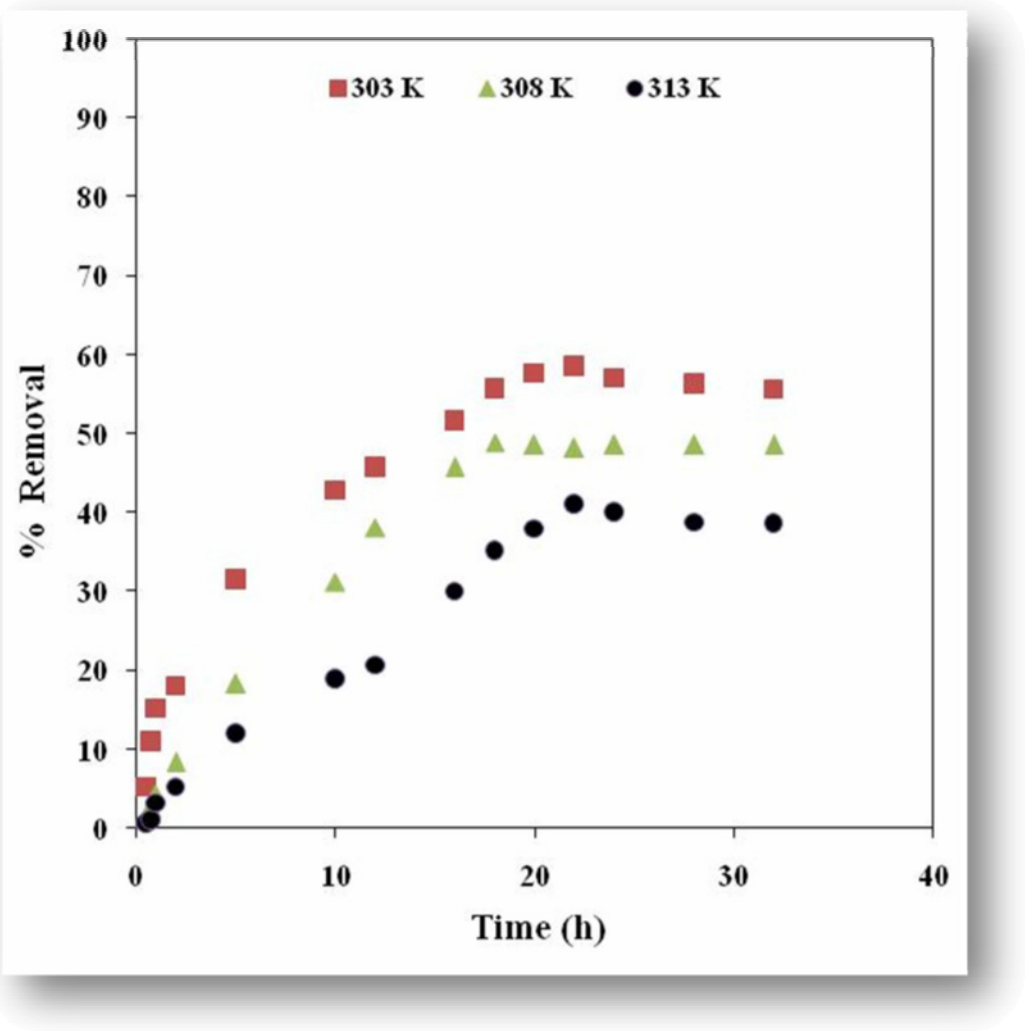


**Figure 5.23 Effect of time on removal of DBT by SZC893 at various temperature (T) [$C_o$=1000 mg/l; $m$ = 10 g/l].**

p

Assuming non-dissociating molecular adsorption of DBT molecules on ZD383, ZC893 and SZC893 particles with no DBT molecules initially present on the adsorbent, the uptake of the DBT molecules by the ZD383, ZC893 and SZC893 at any instant (*t*) is given as [Srivastava et al.,2006]

$$q_t = q_e\left[1-\exp\left(-k_f t\right)\right] \tag{5.1}$$

where, $q_e$ = amount of the adsorbate adsorbed on the adsorbent under equilibrium condition and $k_f$ is the pseudo-first order rate constant.

The pseudo-second-order model is represented as [Blanchard et al., 1984; Ho and McKay,1999]

$$q_t = \frac{tk_S q_e^2}{1+tk_S q_e} \tag{5.2}$$

The initial adsorption rate, $h$ (mg/g min), at $t \to 0$ is defined as:

$$h = k_S q_e^2 \tag{5.3}$$

The best-fit values of $k_f$, $h$, $q_e$ and $k_S$ along with the correlation coefficients for the pseudo-first-order and pseudo-second-order models for all the DBT-adsorbents systems are given in tables 5.3-5.5.

The $q_{e,\exp}$ and the $q_{e,cal}$ values for the pseudo-first-order model and pseudo-second-order models are also shown in tables 5.3-5.5. They $q_{e,\exp}$ are closer to the $q_{e,cal}$ values calculated from the pseudo-first-order kinetic model at some places and to the $q_{e,cal}$ values calculated from the pseudo-second-order kinetic model at other places. The calculated coefficient of correlations is also closer to one, and is also closer to each other for both pseudo-second-order kinetics and pseudo first-order kinetic model. It may be seen that the difference in prediction by the two models is small, and any of the two could be used for kinetic modeling. Therefore, the adsorption can be approximated by pseudo-first-order or pseudo-second-order kinetic model for the DBT adsorption from model hydrocarbon onto ZD383, ZC893 and SZC893.

The fitting of the pseudo-second-order kinetic model onto experimental data points for the DBT adsorption from model hydrocarbon onto ZD383, ZC893 and SZC893 is shown by lines in figures 5.24-5.26, respectively. The fitting is found to be satisfactory.

**Table 5.3 Kinetic parameters for the removal of DBT by ZD383.**

| **Pseudo-First-Order Model** | | | | | |
|---|---|---|---|---|---|
| **T (K)** | $q_{e,exp}$ **(mg/g)** | $q_{e,cal}$ **(mg/g)** | $K_f$ **(1/min)** | $R^2$ | **SSE** |
| 303 | 53.8 | 52.0 | 0.0042 | 0.982 | 95.2 |
| 308 | 49.7 | 49.4 | 0.0029 | 0.983 | 95.3 |
| 313 | 41.3 | 45.3 | 0.0019 | 0.981 | 56.9 |
| **Pseudo-Second-Order Model** | | | | | |
| **T (K)** | $q_{e,cal}$ **(mg/g)** | $K_s$**(g/mg min)** | $h$ **(mg/g min)** | $R^2$ | **SSE** |
| 303 | 60.1 | 8.2E-05 | 0.298 | 0.989 | 45.6 |
| 308 | 58.5 | 6.0E-05 | 0.205 | 0.987 | 72.8 |
| 313 | 56.0 | 3.2E-05 | 0.102 | 0.986 | 51.1 |
| **W-M Intra-Particle Diffusion Model** | | | | | |
| **T (K)** | $K_{id,1}$ **(mg/g min$^{1/2}$)** | | $R^2$ | | **SSE** |
| 303 | 1.642 | | 0.994 | | 3.72 |
| 308 | 1.587 | | 0.992 | | 4.69 |
| 313 | 1.420 | | 0.994 | | 2.92 |
| **T (K)** | $K_{id,2}$ **(mg/g min$^{1/2}$)** | | $R^2$ | | **SSE** |
| 303 | 0.042 | | 0.818 | | 2.15 |
| 308 | 0.011 | | 0.865 | | 2.49 |
| 313 | 0.082 | | 0.810 | | 2.76 |

**Table 5.4 Kinetic parameters for the removal of DBT by ZC893.**

| Pseudo-First-Order Model | | | | | |
|---|---|---|---|---|---|
| **T (K)** | **$q_{e,exp}$ (mg/g)** | **$q_{e,cal}$ (mg/g)** | **$K_f$ (1/min)** | **$R^2$** | **SSE** |
| 303 | 56.96 | 53.20 | 0.0052 | 0.959 | 185.5 |
| 308 | 49.40 | 47.60 | 0.0027 | 0.979 | 126.6 |
| 313 | 44.04 | 46.52 | 0.0015 | 0.960 | 127.4 |
| **Pseudo-Second-Order Model** | | | | | |
| **T (K)** | **$q_{e,cal}$ (mg/g)** | **$K_s$ (g/mg min)** | **$h$ (mg/g min)** | **$R^2$** | **SSE** |
| 303 | 60.50 | 1.0E-04 | 0.369 | 0.978 | 87.8 |
| 308 | 55.70 | 6.5E-05 | 0.200 | 0.979 | 77.0 |
| 313 | 58.20 | 2.8E-05 | 0.096 | 0.967 | 108.3 |
| **W-M Intra-Particle Diffusion Model** | | | | | |
| **T (K)** | **$K_{id,1}$ (mg/g min$^{1/2}$)** | | **$R^2$** | | **SSE** |
| 303 | 1.407 | | 0.995 | | 4.32 |
| 308 | 1.320 | | 0.998 | | 0.32 |
| 313 | 1.109 | | 0.989 | | 8.74 |
| **T (K)** | **$K_{id,2}$ (mg/g min$^{1/2}$)** | | **$R^2$** | | **SSE** |
| 303 | 0.280 | | 0.519 | | 3.61 |
| 308 | 0.152 | | 0.975 | | 1.92 |
| 313 | 0.068 | | 0.703 | | 12.53 |

**Table 5.5 Kinetic parameters for the removal of DBT by SZC893.**

| Pseudo-First-Order Model | | | | | |
|---|---|---|---|---|---|
| **T (K)** | **$q_{e,exp}$ (mg/g)** | **$q_{e,cal}$ (mg/g)** | **$K_f$(1/min)** | **$R^2$** | **SSE** |
| 303 | 59.86 | 58.29 | 0.0028 | 0.985 | 113.91 |
| 308 | 49.69 | 56.43 | 0.0018 | 0.980 | 122.88 |
| 313 | 44.16 | 55.89 | 0.0009 | 0.960 | 146.02 |
| **Pseudo-Second-Order Model** | | | | | |
| **T (K)** | **$q_{e,cal}$ (mg/g)** | **$K_s$(g/mg min)** | **$h$ (mg/g min)** | **$R^2$** | **SSE** |
| 303 | 69.20 | 5.0E-05 | 0.238 | 0.986 | 75.42 |
| 308 | 70.48 | 2.4E-05 | 0.117 | 0.983 | 105.30 |
| 313 | 81.50 | 8.0E-05 | 0.053 | 0.963 | 135.15 |
| **W-M Intra-Particle Diffusion Model** | | | | | |
| **T (K)** | **$K_{id,1}$ (mg/g min$^{1/2}$)** | | **$R^2$** | | **SSE** |
| 303 | 1.8 | | 0.997 | | 3.12 |
| 308 | 1.7 | | 0.987 | | 17.42 |
| 313 | 1.4 | | 0.943 | | 35.65 |
| **T (K)** | **$K_{id,2}$ (mg/g min$^{1/2}$)** | | **$R^2$** | | **SSE** |
| 303 | 0.28 | | 0.973 | | 1.53 |
| 308 | 0.01 | | 0.534 | | 7.43 |
| 313 | 0.15 | | 0.643 | | 14.87 |

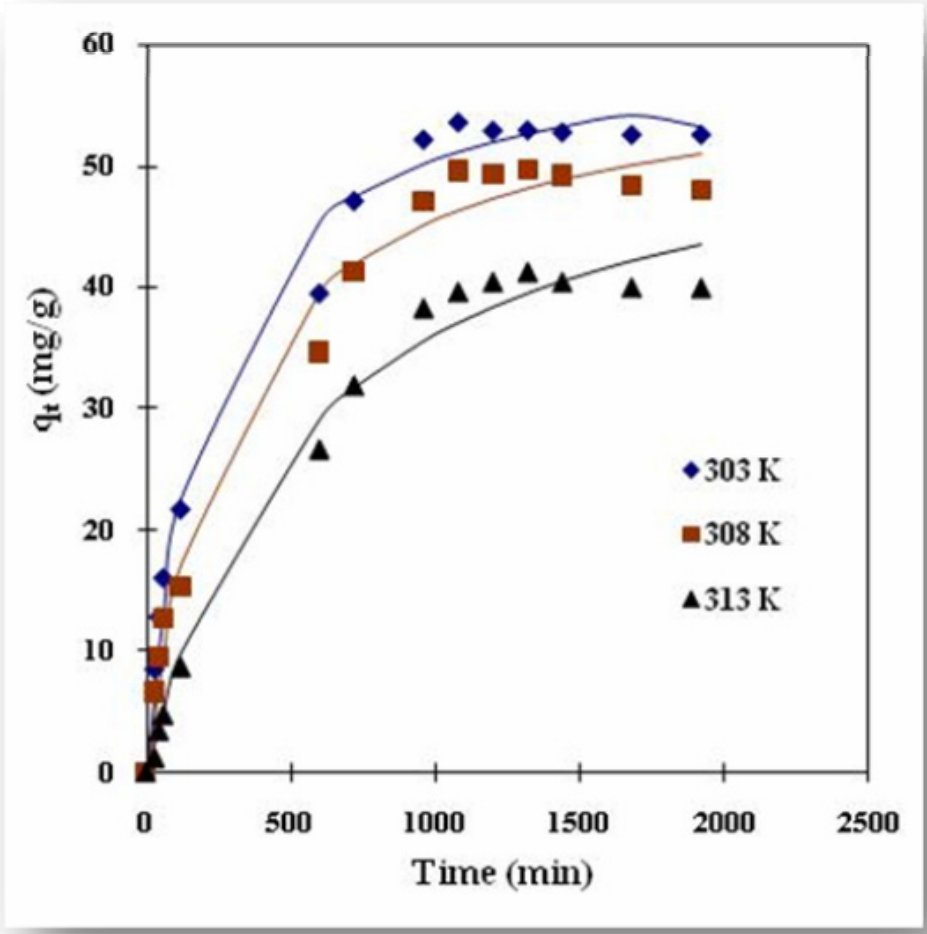


**Figure 5.24 Effect of contact time on the removal of DBT by ZD383. Experimental data points given by the symbols and the lines predicted by the pseudo-second-order model. $C_o$ = 1000 mg/l, $m$ = 10 g/l.**

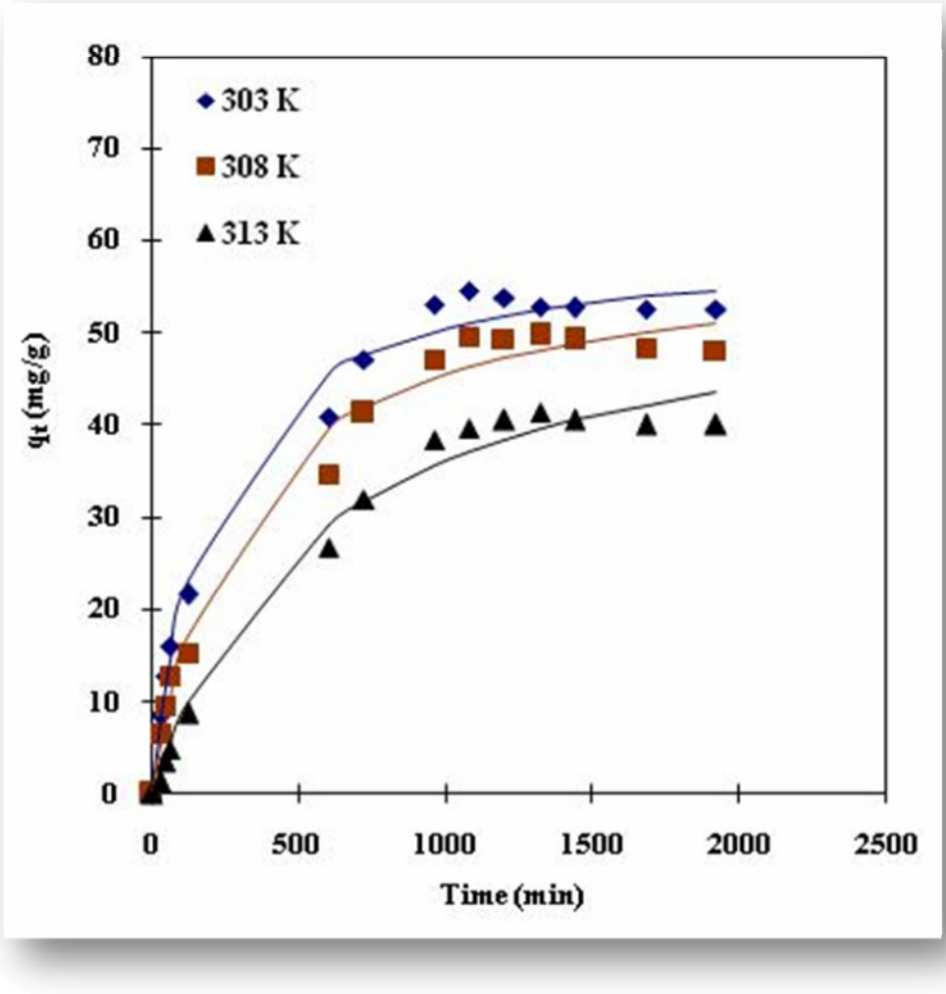


**Figure 5.25 Effect of contact time on the removal of DBT by ZC893. Experimental data points given by the symbols and the lines predicted by the pseudo-second-order model. $C_o$ = 1000 mg/l, $m$ = 10 g/l.**

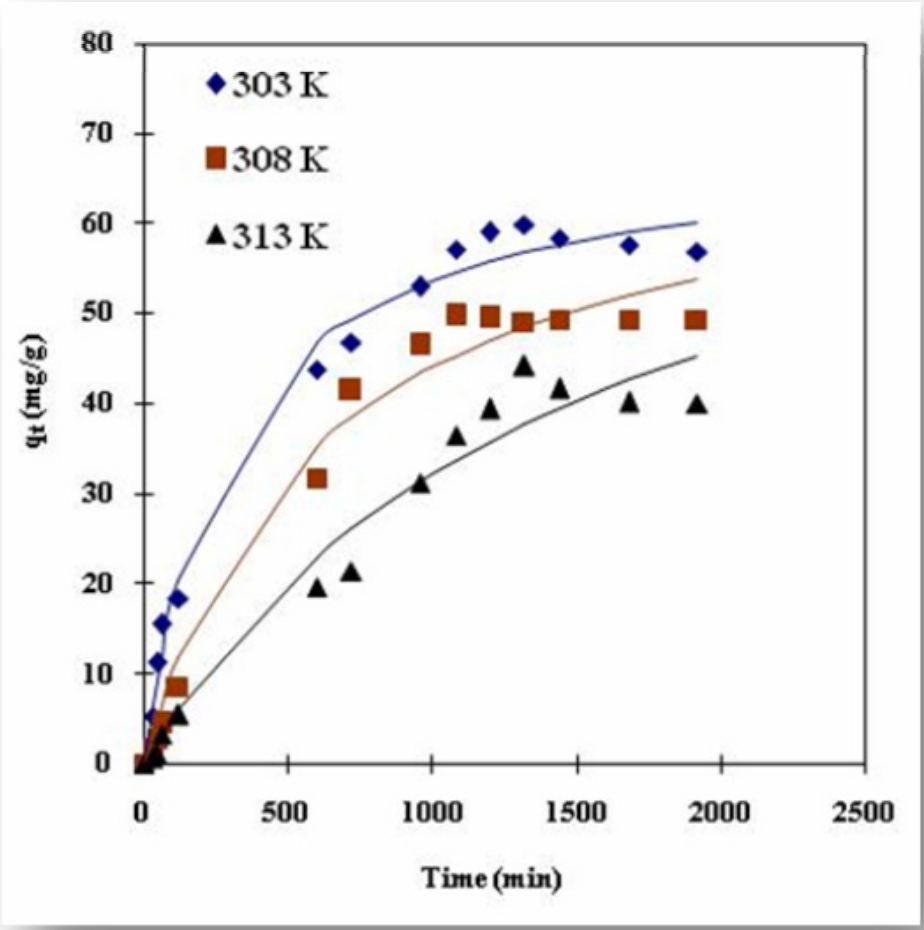


**Figure 5.26 Effect of contact time on the removal of DBT by SZC893. Experimental data points given by the symbols and the lines predicted by the pseudo-second-order model. $C_o$ = 1000 mg/l, $m$ = 10 g/l.**

### 5.2.4.2 Diffusion Study

Interpretation of experimental kinetics data from a mechanistic viewpoint, require the prediction of the rate-limiting step. The transport of adsorbate from the solution phase to the surface of the adsorbent particles occurs in several steps. The overall adsorption process may be controlled either by one or more steps, e.g. film or external diffusion, pore diffusion, surface diffusion and adsorption on the pore surface, or a combination of more than one step. Generally, a process is diffusion controlled if its rate is dependent upon the rate at which components diffuse towards one another. In a rapidly stirred batch adsorption, the diffusive mass transfer can be related by an apparent diffusion coefficient, which will fit the experimental adsorption-rate data.

The possibility of intra-particle diffusion was explored by using the intra-particle diffusion model [Weber and Morris, 1963].

$$q_t = k_{id} t^{0.5} + I \tag{5.4}$$

where, $k_{id}$ is the intra-particle diffusion rate constant, and values of $I$ give an idea about the thickness of the boundary layer. If the Weber-Morris plot of $q_t$ versus $t^{0.5}$ satisfies the linear relationship with the experimental data, then the adsorption process is found be controlled by intra-particle diffusion only. However, if the data exhibit multi-linear plots, then two or more steps influence the overall adsorption process. The first, sharper portion represents the diffusion of adsorbate through the solution to the external surface of adsorbent or boundary layer diffusion of solute molecules. The second linear portion is attributed to the gradual equilibrium stage with intra-particle diffusion dominating. The third portion is the final equilibrium stage for which the intra particle diffusion starts to slow down due to the extremely low adsorbate concentration left in the solution [Crank, 1965; Reichenberg, 1953]. The mathematical dependence of fractional uptake of adsorbate on $t^{0.5}$ is obtained if the adsorption process is considered to be influenced by diffusion in the cylindrical (or spherical) and convective diffusion in the adsorbate solution.

Figures 5.27-5.29 show $q_t$ versus $t^{0.5}$ plot for DBT adsorption from model hydrocarbon onto ZD383, ZC893 and SZC893 at T=303, 308 and 318 K. In the figure the plots are not linear over the whole time range, implying that the more than one process is controlling the adsorption process. The first portion (line not drawn for the clarity of picture) gives boundary layer diffusion, and further two linear portions depict

intra-particle diffusion. In the two linear portions- the first straight portion depicting meso-pore diffusion and the second representing micro-pore diffusion. These show only the pore diffusion data. Extrapolation of the linear portions of the plots back to the y-axis gives the intercepts, which provide the measure of the boundary layer thickness. If the intercept is large, the boundary layer effect will also be large. The deviation of straight lines from the origin may be due to difference in rate of mass transfer in the initial and final stages of adsorption. Further, such deviation of straight line from the origin indicates that the pore diffusion is not the sole rate-controlling step. Therefore, the adsorption proceeds via a complex mechanism [Carbery et al., 1977; Chaturvedi et al., 1988] consisting of both surface adsorption and intra-particle transport within the pores of the adsorbents.

The $k_{id,1}$ and the $I$ values for the Weber-Morris model are also shown in tables 5.3-5.5. The slope of the linear portions of the Weber-Morris Plots - $q_t$ versus $t^{0.5}$ - are defined as a rate parameters ($k_{id,1}$ and $k_{id,2}$), characteristic of the rate of adsorption in the region where intra-particle diffusion is rate controlling. Thus it can be inferred from the figures 5.27-5.29 that the diffusion from the bulk phase to the external surface of the adsorbents, which begins at the start of the adsorption process, is the fastest. It seems that the intra-particle diffusion of DBT into micropores (third portion) is the rate controlling step in the adsorption process. The third portion of the plots is nearly parallel, suggesting that the rate of adsorption DBT in the micropores of ZD383, ZC893 and SZC893 is comparable.

### 5.2.5 Effect of Temperature

Temperature has a pronounced effect on the adsorption capacity of the adsorbents. The effect of temperature on ADS capacity of ZD383, ZC893 and SZC893 was studied by carrying out experiment from 303 to 348 K using different initial DBT concentration. The effect of temperature on the percent DBT removal by ZD383, ZC893 and SZC893 are presented in figures 5.30 through 5.32. It shows that the removal decreased with increase in temperature. The decrease of ADS capacity with the increase in temperature indicated that the ADS by ZD383, ZC893 and SZC893 is exothermic in nature. The decrease in adsorption with the rise of temperature may be due to the weakening of adsorptive forces between the active sites of the adsorbent and adsorbate species and also between the adjacent molecules of the adsorbed phase.

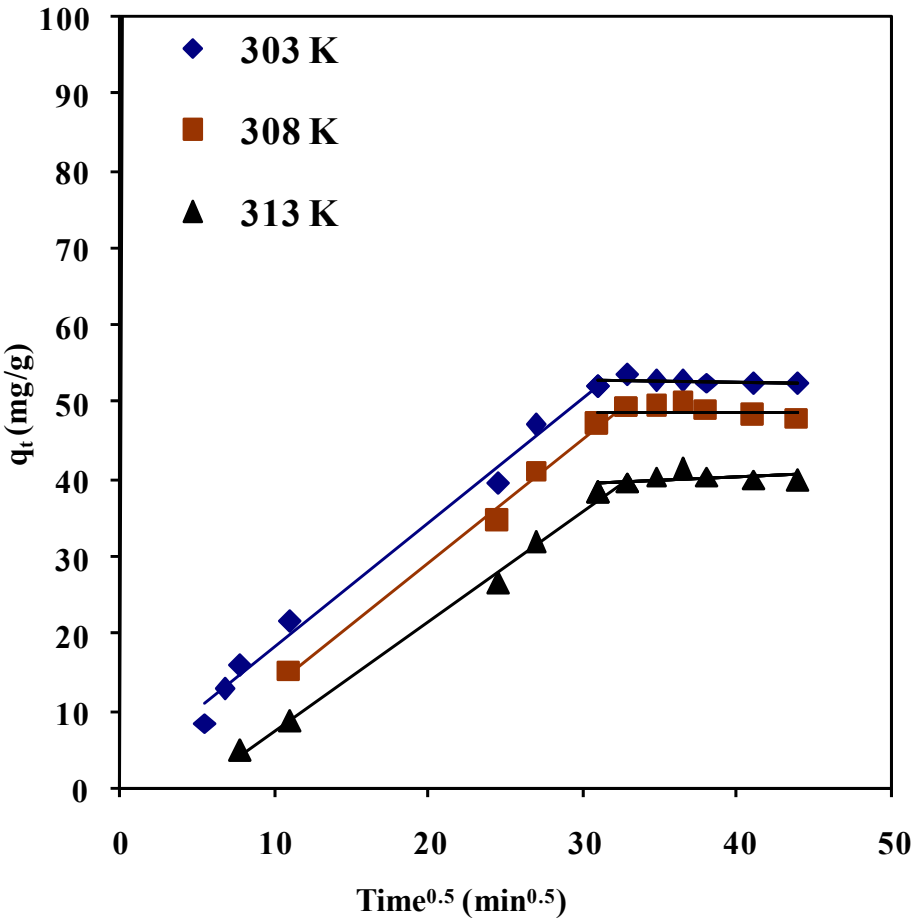


**Figure 5.27 Weber and Morris intra-particle diffusion plot for the removal of DBT ZD383, $C_o$= 1000 mg/l , $m$ = 10 g/l.**

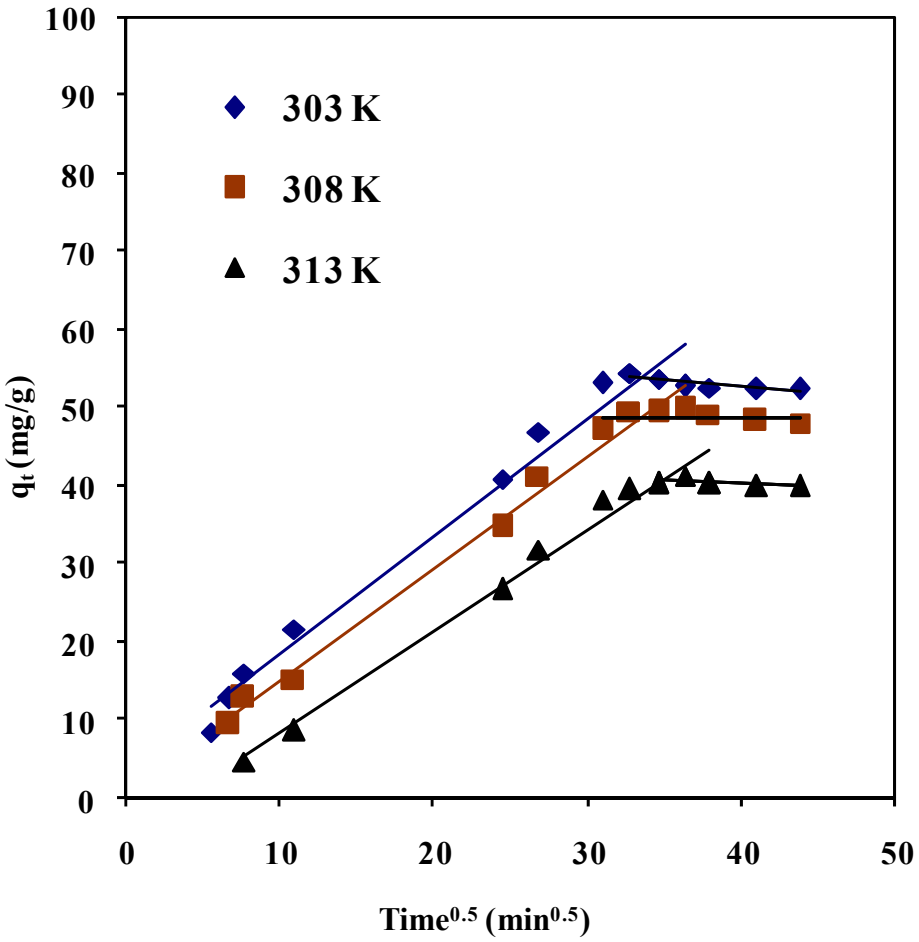


**Figure 5.28 Weber and Morris intra-particle diffusion plot for the removal of DBT ZC893, $C_o$ = 1000 mg/l , $m$ = 10 g/l.**

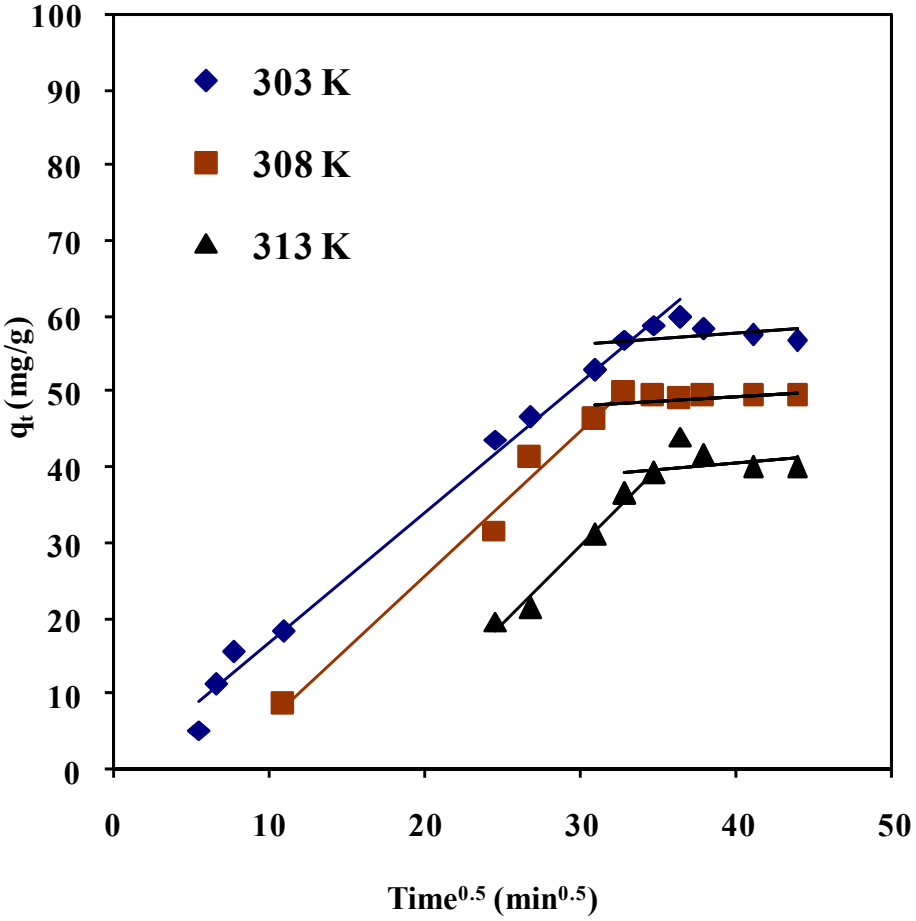


**Figure 5.29 Weber and Morris intra-particle diffusion plot for the removal of DBT SZC893, $C_o$ = 1000 mg/l , $m$ = 10 g/l.**

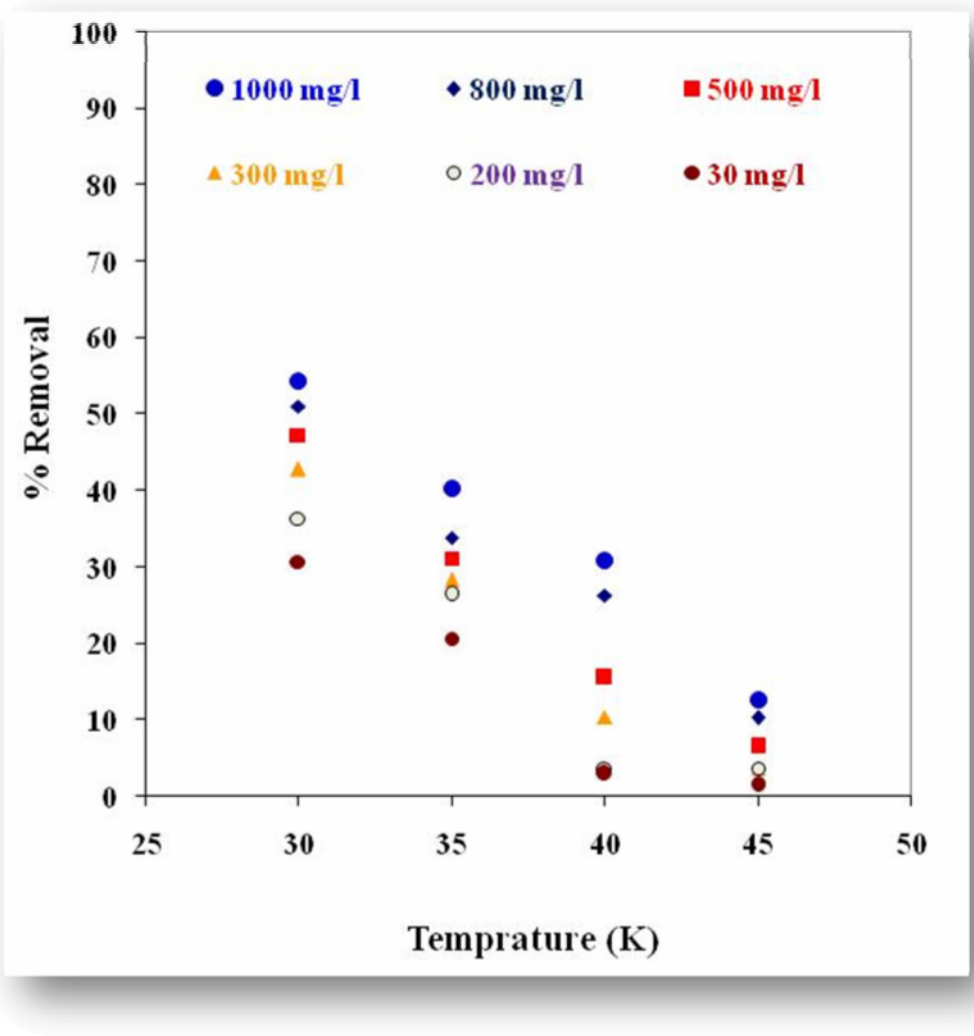


**Figure 5.30 Effect of temperature on removal of DBT by ZD383 at various initial concentrations ($C_o$).**

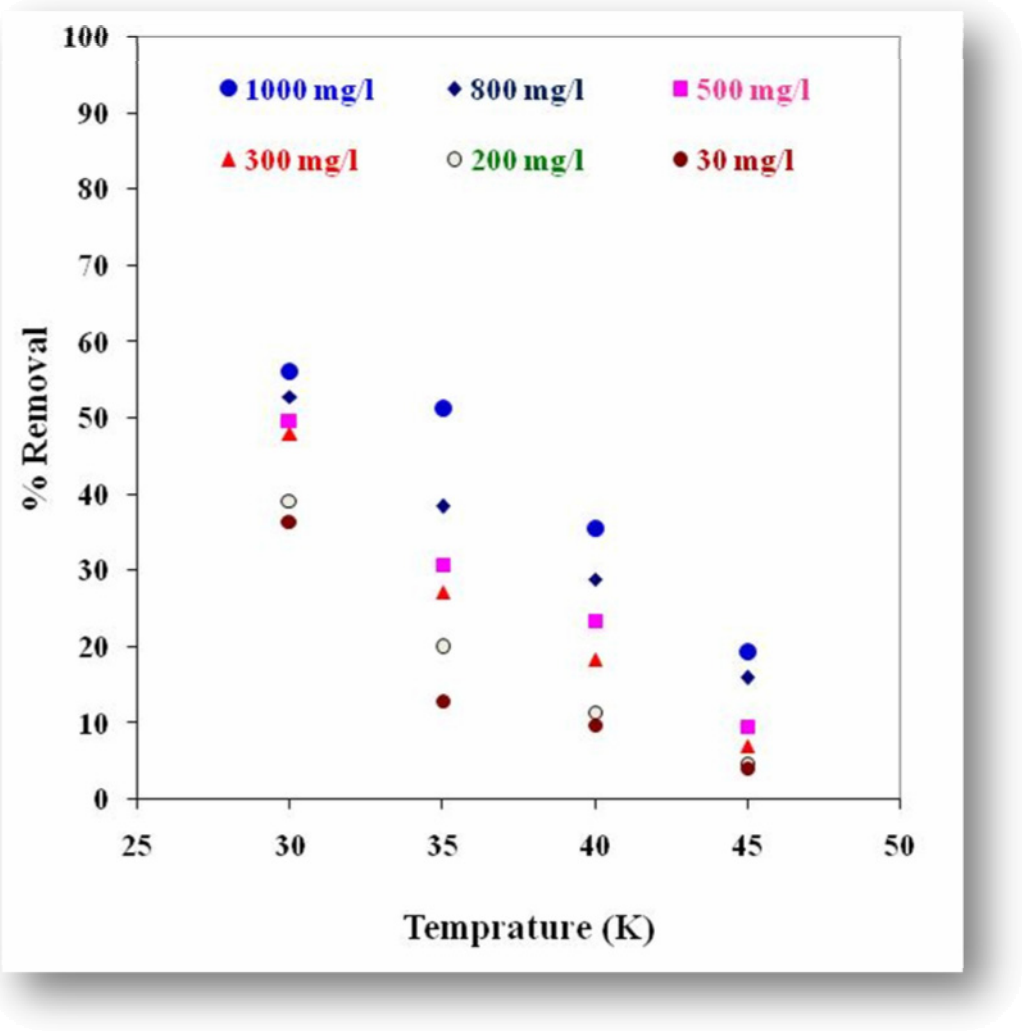


**Figure 5.31 Effect of temperature on removal of DBT by ZC893 at various initial concentrations ($C_o$).**

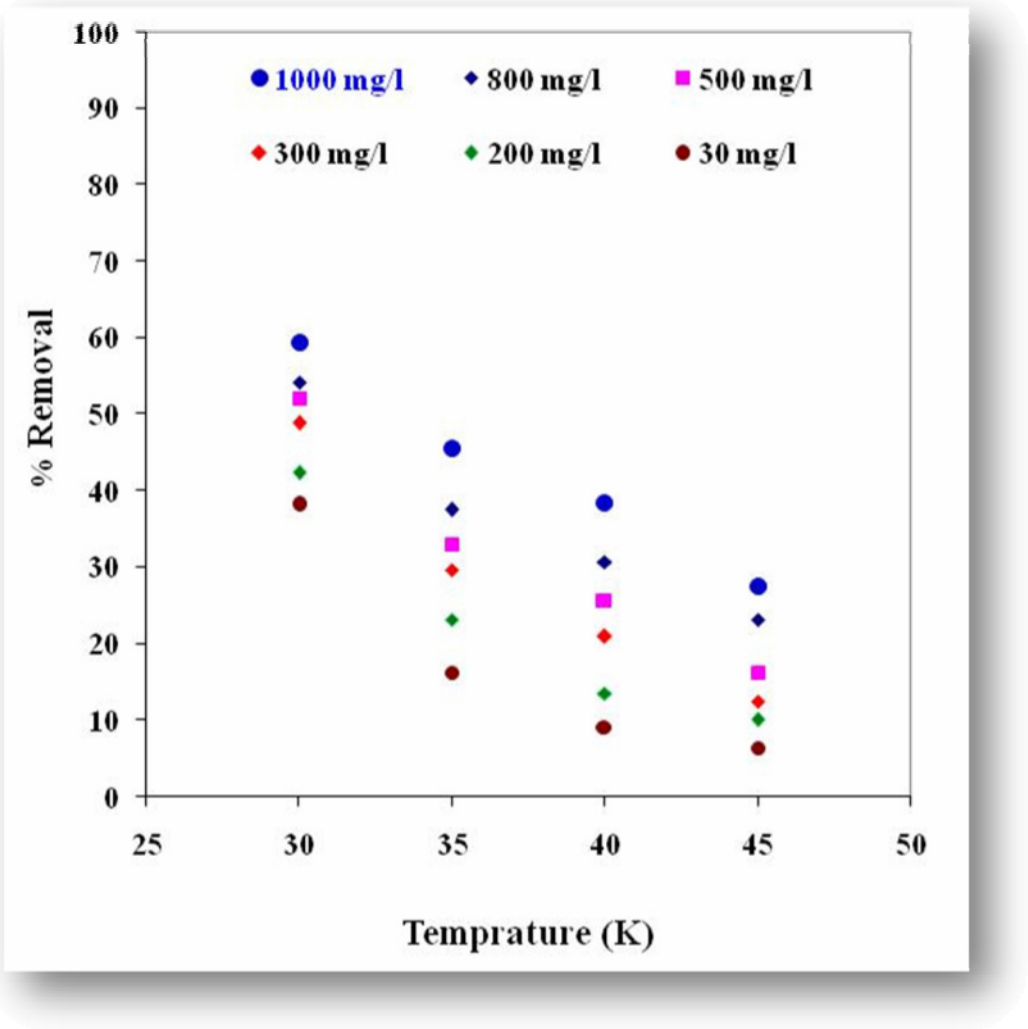


**Figure 5.32 Effect of temperature on removal of DBT by SZC893 at various initial concentrations ($C_o$).**

### 5.2.6 Adsorption Equilibrium Study

The experimental equilibrium adsorption data of DBT adsorption onto ZD383, ZC893 and SZC893 have been tested by using the two-parameter Freundlich, Langmuir, and Tempkin isotherm equations and the three parameter Redlich-Peterson (R-P) and BET isotherm equations. The following equations represent these isotherms:

Freundlich $$q_e = K_F C_e^{1/n} \tag{5.5}$$

Langmuir $$q_e = \frac{q_m K_L C_e}{1 + K_L C_e} \tag{5.6}$$

Tempkin $$q_e = B_T \ln K_T + B_T \ln C_e \tag{5.7}$$

Redlich-Peterson $$q_e = \frac{K_R C_e}{1 + a_R C_e^{\beta}} \tag{5.8}$$

BET $$q_e = \frac{q_{m,B} K_B C_e}{(C_S - C_e)[1 + \{(K_B - 1)(C_e / C_S)\}]} \tag{5.9}$$

The Freundlich isotherm is valid for a heterogeneous adsorbent surface with a non-uniform distribution of heat of adsorption over the surface. The Langmuir isotherm, however, assumes that the sorption takes place at specific homogeneous sites within the adsorbent. R-P model is applicable to both physical and chemical adsorption systems. It also applies to systems involving complex adsorption mechanism.

The Langmuir, Freundlich, R-P and BET isotherm parameters along with $R^2$ and SSE values for the fit of the adsorption of DBT onto ZD383, ZC893 and SZC893 at various temperatures are given in table 5.6 through 5.8, respectively. The $R^2$ values are highest for BET model. The SSE values are smaller for BET model as compared to that for the other models. So, it can be concluded that BET model is the best among the four models for representing the adsorption isotherm data of the DBT adsorption onto ZD383, ZC893 and SZC893 at various temperatures. Figure 5.33 through 5.35 shows the fit of BET isotherms onto experimental data points for DBT adsorption from model hydrocarbon onto ZD383, ZC893 and SZC893 at various temperatures. The $q_{m,B}$ values which represent the adsorption capacity of the adsorbents are found to decrease with an increase in temperature indicating exothermic nature of the adsorption process.

**Table 5.6 Isotherm parameters for the removal of sulfur by ZD383: $C_o$ = 30-1000 mg/l, $m$ = 10 g/l.**

| **Freundlich** | | $q_e = K_F C_e^{1/n}$ | | |
|---|---|---|---|---|
| **T (K)** | **$K_F$ ((mg/g)/(l/mg)$^{1/n}$)** | **1/n** | **$R^2$** | **SSE** |
| 303 | 0.0820 | 0.9884 | 0.9728 | 19.40 |
| 308 | 0.0478 | 0.9999 | 0.9897 | 11.13 |
| 313 | 0.0282 | 0.9999 | 0.9057 | 56.31 |
| 318 | 0.00833 | 0.9999 | 0.7844 | 13.13 |
| **Langmuir** | | $q_e = \frac{q_m K_L C_e}{1 + K_L C_e}$ | | |
| **T (K)** | **$K_L$(l/mg)** | **$q_m$(mg/g)** | **$R^2$** | **SSE** |
| 303 | 1.98E-07 | 387,366 | 0.9744 | 19.16 |
| 308 | 3.95E-06 | 12,234 | 0.9896 | 11.34 |
| 313 | 1.22E-07 | 229,799 | 0.9053 | 56.29 |
| 318 | 9.76E-08 | 85,184 | 0.7965 | 13.18 |
| **Temkin** | | $q_e = B_T \ln K_T + B_T \ln C_e$ | | |
| **T (K)** | **$B_T$(kJ/mol)** | **$K_T$ (l/mg)** | **$R^2$** | **SSE** |
| 303 | 10.7444 | 0.03030 | 0.8108 | 135.17 |
| 308 | 7.8698 | 0.0248 | 0.7407 | 113.56 |
| 313 | 5.8746 | 0.01611 | 0.5638 | 132.53 |
| 318 | 1.9325 | 0.0148 | 0.4537 | 25.29 |
| **Redlich-Peterson** | | $q_e = \frac{K_R C_e}{1 + a_R C_e^{\beta}}$ | | |
| **T (K)** | **$K_R$ (l/g)** | **$a_R$ (l/mg)$^{1/\beta}$** | **$\beta$** | **$R^2$** | **SSE** |
| 303 | 0.0766 | 3.03E-05 | 0.0100 | 0.974 | 19.14 |
| 308 | 0.0478 | 4.82E-05 | 0.0080 | 0.989 | 11.10 |
| 313 | 0.0342 | 2.14E-01 | 0.0020 | 0.905 | 56.28 |
| 318 | 0.0153 | 0.847E-01 | 0.0009 | 0.796 | 13.18 |
| **BET** | | $q_e = \frac{q_{m,B} K_B C_e}{(C_S - C_e)[1 + \{(K_B - 1)(C_e / C_S)\}]}$ | | |
| **T (K)** | **$K_B$(l/mg)** | **$q_{m,b}$(mg/g)** | **$C_s$(mg/L)** | **$R^2$** | **SSE** |
| 303 | 15.41 | 545 | 104463 | 0.977 | 18.7 |
| 308 | 0.26 | 352 | 2604 | 0.999 | 0.4 |
| 313 | 0.14 | 201 | 1804 | 0.982 | 13.7 |
| 318 | 0.03 | 193 | 1770 | 0.950 | 4.1 |

**Table 5.7 Isotherm parameters for the removal of sulfur by ZC893: $C_o$ = 30-1000 mg/l, $m$ = 10 g/l.**

| | **Freundlich** | $q_e = K_F C_e^{1/n}$ | | |
|---|---|---|---|---|
| **T (K)** | **$K_F$ ((mg/g)/(l/mg)$^{1/n}$)** | **1/n** | **$R^2$** | **SSE** |
| 303 | 0.1152 | 0.9990 | 0.9703 | 108.10 |
| 308 | 0.0528 | 0.9990 | 0.9451 | 66.11 |
| 313 | 0.0437 | 0.9990 | 0.9183 | 151.10 |
| 318 | 0.0193 | 0.9990 | 0.9020 | 52.73 |
| | **Langmuir** | $q_e = \frac{q_m K_L C_e}{1 + K_L C_e}$ | | |
| **T (K)** | **$K_L$(l/mg)** | **$q_m$(mg/g)** | **$R^2$** | **SSE** |
| 303 | 3.00E-06 | 38185.42 | 0.9792 | 108.32 |
| 308 | 9.56E-07 | 54969.55 | 0.9452 | 65.97 |
| 313 | 1.27E-06 | 34168.55 | 0.9183 | 150.95 |
| 318 | 1.44E-07 | 133157.14 | 0.9127 | 52.82 |
| | **Temkin** | $q_e = B_T \ln K_T + B_T \ln C_e$ | | |
| **T (K)** | **$B_T$(kJ/mol)** | **$K_T$ (l/mg)** | **$R^2$** | **SSE** |
| 303 | 16.406 | 0.0291 | 0.708 | 738.31 |
| 308 | 8.738 | 0.0225 | 0.639 | 226.12 |
| 313 | 9.523 | 0.0173 | 0.589 | 435.56 |
| 318 | 4.968 | 0.0147 | 0.555 | 149.21 |
| | **Redlich-Peterson** | $q_e = \frac{K_R C_e}{1 + a_R C_e^{\beta}}$ | | |
| **T (K)** | **$K_R$ (l/g)** | **$a_R$ (l/mg)$^{1/\beta}$** | **$\beta$** | **$R^2$** | **SSE** |
| 303 | 0.1427 | 0.246 | 0.0090 | 0.979 | 109.56 |
| 308 | 0.0528 | 0.004 | 0.0034 | 0.945 | 65.91 |
| 313 | 0.0435 | 0.001 | 0.0001 | 0.918 | 150.76 |
| 318 | 0.0193 | 0.006 | 0.0001 | 0.912 | 52.81 |
| | **BET** | $q_e = \frac{q_{m,B} K_B C_e}{(C_S - C_e)[1 + \{(K_B - 1)(C_e / C_S)\}]}$ | | | |
| T (K) | $K_B$(l/mg) | $q_{m,b}$(mg/g) | $C_s$(mg/L) | $R^2$ | SSE |
| 303 | 0.16 | 738 | 1666.3 | 0.997 | 7.3 |
| 308 | 0.12 | 387 | 1488 | 0.998 | 3.3 |
| 313 | 0.07 | 285 | 1344.8 | 0.996 | 4.5 |
| 318 | 0.02 | 224 | 1306.4 | 0.967 | 14.5 |

**Table 5.8 Isotherm parameters for the removal of sulfur by SZC893: $C_o$ = 30-1000 mg/l, $m$ = 10 g/l.**

| | | | | | |
|---|---|---|---|---|---|
| **Freundlich** | | $q_e = K_F C_e^{1/n}$ | | | |
| **T (K)** | **$K_F$ ((mg/g)/(l/mg)$^{1/n}$)** | **1/n** | **$R^2$** | **SSE** | |
| 303 | 1.5925 | 0.5632 | 0.8134 | 726.99 | |
| 308 | 0.0673 | 0.9999 | 0.9265 | 222.67 | |
| 313 | 0.0916 | 0.9027 | 0.9032 | 239.33 | |
| 318 | 0.0587 | 0.9027 | 0.8982 | 117.72 | |
| **Langmuir** | | $q_e = \frac{q_m K_L C_e}{1 + K_L C_e}$ | | | |
| **T (K)** | **$K_L$(l/mg)** | **$q_m$(mg/g)** | **$R^2$** | **SSE** | |
| 303 | 3.41E-07 | 371217.78 | 0.9698 | 169.90 | |
| 308 | 4.20E-07 | 159904.08 | 0.9264 | 222.76 | |
| 313 | 3.45E-07 | 142929.48 | 0.9208 | 190.31 | |
| 318 | 1.55E-07 | 201022.4713 | 0.9345 | 91.91 | |
| **Temkin** | | $q_e = B_T \ln K_T + B_T \ln C_e$ | | | |
| **T (K)** | **$B_T$(kJ/mol)** | **$K_T$ (l/mg)** | **$R^2$** | **SSE** | |
| 303 | 17.7677 | 0.0294 | 0.6858 | 967.23 | |
| 308 | 13.0848 | 0.0199 | 0.6172 | 712.41 | |
| 313 | 10.8246 | 0.0171 | 0.5878 | 561.96 | |
| 318 | 7.5978 | 0.0158 | 0.5826 | 303.90 | |
| **Redlich-Peterson** | | $q_e = \frac{K_R C_e}{1 + a_R C_e^{\beta}}$ | | | |
| **T (K)** | **$K_R$ (l/g)** | **$a_R$ (l/mg)$^{1/\beta}$** | **$\beta$** | **$R^2$** | **SSE** |
| 303 | 0.1268 | 0 | 0.01 | 0.9698 | 169.83 |
| 308 | 0.0673 | 0 | 0.009 | 0.9265 | 222.66 |
| 313 | 0.0493 | 0 | 0.001 | 0.9209 | 190.24 |
| 318 | 0.0311 | 0 | 0.0001 | 0.9345 | 91.89 |
| **BET** | | $q_e = \frac{q_{m,B} K_B C_e}{(C_S - C_e)[1 + \{(K_B - 1)(C_e / C_S)\}]}$ | | | |
| **T (K)** | **$K_B$(l/mg)** | **$q_{m,b}$(mg/g)** | **$C_s$(mg/L)** | **$R^2$** | **SSE** |
| 303 | 0.15 | 935 | 1730 | 0.995 | 19.0 |
| 308 | 0.08 | 415 | 1324 | 0.993 | 13.1 |
| 313 | 0.07 | 319 | 1407 | 0.997 | 4.8 |
| 318 | 0.08 | 273 | 1817 | 0.997 | 2.9 |

Sum of square of errors (SSE) was used as a criterion in finding the best isotherm model to fit the experimental data. The SSE is given by following equation:

$$SSE = \sum_{i=1}^{n} (q_{e,\exp} - q_{e,cal})_i^2 \tag{5.10}$$

where, $q_{e,\exp}$ and $q_{e,cal}$ are the experimental and calculated equilibrium adsorbate uptake, respectively; and $n$ is the number of data points. Figures 5.33 through 5.35 show the fits of various isotherms onto experimental data points for DBT adsorption from model hydrocarbon onto ZD383, ZC893 and SZC893 at various temperatures.

### 5.2.7 Adsorption Thermodynamics

Classical thermodynamics of the adsorption process gives the following relationship between $\Delta G_0$, $\Delta H_0$, $\Delta S_0$ and equilibrium adsorption constant ($K_D$):

$$\ln K_D = \frac{-\Delta G_0}{RT} = \frac{\Delta S_0}{RT} - \frac{\Delta H_0}{R}\frac{1}{T} \tag{5.11}$$

where, T is the absolute temperature (K), $R$ is the universal gas constant ($8.314\times10^{-3}$ kJ/mol K) and $K_D$ ($=q_e/C_e$) is the single point or linear sorption distribution coefficient. Thus, $\Delta H_0$, which is the enthalpy change (kJ/mol), can be determined from the slope of the linear Van't Hoff plot shown in figure 5.36, i.e. $\ln K_D$ versus ($1/T$). This $\Delta H_0$ corresponds to the isosteric heat of adsorption ($\Delta H_{st,0}$) with zero surface coverage (i.e. $q_e$=0). $K_D$ at $q_e$=0 can be obtained from the intercept of the $\ln q_e/C_e$ versus $q_e$ plot [Srivastava et al., 2007].

The adsorption of DBT components onto various samples of zirconia is exothermic in nature, giving a negative value of $\Delta H^0$ (Table 5.9). The negative $\Delta H_0$ value confirms the exothermic nature of the overall-adsorption process. In physisorption, the bond between adsorbate and adsorbent is Van der walls interaction and adsorption energy is typically 5-10 kJ/mol. In the case of chemisorption, a chemical bond is formed between molecules and the surface; the adsorption energy is comparable to the energy of a chemical bond. The chemisorption energy is, generally, 30-70 kJ/mol for [Murzin and Salami, 2005]. Therefore, it seems that the adsorption of DBT components onto ZD383, ZC893 and SZC893 is chemisorptive in nature. The negative value of $\Delta S_0$ suggests decrease in the degree of freedom of the adsorbed DBT molecules. $\Delta G_0$ values are negative indicating that the adsorption process led to a decrease in Gibbs free energy. Negative $\Delta G_0$ indicates the feasibility and spontaneity of the adsorption process.

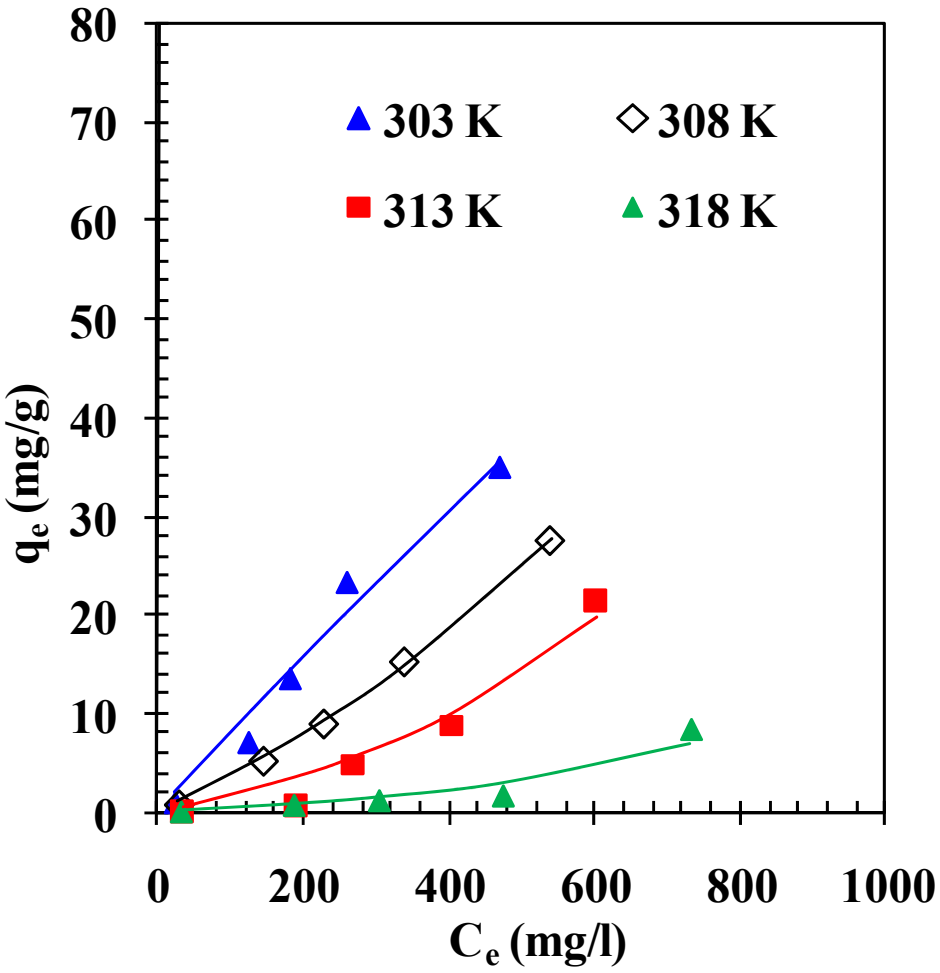


**Figure 5.33** **Equilibrium adsorption isotherms for ZD383 at different temperature. Experimental data points given by the symbols and the lines predicted by the BET Isotherm Model; $C_o$ = 30-1000 mg/l, $m$ = 10 g/l.**

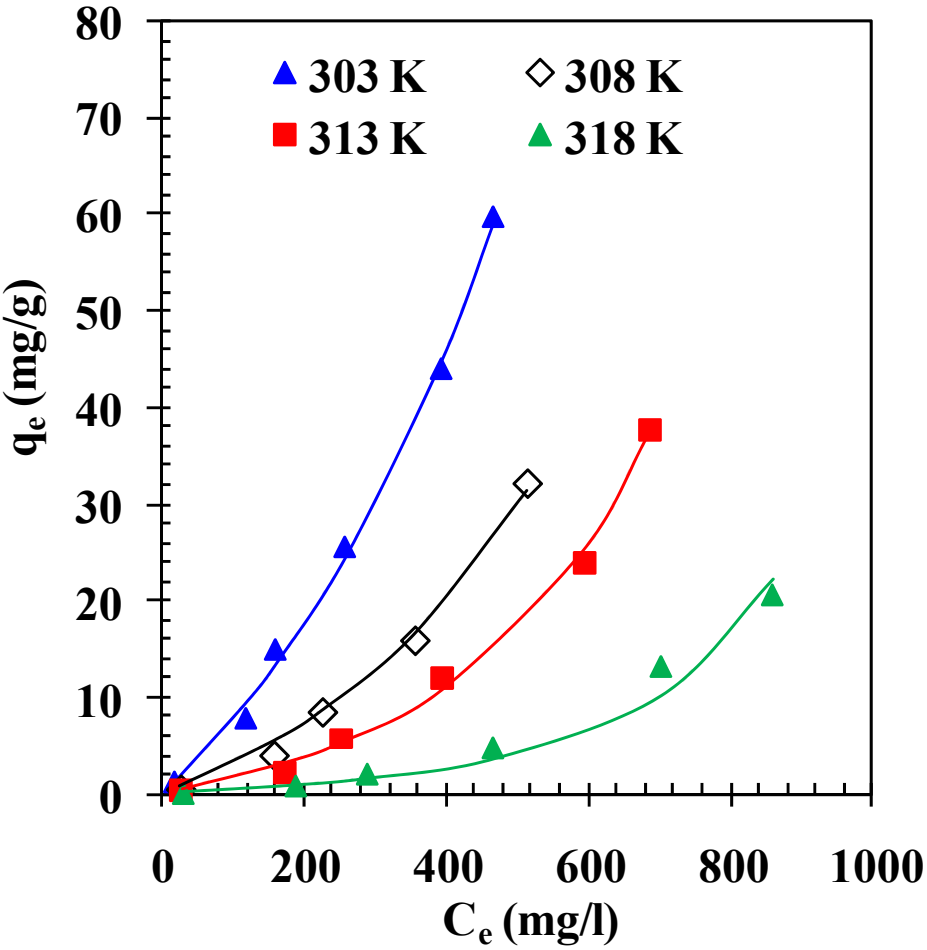


**Figure 5.34** **Equilibrium adsorption isotherms for ZC893 at different temperature. Experimental data points given by the symbols and the lines predicted by the BET Isotherm Model; $C_o$ = 30-1000 mg/l, $m$ = 10 g/l.**

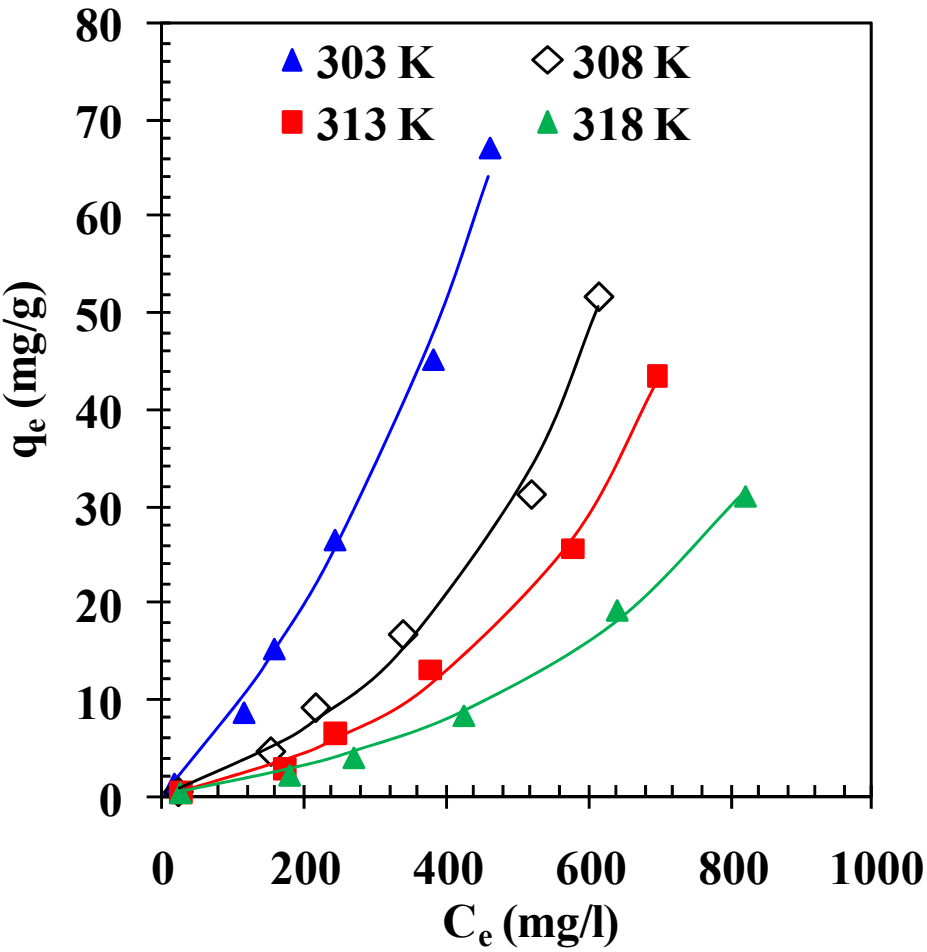


**Figure 5.35** **Equilibrium adsorption isotherms for SZC893 at different temperature. Experimental data points given by the symbols and the lines predicted by the BET Isotherm Model; $C_o$ = 30-1000 mg/l, $m$ = 10 g/l.**

**Table 5.9 Thermodynamics parameters for the removal of DBT by various zirconia supported adsorbents. $C_o$ = 30-1000 mg/l, $m$ = 10 g/l.**

| Temp. (K) | $\Delta G_o$(kJ/mol) | $\Delta H_o$ (kJ/mol) | $\Delta S_o$ (kJ/mol K) |
|---|---|---|---|
| | **ZD383** | | |
| 303 | -10.3625 | -165.3075 | -509.8607 |
| 308 | -9.1528 | | |
| 313 | -5.3621 | | |
| 318 | -3.1053 | | |
| | **ZC893** | | |
| 303 | -10.665 | -125.5165 | -379.371 |
| 308 | -8.3063 | | |
| 313 | -7.2058 | | |
| 318 | -4.7071 | | |
| | **SZC893** | | |
| 303 | -10.9105 | -96.7461 | -284.1312 |
| 308 | -8.8898 | | |
| 313 | -7.7034 | | |
| 318 | -6.5901 | | |

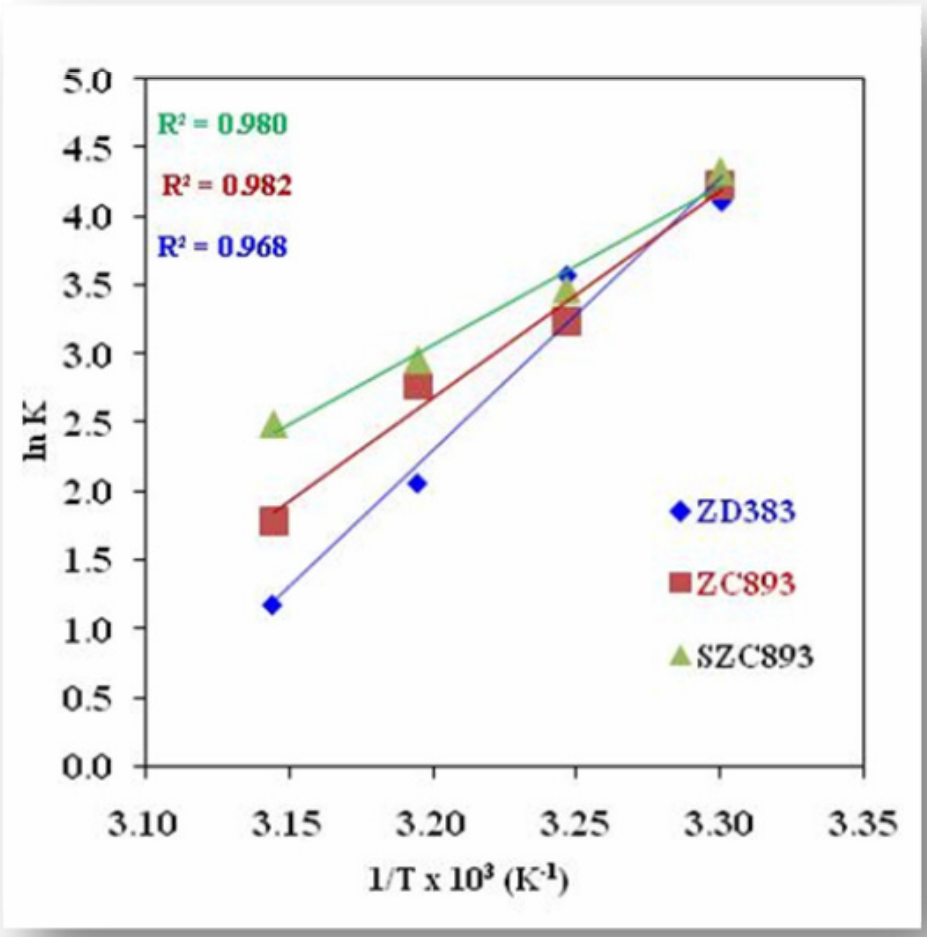


**Figure 5.36 Van't Hoff Plot for the removal of DBT by various zirconia based adsorbents.**

### 5.2.8 Characterization Before and After ADS

#### 5.2.8.1 XRD Analysis

XRD patterns of SZC893 before and after ADS are shown in figure 5.37. It may be seen in figure that after ADS, the peaks get shifted and also the intensity of the gets reduced. Also few new peaks get formed because of the loading of DBT. Also the tetragonal phase of SZC893 gets reduced after ADS signifying to the fact that this phase may be responsible for adsorptive activity of SZC893.

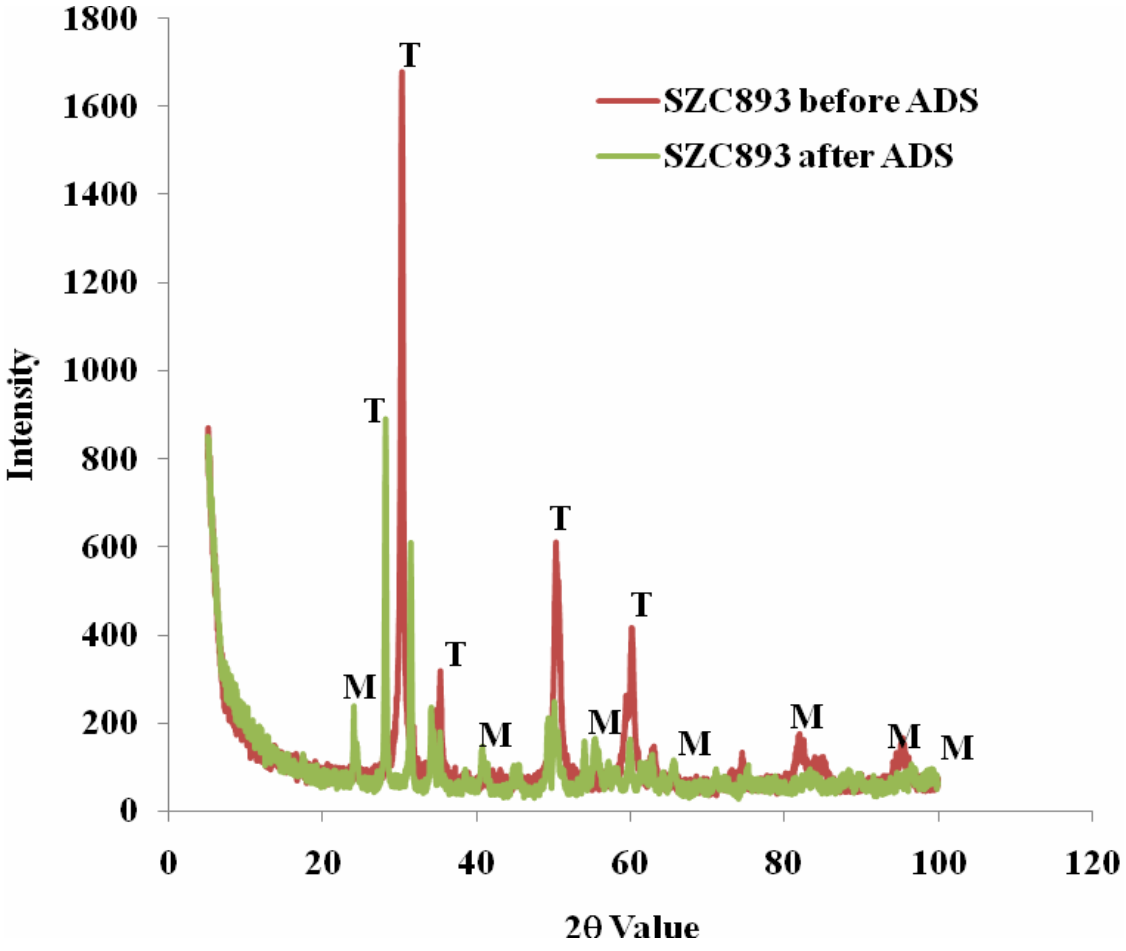


**Figure 5.37 XRD patterns of SZC893 before and after ADS.**

### 5.2.8.2 EDAX analysis

Figures 5.38 and 5.39 show the EDAX patterns of ZD383 and SZC893, respectively, before and after adsorption of DBT. Table 5.10 shows the distribution of the elements in blank and DBT loaded samples. Both, ZD893 and SZC893, show increase in wt% of sulphur after ADS. Increase in sulfur content is due to the loading of DBT on ZD383 and SZC893.

**Table 5.10 Elemental composition of ZD383 and SZC893 before and after ADS determined by EDAX.**

| **ZD383 before ADS** | | | **ZD383 after ADS** | | |
|---|---|---|---|---|---|
| **Element** | **Wt%** | **At%** | **Element** | **Wt%** | **At%** |
| O K | 10.32 | 39.62 | O K | 09.85 | 37.80 |
| S K | Nil | Nil | S K | 01.24 | 02.38 |
| Cr K | Nil | Nil | Cr K | Nil | Nil |
| Zr K | 89.68 | 60.38 | Zr K | 88.91 | 59.83 |
| **SZC893 before ADS** | | | **SZC893 after ADS** | | |
| **Element** | **Wt%** | **At%** | **Element** | **Wt%** | **At%** |
| O K | 11.89 | 42.35 | O K | 07.07 | 29.74 |
| S K | 02.28 | 04.05 | S K | 03.70 | 06.39 |
| Cr K | Nil | Nil | Cr K | Nil | Nil |
| Zr K | 85.83 | 53.60 | Zr K | 90.83 | 66.51 |

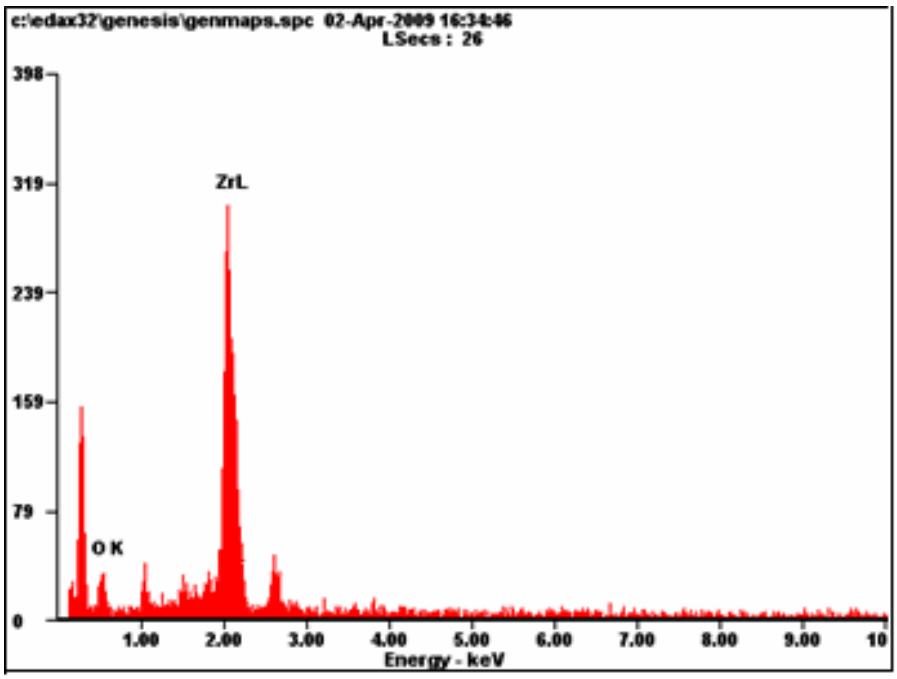


**a. Before ADS**

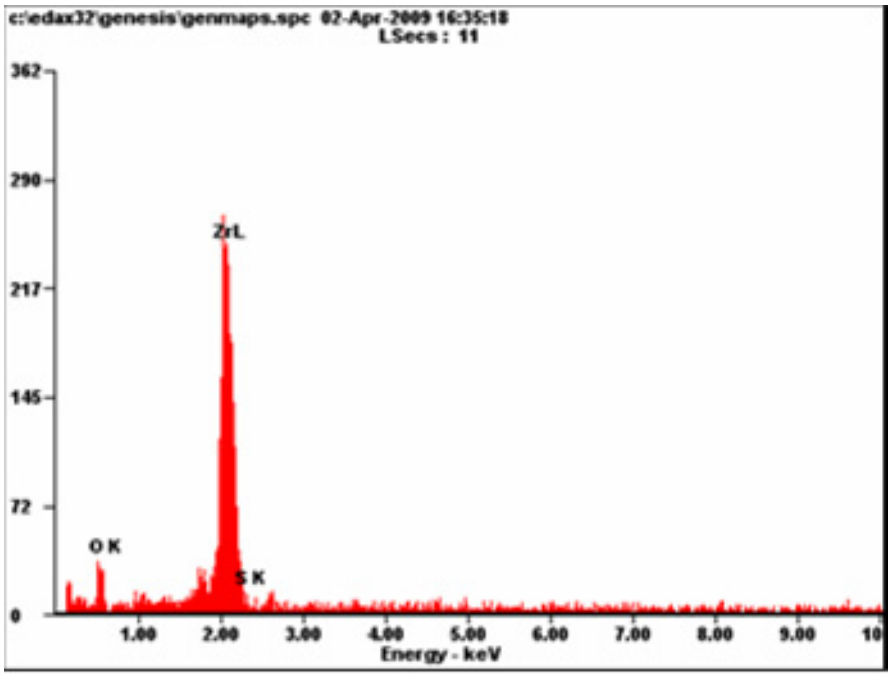


**c. After ADS**

**Figure 5.38 EDAX Spectrum for elemental composition of ZD383 before and after ADS**

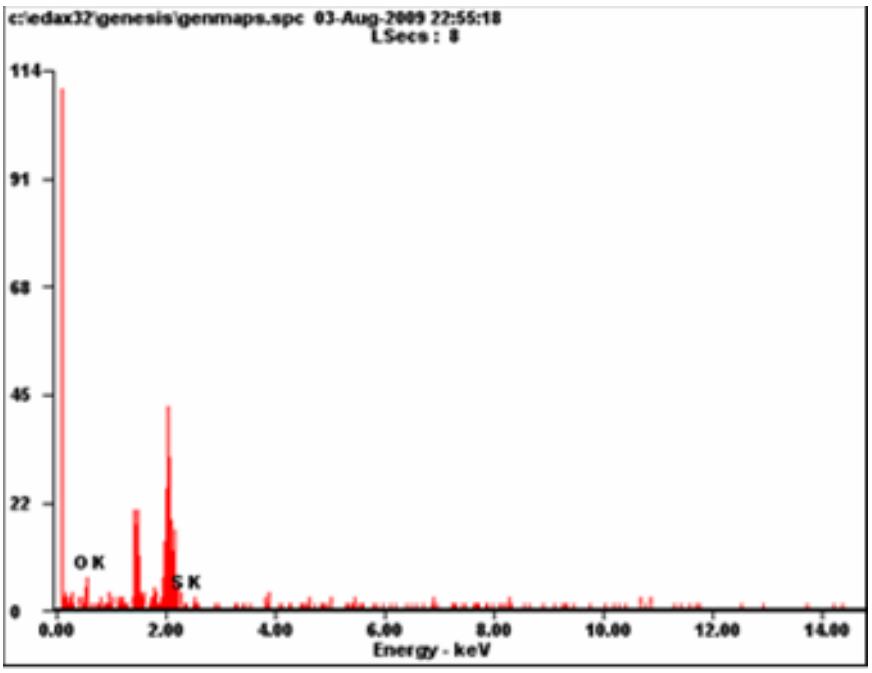


**a. Before ADS**

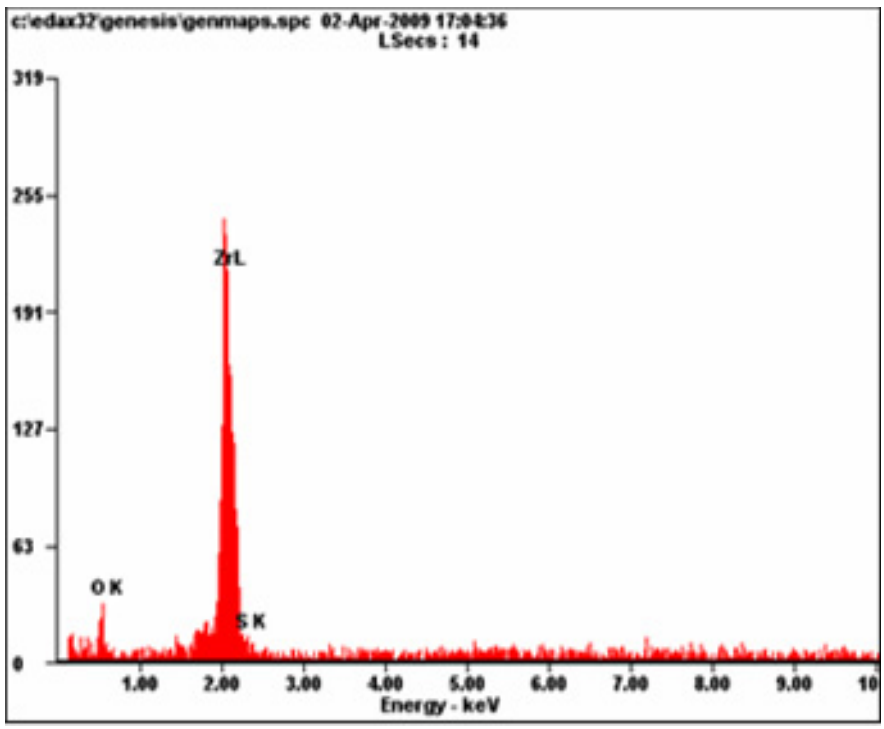


**c. After ADS**

**Figure 5.39 EDAX Spectrum for elemental composition of SZC893 before and after ADS.**

## 5.3 BATCH OXIDATIVE DESULFURIZATION STUDIES

The reactive system consists of model solution-acid-oxidant, and a solid catalyst. Hence, we will present the results obtained from the GC-analysis of the liquid phase, to evaluate the total removal of DBT. The conversion of DBT in simulated diesel was used to calculate the removal of sulfur [Zhua et al., 2011].The solvent phase will be analyzed in order to evaluate the fraction extracted and sulfone yields of DBT.The reaction scheme of oxidation of DBT to DBTO to $DBTO_2$ is shown in figure 5.40.

Total sulfur removal is the fraction of DBT eliminated from the reaction mixture respect to initial concentration in the model solution. This result shows that it is possible to remove very high percentages of DBT under specified conditions. DBT-compounds, which contribute mainly to the sulfur compounds in transportation oil, are removed in about 6 h. With all catalysts, the DBTs extracted reach a maximum upto 6 h and subsequently decrease as reaction time continues. As sulfones were obtained only in solvent phase, these profiles describe a consecutive process scheme [Gomez and Cedeno, 2005]. In ODS, the electrons in the d-orbital of sulfur atom are used for extended bonding allowing them to react easily with oxidizers. The enhanced polarity of sulfoxides and sulfones formed makes it easier to remove them by solvent extraction and /or by adsorption on variety of adsorbents as reported [Collins et al., 1997].

The oxidation of sulfur compounds with $H_2CO_2$ and $H_2O_2$ was carried out at a range of 303- 353 K, using various samples of zirconia as catalyst. Otsuki et al. [2000] have reported the following trend for sulfur compound oxidation reactivity in methanoic acid/$H_2O_2$ system: methyl phenyl sulfide > thiophenol > diphenylsulfide > 4,6-DMDBT > 4- MDBT > DBT > BT > thiophenes.

### 5.3.1 Effect of Catalyst Dose (*w*)

The effect of amount of various catalysts (***w***) on oxidation of DBT by ZD383, ZC893, SZC893 and CSZC893 is shown in figure 5.41, 5.42, 5.43 and 5.44, respectively. These indicate that the conversion of DBT to $DBTO_2$ increases with an increase in *w*. The oxidation efficiency increased significantly with increase in *w* of various catalysts upto 5 g/l. However, further addition of *w* resulted in no increase in conversion of DBT to $DBTO_2$. The conversion at optimum conditions *w* of 5 g/l, $C_o$ of 1000 g/l and *t* of 6 h reached upto 53.92, 58.02, 67.36 and 79.26% for ZD383, ZC893, SZC893 and CSZC893, respectively.

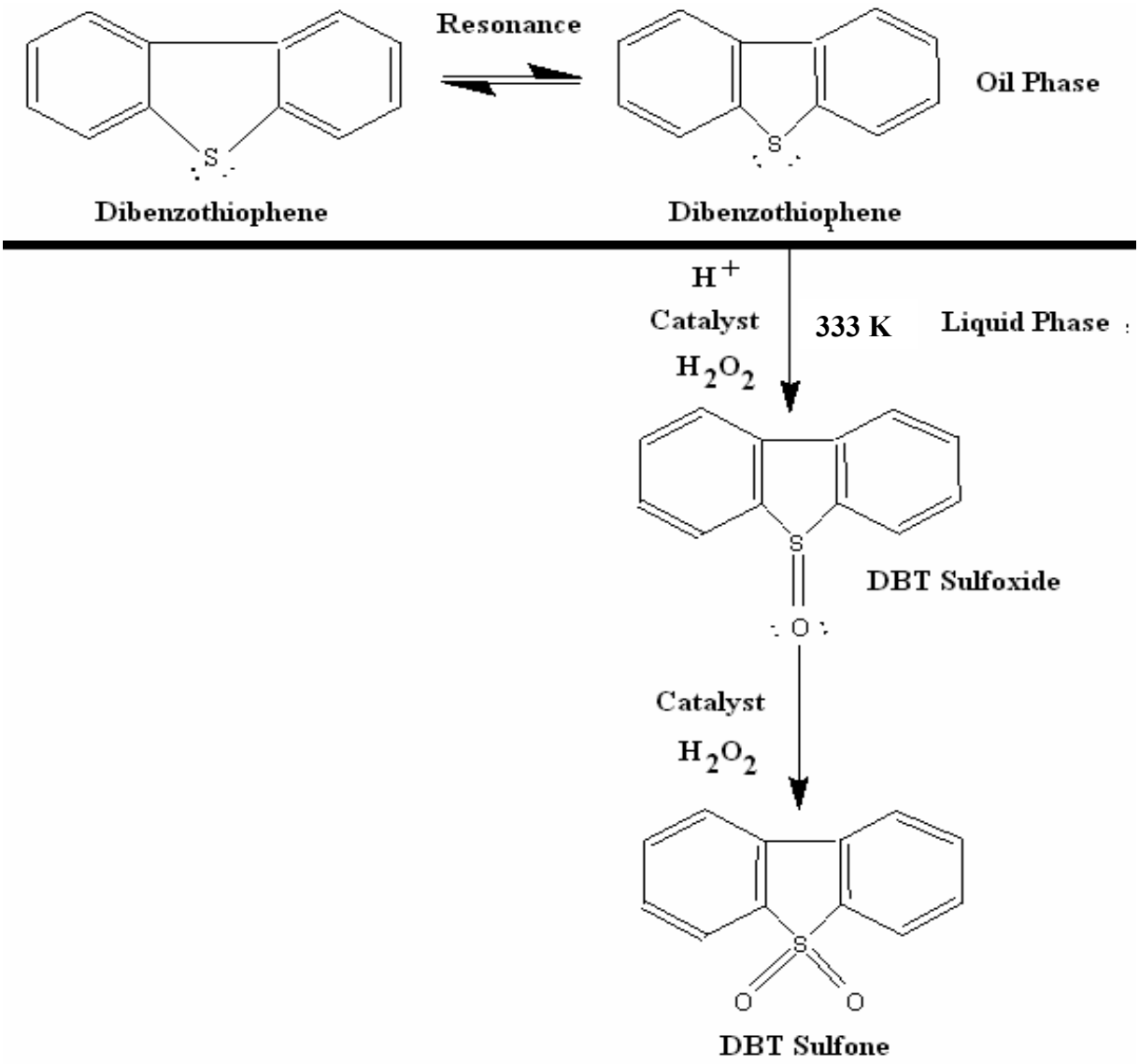


**Figure 5.40 Possible mechanism for conversion pathway from dibenzothiophene to dibenzothiophene-sulfone [Di-shun et al., 2009].**

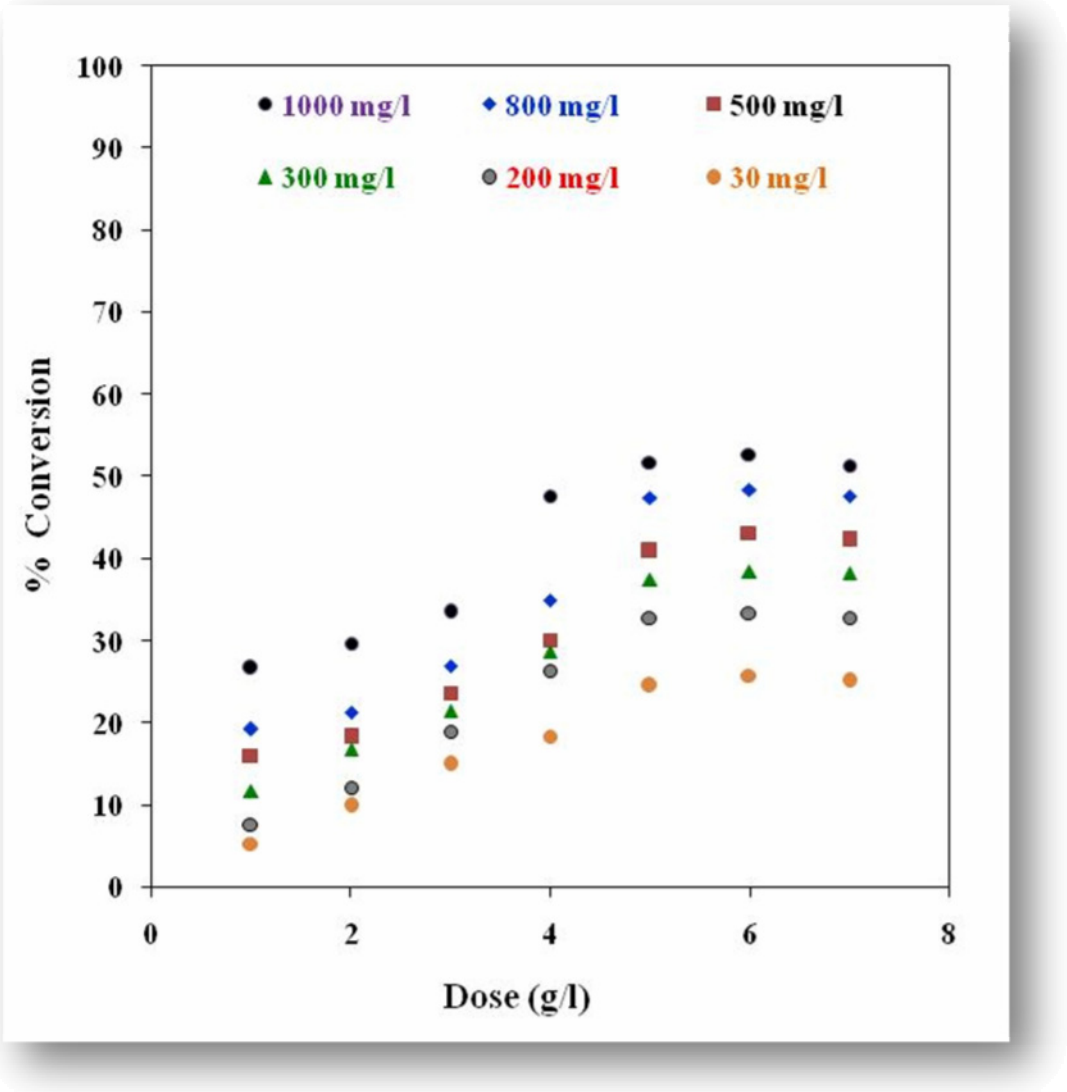


**Figure 5.41 Effect of *w* on conversion of DBT by ZD383 at various initial concentrations ($C_o$) [$t$ = 6 h; T = 333 K]**

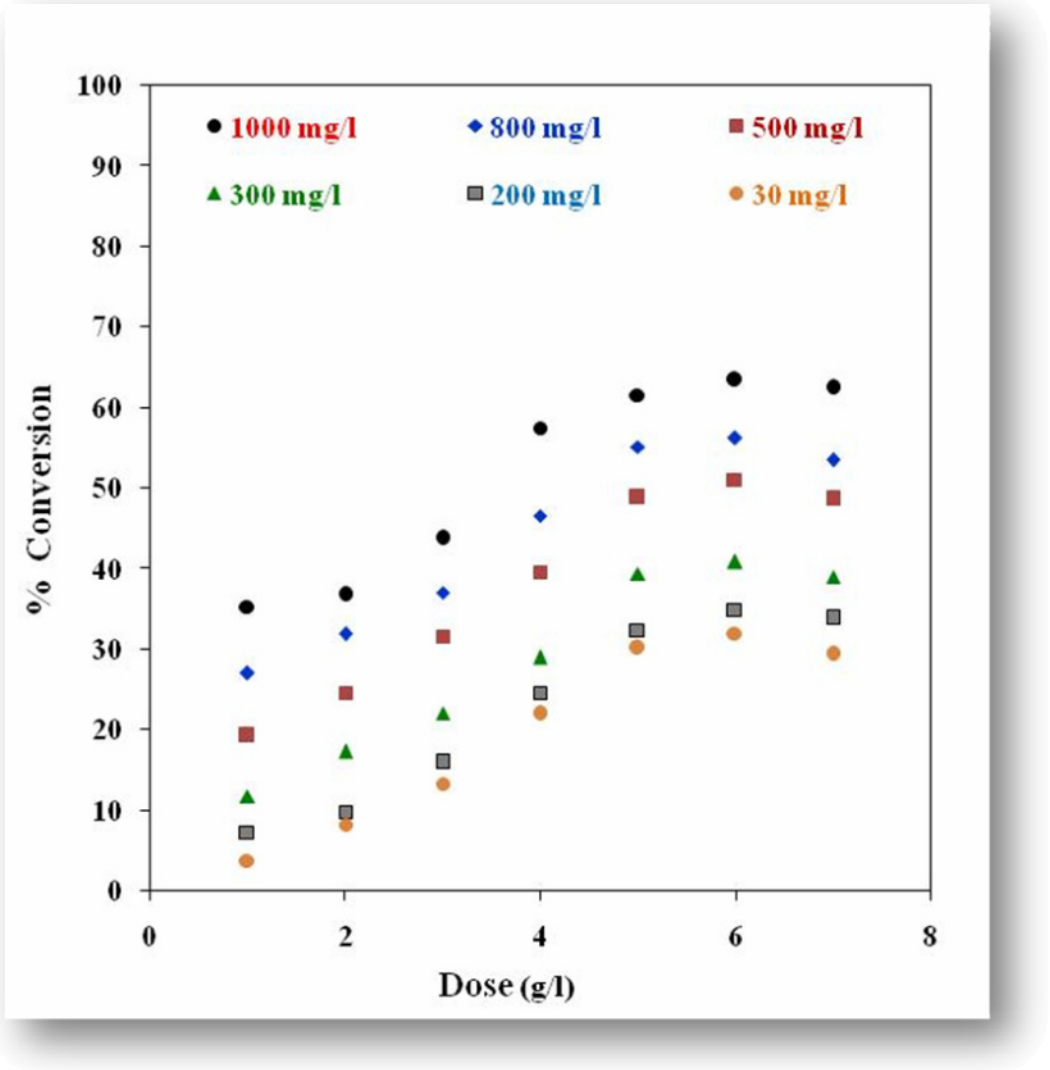


**Figure 5.42 Effect of *w* on conversion of DBT by ZC893 at various initial concentrations ($C_o$) [$t$ = 6 h; T = 333 K]**

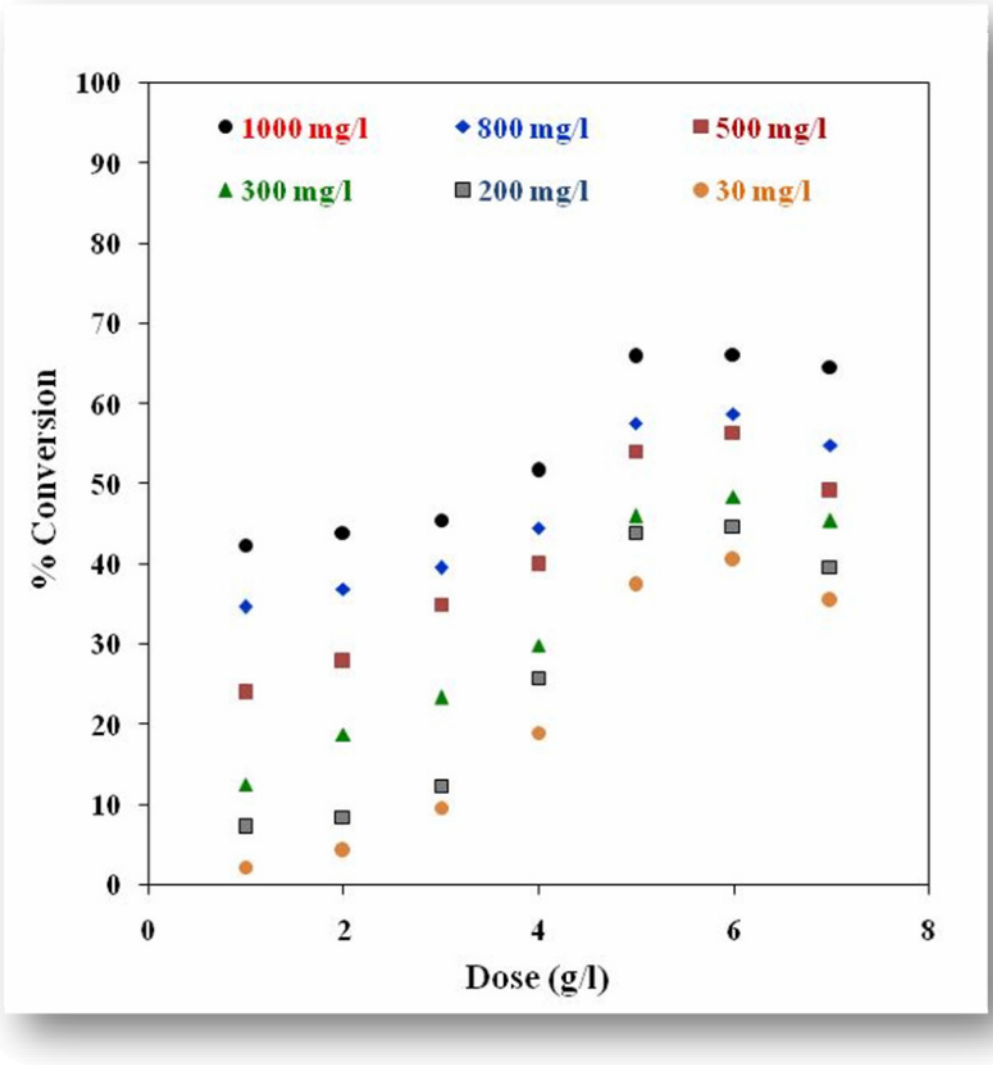


**Figure 5.43 Effect of *w* on conversion of DBT by SZC893 at various initial concentrations ($C_o$) [$t$ = 6 h; T = 333 K]**

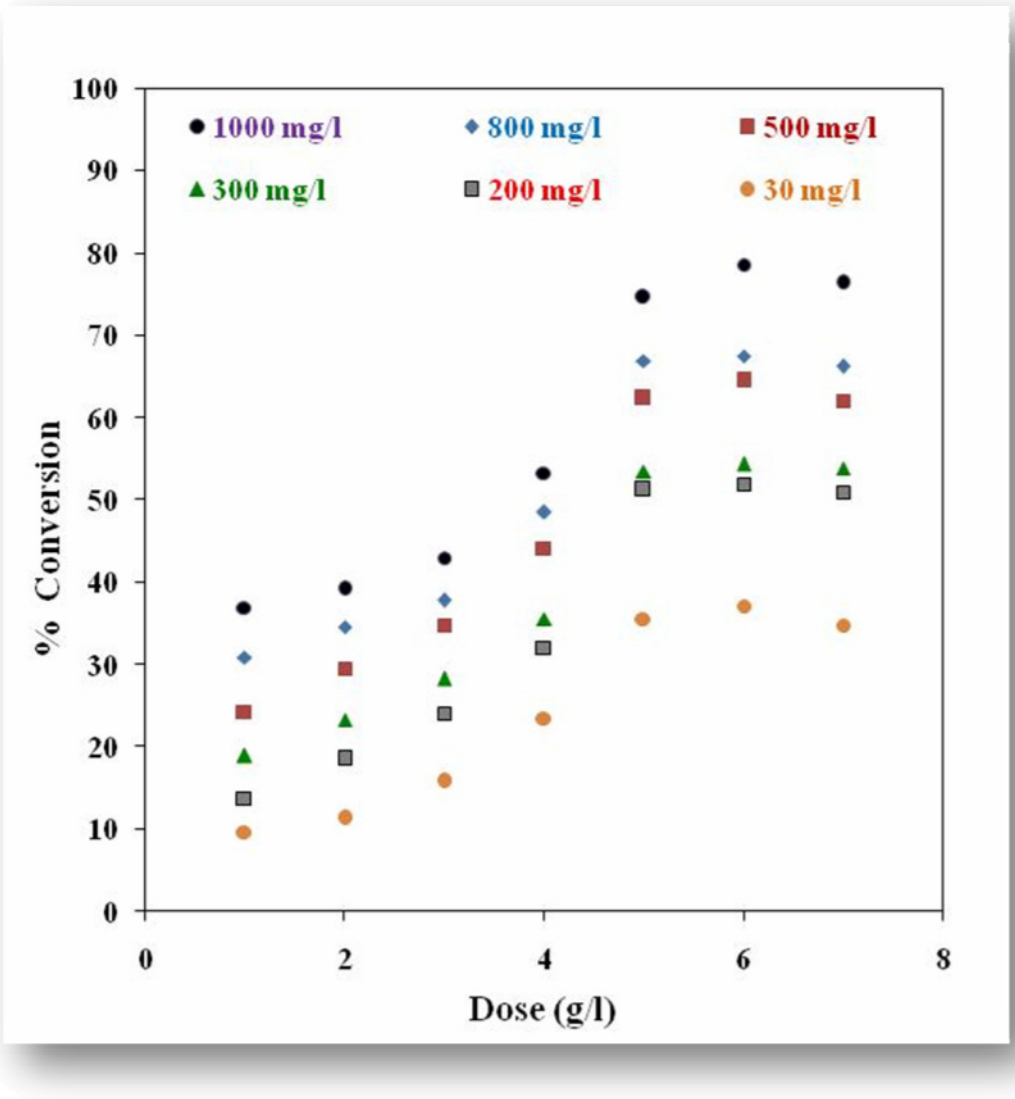


**Figure 5.44 Effect of *w* on conversion of DBT by CSZC893 at various initial concentrations ($C_o$) [$t$ = 6 h; T = 333 K].**

### 5.3.2 Effect of DBT concentration ($C_o$)

The effect of $C_o$ on the extent of conversion of DBT onto various zirconia based catalysts at $w$ = 5 g/l is shown in figure 5.45. It is evident that the DBT conversion increased with an increase in $C_o$. It may be due to the fact that at higher $C_o$, the resistance for DBT molecules to reach the catalyst active sites decreased. This enhanced its conversion.

### 5.3.3 Effect of Reaction Time ($t$)

DBT solutions with different $C_o$ (30,200, 300, 500,800 and 1000 mg/l) were kept in contact with ZD383, ZC893, SZC893 and CSZC893 in a batch reactor upto 8 h. Figure 5.46, 5.47, 5.48 and 5.49 shows the effect of reaction time on the conversion of DBT.

It may be seen that the rate of DBT conversion is nearly constant for 6 h, after which it ceases. It seems that the after 6 h, the active sites of the catalysts get exhausted and are not able to further oxidize DBT. Also, the easily available active sites which are available at the start of the oxidation reaction get saturated after lapse of time and DBT molecules have to traverse farther and deeper to reach the active sites present in the micro-pores. The movement of DBT molecules to active sites present in micro-pore requires larger resistance to be encountered. This results in the slowing down of the oxidation process during the later period of oxidation reaction. Accordingly all the batch DBT oxidation experiments were conducted with a contact time of 6 h for maximum possible conversion of DBT.

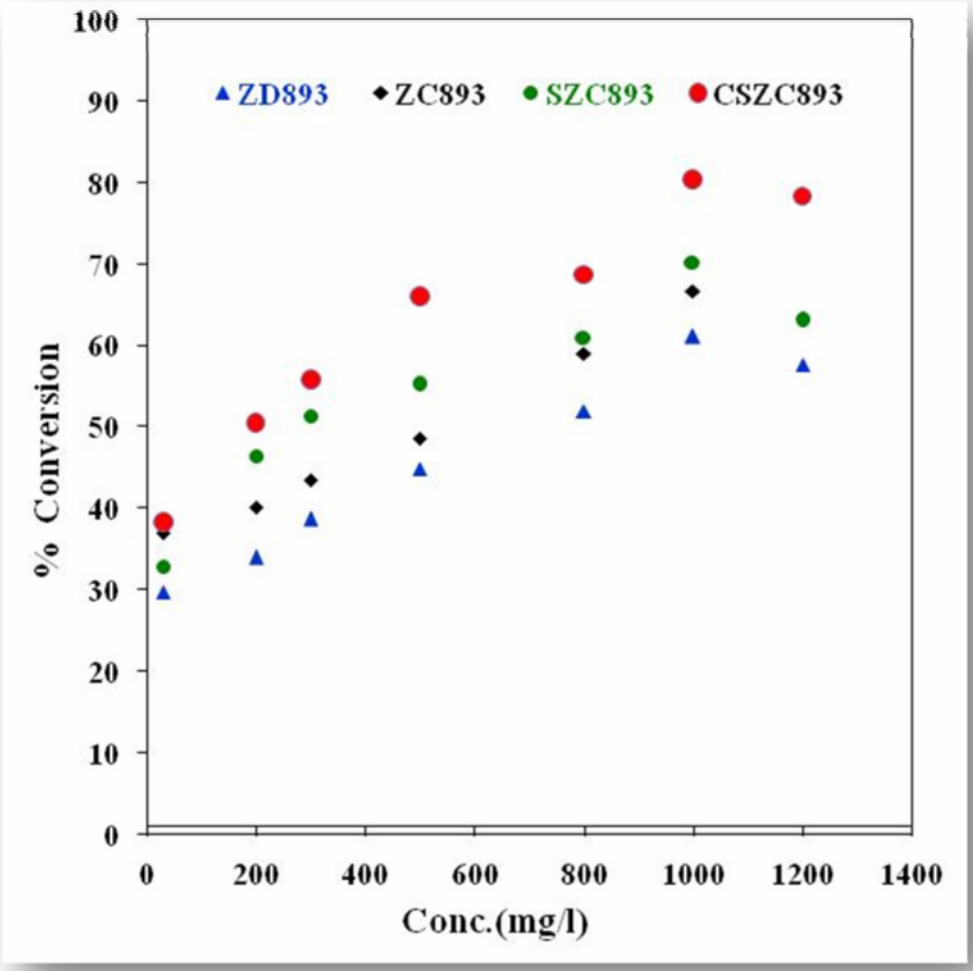


**Figure 5.45 Effect of concentration ($C_o$) on conversion of DBT at T = 333K; t = 22 h; w = 5 g/l, by various samples.**

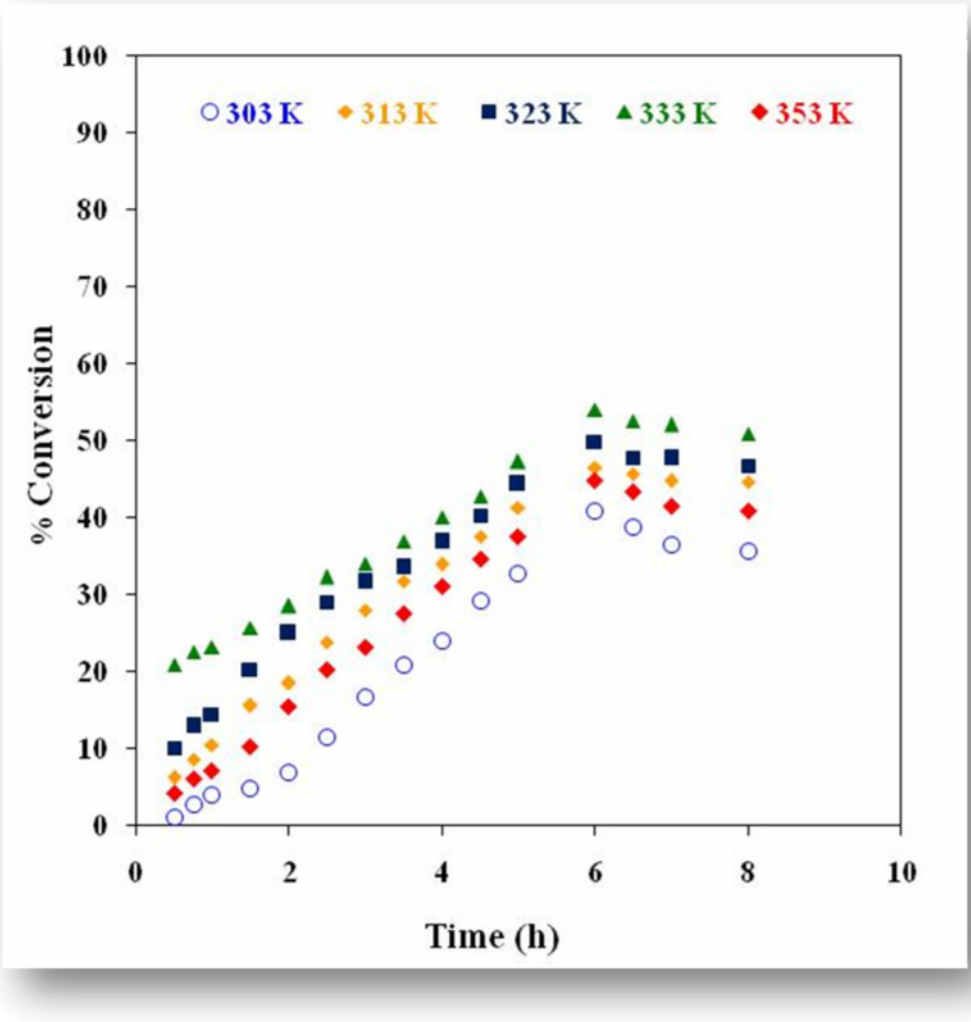


**Figure 5.46 Effect of time on conversion of DBT by ZD383 at various temprature (T) [$C_o$ = 1000 mg/l; $w$ = 5 g/l]**

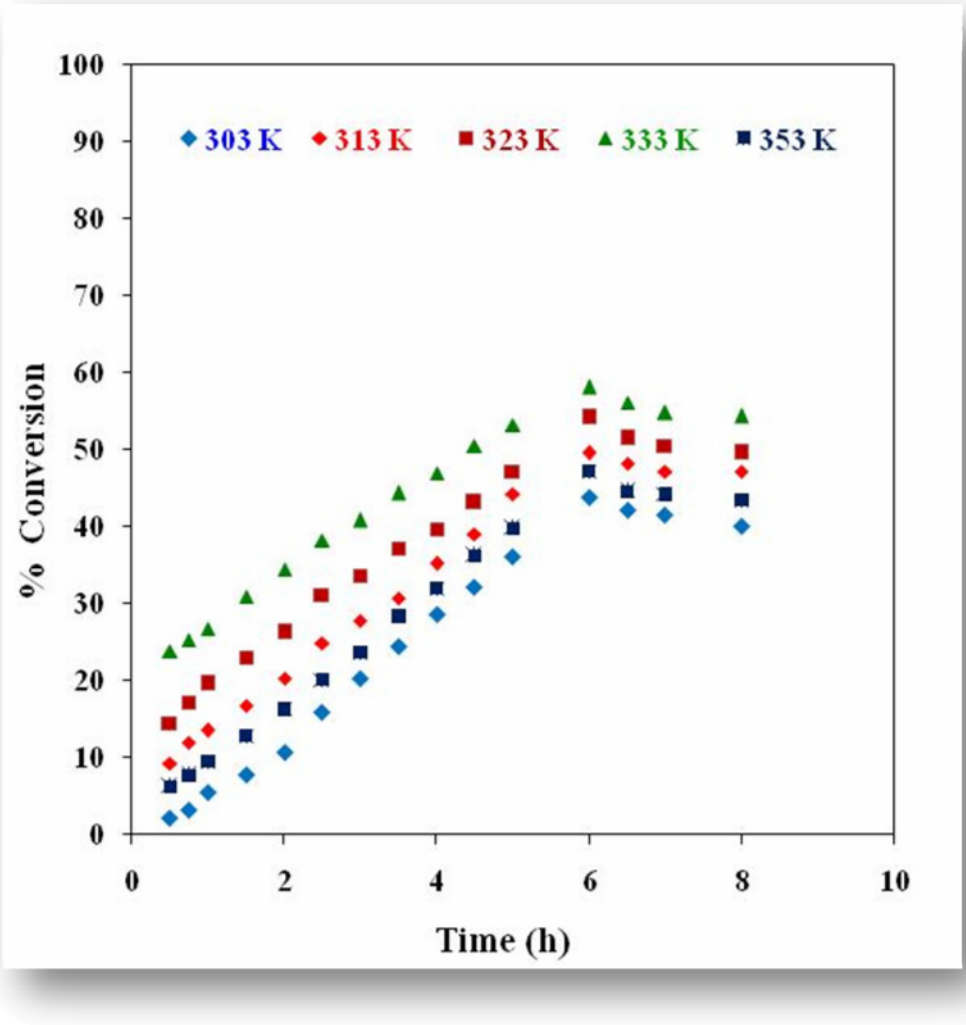


**Figure 5.47 Effect of time on conversion of DBT by ZC893 at various temprature (T) [$C_o$ = 1000 mg/l; $w$ = 5 g/l]**

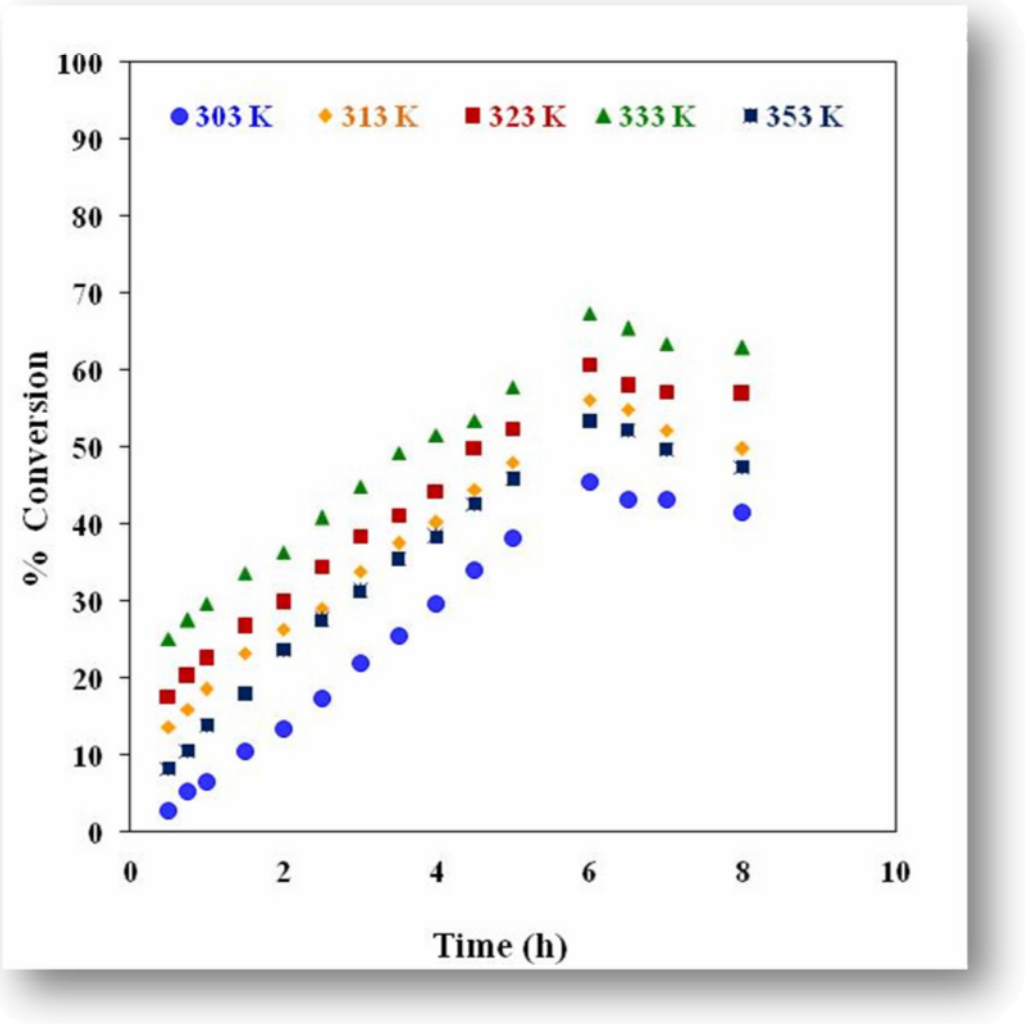


**Figure 5.48 Effect of time on conversion of DBT by SZC893 at various temprature (T) [$C_o$ = 1000 mg/l; $w$ = 5 g/l]**

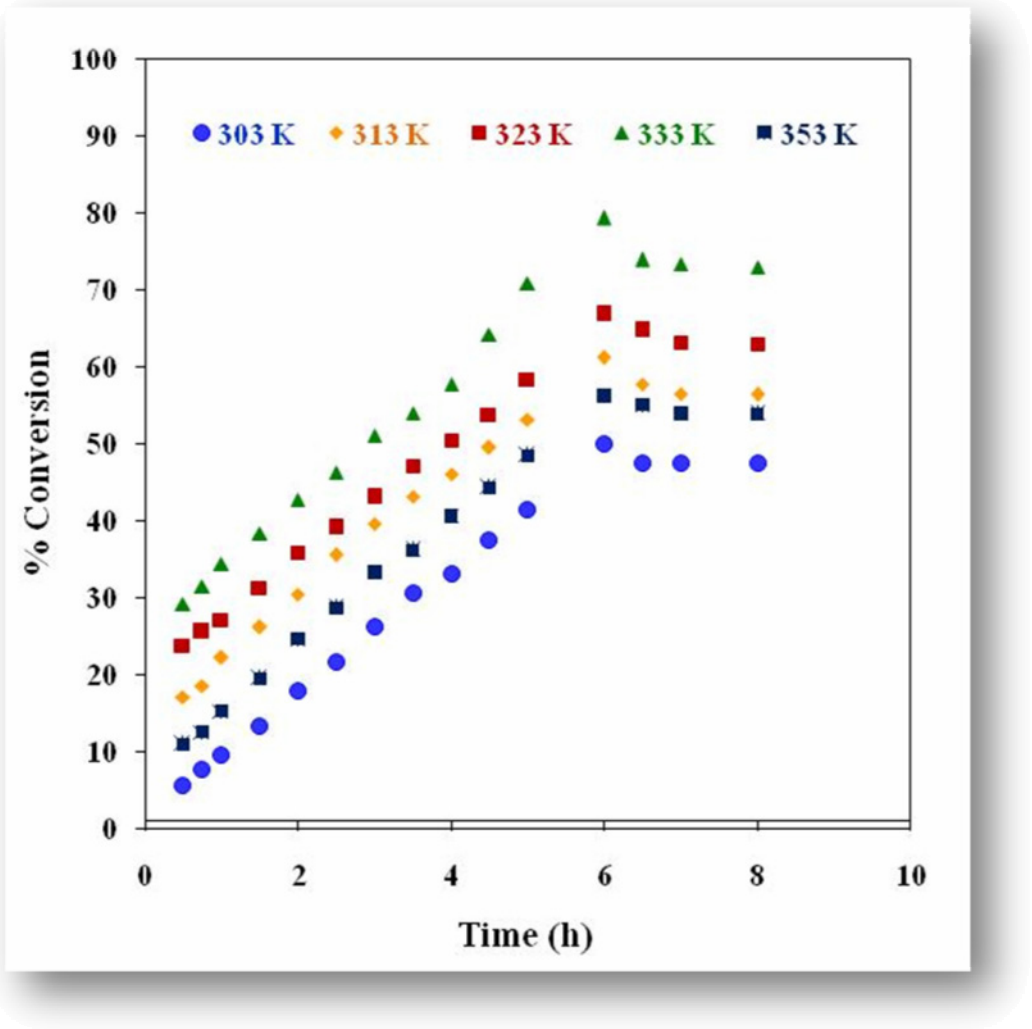


**Figure 5.49 Effect of time on conversion of DBT by CSZC893 at various temprature (T) [$C_o$ = 1000 mg/l; $w$ = 5 g/l]**

### 5.3.3.1 Kinetics of the Oxidative Reaction

Limited work has been reported on mechanistic and kinetic studies of oxidation of organic sulfur compound in zirconia/$H_2O_2$/acid system.

In order to examine the kinetics of the catalytic oxidative reaction, the oxidative reaction of model sulfur compounds under various conditions was carried out at 303, 313, 323, 333, and 353 K. In all the experimental runs, O/S molar ratio 10 whereas $H_2O_2$/methanoic acid molar ratio was 1.

Several studies indicated that in presence of an excess of $H_2O_2$, the oxidation of organic sulfur compounds follows pseudo-first order kinetics [Collins et al., 1997; Te et al., 2001; Otsuki et al., 2000]. Rate of the oxidation of DBT can be written as:

$$r_o = dC_t/dt = - K_o.C_t \quad (5.12)$$

$$\ln C_o/C_t = K_o t \quad (5.13)$$

where, $K_o$ is apparent first-order rate constant.

A plot of ln $C_o/C_t$ vs time should be linear and value of the apprant rate constant $K_o$, can be obtained from the slope of the linear relationship.

In our experiment, the oxidation of DBT at different tempertures with four different zirconia samples was carried. Figures 5.50, 5.51, 5.52 and 5.53 show the plots of ln ($C_o/C_t$) vs time for oxidation of DBT by ZD383, ZC893, SZC893 and CSZC893 under pseudo-first order reaction conditions. The optimum reaction temperature was 333 K. It required extended duration at low temperatures for complete oxidation. At this temperature, the DBT oxidation to DBT sulfone was fast. The kinetic data for oxidation reaction shown in table 5.11 reveals that the reaction is pseudo-first order and demonstrated consistent linear reaction kinetics with correlation factors close to unity for all the catalyst systems tested.

Apparent activation energy for oxidation of DBT derived from the slope of Arrhenius plot are reported in table 5.12.

**Table 5.11 Kinetic parameters for the conversion of DBT by various catalyst samples; $w$ = 5 g/l.**

| T (K) | $K_o$ (min$^{-1}$) | $R^2$ |
|---|---|---|
| **ZD383** | | |
| 303 | 0.0015 | 0.970 |
| 313 | 0.0017 | 0.999 |
| 323 | 0.0017 | 0.994 |
| 333 | 0.0015 | 0.9775 |
| 352 | 0.0016 | 0.9961 |
| **ZC893** | | |
| 303 | 0.0017 | 0.988 |
| 313 | 0.0018 | 0.990 |
| 323 | 0.0018 | 0.993 |
| 333 | 0.0018 | 0.9991 |
| 352 | 0.0017 | 0.989 |
| **SZC893** | | |
| 303 | 0.0017 | 0.989 |
| 313 | 0.0019 | 0.989 |
| 323 | 0.0021 | 0.988 |
| 333 | 0.0023 | 0.977 |
| 352 | 0.0020 | 0.997 |
| **CSZC893** | | |
| 303 | 0.0018 | 0.991 |
| 313 | 0.0022 | 0.994 |
| 323 | 0.0023 | 0.981 |
| 333 | 0.0033 | 0.945 |
| 352 | 0.0020 | 0.994 |

**Table 5.12 Thermodynamics parameters for the conversion of DBT by various catalyst samples; $w$ = 5 g/l.**

| Catalyst | $K_o$ (min$^{-1}$) | $E_a$(kJ/mol) |
|---|---|---|
| ZD383 | 0.0020 | 0.5435 |
| ZC893 | 0.0021 | 0.4878 |
| SZC893 | 0.0062 | 3.0382 |
| CSZ893 | 0.0096 | 3.7900 |

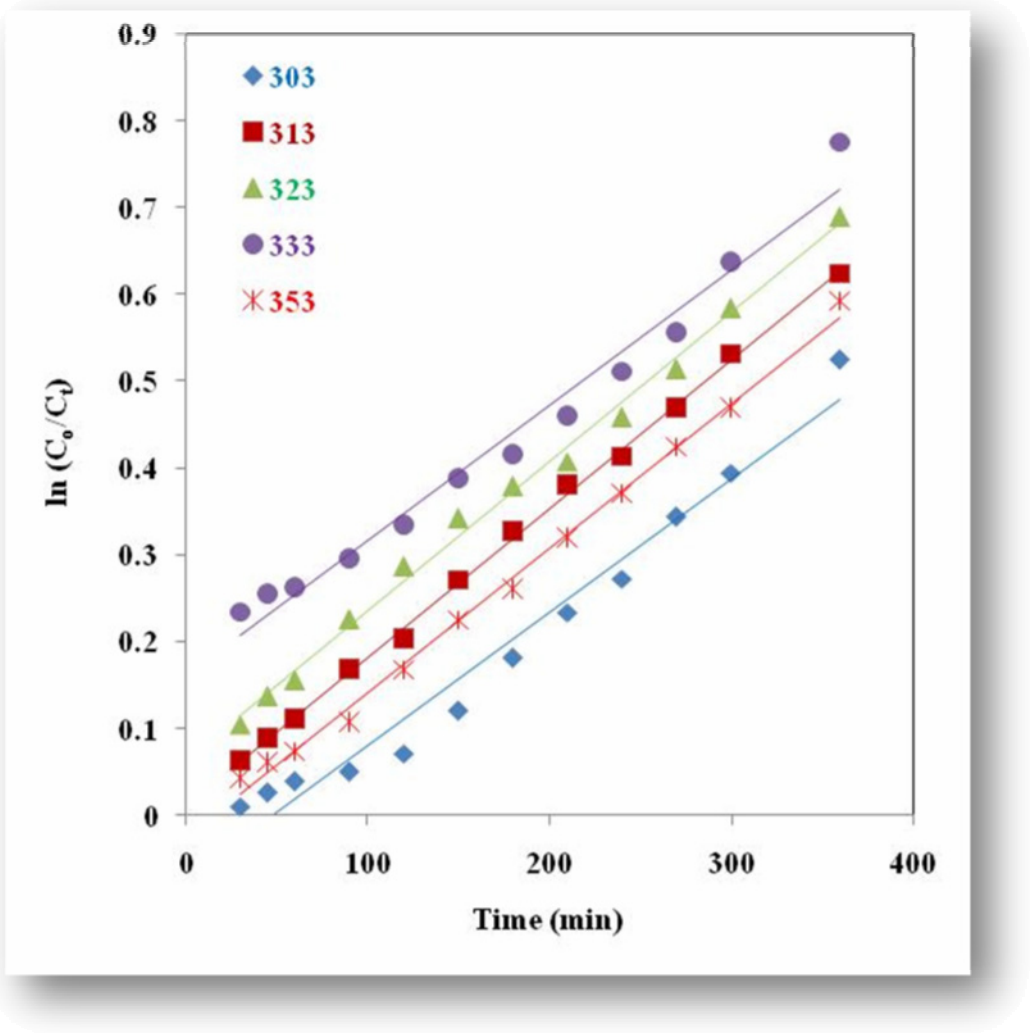


**Figure 5.50 Plot of ln ($C_o/C_t$) vs time for conversion of DBT by ZD383 under pseudo-first order reaction conditions.**

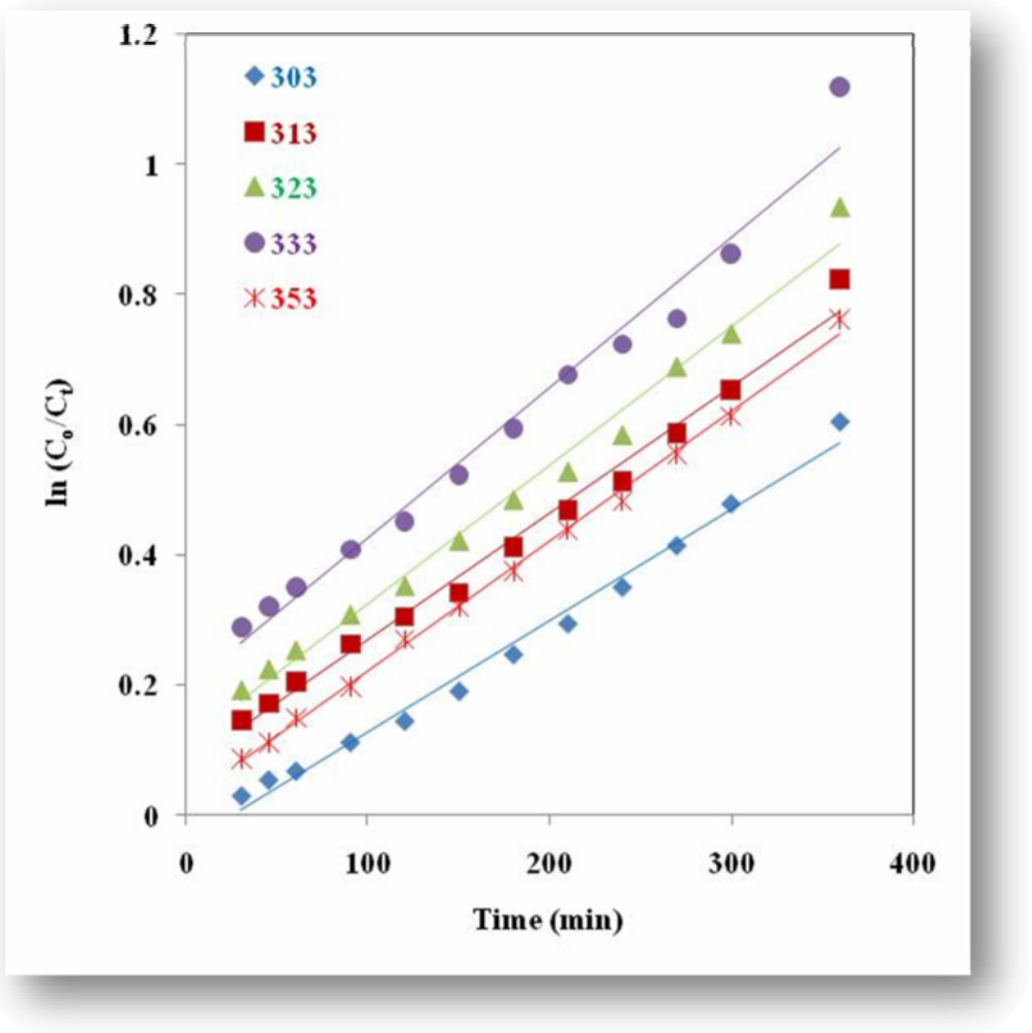


**Figure 5.51** **Plot of ln ($C_o/C_t$) vs time for conversion of DBT by ZC893 under pseudo-first order reaction conditions.**

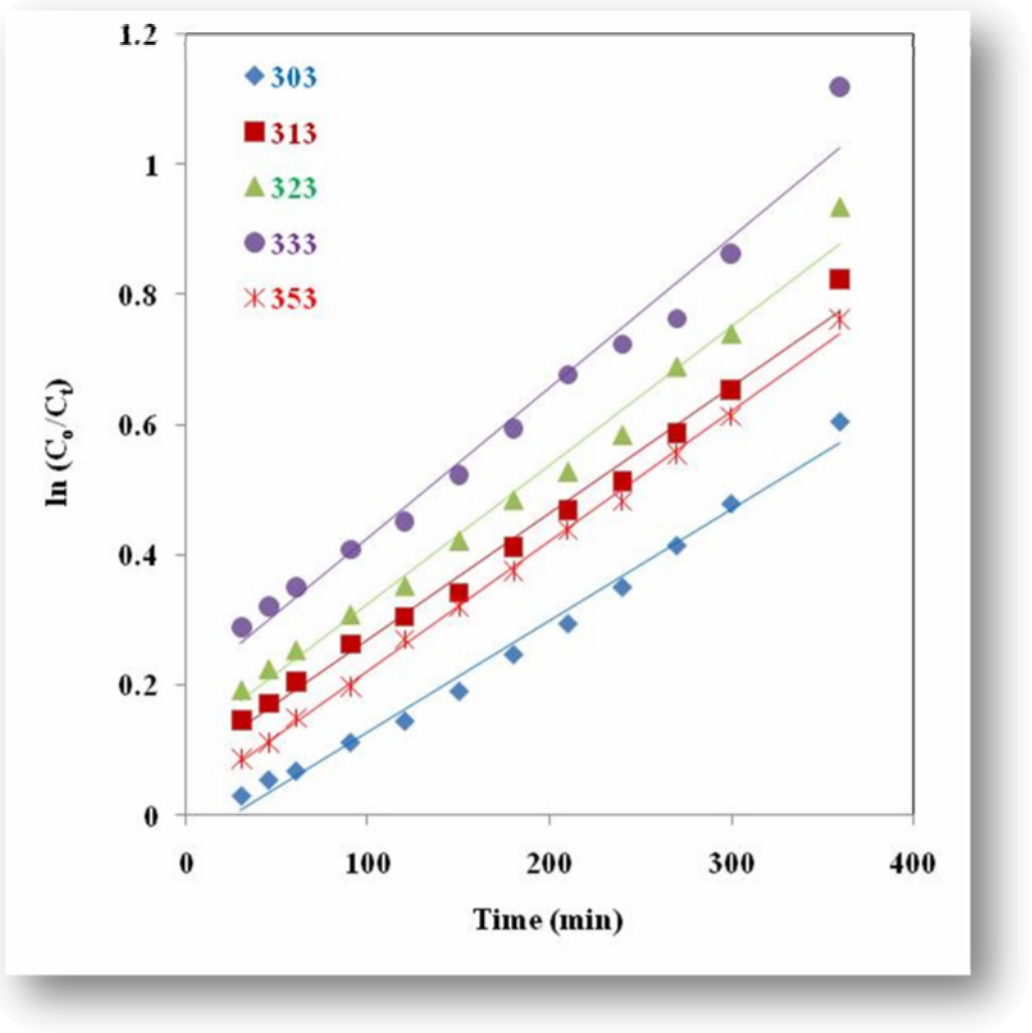


**Figure 5.52 Plot of ln ($C_o/C_t$) vs time for conversion of by SZC893 under pseudo-first order reaction conditions.**

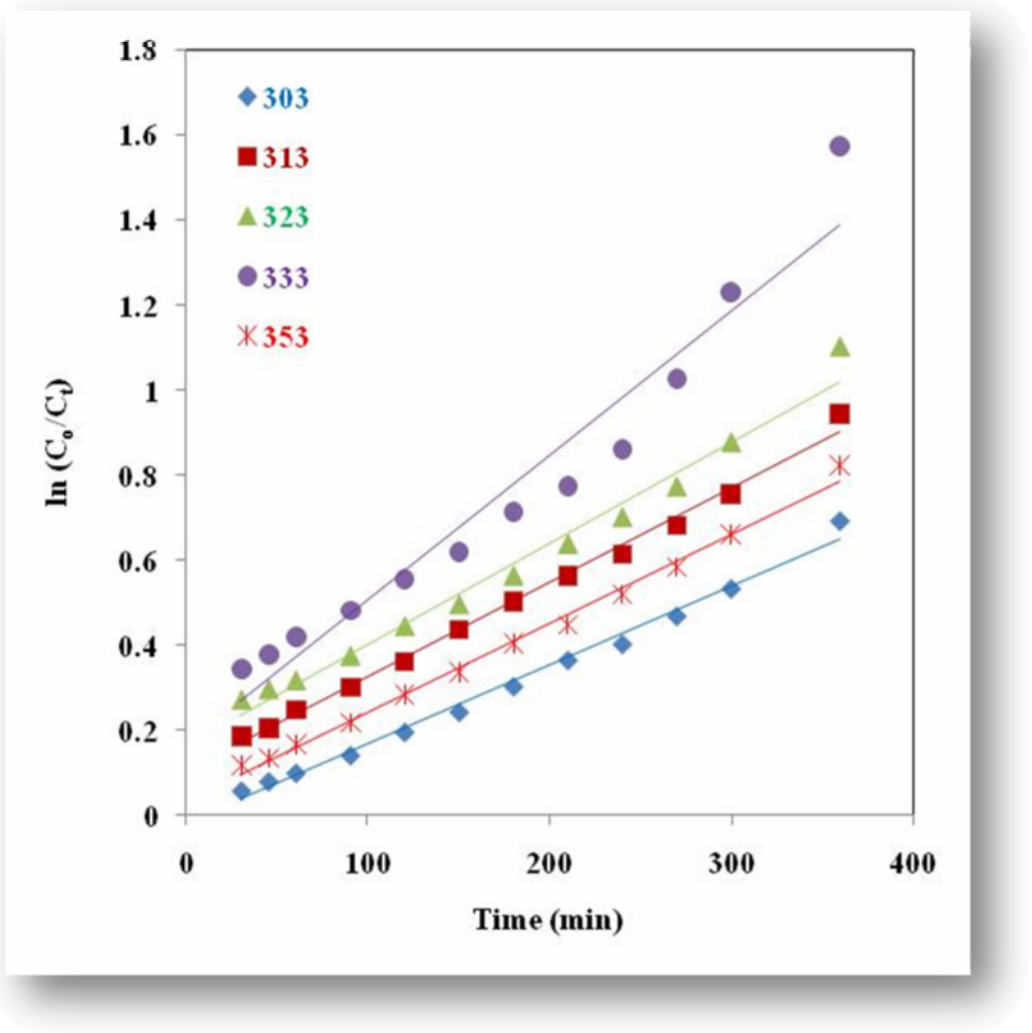


**Figure 5.53 Plot of ln ($C_o/C_t$) vs time for conversion of DBT by CSZC893 under pseudo-first order reaction conditions.**

### 5.3.4 Effect of Reaction Temprature

Generally, increasing temprature will significantly accelerate most organic reactions. Temperature is always one of the important experimental variables to be considering in ODS. It effect observes by performing reaction at different temperature range 303 K–353 K , that the experimental data can be adjusted to first order kinetics, agreed with [Wang et al. 2003; Ishihara et. al., 2005, Moreau et al., 1997].

In our experimental, the reaction temprature of 333 K, concentration 1000 g/l and dose 5 g/l are employed as optimum conditions. Figure 5.55, 5.56, 5.57 and 5.58 shows the conversion of DBT to $DBTO_2$ at various temprature. It is seen that the reaction rate and oxidation efficiency increased with an increase in temperature. At 303 K, for example, the conversion of DBT is found to be 40.84, 43.80, 45.41 and 49.96 % for ZD383, ZC893, SZC893 and CSZC893 at 303 K which increases upto 53.92, 58.02, 67.36 and 79.26% at 333 K at optimum conditions. Further increase in reaction temperature beyond 333 K decreased the conversion of DBT. Borah et al. [2005] indicated that a portion of hydrogen peroxide introduced into the reactor gets decomposed with the evolution of oxygen gas. Oxidation at higher temperature was unfavorable due to the decomposition of hydrogen peroxide to undesirable side products other than hydroxyl radicals which oxidize the DBT [Haw et al., 2010]. Thus, the thermal decomposition of $H_2O_2$ at 353 K decreases the efficiency of desulfurization process [Bernal and Caero, 2005].

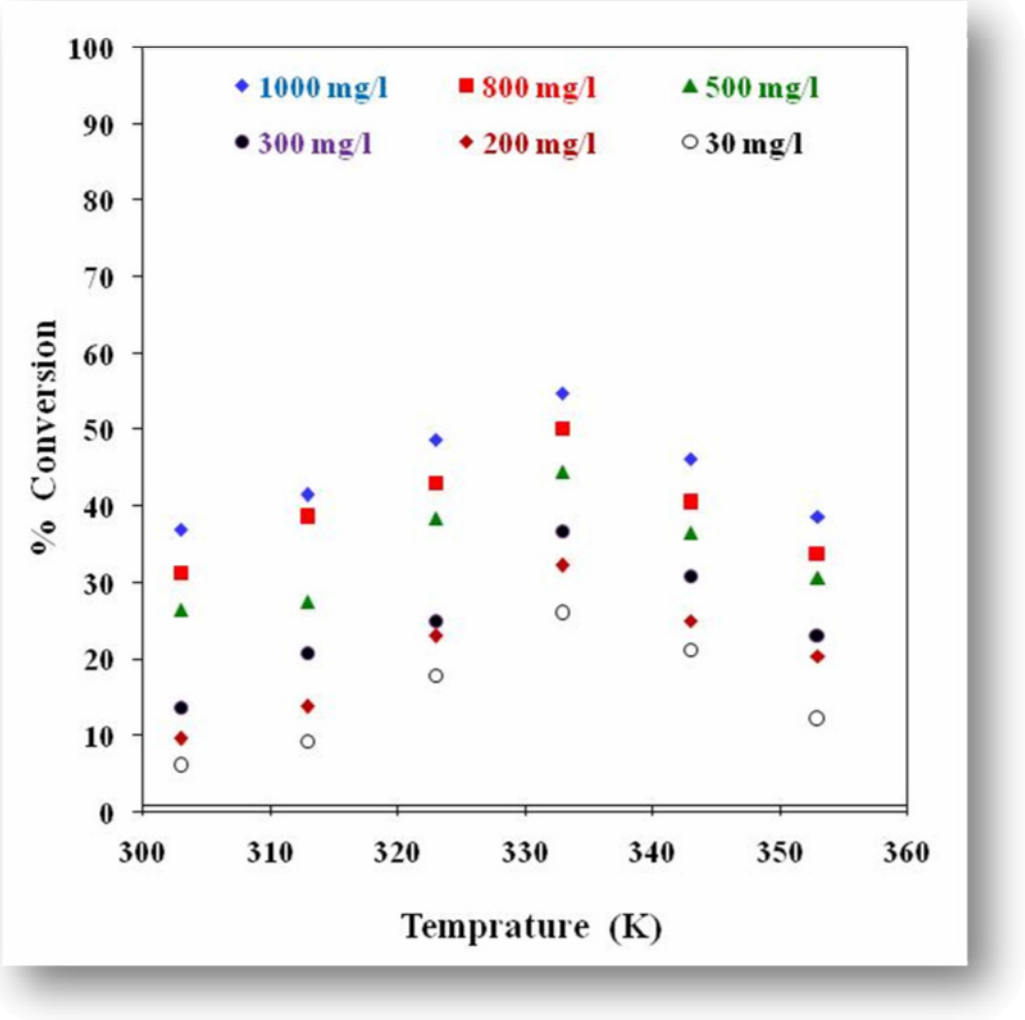


**Figure 5.54 Effect of temperature on conversion of DBT by ZD383 at various initial concentrations ($C_o$).**

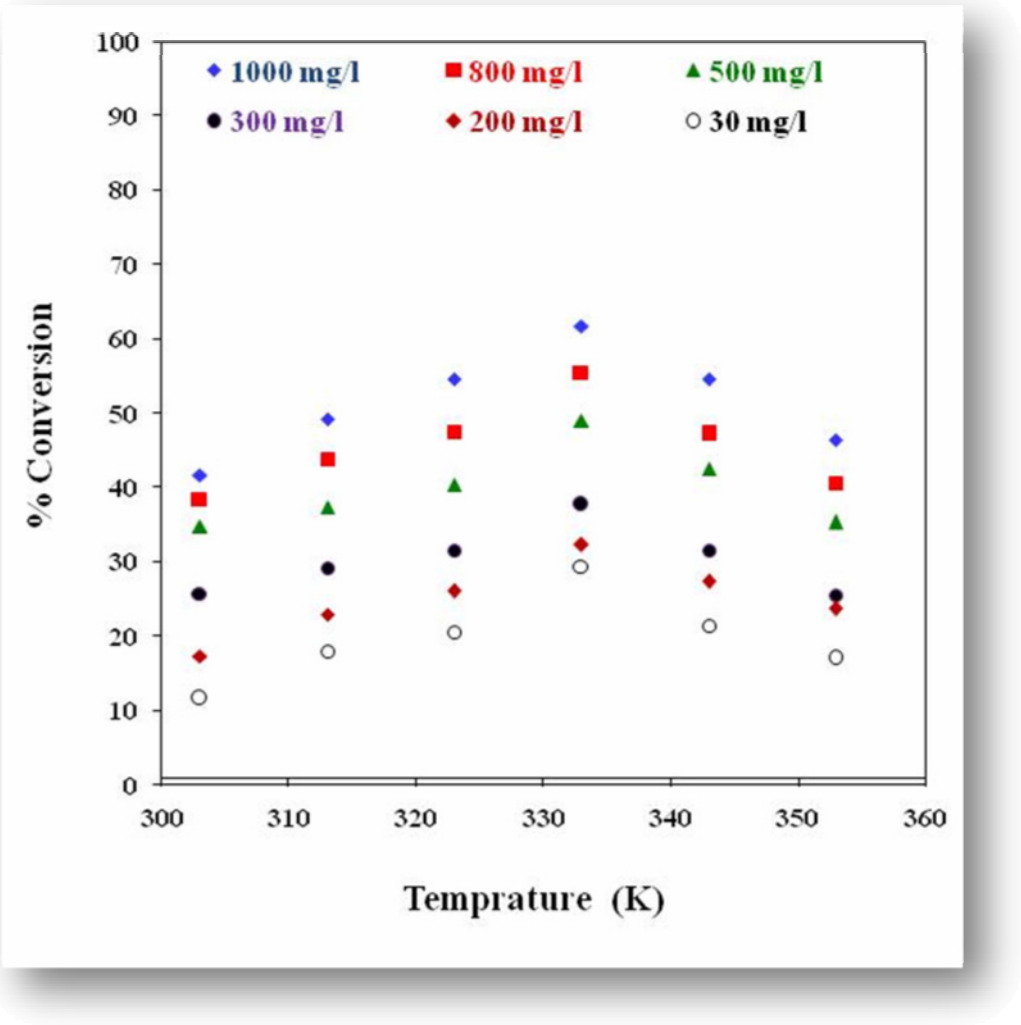


**Figure 5.55 Effect of temperature on conversion of DBT by ZC893 at various initial concentrations ($C_o$).**

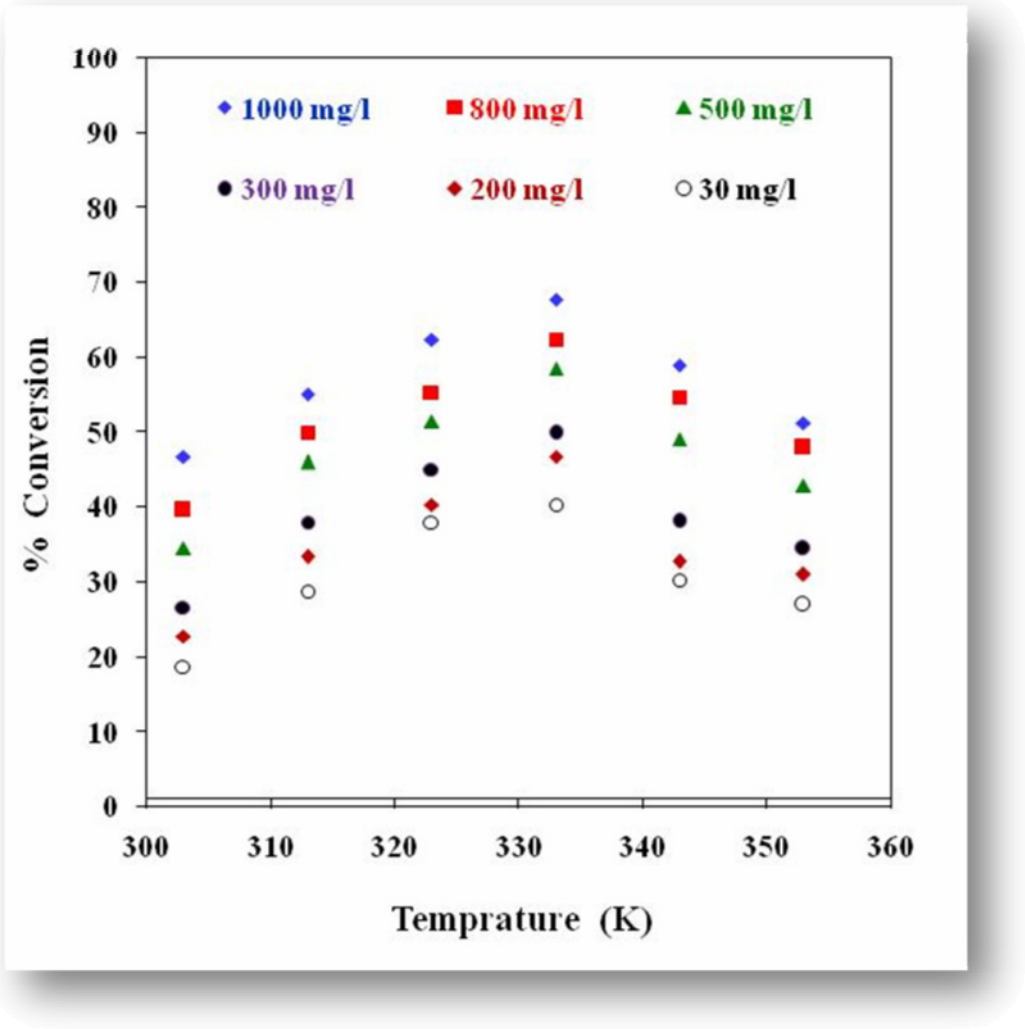


**Figure 5.56 Effect of temperature on conversion of DBT by SZC893 at various initial concentrations ($C_o$).**

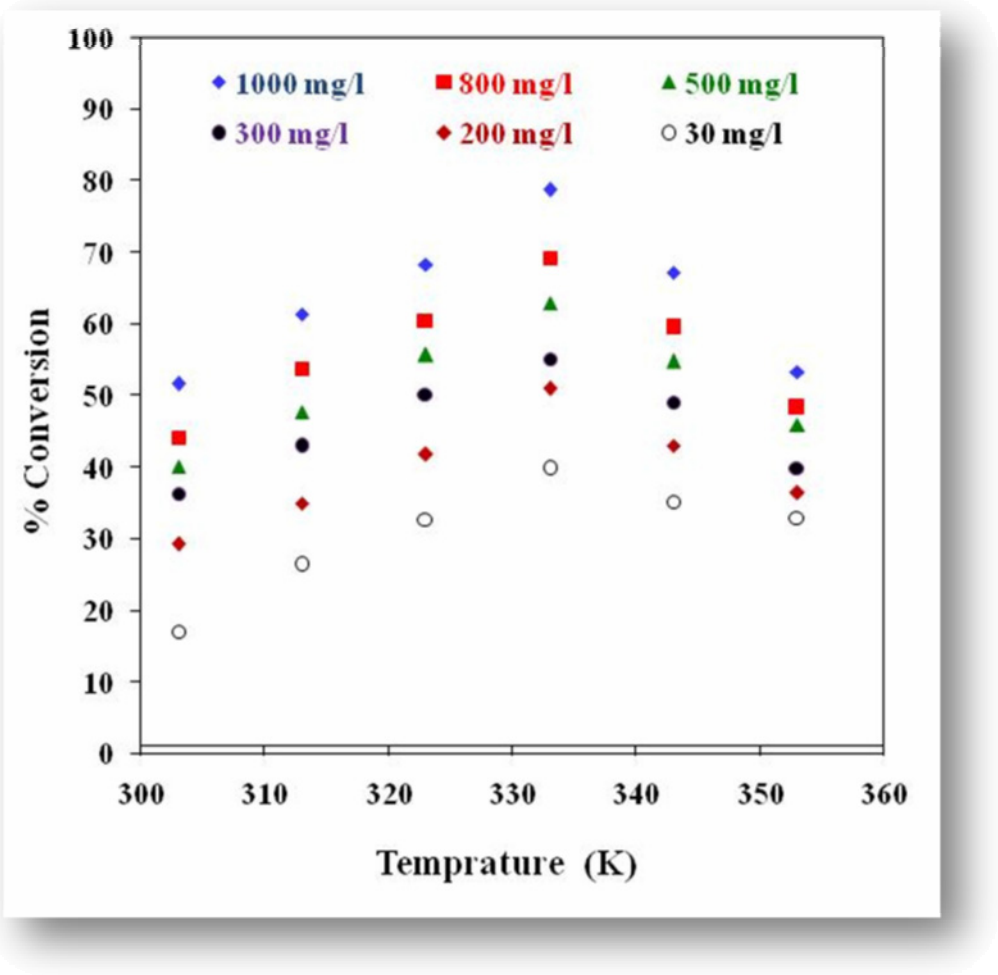


**Figure 5.57 Effect of temperature on conversion of DBT by CSZC893 at various initial concentrations ($C_o$).**

### 5.3.5 Characterization of Catalysts Before and After ODS

#### 5.3.5.1 X-Ray diffraction (XRD) Analysis

XRD patterns of CSZC893 before and after ODS are shown in figure 5.58. It may be seen in figure that, the peaks of CSZC893 get shifted after ODS. Also, the intensity and tetragonal nature of the peaks gets reduced after ODS. This signifies that the fact tetragonal phase is responsible for catalytic activity of CSZC893. Srinivasan et al. [1995] have proposed that surface sites that adsorb oxygen at low temperatures (298–500 K) are responsible for causing the tetragonal–monoclinic transformation at low temperatures.

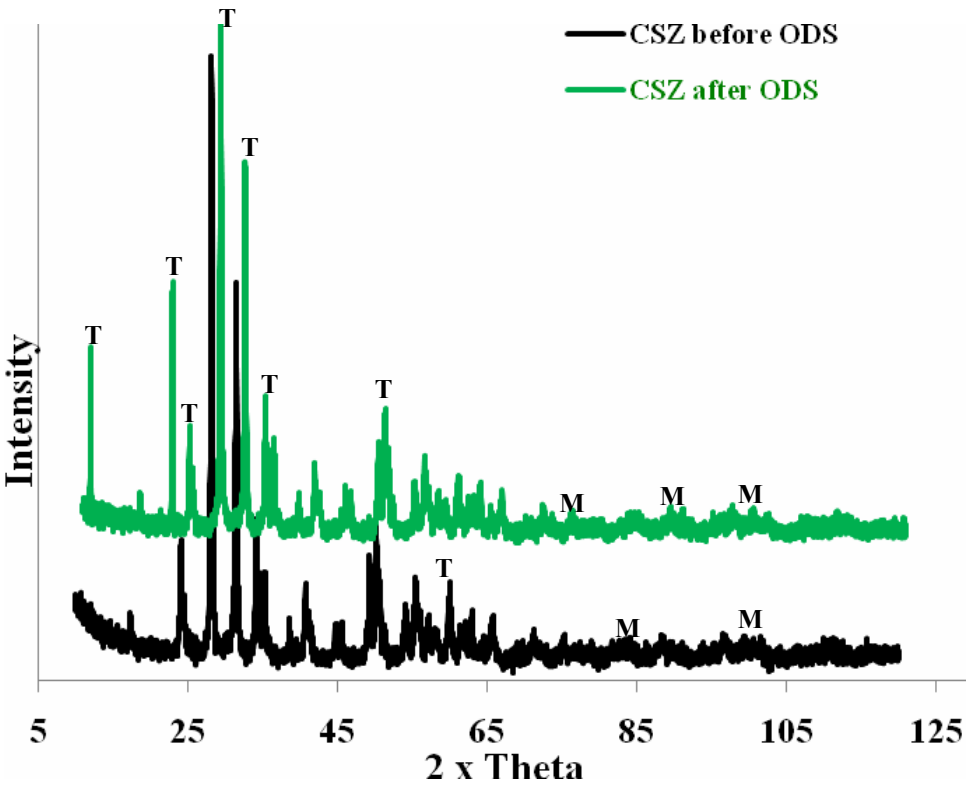


**Figure 5.58 XRD patterns of the CSZC893 before and after ODS reaction (T: Tetragonal $ZrO_2$ M: Monoclinic $ZrO_2$).**

#### 5.3.5.2 Scanning Electron Microscopic (SEM) Study

The SEMs of the CSZC893 before and after ODS at various magnifications are shown in figure 5.59. These figures reveal changes in surface texture of CSZC893 before and after OD. It may be seen that crystalinity of the surface has reduced after ODS and pores have been modified.

#### 5.3.5.3 Electron Probe Microscopic (EPM) Analysis

EPMA analysis of CSZC893 before and after ODS is shown in figure 5.60. It may be seen in the figure that dispersion of both Zr and Cr gets changed in the catalyst. Zr gets well dispersed after the ODS, however, distribution of Cr gets scattered with some voids spaces in between. This may be due to use of sites having Cr for oxidation of DBT.

#### 5.3.5.4 Thermogravimetry (TG) and Differential Thermal Analysis (DTA)

The TGA thermogram of CSZC893 before and after ODS is shown in figure 5.61. It shows that CSZC893 before ODS is fully stable upto 1000 $^{o}$C with a minute 2.2% wt loss from ambient to 1000$^{o}$C. The TGA thermogram of CSZC893 after ODS shows a weight loss of 7.5%. The increase in weight loss is due to the vaporization of DBT-sulfones that may have remained attached on the CSZC893 surface.

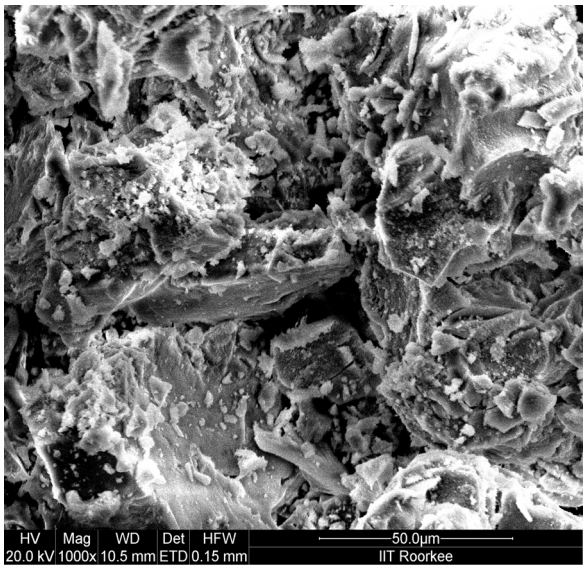


**1000X before ODS**

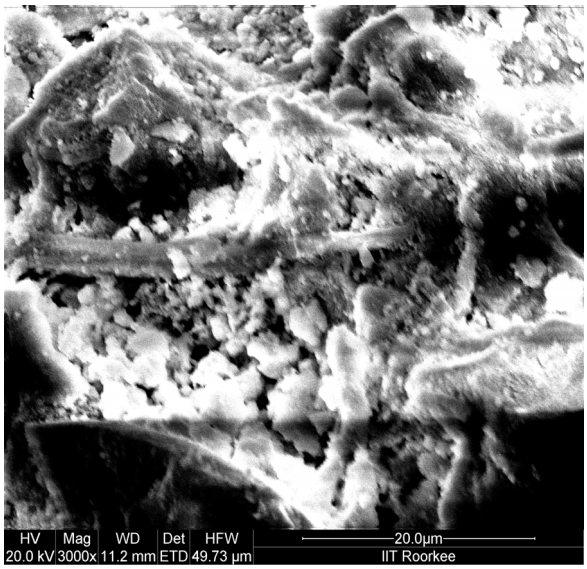


**3000X before ODS**

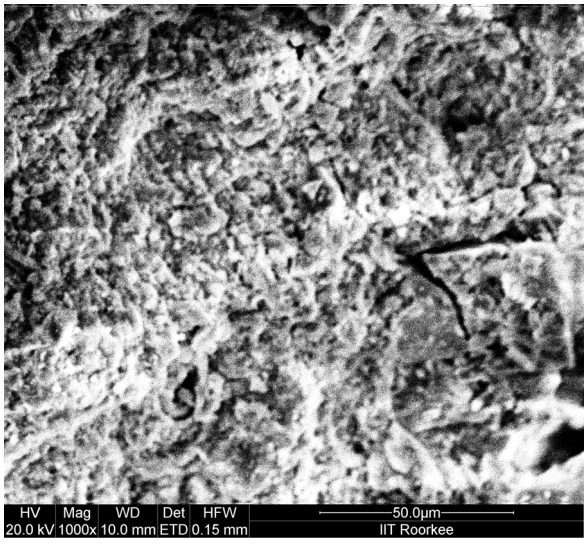


**1000X after ODS**

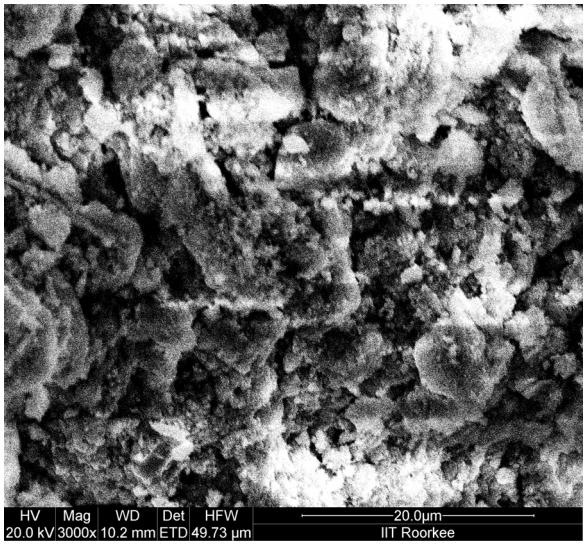


**3000X after ODS**

**Figure 5.59 Scanning Electron Micrographs of CSZC893 before and after ODS.**

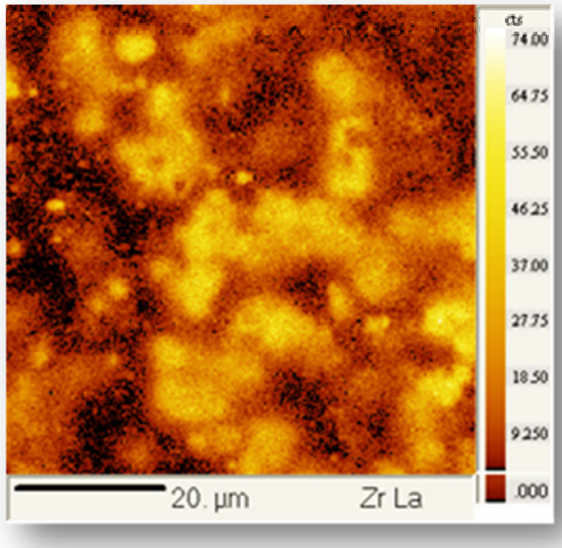


**(a) Zr in CSZC893 before DOS**

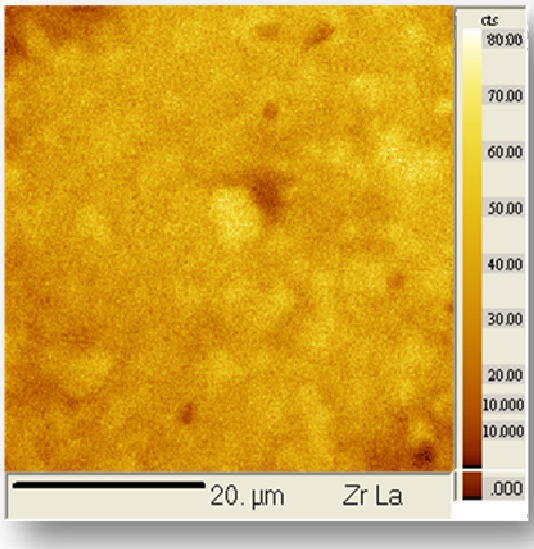


**(a) Zr in CSZC893 after DOS**

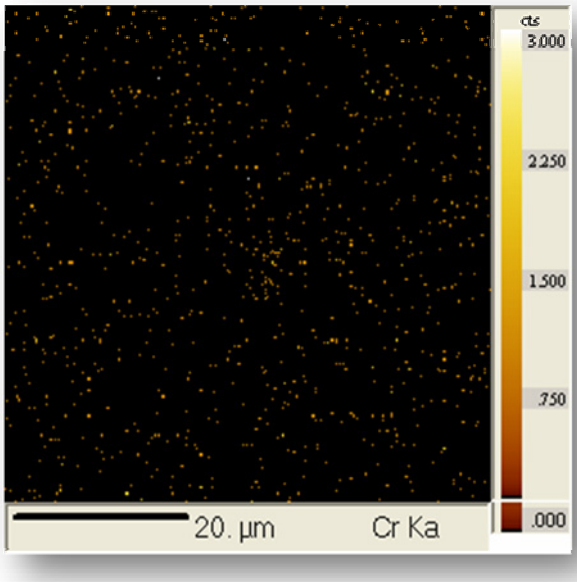


**(b) Cr in CSZC893 before ODS**

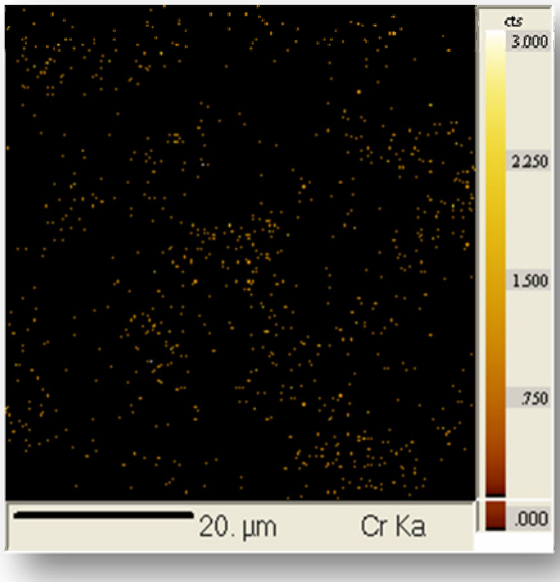


**(c) Cr in CSZC893 after DOS**

**Figure 5.60 Comparative study of EPMA images for dispersion of Zr and Cr metals on CSZC893 before and after ODS.**

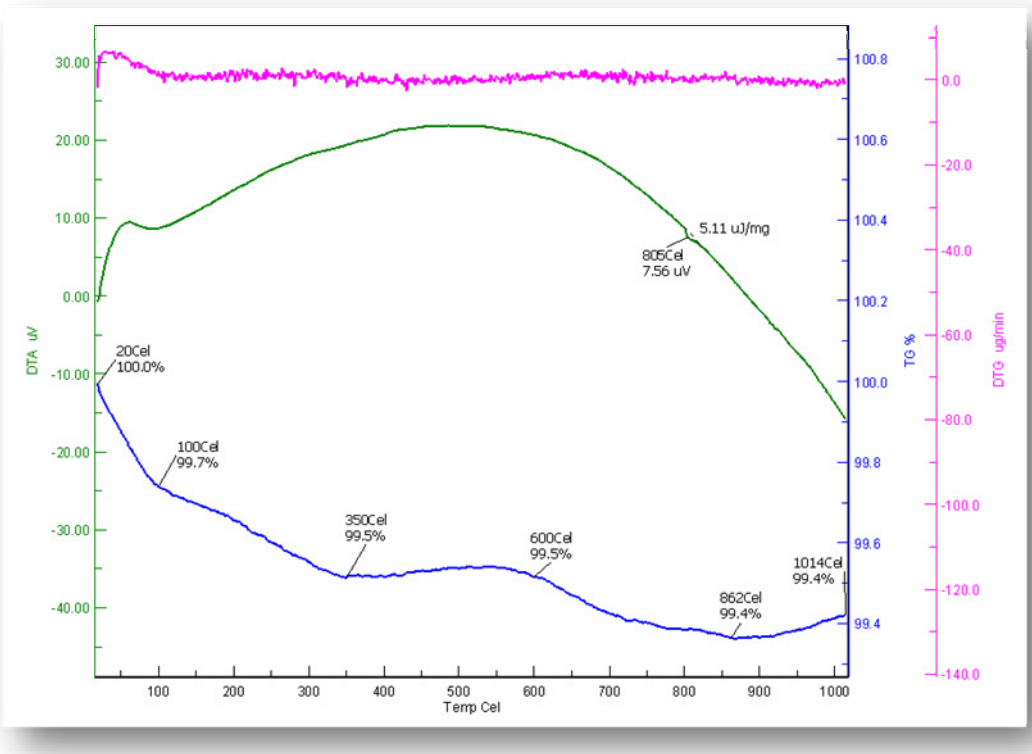


**(a) CSZC893 before ODS.**

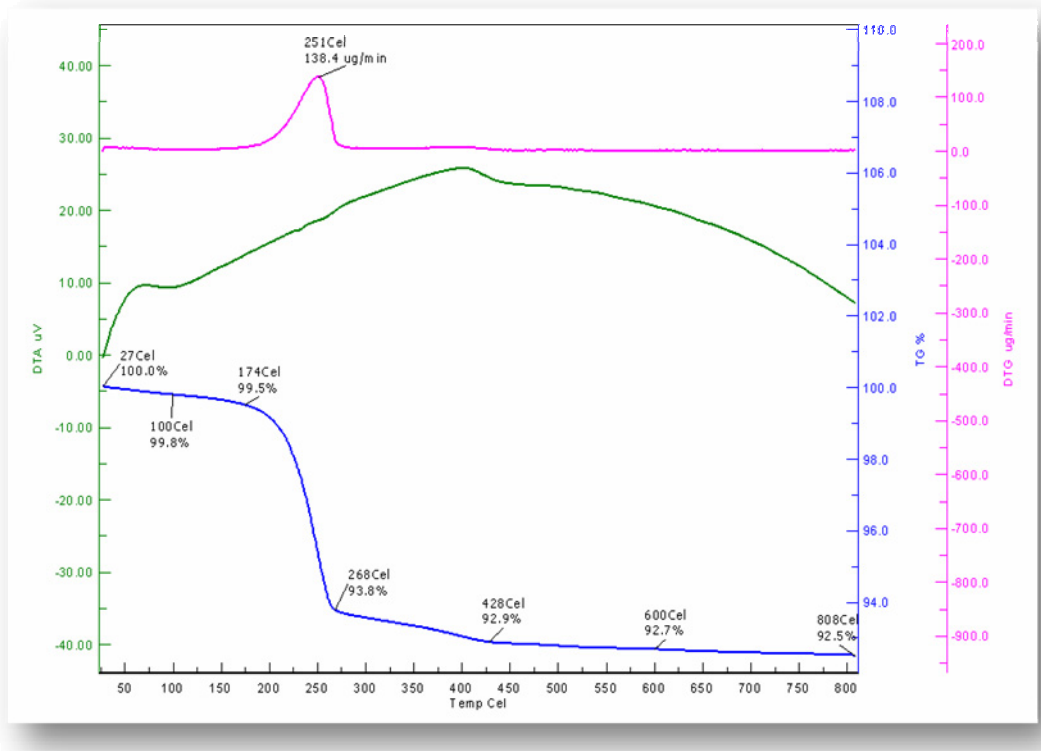


**(b) CSZC893 before ODS**

**Figure 5.61 TG/DTG Thermogram CSZC893 before and after ODS.**

### 5.3.5.5 Electron Spin Resonance (ESR) Spectroscopy

In order to detect the presence of Zr(III) and Cr(III), electron spin resonance (ESR) experiments were performed using a Bruker ESP 300 spectrometer operating at X-band (microwave frequency ν=9.4 GHz) with applied magnetic fields up to 2 Teslas. All the experiments were performed at room temperature and liquid nitrogen temprature. The ESR spectra of the calcined samples are included in figures 5.62 and 5.63. Here we find the effect of Cr (III) on the electronic state of SZ. In figure 5.62 and 5.63 a strong EPR signal appeared at $g_{\perp}$ 1.89 (signal A), associated with Zr (III) and in figure 5.62 two strong signals appeared at $g_{\perp}$1.89 (signal A) and $g_{\perp}$1.96 (signal B), associated with Zr (III) and Cr (III), this shows that the samples are highly paramagnetic. The intensity of signal A decreases after ADS/ODS experiment, this indicates those are lesser in number or bind with some other species. In figure 5.62b signal B become weak (i.e., area decreases) indicates lesser number or nearly no unpaired electrons of Cr (III) present after ODS.

Previous works by other authors [Wong et al., 2005] on polycrystalline samples have associated $Zr^{3+}$ to a narrow and anisotropic line with g-factor values: g ⊥=1.976 and g//= 1.958.These Zr (III) species are usually associated to the presence of oxygen vacancy defects, because the remaining electrons left by the oxygen lost are shared by nearby Zr cations and paramagnetic Zr (III) centers are formed. The spectra in figures 5.62 (a, b) and 5.63 (a, b) correspond to the SZ before and after ODS reaction. Probably, the concentration of paramagnetic species is higher in the refluxed-aged sample. In agreement with [Torralvo et al., 1984; Liue et al., 1995; Che and Tench, 1983; Morterra et al., 94], it can be assigned to the 4d electron of Zr(III). In oxygen atmosphere at room temprature the Zr (III) ions generate superoxide species $O_2^-$ characterized by $g_x$= 2.04, $g_y$=2.010 and $g_z$ = 2.031, well known signals often reported [Torralvo et al., 1984; Liue et al., 1995; Che and Tench, 1983; Morterra et al., 94].The $g_{//}$ components of the Zr (III) ion is the weaker but still present, which shows a contribution of bulk Zr (III) .After evacuation of $O_2$ at room temperature, the EPR spectrum is identical to the spectrum recorded after heating at 573 K,evidencing the low stability of the superoxide species.

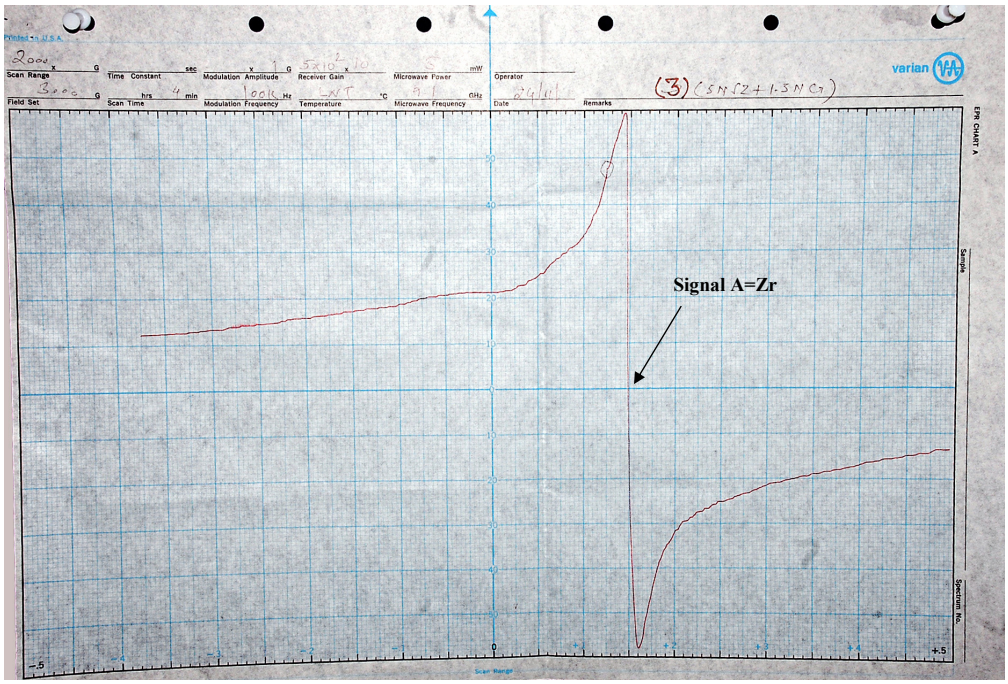


**(a) Before ODS**

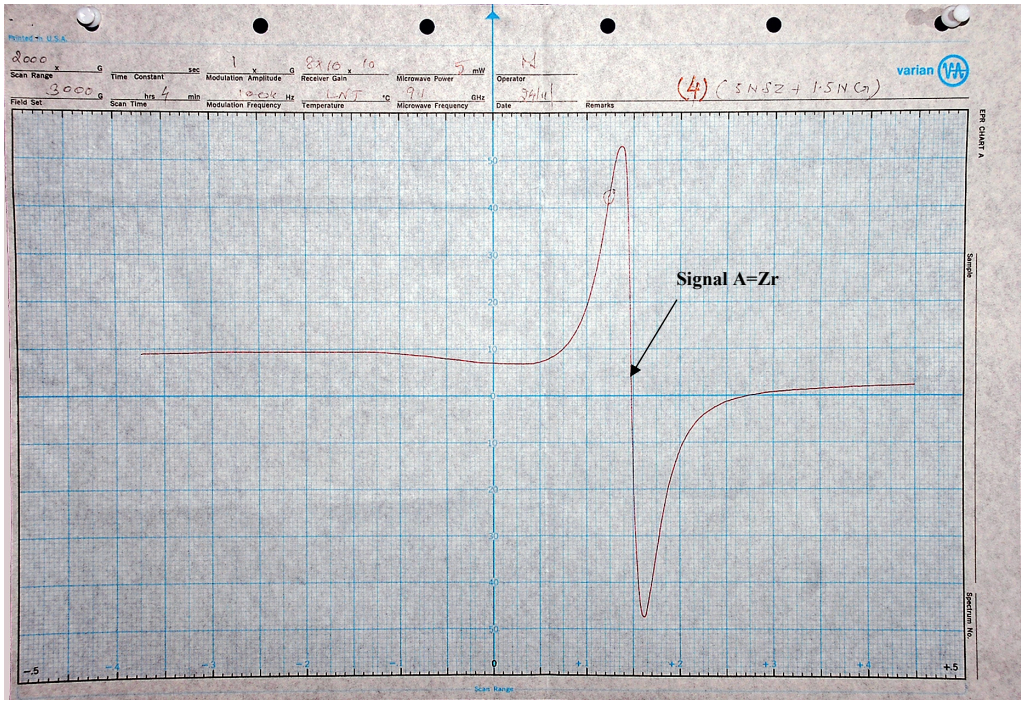


**(b) After ODS**

**Figure 5.62 Electron Spin Resonance Spectrum of CSZ893 before and after ODS at liquid nitrogen temprature (70 K).**

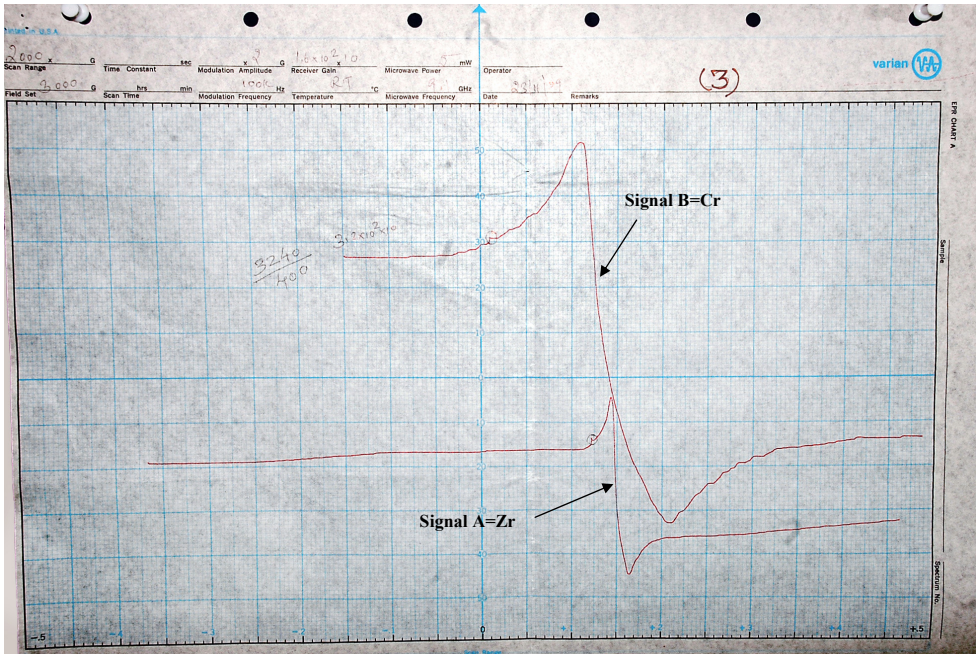


**(a) Before ODS**

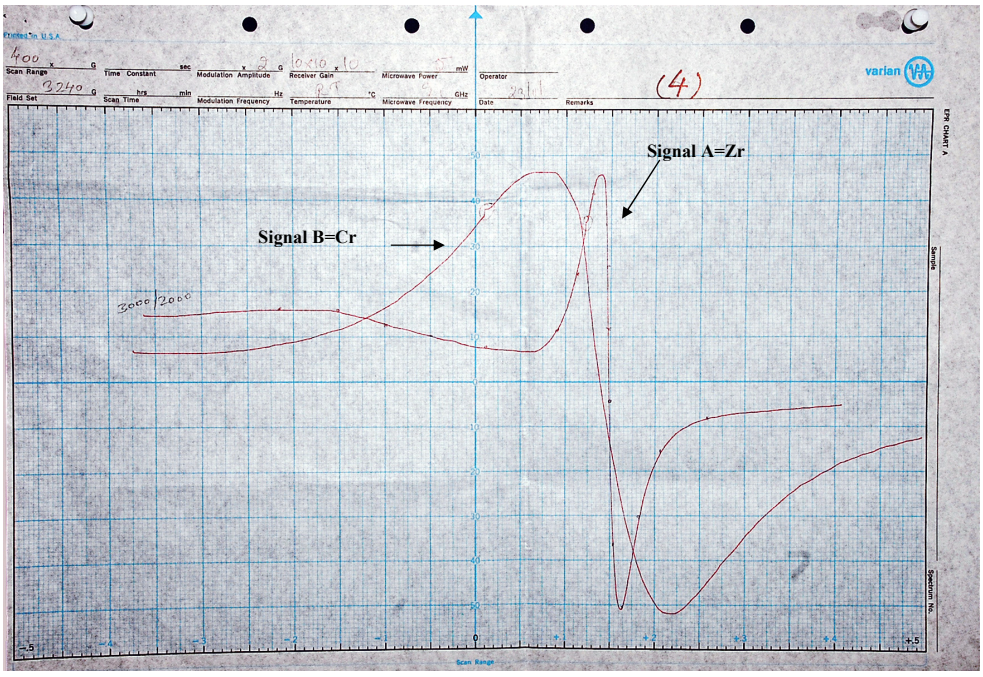


**(b) After ODS**

**Figure 5.63 Electron Spin Resonance Spectrum of SZ before and after ODS at room temprature (298 K)**

#### 5.3.5.6 Summary of ODS

The experimental result in this section indicates that ODS of DBT from model hydrocarbon by various catalysts found to follow the following trend: ZD393 < ZC893 < SZC893 < CSZC893.Table 5.12 shows the comparison ADS and ODS results.

In the present section we conclude that ODS can remove same amount of DBT in lesser time with lesser amount of zirconia material than ADS, though, ODS requires higher temperature than ADS along-with some minor amount additional chemicals like oxidants and acids.

**Table 5.13 Comparative study of desulfurization in ADS and ODS mode.**

| | % Removal of DBT in ADS | | | % Conversion of DBT in ODS | | | |
|---|---|---|---|---|---|---|---|
| $C_o$(mg/l) | ZD383 | ZC893 | SZC893 | ZD383 | ZC893 | SZC893 | CSZC893 |
| 30 | 18.06 | 36.04 | 37.59 | 24.52 | 30.04 | 37.35 | 35.46 |
| 200 | 22.67 | 40.03 | 44.2 | 32.72 | 32.29 | 43.89 | 51.16 |
| 300 | 26.96 | 46.28 | 47.23 | 37.44 | 39.32 | 45.91 | 53.44 |
| 500 | 39.72 | 50.8 | 50.6 | 40.87 | 48.72 | 54.06 | 62.28 |
| 800 | 47.6 | 53.08 | 54.23 | 47.38 | 55.00 | 57.47 | 66.87 |
| 1000 | 56.83 | 58.65 | 60.58 | 51.74 | 61.51 | 65.83 | 74.53 |

# Chapter – VI

# CONCLUSION AND RECOMMENDATIONS

## 6.1 CONCLUSIONS

The present study aimed to synthesize, characterize and utilize zirconia as an adsorbent for use in ADS as well as a catalyst for ODS. These zirconia based samples prepared in laboratory included: zirconia dried at 383 K (ZD393), zirconia calcined at 893 K (ZC893), sulfated zirconia calcined at 893 K (SZC893) and chromium-promoted sulfated zirconia calcined (CSZC893). On the basis of the studies and the results and discussion presented heretofore, the following conclusions can be drawn from different sections of work done:

### 6.1.1 Preparation and Characterization of Various Samples

a. Single-phase monoclinic zirconia with a known specific surface area can be made by means of gel-precipitation method. Though the samples were structurally stable, however the initial specific surface area was lost with an increase in calcination temperature. It was noticed that the activity of samples was markedly improved by acid treatment (i.e. by sulfation). The loading of chromium on the sulfated-zirconia resulted in an improvement in the thermal stability (resistance to sintering) at calcination temperatures upto 893 K.

b. After calcination at 893 K, sample ZC893 showed some crystalline peaks. Majority of these peaks were monoclinic in nature. The introduction of chromium further stabilized the metastable tetragonal zirconia phase and crystallinity was further increased.

c. EDAX analysis showed presence of 0.98 wt% Cr in addition to Zr, O and S in CSZC893.

d. The TGA thermogram of showed that the DBT is thermally stable upto 423 K and vaporized completely at 533 K. ZD383 was found to be fully stable upto 1273 K with a minute 2% wt loss from ambient to 1273 K. SZC393 was found to be stable upto 773 K only.

### 6.1.2 Adsorptive Desulfurization Studies

a. Optimum ZD383, ZC893 and SZC893 dosage as an adsorbent were found to be 10 g/l for DBT removal by ADS.

b. The sorption kinetics of DBT onto ZD383, ZC893 and SZC893 could be well represented by the pseudo-second-order kinetic model.

c. An increase in temperature induced a negative effect on the adsorption process. Brunauer, Emmett and Teller (BET) isotherm generally well represented the equilibrium adsorption of DBT onto various zirconia based adsorbents.

d. ADS of DBT from model hydrocarbon by various adsorbents were found to follow the following trend: ZD393 < ZC893 < SZC893.

### 6.1.3 Oxidative Desulfurization Studies

a. Optimum ZD393, ZC893, SZC893 and CSZC893 dosages for ODS of model hydrocarbon at all concentration level was found to be 5 g/l.

b. Optimum reaction time was found to be 6 h for maximum DBT conversion. Reaction kinetics was found to follow pseudo first order kinetics.

c. Increase in temperature induced a positive effect on the ODS upto 333 K.

d. ODS of DBT from model hydrocarbon by various catalysts was found to follow the following trend: ZD393 < ZC893 < SZC893 < CSZC893.

e. The present study shows that ODS can remove same amount of DBT in lesser time with lesser amount of zirconia material than ADS. However, ODS requires higher temperature than ADS along with some minor amount additional chemicals like oxidants and acids.

## 6.2 RECOMMENDATIONS

On the basis of the present studies, the following recommendations may be made for future studies:

1. Developed material should be further characterized for their physico-chemical and surface characteristics so that they can be correlated in advanced way to preparation technique.
2. Regeneration of various zirconia samples by thermal treatment in presence/absence of inert atmosphere should be explored.
3. Scale-up reactors studies (on Pilot/Mini-Plant/Commercial scale) should be conducted to evaluate the suitability of developed materials as adsorbents/catalysts for adsorptive and oxidative desulfurization of DBT and their derivatives from various commercial liquid fuels.

# REFERENCES


1. Abu II, Das DD, Mishra HK, Dalai AK, Studies on platinum-promoted sulfated zirconia alumina: effects of pretreatment environment and carrier gas on n-butane isomerization and benzene alkylation activities, Journal of Colloid and Interface Science, 267, 2003, 382–390.
2. Adeeva V, de Haan JW, Janchen J, Lei GD, Schunemann V, Ven LJM, Sachtler WHM, Santen RA Acidic Sites in Sulfated and Metal Promoted $ZrO_2$ Catalysts, Journal of Catalysis 151, 1995, 364-368.
3. Ahmad R, Melsheimer J, Jentoft FC, Schlogl RC, Isomerization of n-butane and of n-pentane in the presence of sulfated zirconia: formation of surface deposits investigated by in situ uv-vis diffuse reflectance spectroscopy, Journal of Catalysis 218, 2003, 365-374.
4. Akkari R, Ghorbel A, Essayem N, Figueras F, Synthesis and characterization of mesoporous silica-supported nano-crystalline sulfated zirconia catalysts prepared by a sol–gel process: Effect of the S/Zr molar ratio, Applied Catalysis A-General 44 328, 2007, 43–51.
5. Aladin I, Xian SB, Zhou W, Desulfurization of FCC gas oil by solvent extraction, photo oxidation, and oxidizing agents, Petroleum Science & Technology 22, 2004, 287–301.
6. Al-Barood A and Stanislaus A, Ultra-deep desulfurization of coker and straight-run gas oils: Effect of lowering feedstock 95% boiling point, Fuel Processing Technology 88, 2007, 309–315.
7. Al-Daous MA and Stein A, Preparation and Catalytic Evaluation of Macroporous Crystalline Sulfated Zirconium Dioxide Templated with Colloidal Crystals, Chemistry of Materials 15, 2003, 2638-2645.
8. Ali MF, Al-Malki A, Ahmed S, Chemical desulfurization of petroleum fractions for ultra-low sulfur fuels, Fuel Processing Technology 90, 2009, 536–544.
9. Ali MF, Al-Malki A, El-Ali B, Martinie G, Siddiqui MN, Deep desulphurization of gasoline and diesel fuels using non-hydrogen consuming techniques, Fuel 85, 2006, 1354–1363.
10. Al-Shahrani F, Xiao T, Llewellyn SA, Barri S, Jiang G, Shi H, Martinie G, Green MLH, Desulfurization of diesel via the $H_2O_2$ oxidation of aromatic sulfides to sulfones using a tungstate catalyst, Applied Catalysis B: Environmental 73, 2007, 311–316.

11. Althues H and Kasel S, Sulfated zirconia nanoparticles synthesized in reverse microemulsions: preparation and catalytic properties, Langmuir 18, 2002, 7428-7435.
12. Amiel S, Monographs on neutron activation methods include: Nondestructive activation analysis, Ed., New York: Elesvier, 1981.
13. Anbia M and Parvin Z, Desulfurization of fuels by means of a nanoporous carbon adsorbent, Chemical Engineering Research and Design 89, 2011, 641-647.
14. Ania CO, Parra JB, Arenillas A, Rubiera F, Bandosz TJ, Pis JA, On the mechanism of reactive adsorption of dibenzothiophene on organic waste derived carbons, Applied Surface Science 253, 2007, 5899–5903.
15. Arata K and Hino H in Proceedings, 9th International congress on catalysis, Calgary, 1988, Philips MJ and Ternan M, Eds, 4, 1988, 1727, Institute of Canada,Ottawa.
16. Arata K and Hino M, Journal of the Chemical Society, Synthesis of solid superacid catalyst with acid strength of $H_0 \leq -16.04$, Journal of Chemical Society, Chemical Communications, 1980, 851-852.
17. Arata K and Hino M, Preparation of superacids by metal oxides and their catalytic action, Materials Chemistry & Physics, 26, 1990, 213-237.
18. Arata K, Hino M, Yamagata N, Bull. Chem. Soc. Jpn. 63, 1990, 244.
19. Arata K, Preparation of superacids by metal oxides for reactions of butanes and pentanes, Applied Catalysis A-General 146, 1996, 3-32.
20. Arata K, Preparation of superacids by metal oxides for reactions of butanes and pentanes, Applied Catalysis A 146, 1996, 3-32.
21. Arata K, Solid Superacids, Advances in Catalysis, 37, 1990, 165.
22. Arata.K and Hino.M, Preparation of superacids by metal oxides and their catalytic action, Materials Chemistry & Physics 26, 1990, 213-237.
23. Ardizzone S and Bassi G, Model representation of the zirconia interface: Effects of the temprature of the oxide preparation, Materials Chemistry and Physics 25, 1990, 417-427.
24. Ardizzone S and Bianchi CL, Acidity, sulphur coverage and XPS analyses of $ZrO_2$-$SO_4^{2-}$ powders by different procedures, Applied Surface Science 152, 1999, 63-69.
25. Ardizzone S and Bianchi CL, Journal of Electroanalytical Chemistry, 465, 1999, 136–141.

26. Ardizzone S, Bianchi CL, Signoretto, Zr(IV) surface chemical state and acid features of sulphated-zirconia samples, Applied Surface Science 136, 1998, 213–220.

27. Arias M, Laurenti D, Geantet C, Vrinat M, Hideyuki I, Yoshimura Y, Gasoline desulfurization by catalytic alkylation over silica-supported heteropolyacids: From model reaction to real feed conversion, Catalysis Today 130, 2008, 190–194.

28. Auto Fuel Policy, Ministry of Petroleum and Natural gas, Government of India, 2003. (http://petroleum.nic.in/autoeng.pdf)

29. Babich IV and Moulijn JA, Science and technology of novel processes for deep desulfurization of oil refinery streams: a review, Fuel 82, 2003, 607–631.

30. Babou F, Coudurier G, Vedrine JC, Acidic properties of sulfated zirconia: An infrared spectroscopic study, Journal of Catalysis 152, 1995, 341-349.

31. Babou.Frederic, Coudurier.G and Jacques.C.Vedrine, Acidic properties of Sulfated Zirconia An infrared spectroscopic study, Journal of Catalysis 152, 1995, 341– 349.

32. Baeza P, Aguila G, Gracia F, Araya P, Desulfurization by adsorption with copper supported on zirconia, Catalysis Communications 9, 2008, 751–755.

33. Barton DG Soled SL, Meitzner GD, Fuentes GA, Iglesia E, Structural and Catalytic Characterization of Solid Acids Based on Zirconia Modified by Tungsten OxideJournal of Catalysis 181, 1999, 57-72.

34. Benjaram MR, Sreekanth PM, Vangala RR, Journal of Molecular Catalysis A: Chemical, 225, 2005, 71.

35. Bensitel M, Saur O, lavalley JC, Mabilon G, Acidity of zirconium oxide and sulfated $ZrO_2$ samples, Material Chemistry and Physics. 17, 1987, 249-258.

36. Bensitel M, Saur O, Lavalley JC, Morrow BA, An infrared study of sulfated zirconia, Materials Chemistry & Physics 19, 1988, 147-156.

37. Bergaoui L, Chaabene SB, Ghorbel A, Lambert JF, Grange P, In situ preparation of zirconium sulfate pillared clay: study of acidic properties, Applied Catalysis A-General 268, 2004, 25–31.

38. Bernal HG and Caero LC, Solvent effects during oxidation-extraction desulfurization process of aromatic sulfur compounds from fuels, International Journal of Chemical Reactor Engineering, 3(A28) (2005) 1-7.

39. Blanchard G, Maunaye M, Martin G, Removal of heavy metals from waters by means of natural zeolites, Water Resources 18 (12), 1984, 1501-1507.

40. Blommel.P.G, Gosling.Ch.D and Wilcher.S.A, US Patent 5, 763, 713, 1998.
41. Bogdan VI, Klimenko TA, Kustov LM., Kazansky VB, Supercritical n-butane isomerization on solid acid catalysts, Applied Catalysis A-General 267, 2004, 175–179.
42. Bond, G. C., Heterogeneous Catalysis, Principles and Applications, 2nd edn. Oxford University Press, Oxford, 1987.
43. BP tests alkylation/fractionation process for sulfur removal, Octane Week 9.10.2000.
44. Breitkopf C, A transient TAP study of the adsorption of $C_4$-hydrocarbons on sulfated zirconias, Journal of Molecular Catalysis A: Chemical 226, 2005, 269-278.
45. Bu J, Loh G, Gwie CG, Dewiyanti S, Tasrif M, Borgna A, Desulfurization of diesel fuels by selective adsorption on activated carbons: Competitive adsorption of polycyclic aromatic sulfur heterocycles and polycyclic aromatic hydrocarbons, Chemical Engineering Journal 166, 2011, 207−217.
46. Caero CL, Hernandez E, Pedraza F, Murrieta F, Oxidative desulfurization of synthetic diesel using supported catalysts Part I: Study of the operation conditions with a vanadium oxide based catalyst, Catalysis Today 107–108, 2005, 564–569.
47. Camblor MA, Corma A, Martinez A, Perez-Pariente J, Valencia S, Influence of the synthesis procedure and chemical composition on the activity of titanium in Ti-beta catalysts, UPV-CSIC, 2008.
48. Campelo JM, Climent MS, Martinas JM, Applied Catalysis 3, 1982, 315.
49. Carbery JB, Twardosski OJ, Eberhart DK, Journal of Water Pollution Control Fredration, 49, 1977, 452.
50. Carrier X, Lukinskas P, Kuba S, Stievano L, Wagner FE, Che M, Knozinger H, The State of the Iron Promoter in Tungstated Zirconia Catalysts, Chem Phys. Chem 5, 2004, 1191-1199.
51. Cedeno L, Hernandez E, Pedraza F, Murrieta F, Oxidative desulfurization of synthetic diesel using supported catalysts: Part I, Study of the operation conditions with a vanadium oxide based catalyst, Catalyst Today 107, 2005, 564-569.
52. Chatry M, Henry M, Livage J, Synthesis of non-aggrigated nanometric crystalline zirconia particles, Material Research Bulletin, 29 (5) 1994, 517-522.
53. Chaturbedi AK, Pathak KC, Singh NV, Journal of Applied Clay Science, 3, 1988, 337.

54. Che M and Tench AJ, Characterization and reactivity of molecular oxygen species on oxide surfaces, Advances in Catalysis 32, 1983, 1-148.

55. Chen CL, Cheng S, Lin HP, Wong ST, Mou CY, Sulfated zirconia catalyst supported on MCM-41 mesoporous molecular sieve, Applied Catalysis A-General 215, 2001, 21-30.

56. Chen ER, Coudurier G, Joly JE, Vedrine JC, Superacid and catalytic properties of sulfated zirconia, Journal of Catalysis 143, 1993, 616-626.

57. Chen FR, Coudurier G, Joly JF, Ve-Adrine JC, Prepr. American Chemical Society, Division of Petroleum 36, 1991, 878.

58. Chen FR, Coudurier G, Joly JF, Verdine JC, Superacid and Catalytic Properties of Sulfated $ZrO_2$, Journal of Catalysis 143, 1993, 616-626.

59. Chen XR, Chen CL, Xu NP, Mou CY, Al- and Ga-promoted $WO_3/ZrO_2$ strong solid acid catalysts and their catalytic activities in *n*-butane isomerization, Catalyst Today 93-5, 2004, 129-134.

60. Chen XR, Chen CL, Xu NP, Mou CY, Han S, Ga-Promoted Tungstated Zirconia Catalyst for n-Butane Isomerization, Catalysis Letters 85, 2003, 177-182.

61. Cheng S, Wong ST, Li T, Lee JF, Mou CY Journal of Catalysis 215, 2003, 45.

62. Chica A, Corma A, Domine ME, Catalytic oxidative desulfurization of diesel fuel on a continuous fixed-bed reactor, Journal of Catalysis 242, 2006, 299–308.

63. Chica A, Strohmaier KG, Iglesia E, Effects of zeolite structure and aluminium content on the thiophene adsorption, desorption, and surface reactions, Applied Catalysis B-Environmantal 60, 2005, 223–232.

64. Chokkaram S, Srinivasan R, Milburn DR, Davis BH, Journal of Colloid ad Interface Science 165, 1994, 160.

65. Chuah GK, Jaenicke S, Cheong SA, Chang KS, The influence of preparation conditions on the surface area of zirconia, Applied Catalysis A: General 145, 1996, 267-284.

66. Clearfield A, Serrette GPD, Khazi-Syed AH, Nature of hydrous $ZrO_2$ and sulfated hydrous $ZrO_2$, Catalyst Today 20, 1994, 295-312.

67. Coelho MA, Alvarez WE, Sikabwe EC, White RL, Resasco DE, Induction of activity and deactivation of Fe, Mn promoted sulfated $ZrO_2$ catalysts, Catalyst Today 28 (4) 1996, 415-429.

68. Coelho MA, Resasco DE, Sikabwe EC, White RL, Modification of the catalytic properties of sulfated zirconia by addition of metal promoters, Catalysis Letters 32 (3-4), 1995, 253-262.

69. Collins F.M, Lucy A.R and Sharp C, Oxidative desulphurization of oils via hydrogen peroxide and heteropolyanion catalysis, Journal of Molecular Catalysis A: Chemical 117, 1997, 397-403.

70. Collins FM, Lucy AR, Sharp C, Oxidative desulphurisation of oils via hydrogen peroxide and heteropolyanion catalysis, Journal of Molecular Catalysis A-Chemicals 117, 1997, 397–403.

71. Comelli A, Catalysis Letters 40, 1996, 125.

72. Comelli A, Platinum on a sulfated zirconia surface: effects and interactions, Catalysis Letters 40, 1996, 67-70.

73. Comelli A, Rahul, Carlos RV, Perera JM, Journal of Catalysis 1994, 96 - 101.

74. Comelli RA, Vera CR, Parera JM, Influence of $ZrO_2$ crystalline structure and sulfate ion concentration on the catalytic activity of $SO_4^{2-}$-$ZrO_2$, Journal of Catalysis 151, 1995, 96-101.

75. Cooper BH, Sogaard-Anderson P, Nielsen-Hannerup P, Production of swedish class I diesel using dual-stage process, in Oballa MC, Shih SS (Ed.) Catalytic hydro processing of petroleum and distillates, Marcel Dekker, New York, 1994, 279–290.

76. Corma A, Fornes V, Juanrajadell MI, NietoJ ML, Influence of preparation conditions on the structure and catalytic properties of $SO_4^{2-}/ZrO_2$ superacid catalysts, Applied Catalysis A General 116, 1994, 151-163.

77. Corma A, Inorganic Solid Acids and Their Use in Acid-Catalyzed Hydrocarbon Reactions For a review on inorganic solid acids, Chemical Review 95 (3), 1995, 559-614.

78. da Silva GLJP, da Silva MLCP, Tatiana C, Preparation and Characterization of Hydrous Zirconium Oxide Formed by Homogeneous Precipitation, Material Research, 5, 2002, 1439-1486.

79. Daia Y, Qia Y, Zhaob D, Zhang H, An oxidative desulfurization method using ultrasound/Fenton's reagent for obtaining low and/or ultra-low sulfur diesel fuel, Fuel Processing Technology , 89, 2008, 927–932.

80. Davis BH, AIChE Spring National Meeting 2000, Atlanta GA, March 5–9, 2000, 68a.

81. Davis BH, Effect of pH on Crystal Phase of $ZrO_2$ Precipitated from Solution and Calcined at 600°C, Journal of American Ceramic Sotiety, 67 (8), 1984, C-1680.

82. Davis BH, Keogh RA, Srinivasan R, Sulfated zirconia as a hydrocarbon conversion catalyst Catalyst Today 20, 1994, 219-256.

83. Davis BH, Zhang C, Miranda R, Platinum-sulfated-zirconia, Infrared study of adsorbed pyridine, Catalysis Letters 29, 1994, 349-359.

84. Dehkordi A. M, Kiaei Z, Sobati M. A, Oxidative desulfurization of simulated light fuel oil and untreated kerosene, Fuel Processing Technology 90, 2009, 435–445.

85. Denkewiez JRP, TenhuisenKS, Adair JH, Hydrothermal crystallization and kinetics of m-$ZrO_2$ and t-$ZrO_2$, Journal of Materials Research 5, 1990, 2698-2705.

86. Devassy BM, Shanbhag G, Lefebvre VF, Boehringer W, Fletcher J, Halligudi SB, Zirconia-supported phosphotungstic acid as catalyst for alkylation of phenol with benzyl alcohol, Journal of Molecular Catalysis A: Chemical 230, 2005, 113–119.

87. Di-shun Z, Zhi-min.S, Fa-tang.L, Hai-dan.S, Optimization of oxidative desulfurization of dibenzothiophene using acidic ionic liquid as catalytic solvent, Journal of Fuel Chemistry and Technology, 37 (2), 2009, 196-212.

88. Ebitani K , Konno H, Tanaka T, Hattori H, Journal of Catalysis 143, 1993, 322.

89. Ebitani K, Konishi J, Horie A, Hattori H, Tanabe K in: Tanabe K, Hattori H, Yamaguchi T, Tanaka T Eds. Acid–Base Catalysis, Kodansha, Tokyo, 1989, 491-498.

90. Ebitani K, Tsuji J, Hattori H, Kita H, Dynamic modification of surface acid properties with hydrogen molecules for $ZrO_2$ oxide promoted by Pt and $SO_4^{2-}$, Journal of Catalysis 135, 1992, 609-614.

91. Ecormier MA, Lee AF, Wilson K, High activity templated mesoporous $SO_4/ZrO_2$/HMS catalysts with controlled acid site density for alpha-pinene isomerisation, Microporous Mesoporous Materials 80, 2005, 301-308.

92. EPA-Gasoline RIA, Regulatory Impact Analysis—Control of Air Pollution from New Motor Vehicles: Tier 2 Motor Vehicle Emissions Standards and Gasoline Sulfur Control Requirements, US Environmental Protection Agency, Air and Radiation, EPA420-R-99-023, December 1999.

93. Fairbridge C, Te M, Ring Z, Oxidation reactivities of dibenzothiophenes in polyoxometalate/$H_2O_2$ and formic acid/$H_2O_2$ systems, Applied Catalysis A-General 219, 2001, 267-274.

94. Farcasiu and Li JQ, Preparation of sulfated zirconia catalysts with improved control of sulfur content: III, Effect of conditions of catalyst synthesis on physical properties and catalytic activity, Applied Catalysis A-General 175, 1998, 1-9.

95. Farcasiu D and Li JQ, Preparation of sulfated zirconia catalysts with improved control of sulfur content, Applied Catalysis A-General 128 (9) 1995, 97-105.

96. Farcasiu D, Li JQ, Cameron S, Preparation of Sulfated Zirconia Catalysts with Improved Control of Sulfur-Content .2. Effect of Sulfur-Content on Physical-Properties and Catalytic Activity Applied Catalysis A-General 154 (1-2) 1997, 173-184.

97. Farcasiu et al., USA Patent 4, 171, 260, Oct.16, 1979.

98. Feigl F, Anger V, Oesper RP, Chromium in Spot Tests in Inorganic Analysis, Inorganic Halogenated Chemistry, 2003, 187.

99. Feng RM, Yang XJ, Ji WJ, Au CT, Hydrothermal synthesis of stable mesoporous $ZrO_2$–$Y_2O_3$ and $CeO_2$–$ZrO_2$–$Y_2O_3$ from simple inorganic salts and CTAB template in aqueous medium, Material Chemistry and Physics 107 (1) 2008, 132–136.

100. Feng-Chau Wu, The crystallization and phase transformation of stabilizer-doped zirconia powder with $H_2SO_4$ additive, Journal of Crystal Growth 96, 1989, 96 - 100.

101. Fiona CM, Woudenberg, Sager WFC, Elshof JE, Henk V, Nanostructures dense $ZrO_2$ thin films from nanoparticles obtained by emulsion precipitation, Journal of American Ceramic Society 87 (8) 2004, 1430–1435.

102. Flora T, Ng T, Horvat H, Applied Catalysis 123, 1995, L197.

103. Fogash KB, Larson RB, Gonzalez MR, Kobe JM, Dumesic JA, Kinetics, and deactivation of sulfated $ZrO_2$ catalyzed for butane isomerization, Journal of Catalysis 163, 1996, 138-145.

104. Fogash KB, Yaluris G, Gonzalez MR, Ouraipryvan P, Ward DR, Kobe I, Dumesic JA, Characterization and selective poisoning of acid sites on sulfated zirconia, Catalysis Letters 32, 3,4, 1995, 241-51.

105. Funamoto T, Nakagawa T, Segawa K, Isomerization of n-butane over sulfated zirconia catalyst under supercritical conditions, Applied Catalysis A-General 80 286, 2005, 79–84.

106. Furimsky E and Massoth FE, Deactivation of hydroprocessing catalysts, Catalysis Today 1999, 52, 381-495.

107. Furimsky E, Yumura M, Erdol and Kohle-Erdgas-Pertochemie vereinigt mit Brennstoff-Chemie Bd. 39, Heft 4, 1986, 163–172.

108. Gao Z, Xia YD, Hua WM, Miao CX, New catalyst of $SO_4^{2-}/Al_2O_3$- $ZrO_2$ for n-butane isomerizationTopics in Catalysis 6 (1-4), 1998, 101-106.

109. Garcia CL and Lercher JA, Adsorption and surface reactions of thiophene on ZSM-Zeolites, Journal of Physical Chemistry 96, 1992, 2669–2675.

110. Garcıa EA, Rueda EH, Rouco AJ, Sulfated zirconia catalysts promoted with Fe and Mn: Mn effect in the Fe dispersion, Applied Catalysis A-General 210, 2001, 363–370.

111. Garcia MAV, Arjona AM, Arean CO, Parra Soto JB, Anales de Quimica 76, 1980, 224.

112. Garin F, Andriamassinoro D, Abdulsamad A, Sommer J, Conversion of butane over the solid superacid $ZrO_2/SO_4^{2-}$ in the presence of hydrogen, Journal of Catalysis 131, 1991, 199-203.

113. Garvie RC, The Occurrence of Metastable Tetragonal Zirconia as a Crystallite Size Effect, Journal of Physical Chemistry 69 (4), 1965, 1238-1243.

114. Gbondo-Tugbawa SS and Driscoll CT, Evaluation of the effects of future controls on sulfur dioxide and nitrogen oxide emissions on the acid–base status of a northern forest ecosystem, Atmospheric Environment 36, 2002, 1631–1643.

115. Ghedini E, Signoretto M, Pinna F, Cerrato G, Morterra C, Studies in Surface Science and Catalysis, Applied Catalysis-B, 67, 2006, 24-30.

116. Gomez H and Cedeno L, Solvent Effects during oxidation-extraction desulfurization

117. Gomez-Bernal H, Cedeno-Caero L, Gutierrez-Alejandre A, Liquid phase oxidation of dibenzothiophene with alumina-supported vanadium oxide catalysts: An alternative to deep desulfurization of diesel, Catalysis Today 142, 2009, 227–233.

118. Gonzalez MR, Fogash KB, Dumesic JA, Promotion of n-butane isomerization activity by hydration of sulfated $ZrO_2$, Journal of Catalysis 160, 1996, 290-298.

119. Gonzalez MR, Fogash KB, Kobe JM, Dumesic J, Promotion of n-butane Isomerization by hydroxyl groups on Sulfated $ZrO_2$, Catalysis Today 33, 1997, 303-312.

120. Gonzalez-Garcıa O and Cedeno-Caero L, V-Mo based catalysts for oxidative desulfurization of diesel fuel, Catalysis Today, 2009.

121. Gore, USA Patent 6, 160, 193, Dec.2, 2000.

122. Grossman MJ, Lee MK, Prince RC, Bernero-Minak V, George GN, Pickering IJ, Deep Desulfurization of Extensively Hydrodesulfurized Middle Distillate Oil by *Rhodococcus* sp. Strain ECRD-1, Applied and Environmental Microbiology, April 2001, 1949-1952.

123. Guo C, Yao S, Cao J, Qian Z, Alkylation of isobutane with butenes over solid superacids, $SO_4^{2-}/ZrO_2$ and $SO_4^{2-}/TiO_2$, Applied Catalysis A-General 107, 1994, 229-238.

124. Hahn A, Ressler T, Jentoft RE, Jentoft FC, The Role of the "Glow Phenomenon" in the Preparation of Sulfated Zirconia Catalysts, Chemical Communications, 2001, 537–538.

125. Haines BL and Carlson CL, Effects of acidic precipitation on trees, In: Adrino DC, Johnson AH, Acidic precipitation: Biological and ecological effects, Advances in Environmental Sciences, 2, 1989, 1– 23.

126. Hammache S and Goodwin JG, Characteristics of Activities on Sulfated $ZrO_2$ for n-Butane Isomerization, Journal of Catalysis 218, 2003, 258.

127. Hattiangadi U, Spoor M, Pal SC, Petrotech Quart 2000, 4, 35.

128. Hattori H, Ebitani K, Konno H, Tanaka T, Journal of Catalysis 143, 1993, 322.

129. Hattori H, Studies in Surface Science and Catalysis 77, 1993, 69.

130. Haw KG, Bakar WAWA, Ali R, Chong JF, Kadir AAA, Catalytic oxidative desulfurization of diesel utilizing hydrogen peroxide and functionalized-activated carbon in a biphasic diesel–acetonitrile system. Fuel Processing Technology 91, 2010, 1105–1112.

131. Haw KG, Bakara WAWA, Ali R, Chong JF, Kadir AAA, Catalytic oxidative desulfurization of diesel utilizing hydrogen peroxide and functionalized-activated carbon in a biphasic diesel–acetonitrile system, Fuel Processing Technology 91, 2010, 1105–1112.

132. Hernandez SP, Fino D, Russo N, High performance sorbents for diesel oil desulfurization, Chemical Engineering Science 2009.

133. Hernandez-Maldonado AJ and Yang R, Journal of Amrican Chemical Society 126, 2004a, 992.

134. Hernandez-Maldonado AJ and Yang RJ, Denitrogenation of Transportation Fuels by Zeolites at Ambient Temperature and Pressure, You have full text access to this content, Angewandte Chemie International Edition, 43, 2004b, 1004-1006.

135. Hernández-Maldonado AJ and Yang RT, Desulfurization of commercial liquid fuels by selective adsorption via π-complexation with Cu-(I)-Y zeolite, Industrial & Enginering Chemistry Research 42, 2003b, 3103-3110.

136. Hernández-Maldonado AJ and Yang RT, Desulfurization of liquid fuels by adsorption via π-complexation with Cu(I)-Y and Ag-Y zeolites, Industrial & Enginering Chemistry Research 42, 2003a, 123-128.

137. Hernandez-Maldonado AJ, Yang FH, Desulfurization of transportation fuels by p-complexation sorbents: Cu(I)-, Ni(II)-, and Zn(II)-zeolites, Applied Catalysis B: Environmental 56, 2005, 111–126.

138. Hertl W, Langmuir 5, 1989, 96.

139. Heuer AH and Ruihle M, in Claussen NC, Riihle M and Heuer AH (Editors), Advances in Ceramics, Am. Ceram. Sot., Columbus, OH, 12, 1984, l-13.

140. Hino M and Arata K, Synthesis of solid superacid catalyst with acid strength of $H_o \leq -16.04$, Journal of the Chemical Society, Chemical Communications 18, 1980, 851-200.

141. Hino M and Arata K Reaction Kinetics, Catalysis Letters 19, 1982, 101.

142. Hino M and Arata K, Catalysis Letters 30, 1995, 25.

143. Hino M and Arata K, Catalysis Letters 34, 1996, 125.

144. Hino M and Arata K, Chemistry Letters 1979b, 1259.

145. Hino M and Arata K, Journal of Chemical Society and Chemical Communications 1979a, 1148.

146. Hino M, Kobayashi S, Arata K, Journal of Amrican Chemical Society 101 (21) 1979c, 6439–6441.

147. Ho et al., USA Patent 5958224, Sept.28, 1999.

148. Ho YS and McKay G, Pseudo-second order model for sorption processes, Process Biochemistry, 34, 1999, 451-465.

149. Holm VCF and Bailey GC, US Patent No. 3032599, 1962.

150. Hosoi T, Shimidzu T, Itoh S, Baba S, Takaoka H, Imai T, Yokoyama N in: Proceedings of the American Chemical Society, Los Angeles, 1988, 562.

151. Hsu CY, Heimbuck CR, Armes CT, Gates BC 3, Chem. Soc. Chemical Communications 1992, 1645.

152. Hua WM, Goeppert A, Sommer J, Journal of Catalysis 197, 2001, 406.

153. Hua WM, Miao XC, Chen JM, Gao Z, Catalysis Letter 37, 1996, 187.

154. Hua WM, Yue YH, Gao Z, Journal of Molecular Catalysis A 170, 2001, 195.

155. Huang D, Wang YJ, Cui YC, Luo GS, Direct synthesis of mesoporous $TiO_2$ and its catalytic performance in DBT oxidative desulfurization, Microporous and Mesoporous Materials 116, 2008, 378–385.

156. Huang J, Zhao J, Wei X, Wang Y, Bu X, Kinetic studies on the sulfidation and regeneration of zinc titanate desulfurization sorbent, Powder Technology 180, 2008, 196–202.

157. Huang YY, McCarthy TJ, Sachlter WMH, Preparation and catalytic testing of mesoporous sulfated zirconium dioxide with partially tetragonal wall structure, Applied Catalysis A 148, 1996, 135-142.

158. Hulea V, Moreau P, The solvent effect in the sulfoxidation of thioethers by hydrogen peroxide using Ti-containing zeolites as catalysts, Journal of Molecular Catalysis A: Chemicals 113, 1996, 499-505.

159. Iglesia E and Biscardi JA, Isotopic tracer studies of propane reactions on H-ZSM5 zeolite, Journal of Physical Chemistry-B 102, 1998, 9284–9289.

160. Iglesia E, Soled SL, Kramer GL, Journal of Catalysis, 144 (1) 1993, 238.

161. Irvine RL and Varraveto DM, Petro Tech Quart 1999, 3, 37.

162. Irvine RL, Benson BA, Varraveto DM, Frye RA NPRA 1999, Annual Meeting, AM-99-42, San Antonio, Texas, March 21–23, 1999.

163. Irvine RL, US Patent 5, 730, 860, 1998.

164. Ishida T, Yamaguchi T, Tanabe K, Chemistry Letters, 1988, 1869.

165. Ishihara A, Wang D, Dumeignil F, Amano H, Qian EW, Kabe T Oxidative desulfurization and denitrogenation of a light gas oil using an oxidation/adsorption continuos flow process, Applied Catalysis A-General 279, 2005, 279-287.

166. Ismagilov ZR, Yashnik SA, Startsev AN, Boronin AI, Stadnichenko AI, Kriventsov VV, Kasztelan S, Guillaume D, Makkee M, Moulijn JA, Deep desulphurization of diesel fuels on bifunctional monolithic nanostructured Pt-zeolite catalysts, Catalysis Today 44 (3-4), 2009, 235-250.

167. Jatia A, Chang C, Macleod JD, Okubo T, Davis ME, Catalysis Letters 25, 1994, 21.

168. Jentoft FC, Hahn A, Krohnert J, Lorenz, Gisela, Jentoft RE, Ressler T, Wild U, Schlogl R, Hassner C, Kohler K, Incorporation of manganese and iron into the zirconia lattice in promoted sulfated zirconia catalysts, Journal of Catalysis 224 (1) 2004, 124-137.

169. Jeyagowry T, Sampanthar, Xiao H, Dou J, Nah TY, Rong X, Kwan W, A novel oxidative desulfurization process to remove refractory sulfur compounds from diesel fuel, Applied Catalysis B: Environmental 63, 2006, 85–93.

170. Jiang X, Li H, Zhu W, He L, Shu H, Lu J, Deep desulfurization of fuels catalyzed by surfactant-type decatungstates using $H_2O_2$ as oxidant, Fuel 88, 2009, 431–436.

171. Jiang ZX, Liu Y, Sun X, Tian FP, Sun FX, Liang CH, You WS, Han CR, Li C, Activated carbons chemically modified by concentrated $H_2SO_4$ for the adsorption of the pollutants from wastewater and the dibenzothiophene from fuel oils, Langmuir 19, 2003, 731–736.

172. Jin C, Li G, Wang X, Wang Y, Zhao L, Sun D, A titanium containing micro/mesoporous composite and its catalytic performance in oxidative desulfurization, Microporous and Mesoporous Materials 111, 2008, 236-242.

173. Jin T, Yamaguchi T, Tanabe K, Journal of Physical Chemistry, 90, 1986, 4794.

174. Jolly SC, Meat Extract in Official Standardized and Recommendation Methods of Analysis: The Society for Analytical Chemistry, 1963, 130.

175. Jones CW and Clark JH, Application of Hydrogen Peroxide and Derivatives, 1st ed., Royal Society of Chemistry, Cambridge, 1999, 21-30.

176. Kaczorowska K, Kolarska Z, Mitka K, Kowalski P, Oxidation of sulfides to sulfoxides: Part II, Oxidation by hydrogen peroxide, Tetrahedron 61 (35) 2005, 8315-8327.

177. Kaya C, He JY, Gu X, Butler EG, Nano-structured ceramic powders by hydrothermal synthesis and their applications, Microporous Mesoporous Mater. 54, 2002, 37–49.

178. Kayo A, Yamaguchi T, Tanabe K, ibid. 83, 1983, 99.

179. Keogh RA, Sparks D, Hu J, Wender I, Tierney JW, Wang W, Davis BH, Energy & Fuels 8 (3), 1994, 755–762.

180. Keogh RA, Srinivasan R, Davis BH, Journal of Catalysis, 151, 1995, 292.

181. Khodakov A, Yang J, Su S, Iglesia E, Bell AT, Journal of Catalysis 177, 1998, 343.

182. Kim JH, Ma X, Zhou A, Song C, Ultra-deep desulfurization and denitrogenation of diesel fuel by selective adsorption over three different adsorbents: A study on adsorptive selectivity and mechanism, Catalysis Today 111, 2006, 74–83.

183. Kim SY, Goodwin JG, Farcasiu.D, The effects of reaction conditions and catalyst deactivation on the mechanism of n-butane isomerization on sulfated zirconia, Applied Catalysis A-General 207, 2001, 281–286.

184. King DL, Faz C, Flynn T, Desulfurization of gasoline feedstocks for application in fuel reforming, SAE paper 2000-01-0002, Detroit, Soc. Automot. Eng., 2000, 9–13.

185. Kobe JM, Gonzalez MR, Fogash KB, Dumesic JA, Effects of Water on the performance of sulfated zirconia catalysts for butane isomerization, Journal of Catalysis 164, 1996, 459–466.

186. Kobe JM, Gonzalez RD, Fogash KB, Dumesic JA, Effects of water on the performance of sulfated $ZrO_2$, catalysts for butane isomerization, Journal of Catalysis 164, 1996, 459-468.

187. Kocal et al., USA Patent 6, 277, 271, Aug. 21, 2001.

188. Komarnisky LA, DVM, Christopherson RJ, Basu TK, Sulfur: Its Clinical and Toxicologic Aspects, Nutrition, 19, 2003, 54–61.

189. Kong L, Li G, Wang W, Catalyst Today 93, 2004, 341.

190. Kong L, Li G, Wang X, Mild oxidation of thiophene over TS-1/$H_2O_2$, Catalysis Today 93–95, 2004, 341–345.

191. Kong LY, Li G, Wang XS, Kinetics and mechanism of liquid-phase oxidation of thiophene over TS-1 using $H_2O_2$ under mild conditions, Catalysis Letters, 92, 2004, 163- 167.

192. Koranyi TI, Jentys A, Vinek H, Adsorption and reaction of thiophene over nickel and cobalt containing zeolites, Study Surface Science Catalysis 94, 1995, 582–589.

193. Kropp KG and Fedorak PM, A review of the occurrence, toxicity, and biodegradation of condensed thiophenes found in petroleum, Canadian Journal of Microbiology 44, 1998, 605–22.

194. Kuba S, Heydorn PC, Grasselli RK, Gates BC, Che M, Knozinger H, Phys. Chem. Chem. Phys. 3, 2001, 146.

195. Kumagai S, Ishizawa H, Toida Y, Influence of solvent type on dibenzothiophene adsorption onto activated carbon fiber and granular coconut-shell activated carbon, Fuel 89, 2010, 365-371.

196. Kumagai S, Shimizu Y, Toida Y, Enda Y, Removal of dibenzothiophenes in kerosene by adsorption on rice husk activated carbon, Fuel 88, 2009, 1975–1982.

197. Kumar S, Srivastava V. C, Badoni R. P, Oxidative desulfurization by chromium promoted sulfated zirconia, Fuel Processing Technology 93, 2012, 18–25.

198. Kumbhar PS, Yadav VM, Yadav GD in: Leyden DE, Collins WT (Eds.) Morterra C, Pinna F, Signoretto N, Strukul G, Cerrato G, Catalysis Letters 26, 1994, 339.

199. Kumbhar PS, Yadav VM, Yadav GD, in: Leyden DE, Collins WT (Eds.), chemically modified oxide surfaces, Gordon and Breach, 1989, 81.

200. Kustov LM, Kazansky VB, Figueras F, Tichit D, Investigation of the acidic properties of $ZrO_2$ modified by $SO_4^{2-}$ anions, Journal of Catalysis 150, 1994, 96 -101.

201. Lambert J and Muir TA, Acidimetery and Alkalimetery, in Practical Chemistry, 2ed ed., 1965, 273.

202. Landau MV, Titelman L, Vradman L, Wilson P, Chemical Communications, 2003, 594.

203. Lanju C, Shaohui G, Dishun Z, Oxidative desulfurization of simulated gasoline over metal oxide-loaded molecular sieve, Chinese Journal of Chemical Engineering, 15(4) 2007, 520-523.

204. Larsen G, Lotero E, Nabity M, Petkovic LM, Shobe DS, Journal of Catalysis 164, 1996, 246.

205. Lee D, Ko EY, Lee HC, Kim S, Park ED, Adsorptive removal of tetrahydrothiophene (THT) and tert-butylmercaptan (TBM) using Na-Y and AgNa-Y zeolites for fuel cell applications, Applied Catalysis A: General 334, 2008, 129–136.

206. Li X, Nagaoka K, Simon LJ, Lercher JA, Olindo R, Interaction between sulfated zirconia and alkanes: prerequisites for active sites-formation and stability of reaction intermediates, Journal of Catalysis 232 (2) 2005, 456-466.

207. Li B and Gonzalez RD, Industrial & Enginering Chemistry Research 35, 1996, 3141.

208. Li B, Ma W, Liu J, Han C, Zuo S, Li X, Synthesis of the well-ordered hexagonal mesoporous silicate incorporated with phosphotungstic acid through a novel method and its catalytic performance on the oxidative desulfurization reaction, Catalysis Communications 13, 2011, 101-105.

209. Li BH and Gonzalez RD, TGA/FT-IR studies of the deactivation of sulfated zirconia catalysts, Applied Catalysis A-General 165 (1–2) 1997, 291–300.

210. Li C and Stair PC, Catalysis Letters 36, 1996, 119.

211. Li X, Wang A, Egorova M, Prins R, Kinetics of the HDS of 4,6-dimethyl dibenzothiophene and its hydrogenated intermediates over sulfided Mo and NiMo on $\gamma$ -$Al_2O_3$, Journal of Catalysis 250, 2007, 283–293.

212. Li X, Wang A, Wang Y, Cehn Y, liu Y, hu Y, Hydrodesulfurization of dibenzothiophene over Ni-Mo sulfides supported by proton-exchanged siliceous MCM-41, Catalysis Letters, 84, 2002, 12-21.

213. Li Y, Yang FH, Qi G, Yang RT, Effects of oxygenates and moisture on adsorptive desulfurization of liquid fuels with Cu (I) Y zeolite , Catalysis Today 116, 2006, 512–518.

214. Li.X, Nagaoka.K, Lercher JA, Krohnert J, Klaeden K, Jentoft FC, Breitkopf C, Papp H, XXXVII. Jahrestreffen Deutscher Katalytiker in Verbindung mit dem Fachtreffen Reaktionstechnik 17–19, Marz 2004, Weimar.

215. Lin.C.H and Hsu.C.Y, Chem. Soc. Chemical Communications 1992, 1479.

216. Liotta FJ and Han Y, NPRA, AM-03-23, Annual Meeting, March 23-25, 2003.

217. Liu D, Gui J, Sun Z, Adsorption structures of heterocyclic nitrogen compounds over Cu (I)Y zeolite: A first principle study on mechanism of the denitrogenation and the effect of nitrogen compounds on adsorptive desulfurization, Journal of Molecular Catalysis A: Chemical 291, 2008, 17–21.

218. Liu H, Feng L, Zhang X, Xue Q, ESR characterization of $ZrO_2$ nano powder, Journal of Physical Chemistry 99, 1995, 332-334.

219. Liu H, Lei GD, Sachtler WMH, Alkane isomerization over solid acid catalysts effect of non-specific olefine addition, Applied Catalysis A-General 137, 1996a, 167-172.

220. Liu H, Lei GD, Sachtler WMH, Pentane and butane isomerization over Pt-promoted sulfated Cctalysts, Applied Catalysis A-General 146, 1996b, 65-69

221. Lohitharn N, Goodwin JG, n-Butane isomerization on sulfated zirconia: How olefins affect surface intermediate concentration, Journal of Catalysis 245, 2007, 198-204.

222. Lu H, Gao J, Jiang Z, Jing F, Yang Y, Wang G, Li C, Ultra-deep desulfurization of diesel by selective oxidation with $[C_{18}H_{37}N(CH_3)_3]_4$-$[H_2NaPW_{10}O_{36}]$ catalyst assembled in emulsion droplets, Journal of Catalysis 239, 2006, 369–375.

223. Lu H, Gao J, Jiang Z, Jing F, Yang Y, Wang G, Li C, Ultra-deep desulfurization of diesel by selective oxidation with $[C_{18}H_{37}N(CH_3)_3]_4[H_2NaPW_{10}O_{36}]$ catalyst assembled in emulsion droplets, Journal of Catalysis 239, 2006, 369–375.

224. Lukinskas P, Kuba S, Spliethoff B, Grasselli RK, Tesche B, Knozinger H, Topics in Catalysis 23, 2003

225. Lunsford JH, Sang H, Campbell Sh M, Liang Ch-M, Anthony RG, Catalysis Letter 27, 1994, 305.

226. Luzgin MV, Arzumanov SS, Shmachkova VP, Kotsarenko NS, Rogov VA, Stefano AG, n-Butane conversion on sulfated zirconia: the mechanism of isomerization and $^{13}C$-label scrambling as studied by in situ $^{13}C$MAS NMR and ex situ GC-MS, Journal of Catalysis 220, 2003, 233–239.

227. Ma X, Sprague M, Sun Lu, Song C, Deep desulfurization of liquid hydrocarbons by selective adsorption for fuel cell applications, American Chemical Society. Division of Petroleum Chemistry Prepration, 47 (1) 2002, 48-49.

228. Ma XL, Sprague M, Song CS, Deep desulfurization of gasoline by selective adsorption over nickel-based adsorbent for fuel cell applications, Industrial and Enginering Chemistry Research 44, 2005, 5768–5775.
229. Ma XL, Sun L, Song CS, A new approach to deep desulfurization of gasoline, diesel fuel and jet fuel by selective adsorption for ultra-clean fuels and for fuel cell applications, Catalyst Today 77, 2002, 107–116.
230. March J, Advanced Organic Chemistry, John Wiley & Sons, New York, 1985.
231. McIntosh DJ and Kydd RA, Microporous Mesoporous Materials 37, 2000, 281.
232. McKinley SG and Angelici RJ, Chemical Communications 20, 2003, 2620.
233. Mei H, Mei BW, Yen TF, Fuel 82, 2003, 405.
234. Miao CX, Hua WM, Chen JM, Gao Z, Catalysis Letters 39, 1996, 406.
235. Miao CX, Hua WM, Gao Z, Chinese Journal of Catalysis 18, 1997, 13.
236. Mikhail S, Zaki T, Khalil L, Desulfurization by an economically adsorption technique, Applied Catalysis A: General 227, 2002, 265–278.
237. Miller RB, Macris A, Gentry AR, Petr Tech Quart 2001, 2, 69.
238. Mishra HK and Parida KM, Studies on sulphated zirconia: synthesis, physico-chemical characterization and n-butane isomerisation activity, Applied Catalysis A-General 224, 2002, 179–189.
239. Mishra HK and Parida KM, Studies on sulphated zirconia: synthesis, physico-chemical characterisation and n-butane isomerisation activity, Applied Catalysis A-General 224, 2002, 179–189.
240. Mishra HK, Dalai AK, Parida KM, Bej SK, Butane isomerization over persulfated zirconia, Applied Catalysis A-General 217, 2001, 263–273.
241. Mishra HK, Dalai AK, Parida KM, Bej SK, Butane isomerization over persulfated zirconia, Applied Catalysis A-General 217, 2001, 263–273.
242. Mishra HK, Dalai AK, Parida KM, Studies on the effects of $CO_2$ and CO on n-butane isomerisation activity over sulfated zirconia, Journal of Molecular Catalysis A: Chemical 185, 2002, 237–248
243. Mishra MK, Tyagi B, Jasra RV, Effect of synthetic parameters on structural, textural, and catalytic properties of nanocrystalline sulfated zirconia prepared by sol-gel technique, Industrial and Enginering Chemistry Research 42, 2003, 5727-5736.
244. Moreau P, Hulea V, Gomez S, Brunel D , Di Renzo F, Oxidation of sulfoxides to sulfones by hydrogen peroxide over Ti-containing zeolite, Applied Catalysis A: General 155, 1997, 253-263.

245. Moreno JA and Poncelet G, Isomerization of n-butane over sulfated Al- and Ga-promoted zirconium oxide catalysts: Influence of promoter and preparation method, Journal of Catalysis 203, 2001, 453-465.

246. Morterra C and Marchese L in Tanabe K, Hattori H, Yamaguchi T and Tanaka T Eds., Acid-Base Catalysts, Kodansha, Tokyo, 1989 a, 363.

247. Morterra C and Marchese L, in Tanabe K, Hattori H, Yamaguchi T and Tanaka T Eds., Acid-Base Catalysts, Kodansha, Tokyo, 1989 b, 197.

248. Morterra C, Cerrato G, Di Ciero S, Signoretto M, Pinna F, Strukul G, Platinum Promoted and unpromoted sulfated $ZrO_2$ catalysts prepared by a one step aerogel procedure:1, physico-chemical and morphological characterization, Journal of Catalysis. 165, 1997, 172-183

249. Morterra C, Cerrato G, Emanuel C, Bolis V, Journal of Catalysis 142, 1993, 349.

250. Morterra C, Cerrato G, Emanuel C, Bolis V, On the surface acidity of some sulfate-doped $ZrO_2$ catalysts, Journal of Catalysis 142, 1993, 349-367.

251. Morterra C, Cerrato G, Pinna F, Signoretto M , Brosted acidity of a superacid sulfate-doped $ZrO_2$ system, Journal of Physical Chemistry, 98, 1994, 12373-12381.

252. Morterra C, Cerrato G, Pinna F, Signoretto M, Strukul G, On the Acid-catalyzed isomerization of light paraffins over a $ZrO_2/SO_4^{2-}$ system: the effect of hydration, Journal of Catalysis 149, 1994, 181-188.

253. Morterra C, Giamello E, Orio L, Volante M, Formation and reactivity of zirconium (3+) centers at the surface of vacuum-activated monoclinic zirconia, Journal of Physical Chemistry 94, 1990, 3111-3116.

254. Murata S, Murata K, Kidena K, Nomura M, Energy & Fuels 18, 2004, 116.

255. Murzin D and Salmi T, Mechanism of catalytic reactions and characterization of catalysts, Catalytic Kinetics, Table 2.1, P 45.

256. Muzica M, Sertic-Biondaa K, Gomzia Z, Podolskib S, Telenb S, Study of diesel fuel desulfurization by adsorption, chemical engineering research and design 88, 2010, 487-495.

257. Nakano Y, Lizuka T, Hattori H, Tanabe K, Surface properties of zirconium oxide and its catalytic activity for isomerization of 1-butene, Journal of Catalysis 57, 1979, 1-10.

258. Nascimento P, Akratopoulou C, Oszagyan M, Coudurier G, Travers C, Joly JF, Vedrine JC, Study Surface Science Catalysis 75, 1993, 1197.

259. Nava R, Ortega RA, Alonso G, Ornelas C, Pawelec B, Fierro JLG, CoMo/Ti-SBA-15 catalysts for dibenzothiophene desulfurization, Catalysis Today 127, 2007, 70–84.

260. Nemeth L, Bare SR, Rathbun W, Gatter M, Low J, Oxidative desulfurization of sulfur compounds: Oxidation of thiophene and derivatives with hydrogen peroxide using Ti-Beta catalyst, UOP LLC, 2008.

261. Ngamcharussrivichai C, Chatratananon C, Nuntang S, Prasassarakich P, Adsorptive removal of thiophene and benzothiophene over zeolites from Mae Moh coal fly ash, Fuel 87, 2008, 2347–2351.

262. Niwa M, Habuta Y, Okumura K, Katada N, Solid acidity of meta oxide monolayer and its role in catalytic reactions, Catalyst Today 87, 2003, 213-220.

263. Nonaka OS, Takashima T, Qian WH, Gakkaisi S, Journal of the Japan Petroleum Institute 42, 1999, 315.

264. Okamoto Y, Kubota T, Ohto Y, Nasu S, Metal oxide support interactions in $Fe/ZrO_2$, catalysts, Journal of Physical Chemistry B 104, 2000, 8462-8470.

265. Olindo R, Pinna F, Strukul G, Canton P, Riello P, Cerrato G, Meligrana G, Morterra C, $Al_2O_3$ Promoted sulfated $ZrO_2$ catalysts for the isomerization of n-Butane, Study Surface Sciences Catalysis130, 2000, 2375-2380.

266. Otsuki S, Nonaka T, Takashima N, Qian W, Ishihara A, Imai T, Kabe T, Oxidative desulfurization of light gas oil and vacuum gas oil by oxidation and solvent extraction, Energy and Fuels 14, 2000, 1232–1239.

267. Oviedo A, Torres-Nieto J, Arévalo A, Garcia JJ, Deoxydesulfurization of sulfones derived from dibenzothiophene using nickel compounds, Journal of Molecular Catalysis A: Chemical 293, 2008, 65–71.

268. Parera JM, Promotion of zirconia acidity by addition of sulfate ion, Catalyst Today 15, 1992, 481-490.

269. Park JG, Ko CH, Yi KB, Park JH, Han SS, Cho SH, Kim JN, Reactive adsorption of sulfur compounds in diesel on nickel supported on mesoporous silica, Applied Catalysis B: Environmental 81, 2008, 244–250

270. Paukshtis EA, Kotsarenko NS, Shmachkova VP, Interaction of hydrogen and *n*-pentane with sulfated zirconia, Catalysis Letters 69, 2000, 189–193.

271. Platero EE and Mentruit MP, IR characterization of sulfated zirconia derived from zirconium sulphate, Catalysis Letters 30, 1995, 31-39.

272. process of aromatic sulfur compounds from fuels, International Journal of Chemical Reactor Engineering, 3 (A28) 2005, 1-11.

273. Qi R, Wang Y, Chen J, Li J, Zhu S, Removing thiophenes from *n*-octane using PDMS–AgY zeolite mixed matrix membranes, Journal of Membrane Science 295, 2007, 114–120.

274. Qin W, Xiao-yi L, Rui Z, Chao-jun L, Xiao-jun L, Wen-ming Q, Liang Z , Li-cheng L, Preparation of polystyrene-based activated carbonspheres and their adsorption of dibenzothiophene, New Carbon Materials 24 (1) 2009.

275. Radojevic M and Baskin VN, Practical Environmental Analysis, RSC Publishing, 2006, 2ed Ed., 63.

276. Ramırez-Verduzco LF, Torres-Garcıa E, Gomez-Quintana R, Gonzalez-Pena V, Murrieta-Guevara F, Desulfurization of diesel by oxidation/extraction scheme: influence of the extraction solvent, Catalysis Today 98, 2004, 289–294.

277. Rang H, Kann J, Oja V, Advances in desulfurization research of liquid fuel, Oil Shale, 23 (2) 2006, 164–176.

278. Rappas AS, Unipure Corporation, US Patents US 6, 402, 940; US 6, 406, 616, Wachs WO 03/051798.

279. Ratnasamy P, Srinivas D, Kn ozinger H, Active Sites, Reactive intermediates in titanium silicate molecular sieves, Advance Catalysis 48, 2004, 1−169.

280. Reddy BM, Sreekanth PM, Reddy VR, Modified zirconia solid acid catalysts for organic synthesis and transformations, Journal of Molecular Catalysis A: Chemical 225, 2005, 71–78.

281. Reimann C and Bredow T, Adsorption of nitrogen and ammonia at zirconia surfaces, Journal of Molecular Structure: Theochem, 2009, 89–99.

282. Reut S and Prakash A, Evaluation of sorbents for thiophene removal from liquid hydrocarbons, Fuel Processing Technology 87, 2006, 217 – 222.

283. Rezaei M, Alavi SM, Sahebdelfar S, Yan ZF, Tetragonal nanocrystalline zirconia powder with high surface area and mesoporous structure, Powder Technology 168, 2006, 59–63.

284. Richardeau D, Joly G, Canaff C, Magnoux P, Guisnet M, Thomas M, Nicolaos A, Adsorption and reaction over HFAU zeolites of thiophene in liquid hydrocarbon solutions, Applied Catalysis A-General 263, 2004, 49–61.

285. Riemer T, Spielbaker D, Hunger M, Mekhemer CAH, Knozinger H J. Chem. Soc., Chemical Communications 1994, 1181.

286. Rijnten HT in Linsen BC (Editor), Physical Chemistry and Aspects of Adsorbents and Catalysts, Academic Press, New York, 1970, 315-372.

287. Robert AK and Burtron HD, Hydroconversion of *n*-hexadecane with Pt-promoted monoclinic and/or tetragonal sulfated zirconia catalysts, Catalysis Letters 57, 1999, 33–35.

288. Roger A, Sheldon RA, Dakka J, Heterogeneous catalytic oxidations in the manufacture of fine chemicals, Catalysis Today 19 (2) 1994, 215−245.

289. Salem ABSH and Hamid HS, Naphtha desulfurization by adsorption Industrial & Engineering Chemistry Research, 1994, 33, 336-340.

290. Salem ABSH and Hamid HS, Removal of Sulfur Compounds from Naphtha Solutions Using Solid Adsorbents, Chemical Engineering Technology 1997, 20, 342.

291. Salem.A.S and Hamid.H.S, Chemical Engineering Technology 20, 1997, 342.

292. Samokhvalova A, Duinb EC, NairaS, Tatarchuka BJ, Adsorption and desorption of dibenzothiophene on Ag-titania studied by the complementary temperature-programmed XPS and ESR, Applied Surface Science 257, 2011, 3226–3232.

293. Sampanthar JT, Rong X, Dautzenberg FM, PCT Patent Application PCT/SG2004/000160.

294. Sano Y, Choi KH, Korai Y, Mochida I, Adsorptive removal of sulfur and nitrogen species from straight run gas oil over activated carbons for its deep hydrodesulfurization, Applied Catalysis B: Environmental 49, 2004, 219–225.

295. Sarzanini C, Sacchero G, Pinna F, Signoretto M, Cerrato G, Morterra C, Amount and nature of sulfates at the surface of sulfate-doped zirconia catalysts, Journal of Materials Chemistry, 5, 1995, 353.

296. Saur O, Bensitel M, Mohammed AB, LavaIley JC, Tripp CP, Morrow BA, Journal of Catalysis, 99, 1986, 104.

297. Savage DW, Kaul BK, Dupre GD, O'Bara JT, Wales WE, Ho TC, US Patent 5, 454, 933, 1995.

298. Sayari A and Dicko A, The State of Platinum in Pt on Sulfated Zirconia Superacid Catalysts, Journal of Catalysis 145, 1994, 561-564.

299. Sayari A, Dicko A, Song X, Adnot A, Characterization of platinum on sulfated zirconia catalysts by temperature programmed reduction, Journal of Catalysis 150, 1994, 254-261.

300. Scheithauer M, Jentoft RE, Gates BC, Knozinger H, n-Pentane isomerization catalyzed by Fe- and Mn-containing tungstated zirconia characterized by raman spectroscopy, Journal of Catalysis 191, 2000, 271-274.

301. Schulz H, Bohringer W, Waller P, Ousmanov F, Gas oil deep hydrodesulfurization, refractory compounds and retarded kinetics, Catalaysis Today 49, 1999, 87–97.

302. Scott GM and Robert JA, Chemical Communications, 2003, 2620.

303. Scott WW, Standard Methods of Chemical Analysis: A Mannul of Analytical Methods and general reference for the analytical chemist and for advanced students, Princeton, New Jersey, 2, 1959a, 2194-2207.

304. Scott WW, Standard Methods of Chemical Analysis: A Manual of Analytical Methods and general reference for the analytical chemist and for advanced students, Princeton, New Jersey, Vol.2, 1959b, 5109-5114.

305. Scurrel MS, Applied Catalysis A: General 34, 1987, 109.

306. Selvavathi V, Chidambaram V, Meenakshisundaram V, Sairam B, Sivasankar B, Adsorptive desulfurization of diesel on activated carbon and nickel supported systems, Catalysis Today 141, 2009, 99–102.

307. Semmer V, Batamack P, Doremieux-Morin C, Vincent R, Fraissard J, The acids strength of sulfated zirconia measured by two $^{1}H$ NMR techniques in the presence of water: 4 K broad-line and 300 K high resolution MAS, Journal of Catalysis 161, 1996, 186–193.

308. Sentorun-Shalaby C, Saha SK, Ma X, Song C, Mesoporous-molecular-sieve-supported nickel sorbents for adsorptive desulfurization of commercial ultra-low-sulfur diesel fuel, Applied CatalysisB:Environmental 101 (3-4) 2011, 718-726.

309. Seredych M, Lison J, Jans U, Bandosz TJ, Textural and chemical factors affecting adsorption capacity of activated carbon in highly efficient desulfurization of diesel fuel, Carbon 47, 2009, 2491-2500.

310. Shan G, Liu H, Xing J, Zhang G, Wang K, Separation of polycyclic aromatic compounds from model gasoline by magnetic alumina sorbent based on π–complexation Industrial and Enginering Chemistry Research 43, 2004, 758–761.

311. Sharma LR, Kalia KC, Puri BR, The d-block elements-General characteristic, Principles of Inorganic Chemistry , Vishal Publications, 2001, 742-747.

312. Sharma LR, Kalia KC, Puri BR, The d-block elements-General characteristic, Principles of Inorganic Chemistry Principles of Inorganic Chemistry, Vishal Publications, 2001, 269-270.

313. Sheldon RA, Arends IWCE, Lempers HEB, Liquid phase oxidation at metal ions and complexes in constrained environments, Catalysis Today 41 (4) 1998, 387−407.

314. Shennan JL, Microbial attack on sulphur-containing hydrocarbons: implications for the biodesulphurisation of oils and coals, Journal of Chem Technol Biotechnol, 67, 1996**,** 109–123.

315. Shimizu K, Kounami N, Wada H, Shishido T, Hattori H, Isomerization of n-butane by sulfated zirconia: the effect of calcination temperature and characterization of its surface acidity, Catalysis Letters 54, 1998, 153-158.

316. Shiraishi Y and Hirai T, Desulfurization of vacuum gas oil based on chemical oxidation followed by liquid-liquid extraction, Energy & Fuels, 18, 2004, 37-40.

317. Shiraishi Y, Hirai T, Komasawa I, A Deep Desulfurization process for light oil by photochemical reaction in an organic two-phase liquid-liquid extraction system, Industrial and Engineeringg Chemistry Research, 37, 1998, 203-211.

318. Shiraishi Y, Hirai T, Komasawa I, Photochemical desulfurization and denitrogenation process for vacuum gas oil using an organic two-phase extraction system, Industrial and Engineeringg Chemistry Research 2001, 40, 293-303.

319. Shiraishi Y, Taki Y, Hirai T, Komasawa I, Visible light-induced deep desulfurization process for light oils by photochemical electron-transfer oxidation in an Organic Two-Phase Extraction System, Industrial and Engineering Chemistry Research 1999a, 38, 3310-3318.

320. Shiraishi Y, Taki Y, Hirai T, Komasawa I, Visible light-induced deep desulfurization process for catalytic-cracked gasoline using an organic two-phase extraction system, Industrial and Engineering Chemistry Research 1999b, 38, 4538-4544.

321. Shiraishi.Y, Tachibana K, Hirai T, Komasawa I, Desulfurization and denitrogenation process for light oils based on chemical oxidation followed by liquid-liquid extraction, Industrial and Engineering Chemistry Research, 41, 2002, 3662-4375.

322. Signoretto M, Breda A, Somma F, Pinna F, Cruciani G, Mesoporous sulphated zirconia by liquid-crystal templating method, Microporous Mesoporous Materials 91, 2006, 23-32.

323. Signoretto M, Pinna F, Strukul G, Chies P, Cerrato G, Di Ciero S, Morterra C, Pt-Promoted and Unpromoted Sulfated zirconia Catalysts Prepared by a One-Step Aerogel Procedure, Journal of Catalysis 167, 1997, 522.

324. Sohn JR and Jang HJ, Characterization of $ZrO_2$-$SiO_2$ unmodified or modified with $H_2SO_4$ and acid catalysis, Journal of Molecular Catalysis, 64, 1991, 349-360.

325. Sohn JR and Kim HW, Catalytic and surface properties of $ZrO_2$ modified with sulfur compounds, Journal of Molecular Catalysis 52, 1989, 361-374.

326. Sohn JR, Lee SH, Lim JS, New solid superacid catalyst prepared by doping $ZrO_2$ with Ce and modifying with sulfate and its catalytic activity for acid catalysis, Catalysis Today 116, 2006, 143–150

327. Soleimani M, Bassi A, Margaritis A, Biodesulfurization of refractory organic sulfur compounds in fossil fuels, Biotechnology Advances 25, 2007, 570–596.

328. Song C and Ma X, New design approaches to ultra-clean diesel fuels by deep desulfurization and deep dearomatization, Applied Catalysis B: Environmental 41, 2003, 207-238.

329. Song C, An overview of new approaches to deep desulfurization for ultra-clean gasoline, diesel Fuel and jet Fuel, Catalysis Today 86, 2003, 211–263.

330. Song C, Catalytic Fuel processing for Fuel cell applications. Challenges and opportunities, Am. Chem. Soc. Div. Fuel Chem. Prepr. 46 (1) 2001, 8–13.

331. Song C, Hsu S, Mochida I (Eds.) Chemistry of Diesel Fuels, Taylor & Francis, New York, 2000a.

332. Song C, Keynote: new approaches to deep desulfurization for ultra-clean gasoline and diesel Fuels: an overview, Am. Chem. Soc., Div. Fuel Chem. Prepr. 47, 2002, 438-442.

333. Song SC and Ma XL, New design approaches to ultra-clean diesel fuels by deep desulfurization and deep dearomatization, Applied Catalysis B: Environmental, 41, 2003b, 207-212.

334. Song SX and Kydd RA, Activation of sulfated zirconia catalysts Effect of water content on their activity in *n*-butane isomerization, Journal of Chemical Society Faraday Trans.94, 1998, 1333-1338.

335. Song SX and Kydd RA, The effect of pretreatment procedures on the activities of Fe- and Mn-promoted sulfated zirconia catalysts, Catalysis Letters 51, 1998, 95–100.

336. Song SX, Pilko M, Kydd RA, Catalysis Letters, 55, 1998a, 97.

337. Song X and Sayari A, Chemtech, 1995, 27.

338. Song XM and Sayari A, Sulfated zirconia-based strong solid-acid catalysts, Catalysis Reviews Science & Engineering 38 (3) 1996, 329–412.

339. Spielbauer D, Mekhemer GAH, Bosch E, Knozinger H, *n*-butane isomerization on sulfated zirconia. Deactivation and regeneration as studied by Raman, uv-vis diffuse reflectance and ESR spectroscopy, Catalysis Letters 36, 1996, 59-68.

340. Srinivasan R and Davis BH, Influence of zirconium salt precursors on the crystal structures of zirconia, Catalysis Letters 14, 1992, 165-170.

341. Srinivasan R and Davis BH, Prepr. Am. Chem. Petrol. Chem.Div. 36 1991, 635.

342. Srinivasan R, Harris MB and De Angehs RJ, Journal of Materials Research, 3, 1988, 787.

343. Srinivasan R, Keogh RA, Milburn DR, Davis BH, Sulfated zirconia catalysts: characterization by TGA/DTA mass spectrometry, Journal of Catalysis 153, 1995, 123–130.

344. Srinivasan R, Taulbee D, Davis BH, The effect of sulfate on the crystal structure of zirconia Catalysis Letters 9, 1991, 1-7.

345. Srinivasan R, Watkins TR, Hubbard CR, Davis BH, Sulfated zirconia catalysts, The crystal phases and their transformations, Chemistry of Materials 7, 1995, 725-730.

346. Srinivasan, R, Chokkaram S, Milburn DR, Davis BH, Ion exchange and thermal studies of sulfated zirconia, Journal of Colloid and Interface Science 165 (1) 1994, 160-168.

347. Srivastav A and Srivastava VC, Adsorptive desulfurization by activated alumina, Journal of Hazardous Materials 170, 2009, 1133–1140.

348. Srivastava VC, Mall ID, Mishra IM, Adsorption thermodynamics and isosteric heat of adsorption of toxic metal ions onto bagasse fly ash (BFA) and rice husk ash (RHA) Chemical Engineering Journal 132, 2007, 267–278.

349. Srivastava VC, Swamy MM, Mall ID, Prasad B, Mishra, Adsorptive removal of phenol by bagasse fly ash and activated carbon: equilibrium, kinetics and thermodynamics, Colloid Surf. A: Physicochem. Eng. Aspects 272, 2006, 89-104.

350. Strukul G in Strukul G (Ed.) Catalytic Oxidation with hydrogen peroxide as oxidant, Kluwer Academic Publisher, 1992a, 1-4.

351. Strukul G in Strukul G ed., Catalytic Oxidation with hydrogen peroxide as oxidant, Kluwer Academic Publisher, 1992b, 177-183.

352. Suchanek A, How to make low-sulfur, low aromatics, high cetane diesel fuel, ACS Div. Petroleum Chemistry Prepraration 41, 1996, 583–584.

353. Sugeng T, Abdullah Z, Jali AA, The effect of sulfate ion on the isomerization of n-butane to iso-butane, Journal of Natural Gas Chemistry 15, 2006, 247-252.

354. Sughrue, et al., Fish and Dollar, US Patent Application 20, 040, 007, 501.

355. Sun YY, Ma SQ, Du YC, Yuan LN, Wang SC, Yang J, Deng F, Xiao FS, Journal of Physical Chemistry B 109, 2005, 2567.

356. Sun YY, Yuan LN, Wang W, Chen CL, Xiao FS, Catalysis Letters 87, 2003, 57.
357. Sun YY, Zhu L, Lu HJ, Wang RW, Lin S, Jiang DJ, Xiao FS, Sulfated zirconia supported in mesoporous materials, Applied Catalysis A-General 237, 2002, 21-26.
358. Suzuku T and Okuhara T, Chemistry Letters 470, 2000.
359. Tabora JE and Davis RJ, Structure of Fe, Mn-promoted sulfated zirconia catalyst by X-ray and IR absorption spectroscopies, Journal of Chemical Society Faraday Trans. 91, 1995, 1825-1833.
360. Takahashi A and Yang RT, Cu(I)-Y-zeolite as a superior adsorbent for diene/olefin separation, Langmuir 17, 2001, 8405–8413.
361. Takahashi A, Yang FH, Yang RT, New sorbents for desulfurization by π-complexation: thiophene/benzene adsorption, Industrial and Enginering Chemistry Research, 41, 2002, 2487-2496.
362. Tam PS, Kittrell JR, Eldridge JW, Desulfurization of fuel oil by oxidation and extraction:1, Enhancement of extraction oil yield Industrial & Enginering Chemistry Research 29, 1990, 321-324.
363. Tanabe K and Holderich WF, Industrial application of solid acid–base catalysts, Applied Catalysis A: General 181, 1999, 399-406.
364. Tanabe K and Takeshita Y, Catalytic Activity and Acidic Property of Solid Metal Sulfates, Advances in Catalysis, 17, 1967, 315-349.
365. Tanabe K, Hattori H, Yamaguchi T, Critical Reviews in Surface Chemistry, 1, 1990, 353-357.
366. Tanabe K, in Catalysis Science and Technology (J.R Anderson and M.Boudart, Ed.) 231, Springer-Velag, Berlin 1981.
367. Tanabe K, Misono M, Ono Y, Studies in Surface Scienc and Catalysis 51, 1989, 1909.
368. Tanabe K, Surface and catalytic properties of $ZrO_2$, Materials Chemistry and Physics 13, 1985, 347-364.
369. Tang K, Song L, Duan L, Li X, Gui J, Sun Z, Deep desulfurization by selective adsorption on a heteroatoms zeolite prepared by secondary synthesis, Fuel Processing Technology, 89, 2008, 1-6.
370. Tao H, Nakazato T, Sato S, Energy-efficient ultra-deep desulfurization of kerosene based on selective photooxidation and adsorption, Fuel 88, 2009, 1961–1969.
371. Te M, Fairbridge C, Ring Z, Oxidation reactivities of dibenzothiophenes in polyoxometalate/$H_2O_2$ and formic acid/$H_2O_2$ systems,Applied Catalysis A-General 219, 2001, 267-280.

372. Tian F, Wu W, Jiang W, Liang C, Yang Y, Ying P, Sun X, Cai T, Li C, The study of thiophene adsorption onto La(III)-exchanged zeolite NaY by FT-IR spectroscopy , Journal of Colloid and Interface Science 301, 2006, 395–401.

373. Tichit D, Coq B, Armendariz H, Figueras F, One-step sol-gel synthesis of sulfated-zirconia catalysts, Catalysis Letters 38, 1996, 109-113.

374. Tichit D, El Alami D, Figueras F, Preparation and anion exchange properties of zirconia, Applied Catalysis A 145, 1996, 195-210.

375. Topsøe H, Clausen BS, Massoth FE, Catalysis Science and Technology, 11, 1996, 310.

376. Torralvo MJ, Alario MA, Soria, Crystallization behavior of zirconium oxide gels, Journal of Catalysis 86 (2) 1984, 473–476.

377. US Patent 4, 493, 765, and 1998.

378. Valigi M, Gazzoli D, Pettiti I, Mattei G, Colonna S, De Rossi S, Ferraris G, $WO_x/ZrO_2$ catalysts Part 1: Preparation, bulk and surface characterization, Applied Catalysis A-General 231, 2002, 159–172.

379. Vaudagna SR, Comelli RA, Figoli NS, Influence of the preparation conditions on the textural properties and n-hexane isomerization activity of $Pt/SO_4^{2-}$ $ZrO_2$, Reaction Kinetics and Catalysis Letters 58, 1996, 111-117.

380. Vaudagna SR, Comelli RA, Figoli NS, Modification of $SO_4^{2-}$- $ZrO_2$ and $Pt/SO_4^{2-}$- $ZrO_2$ properties during n-hexane isomerization, Catalysis Letters 47 (3, 4) 1997, 259-264.

381. Veiga Blanco ML, valet Regi M, Mata Arjona A, Gutierrez RE, An. Quimica, 76, 1980, 218.

382. Velu S, Ma XL, Song CS, Selective adsorption for removing S from jet fuel over zeolite-based adsorbents, Industrial and Enginering Chemistry Research 42, 2003, 5293.

383. Velu S, Song CS, Engelhard EH, Chin YH, Adsorptive removal of organic S compounds from jet fuel over K-exchanged NiY zeolites prepared by impregnation and ion exchange, Industrial and Enginering Chemistry Research 44, 2005, 5740–5749.

384. Venner SF, Hydrocarbon Processing 2000, 5, 51.

385. Vera.C.R, Pieck.C.L, Shimizu.K, Querini.C.A, Parera.J.M, "Coking of $SO_4^{2-}$-$ZrO_2$ catalysts during isomerization of n-butane and its relation to the reaction mechanism", Journal of Catalysis 187, 1999, 39-49.

386. Vogel AI, A Text Book of Quantitative Inorganic Analysis, 3$^{ed}$. Wiley, New York, 1966.

387. Wan KT, Khouw CB, Davis ME, Studies on the catalytic activity of zirconia promoted with sulfate, iron, and manganese, Journal of Catalysis 158, 1996, 311-326.

388. Wan KT, Khouw CB, Davis ME, Studies on the catalytic activity of $ZrO_2$ promoted with sulfate, iron, and manganese, Journal of Catalysis 158, 1996, 311.

389. Wang A, Wang Y, Kabe T, Cehn Y, Ishihara A, Qian W, Journal of Catalysis 199, 2001, 19-29.

390. Wang B, Zhu J, Ma H, Desulfurization from thiophene by $SO_4^{2-}/ZrO_2$ catalytic oxidation at room temperature and atmospheric pressure, Journal of Hazardous Materials 164, 2009, 256–264.

391. Wang D, Li W, Tang H, Liu Q, Xing J, Yang M, Li X, Liu H, Deep desulfurization of diesel by integrating adsorption and microbial method, Biochemical Engineering Journal 44, 2009, 297–301.

392. Wang D, Qian EW, Amano H, Okata K, Ishihara A, Kabe T, Oxidative desulfurization of Fuel oil: Part I, Oxidation of dibenzothiophenes using tert-butyl hydroperoxide, Applied Catalysis A-General 253, 2003 91-99.

393. Wang JH, Mou CY, Alumina-promoted mesoporous sulfated zirconia catalyst for n-butane isomerization, Applied Catalysis A-General 286, 2005, 128–136.

394. Wang S, Matsumura S, Toshima K, Sulfated zirconia as a reusable solid acid catalyst for the Mannich-type reaction between ketene silyl acetals and aldimines, Tetrahedron Letters 48, 2007, 6449–6452.

395. Wang SY, Li XA, Zhai YC, Wang KM, Preparation of homodispersed nano zirconia, Powder Technology 168 (2) 2006, 53–58.

396. Wang W, Wang S, Liu H, Wang Z, Desulfurization of gasoline by a new method of electrochemical catalytic oxidation, Fuel 86, 2007b, 2747–2753.

397. Wang W, Wang S, Wang Y, Liu H, Wang Z, A new approach to deep desulfurization of gasoline by electrochemically catalytic oxidation and extraction, Fuel Processing Technology 88, 2007a, 1002–1008.

398. Wang Y, Yanga RT, Heinzelb JM, Desulfurization of jet fuel by π-complexation adsorption with metal halides supported on MCM-41 and SBA-15 mesoporous materials, Chemical Engineering Science 63, 2008, 356 – 365.

399. Wanga J, Xub F, Xiec W, Meib Z, Zhanga Q, Caib J, Caia W, The enhanced adsorption of dibenzothiophene onto cerium/nickel-exchanged zeolite Y, Journal of Hazardous Materials 163, 2009, 538–543.

400. Waqif M, Bachelier J, Saur O, Lavalley JC, Journal of Molecular Catalysis, 72, 1992, 127.

401. Ward DA and Ko EI, One-Step Synthesis and Characterization of Zirconia-Sulfate Aerogels as Solid Superacids, Journal of Catalysis 150, 1994, 18-33.

402. Ward DA and Ko EI, Sol-Gel Synthesis of Zirconium Supports: Important Properties for Generating n-Butane Isomerization Activity upon Sulfate Promotion, Journal of Catalysis 157, 1995, 321.

403. Wardencki W and Straszewski R, Dynamic adsorption of thiophenes, thiols and sulfides from n-heptane solutions on molecular sieve 13X, J. Chromatogr. 91, 1974, 715–722.

404. Watanabe K, Kawakami T, Baba K, Oshio N, Kimura T, Effect of metals on the catalytic activity of sulfated zirconia for light naphtha isomerization, Catalytic Surveys from Asia 9 (1) 2005, 17-24.

405. Weber Jr. WJ and Morris JC, Kinetics of adsorption on carbon from solution, Journal of Sanitary Engineering Diviison. ASCE 89, 1963, 31-59.

406. Weitkamp J, Schwark M, Ernest S, Journal of Chemical Society, Chemical Communications 1991, 1133.

407. Wen MY, Wender I, Tierney JW, Hydroisomerization and hydrocracking of n-heptane and n-hexadecane on solid superacids Energy and Fuels 4, 1990, 372-379.

408. Wong ST, Li T, Lee JF, Mou CY, Cheng S, Journal of Catalysis 215, 2003, 45.

409. Wong T, Li T, Cheng S, Lee JF, Mou CY, Platinum- and iron-doubly promoted tungstated zirconia catalyst for n-butane isomerization reaction, Applied Catalysis A: General 296, 2005, 90–99.

410. Xia QH, Hidajat K, Kawi S, Effect of $ZrO_2$ Loading on the structure, acidity, and catalytic activity of the $SO_4^{2-}/ZrO_2$/MCM-41 acid catalyst, Journal of Catalysis 205, 2002, 318-331.

411. Xia Y, Hua W, Gao Z, A new catalyst for n-butane isomerization: persulfate-modified $Al_2O_3$–$ZrO_2$, Applied Catalysis A-General 185, 1999, 293–300.

412. Xie Y, Preparation of ultrafine zirconia particles, Journal of American Ceramic Society 82, 1999, 768–770.

413. Xu BQ and Sachtler WMH, Reduction of $SO_4^{2-}$ ions in sulfated zirconia catalysts, Journal of Catalysis 167 (1) 1997, 224-233.

414. Xue M, Chitrakar R, Sakane K, Hirotsu T, Ooi K, Yoshimura Y, Feng Q, Sumida N, Selective adsorption of thiophene and 1-benzothiophene on metal-ion-exchanged zeolites in organic medium, Journal of Colloid Interface Science 285, 2005, 487-492.

415. Yadav GD and Nair JJ, Sulfated $ZrO_2$ and its modified versions as promising catalysts for industrial processes, Microporous and Mesoporous Materials 33, 1999, 4-7.

416. Yahia A, Alhamed, Hisham S, Bamufleh, Sulfur removal from model diesel fuel using granular activated carbon from dates' stones activated by $ZnCl_2$, Fuel 88, 2009, 87–94.

417. Yamaguchi T, Application of $ZrO_2$ as a catalyst and a catalyst support, Catalysis Today 20, 1994, 199-217.

418. Yamaguchi T, Jin T, Ishida T, Tanabe K, Structural identification of acid sites of sulfur-promoted solid super acid and construction of its structure on silica support, Materials Chemistry Physics 17, 1987, 3-19.

419. Yamaguchi T, Recent progress in solid superacid, Applied Catalysis A: General 61, 1990, 1-25.

420. Yamaguchi T, Tanabe K, Jin T, Mechanism of acidity generation on sulfur-promoted metal oxides, Journal of Physical Chemistry 90, 1986, 4794-4796.

421. Yamaguchi T, Tanabe K, Kung YC, Nano zirconia and sulfated zirconia from ammonia zirconium carbonate, Materials Chemistry & Physics 16, 1986, 67-73.

422. Yamamoto T, Tanaka T, Takenaka S, Yoshida S, Onari T, Takahashi Y, Kosaka T, Hasegawa S, Kudo M, Structural analysis of iron and manganese species in iron- and manganese promoted sulfated zirconia, Journal of Physical Chemistry B103, 1999, 2385-2393.

423. Yang L, Li J, Yuan X, Shen J, Qi Y, One step non-hydrodesulfurization of fuel oil: Catalyzed oxidation adsorption desulfurization over HPWA-SBA-15, Journal of Molecular Catalysis A: Chemical 262, 2007, 114–118.

424. Yang RT, Hernandez-Maldonado AJ, Cannella W, Science 301, 2003, 79.

425. Yang X, Jentoft FC, Jentoft RE, Girgsdies F, Ressler T, Sulfated zirconia with ordered mesopores as anactive catalyst for *n*-butane isomerization, Catalysis Letters 81, 2002, 25-31.

426. Yazu K, Yamamoto Y, Furuya T, Miki K, Ukegawa K, Energy & Fuels 15, 2001, 1535.

427. Yen et al., USA Patent 66, 402, 939, June 11, 2002.

428. Yongna Z, Lu W, Yuliang W, Zongxuan J, Can L, Ultra-deep Oxidative Desulfurization of Fuel Oil Catalyzed by Dawson-type Polyoxotungstate Emulsion Catalysts, Chinese Journal of Catalysis, 32 (2) 2011, 235–239.

429. Yoona YI, WookKim M, Yoonb YS, Kima SH, A kinetic study on medium temperature desulfurization using a natural manganese ore, Chemical Engineering Science 58, 2003, 2079 – 2087.

430. Yori JC, D'Amato MA, Costa G, Parera JM, Journal of Catalysis 153, 1995, 218.

431. Yori JC, Luy JC, Parera JM, Deactivation of H-mordenite and $ZrO_2/SO_2^{-4}$ during n-butane isomerization, Applied Catalysis 46, 1989, 103-108.

432. Yori JC, Luy JC, Parera JM, n-Butane isomerization on solids, Catalyst Today 5, 1989, 493.

433. Yu G, Lu S, Chen H, Zhu Z, Diesel fuel desulfurization with hydrogen peroxide promoted by formic acid and catalyzed by activated carbon, Carbon 43, 2005, 2285–2294.

434. Yu G, Lu S, Chen H, Zhu Z, Oxidative desulfurization of diesel fuels with hydrogen Peroxide in the Presence of Activated Carbon and formic, Acid Energy and Fuels 19, 2005, 447-452.

435. Yu M, Li Z, Xia Q, Xi H, Wang S, Desorption activation energy of dibenzothiophene on the activated carbons modified by different metal salt solutions, Chemical Engineering Journal 132, 2007, 233–239.

436. Yu M, Li, Ji Q, Wang S, Su D, Lin YS, Effect of thermal oxidation of activated carbon surface on its adsorption towards dibenzothiophene, Chemical Engineering Journal 148, 2009, 242–247.

437. Yuan PQ, Cheng ZM, Jiang WL, Zhang R, Yuan WI, Catalytic desulfurization of residual oil through partial oxidation in supercritical water, J. of Supercritical Fluids 35, 2005, 70–75.

438. Zaki T, Riad M, Saad L, Mikhail S, Selected oxide materials for sulfur removal, Chemical Engineering Journal 113, 2005, 41–46.

439. Zalewski DJ, Alerasool S, Doolin PK, Characterization of catalytically active sulfated zirconia,

440. Zane F, Melada S, Signoretto M, Pinna F, Active and recyclable sulphated zirconia catalysts for the acylation of aromatic compounds, Applied Catalysis A-General 138 299, 2006, 137–144.

441. Zapata B, Pedraza F and Valenzuela MA, Catalyst screening for oxidative desulfurization using hydrogen peroxide. Catalysis Today 106, 2005, 219-221.

442. Zapata B, Pedraza F, Valenzuela MA, Catalyst screening for oxidative desulfurization using hydrogen peroxide, Catalysis Today 106, 2005, 219–221.

443. Zeng J, Zhong B, Luo Q, Wang Q, Ranliao Huaxue uebao 22 (2), 1994, 145.

444. Zepeda TA, Pawelec B, Fierro JLG, Halachev T, Removal of refractory S-containing compounds from liquid fuels on novel bifunctional CoMo/HMS catalysts modified with Ti, Applied Catalysis B: Environmental 71, 2007, 223–236.

445. Zhang C, Miranda R, Davis BH, Platinum-sulfated-zirconia. Infrared study of adsorbed pyridine, Catalysis Letters 29, 1994, 349-359.

446. Zhang ZY, Shi TB, Jia CZ, Ji WJ, Chen Y, He MY, Adsorptive removal of aromatic organosulfur compounds over the modified NaY zeolites, Applied Cataysis. B: Environmental, 82, 2008, 1-10.

447. Zhang ZY, Shi TB, Jia CZ, Ji WJ, Chen Y, He MY, Adsorptive removal of aromatic organosulfur compounds over the modified Na-Y zeolites, Applied Catalysis B: Environmental 82, 2008, 1–10.

448. Zhao J, Huffman GP, Davis BH, XAFS study of the state of platinum in a sulfated zirconia catalyst, Catalysis Letters 24, 1994, 385-389.

449. Zhou A, Maa X, Song C, Effects of oxidative modification of carbon surface on the adsorption of sulfur compounds in diesel fuel, Applied Catalysis B: Environmental 87, 2009, 190–199.

450. Zhua W, Li H, Gua Q. Q, Wua P, Zhua G, Yana Y, Chen G, Kinetics and mechanism for oxidative desulfurization of fuels catalyzed by peroxo-molybdenum amino acid complexes in water-immiscible ionic liquids, Journal of Molecular Catalysis A: Chemical 336, 2011, 16–22.

451. Zhua W, Zhub G, Li H, Chaob Y, Changa Y, Chena G, Hana C, Oxidative desulfurization of fuel catalyzed by metal-based surfactant-type ionic liquids, Journal of Molecular Catalysis A: Chemical 347, 2011, 8-14.

452. Ziolek M, Catalytic liquid-phase oxidation in heterogeneous system as green chemistry goal−advantages and disadvantages of MCM-41 used as catalyst, Catalysis Today 90 (1/2) 2004, 145-150.

# LIST OF PUBLICATIONS

**Research Papers Published/Accepted/Communicated in SCI (International) Journals**

1. Sachin Kumar, VC Srivastava, RP Badoni "Studies on adsorptive desulfurization by zirconia based adsorbents", **Fuel 90, 2011, 3209-3216; Impact Factor: 3.602.**
2. Sachin Kumar, VC Srivastava, RP Badoni "Deep desulfurization of liquid fuel stream by chromium promoted zirconia based catalytic-oxidation", **Fuels Processing Technology, 93, 2012, 1825-1831; Impact Factor: 2.781.**
3. Sachin Kumar, VC Srivastava, RP Badoni "Ooxidative desulfurization of dibenzothiophene by zirconia based catalysts", **International Journal of Chemical Reactor Engineering (Accepted); Impact Factor: 0.64.**
4. Sachin Kumar, VC Srivastava, RP Badoni "Effect of the precipitation procedure on zirconia based catalysts used for oxidative desulfurization of liquid fuel", communicated in **Petroleum Science & Technology Journal (Communicated 2011)**; **Impact Factor: 0.345.**
5. Sachin Kumar, VC Srivastava, RP Badoni "A critical review on catalytic activation of alkane to valuated Petrochemicals", **Catalysis Review (Communicated 2011); Impact Factor: 9.256.**

**International / National Conferences**

1. Sachin Kumar, Priyanshu Vajpeyi, Saurabh Kulshrestha "*A critical review of the adsorption of sulfur derivatives on low cost adsorbents and their potential applications in their removal from fuel streams*", poster presented at **School of Environmental Science, Jawharlal Nehru University, New Delhi, India.**
2. Sachin Kumar, VC Srivastava, RP Badoni, S Suresh "*Catalytic oxidative desulfurization for removal of sulphur compounds from synthetic fuel stream*", Abstract accepted for poster presentation in **PSE ASIA 2010 at National University of Singapore.**

3. Sachin Kumar, VC Srivastava, RP Badoni "Preparation and characterization of zirconia catalysts for the removal of sulfur compounds in distillate fuels", paper oral presentation in **Petrotech 2010, 9th International Oil & Gas Conference & Exhibition, New Delhi, India.**
4. Sachin Kumar, VC Srivastava, RP Badoni, S Suresh "Catalytic desulfurization for the removal of sulphur compounds chemical oxidative process", Abstract accepted for oral presentation in **5th International Conference on Environmental Science and Technology 2010 at Environmental Conference Program, American Academy of Sciences, Houston, TX.**
5. Sachin Kumar, VC Srivastava, RP Badoni, S Suresh "Adsorptive desulfurization for the removal of DBT & derivatives compounds by Granular activated Carbon (GAC", Abstract accepted for oral presentation in **International Conference on Nanotechnology: Fundamentals and Applications, August 4 - 6, 2010: International-ASET Ottawa, Ontario, Canada K1J 1C7.**

**International / National Conferences (Communicated 2011)**

1. Sachin Kumar, VC Srivastava, RP Badoni "Effect of the preparation procedure on zirconia based catalysts for oxidative desulfurization of liquid fuel" communicated in **8th Symposium in the series, i.e., ISFL-2012 will be organized during March 5-7, 2012, in Habitat World at India Habitat Centre, New Delhi, India. The theme of this symposium is "Advances in Fuels, Lubricants and Alternatives".**
2. Sachin Kumar, VC Srivastava, RP Badoni, S Suresh, Urban Environmental Pollution, 17th June 2012, Amsterdam, The Netherlands': Under the category-Pollution problems and possible solutions.
3. Sachin Kumar, VC Srivastava, GK Vramireddy, CHEMCON - 2011: "Catalytic Oxidation of 4-Chlorophenol using α-FeOOH", 64 Annual Session of the Indian Institute of Chemical Engineers will be held during December 27 - 29, 2011, Bangalore.

**APPENDIX – A**

# LIST OF ABBREVIATIONS

| | |
|---|---|
| ACF | activated carbon fiber |
| GCSAC | granular coconut-shell activated carbon |
| 2-MBT | 2-methylbezothiophene |
| 2-MT | 2-methylthiophene |
| 4,6-DMDBT | 4,6-dimethyldibenzothiophene |
| 4-E-6MDBT | 4-ethyl, 6-methyl-DBT |
| 4-MDBT | 4-methyldibenzothiophene |
| 2,5-DMT | 2,5-dimethythiophene |
| AC | Activated Carbon |
| ACF | Activated Carbon Fiber |
| ADS | Adsorptive desulphurization |
| BT | Benzothiophene |
| BET | Brunauer-Emmett-Teller |
| C | Cubic |
| CGO | Coker Gas Oil |
| CVD | Chemical vapor deposition |
| CSZC893 | Chromium Promoted Sulfated Zirconia calcined @ 893 K |
| CUS | Coordinately unsaturated sites |
| CeSZ | Cerium Promoted Sulfated Zirconia calcined @ 923 K |
| DBT | Dibenzothiophene |
| DBT-MO | Dibenzothiophene-monooxygenase |
| DBTO | Dibenzothiophene-5-oxide, DBT sulfoxide |
| DBTO2 | Dibenzothiophene-5,5-dioxide, DBT sulfone |
| $DBTO_2$-MO | Dibenzothiophene-5,5-dioxide-monooxygenase |

| | |
|---|---|
| DDS | Direct desulfurization |
| DLCO | Deeply desulphurized Light Cycle Oil |
| DMBPh | Dimethylbiphenyl |
| DMDBT | DiMethyl Dibenzothiophene |
| DMDS | Dimethyl disulfide |
| DMSO | Dimethyl sulfoxide |
| DPS | Diphenylsulfide |
| EDF | Equilibrium deposition filtration |
| EDXFS | Energy-dispersive X-ray fluorescence spectrometry |
| EPA | Environmental protection agency |
| EPMA | Electron Probe Microscopic Analysis |
| EPR/ESR | Electron Paramagnetic Resonance/ Electron Spin Resonance |
| FCC | Fluid catalytic cracking |
| FID | Flame ionization detector |
| FTIR | Fourier Transform Infrared Spectroscopy |
| GC | Gas Chromatography |
| GC-MS | Gas Spectroscopy-Mass Spectroscopy |
| HDS | Hydrodesulfurization |
| HDN | Hydrodenitrogenation |
| HT | Hydrotreated |
| HYD | Hydrogenation Benzene |
| HYD | Hydrogenation |
| HMS | Hexagonal mesoporous silicate |
| M | Monoclinic |
| MDBT | Methyl Dibenzothiophene |
| MT | Methylthiophene |
| MINAS | Minimal national standard |

| | |
|---|---|
| MPSD | Marquardt's percent standard deviation |
| MW | Molecular weight |
| NA | Naphthalene |
| NAA | Neutron Activation Analysis |
| $S_N2$ | Nucleophilic bimolecular substitution |
| $NO_x$ | Oxides of nitrogen |
| ODS | Catalytic-Oxidative desulphurization |
| OECD | Organization for Economic Co-operation and Development |
| ppmw | Parts per million by weight |
| HPW | phosphotungstic acid |
| PASHs | polycyclic aromatic sulfur heterocycles |
| PAHS | polycyclic aromatic hydrocarbons |
| SCANfining | Selective cat naphtha hydrofining process developed by ExxonMobil |
| SCW | Supercritical Water |
| SEM | Scanning Electron Microscopy |
| SOx | Oxides of sulfur |
| SRGO | Straight Run Gas Oil |
| SRGO | Straight (distillation) run gas oil |
| SZ | Sulfated Zirconia |
| SZC893 | Sulfated Zirconia calcined @ 893 K |
| SSE | Sum of squares of error |
| SSR | Residual sum of squares |
| T | Tetragonal |
| TH2MT | Tetrahydro-2-methylthiophene |
| TOF | Turnover frequency |
| TH | Thiophene |

| | |
|---|---|
| TAP | Temporal Analysis of Products |
| TEM | Transmission Electron Microscopy |
| TPD | Temperature-programmed desorption |
| TPR | Temperature-programmed reduction/temperature-programmed reaction |
| TG | Thermo-Gravimetric |
| TGA | Thermo-Gravimetric Analysis |
| THDBT | Tetra hydrodibenzothiophene |
| THT | Tetra hydrothiophene |
| TPR | Temperature-Programmed Reduction |
| ULSD | ultra low sulfur diesel |
| VR | Vacuum Residuum |
| XPS | X-Ray Photoelectron Spectroscopy |
| XRD | X-Ray Diffraction |
| Z | Zirconia Raw |
| ZC893 | Zirconia (normal) calcined @ 893 K |
| ZD393 | Zirconia (normal) drying @ 393 K |

**APPENDIX – B**

# SAFETY POINTS [http://www.des.umd.edu/ls/labguide/one.htm]

1. Be alert to unsafe conditions and actions, and call attention to them so that corrections can be made as soon as possible.
2. Label all storage areas, refrigerators, etc., appropriately, and keep all chemicals in properly labeled containers.
    - Date all bottles when received and when opened.
    - Note expiration dates on chemicals.
    - Note special storage conditions.
3. Be familiar with the appropriate protective measures to take when exposed to the following classes of hazardous materials:

    Flammables; Corrosives; Biohazards; Toxics; Carcinogens; Reactive; Compressed Gases
4. Segregate chemicals by compatibility groups for storage.
5. Post warning signs for unusual hazards such as flammable materials, biohazards or other special problems.
6. Pour more concentrated solutions into less concentrated solutions to avoid violent reactions (i.e., always add acid to water; not water to acid).
7. Avoid distracting any other worker. Practical jokes or horseplay have no place in the laboratory.
8. Position and secure apparatus used for hazardous reactions in order to permit manipulation without moving the apparatus until the entire reaction is complete.